Evaluation of Single-Bounce Attenuated Total Reflectance/Fourier Transform Infrared and Two-Dimensional Correlation Spectroscopy in Quantitative Analysis

Robert Arthur Cocciardi

Department of Food Science and Agricultural Chemistry

McGill University

A thesis submitted to the Faculty of Graduate Studies and Research in partial fulfillment

of the requirements for the degree of Doctor of Philosophy

Short title:

SB-ATR/FTIR AND 2D CORRELATION SPECTROSCOPY IN QUANTITATIVE ANALYSIS

ABSTRACT

The utility of single-bounce attenuated total reflectance (SB-ATR) and heterospectral two-dimensional correlation spectroscopy (H2D-CS) in quantitative analysis by Fourier transform infrared (FTIR) spectroscopy was investigated by exploring several potential applications of these techniques. Enzymatic hydrolysis of lactose in milk was monitored by SB-ATR/FTIR spectroscopy, and changes in the concentrations of glucose, galactose and lactose during the process were successfully measured quantitatively. SB-ATR/FTIR spectroscopy was shown also to perform comparably to Fourier transform near-infrared (FT-NIR) spectroscopy for the determination of the alcohol content of distilled liquors and better than FT-NIR spectroscopy and comparably to transmission FTIR spectroscopy for the analysis of alcohol, total reducing sugar, total acidity and pH in wines. In addition, a set of 149 pre-analyzed wine samples was employed to develop and validate an SB-ATR/FTIR calibration for 11 different parameters and constituents in wines with the use of partial-least-squares (PLS) regression, demonstrating the potential utility of this method in the routine analysis of wines. The application of SB-ATR/FTIR spectroscopy and H2D-CS in the selection of wavelengths for multiple linear regression (MLR) calibration for FT-NIR analysis of ternary aqueous solutions of fructose, glucose and galactose was also investigated. NIR wavelengths were identified for the three sugars by H2D-CS of the SB-ATR/FTIR spectra of binary sugar solutions in relation to their FT-NIR spectra. An MLR calibration developed based on these wavelengths gave better results than PLS calibrations and comparable results to those obtained by MLR using wavelengths selected by examination of 1^{st} and 2^{nd} derivative spectra. H2D-CS was extended to include 2D correlations between high-pressure liquid chromatography (HPLC) and SB-ATR/FTIR data for the purpose of identifying HPLC peaks without the need to isolate the eluted compounds. The potential utility of this approach, termed spectroscopic/chromatographic 2D correlation (SC2D-C), was investigated by generating FTIR slice spectra corresponding to the HPLC peaks of wines spiked with sucrose, glucose and fructose and comparing them to 404 reference spectra in an IR spectral library. It was found that these constituents were correctly identified provided there was sufficient random variability of their concentrations in the samples analyzed.

RÉSUMÉ

La pertinence de la réfléctance totale atténuée à un point (SB-ATR) et de la corrélation hétérospectrale en deux dimensions (H2D-CS) comme outils d'analyse quantitative par spectroscopie infrarouge à transformée de Fourier (FTIR) a été sondée en utilisant plusieurs applications de ces méthodes. L'hydrolyse enzymatique du lactose dans le lait a été étudiée par spectroscopie SB-ATR/FTIR et les changements de concentration en glucose, en galactose et en lactose durant la réaction ont été mesurés adéquatement. Les résultats ont démontré que la performance de la spectroscopie SB-ATR/FTIR était comparable à la spectroscopie proche-infrarouge à transformée de Fourier (FT-NIR) pour l'analyse du contenu en alcool des boissons alcoolisées distillées tandis qu'elle était supérieure à la spectroscopie FT-NIR et comparable à la spectroscopie FTIR de transmission en ce qui a trait à l'analyse du contenu en alcool et en sucres réducteurs, de l'acidité totale et du pH des vins. De plus, un totale de 149 échantillons de vins préalablement analysés ont été utilisés pour le développement et la validation d'une méthode SB-ATR/FTIR à 11 paramètres et composantes du vin dont la calibration a été dévelopée en utilisant la méthode des moindres-carrés-partiels (PLS) et démontrant l'applicabilité de cette méthode dans l'analyse oenologique de routine. L'applicabilité de la spectroscopie SB-ATR/FTIR et H2D-CS dans la séléction des longueurs d'ondes nécessaires à une régression linéaire multiple (MLR) pour l'analyse FT-NIR de solutions tertiaires de fructose, glucose et galactose a aussi été évaluée. Les longueurs d'ondes NIR on été identifiées pour les trois sucres mentionnés en faisant l'analyse H2D-CS des spectres SB-ATR/FTIR de solutions binaires de ces sucres avec leur spectres FT-NIR correspondant. L'étalonnage MLR basé sur ces longueurs d'ondes a donné des résultats supérieurs comparer aux résultats obtenus par la méthode PLS et comparables aux résultats obtenus par les étalonnages MLR dont les longueurs d'ondes ont été sélectionées par évaluation des spectres de la première et de la deuxième dérivée. La méthode H2D-CS a aussi compris des corrélations 2D entre les donnés de la chromatographie à haute performance (HPLC) et celles de la spectroscopie SB-ATR/FTIR pour l'identification des sommets HPLC dans le but d'éliminer l'étape d'isolation des composantes éluées. Le potentiel d'applicabilité de cette méthode qu'est la corrélation spectroscopie/chromatographie 2D (SC2D-C) a été évaluée en examinant les spectres unidimensionels FTIR, obtenus par SC2D-C des sommets HPLC des échantillons de vins dans lesquels différentes quantités de sucrose, de glucose et de fructose avaient été ajoutées. En comparant ces spectres unidimensionels avec 404 spectres de référence contenus dans une banque de spectres à infrarouge, il a été démontré que ces composantes peuvent être indentifiées si il y a suffisamment de variabilité de leurs concentrations dans les échantillons analysés.

STATEMENT FROM THE THESIS OFFICE

In accordance with the regulations of the Faculty of Graduate Studies and Research of McGill University, the following statement from the Guidelines for Thesis Preparation is included:

Candidates have the option of including, as part of the thesis, the text of one or more papers submitted, or to be submitted, for publication, or the clearly-duplicated text of one or more published papers. These texts must conform to the "Guidelines for Thesis Preparation" and must be bound together as an integral part of the thesis.

The thesis must be more than a collection of manuscripts. All components must be integrated into a cohesive unit with a logical progression from one chapter to the next. In order to ensure that the thesis has continuity, connecting texts that provide logical bridges between the different papers are mandatory.

The thesis must conform to all other requirements of the "Guidelines for Thesis Preparation" in addition to the manuscripts.

As manuscripts for publication are frequently very concise documents, where appropriate, additional material must be provided in sufficient detail to allow a clear and precise judgement to be made of the importance and originality of the research reported in the thesis.

In general when co-authored papers are included in a thesis, the candidate must have made a substantial contribution to all papers included in the thesis. In addition, the candidate is required to make an explicit statement in the thesis as to who contributed to such work and to what extent. This statement should appear in a single section entitled "Contributions of Authors" as a preface to the thesis.

When previously published copyright material is presented in a thesis, the candidate must obtain, if necessary, signed waivers from the co-authors and publishers and submit these to the Thesis Office with the final deposition.

ACKNOWLEDGMENTS

"I can do everything through Him who gives me strength" **(Php 4:13)**

This thesis is dedicated to the Lord our God and to His Son Jesus Christ to whom I thank for the grace, guidance, wisdom, knowledge and strength He provided me to complete this work. I would also like to express my deepest gratitude to my parents who have always supported me and given me their best. I also thank my newly wed wife, Fleur de Marie, for supporting me financially through the final year of my doctoral studies.

I would like to express my appreciation to my supervisor, Dr. Ashraf A. Ismail, who guided me through this work and who was always willing to give his support and help. I especially like to express my gratitude to Dr. Jacqueline Sedman, who always gave valuable advice and encouragement and who was always available for help. I would also like to thank her for editing this thesis. I would like to thank Dr. Frederick van de Voort for his advice and input. I also express great thanks to Mr. David Pinchuk of Thermal-Lube Inc. who supported me financially during my doctoral studies through the NSERC industrial post-graduate scholarship program. Finally I would like to thank Dr. Yan Wang for his advice and assistance in this work.

CONTRIBUTION OF AUTHORS

Chapters 3-6 of this thesis are the text of papers to be submitted for publication, as listed below. The present author was responsible for the concepts, design of experiments, experimental work, and manuscript preparation. Dr. Ashraf A. Ismail, thesis supervisor, had direct advisory input into the work as it progressed. Dr. Jacqueline Sedman contributed her expertise and knowledge of FTIR spectroscopy and chemometrics in the interpretation and discussion of the results. Dr. Frederick van de Voort and Dr. Yan Wang provided their knowledge in IR milk analysis and 2D correlation spectroscopy, respectively, in the interpretation and discussion of the results for Chapters 3 and 5, respectively.

Chapter 3
Cocciardi, R.A., van de Voort, F.R., Sedman, J. and Ismail, A.A. Monitoring of lactose hydrolysis in milk by single-bounce attenuated total reflectance Fourier transform infrared spectroscopy

Chapter 4
Cocciardi, R.A., Ismail, A.A. and Sedman, J. Investigation of the potential utility of single-bounce attenuated total reflectance Fourier transform infrared spectroscopy in the analysis of distilled liquors and wines.

Chapter 5
Cocciardi, R.A., Ismail, A.A., Wang, Y. and Sedman, J. Heterospectral two-dimensional correlation spectroscopy of Fourier self-deconvolved Fourier transform near-infrared and Fourier transform mid-infrared spectra of sugar solutions.

Chapter 6
Cocciardi, R.A., Ismail, A.A. and Sedman, J. Compound identification by two-dimensional correlation of high-pressure liquid chromatograms with single-bounce attenuated total reflectance Fourier transform infrared spectra using wines as a model system

TABLE OF CONTENTS

LIST OF TABLES

LIST OF FIGURES

LIST OF ABBREVIATIONS

AOAC	Association of Official Analytical Chemists
AOCS	American Oil Chemists' Society
ATR	Attenuated total reflectance
AV	Anisidine value
BSVS	Backward stepwise variable selection
CIRCLE	Cylindrical internal reflectance cell for liquid evaluation
CLS	Classical-least-squares
DA	Discriminant analysis
DRIFT	Diffuse reflectance infrared Fourier transform
DTGS	Deuterated triglycine sulfate
FAME	Fatty acid methyl ester
FSD	Fourier self-deconvolution
FTIR	Fourier transform infrared
FT-NIR	Fourier transform near-infrared
GC	Gas chromatography
HPLC	High-pressure liquid chromatography
H2D-CS	Heterospectral two-dimensional correlation spectroscopy
ILS	Inverse-least-squares
IR	Infrared
IRE	Internal reflection element
IV	Iodine value
LDA	Linear discriminant analysis
MB-ATR	Multiple-bounce attenuated total reflectance
MCT	Mercury-cadmium-telluride
MD_a	Mean difference for accuracy
MLR	Multiple linear regression
NIR	Near-infrared
NMA	N-Methylacetamide
NMR	Nuclear magnetic resonance

OW	Optothermal window
PAS	Photoacoustic spectroscopy
PCA	Principal component analysis
PCR	Principal component regression
PLS	Partial-least-squares
PPE	Poly(2,6-dimethyl-1,4-phenylene ether)
PRESS	Predicted residual error sum of squares
PS	Polystyrene
PV	Peroxide value
R	Correlation coefficient
RSD	Relative standard deviation
SAQ	Société des alcools du Québec
SB-ATR	Single-bounce attenuated total reflectance
SC2D-C	Spectroscopic/chromatographic two-dimensional correlation
SD	Standard deviation
SDD_a	Standard deviation of the differences for accuracy
SDD_r	Standard deviation of the differences for reproducibility
SEP	Standard error of prediction
SN	Saponification number
S/N	Signal-to-noise ratio
UV	Ultraviolet
1D	One-dimensional
2D	Two-dimensional
3D	Three-dimensional

CHAPTER 1

INTRODUCTION

Mid-infrared (mid-IR) spectroscopy is well established as a powerful tool for qualitative analysis because of the detailed information about composition and molecular structure provided in the IR spectrum of a material[1]. Mid-IR spectroscopy has also found application as a means of quantitative analysis, although traditionally to a much lesser extent, except in the case of gas analysis, primarily owing to its limited sensitivity, the spectral complexity of multicomponent systems and, last but not least, fairly severe sample-handling limitations. However, although mid-IR spectroscopy is one of the oldest instrumental methods of analysis, it has rapidly evolved over the past few decades, beginning with the development of Fourier transform infrared (FTIR) spectroscopy. In terms of quantitative analysis, for example, major advances have been made through the application of chemometrics in the multicomponent analysis of complex samples[2] and the development of new sample-handling techniques[3], but there remains much potential to broaden the scope of FTIR quantitative analysis by taking advantage of new research findings and technological developments.

Food analysis by FTIR spectroscopy is an area that has been the subject of substantial research interest owing to its potential utility in the food industry. However, despite providing the possibility of highly rapid, automatable and solvent/reagent-free analysis, FTIR spectroscopy has had little impact in the food industry. In contrast, near-infrared (NIR) spectroscopy, which offers these same advantages, has found widespread application[4]. This difference can be largely attributed to the sample-handling difficulties associated with mid-IR spectroscopy, which are not shared by NIR spectroscopy. On the other hand, mid-IR calibrations are generally much simpler to develop because mid-IR spectra exhibit distinct bands that can be assigned to specific functional groups or components. In contrast, NIR spectra consist of ill-defined bands that are difficult to interpret and assign, making calibration development a time-consuming, empirical process that can require exceedingly large calibration sets. Nevertheless, this disadvantage largely continues to be overridden by the sample-handling advantages provided by NIR instrumentation.

In this context, two recent advances in FTIR spectroscopy, namely, the development of single-bounce attenuated total reflectance (SB-ATR) sample-handling accessories and the advent of generalized two-dimensional (2D) correlation spectroscopy, have the potential to prove valuable in quantitative analysis, including that of food systems. For this reason, several applications of these techniques were investigated in the research described in this thesis. In this chapter, a brief overview of quantitative analysis of foods by mid-IR spectroscopy will be presented followed by a discussion of the rationale and objectives of this research.

1.1. MID-IR SPECTROSCOPY IN QUANTITATIVE ANALYSIS OF FOODS

Molecules absorb IR radiation at the frequencies that promote transitions between the rotational and vibrational energy levels of the ground electronic energy state. The characteristic absorption bands of a species can be employed for quantitative analysis as their intensity is proportional to the concentration of the species in the sample, as expressed by the Bouguer-Beer-Lambert law, also known as Beer's law :

$$A_\nu = \varepsilon_\nu bc \quad [1.1]$$

where A_ν is the absorbance measured at frequency ν, ε_ν is the absorption coefficient of the absorbing species at the same frequency, b is the pathlength of the cell and c is the concentration of the absorbing species[5]. IR quantitative analysis requires that a calibration be developed by relating the change in concentration to the change in absorbance of a species at a fixed pathlength (to determine $\varepsilon_\nu b$ in Equation [1.1]). Once the relationship is established, the concentration of an unknown sample can be predicted using the calibration devised. Although simple in theory, in practice implementation of quantitative IR spectroscopy can be complicated by underlying absorptions due to other components as well as intermolecular and intramolecular interactions in the sample matrix[2].

The major components in foods, fat, protein and carbohydrates, all have well defined mid-IR absorptions that can be exploited for quantitative analysis. Table 1.1 presents some of the characteristic absorption frequencies of these components and their assignments to functional groups. The frequencies of these functional group absorptions are fairly consistent, although the exact frequency at which IR radiation is

Table 1.1: Functional group absorptions commonly used in food analysis[a].

Functional Group	Frequency (cm^{-1})	Remarks
-OH	3600-3200	O-H stretching vibration, strong water absorption band.
$-CH_2$	2926 (±10), 2853 (±10)	C-H stretching doublet, fatty acid chains.
-C=O	1745-1725	C=O stretching, triglyceride ester linkages, fats and oils
	1700-1600	Amide I band, peptide linkages of proteins.
-C=C-	1678-1665	C=C stretching, *trans* double bonds, fats and oils.
	1662-1648	C=C stretching, *cis* double bonds, fats and oils.
H-O-H	1650	H-O-H bending vibration, strong water absorption band.
-N-H-	1590-1500	Amide II band, proteins.
-C-O-H	1250-800	C-O stretching and C-O-H bending vibrations, carbohydrates and alcohols
-C=C-H	967	C=C-H bending, characteristic of isolated *trans* double bonds, fats and oils.

[a]adapted from reference 2.

absorbed by a functional group is affected by electrical effects, steric effects, electronegativity of neighboring atoms, phase changes and hydrogen bonding[2].

Two of the earliest and most noteworthy examples of applications of mid-IR analysis of foods are the determination of *trans* content in edible oils and the determination of fat, protein and lactose in milk, both of which have been established as official method of analysis[6,7]. *Trans* analysis by IR spectroscopy dates back about 50 years and is based on the characteristic absorption of isolated *trans* bonds at 966 cm^{-1} (10.3 μm), which is due to the *trans* C=C-H bending vibrations. The original method was modified to require saponification and methylation of the oil to remove underlying triglyceride absorptions which give rise to significant errors when measuring samples containing low levels of *trans* isomers (<15%)[8]. Another disadvantage of the traditional method is the need to quantitatively dissolve the sample in carbon disulfide, a volatile and noxious solvent, in order to inject it into a fixed-pathlength transmission cell. Milk analysis by mid-IR spectroscopy was developed by Biggs in 1967 and evolved into a standard method of the Association of Official Analytical Chemists (AOAC) that is widely used for milk payment, herd milk analysis and routine quality control in the dairy industry[6,9,10]. Although milk analysis was originally developed using dispersive spectrometers, filter-based instruments became the norm. Quantitation of each component is based on measurements at two specific wavelengths, one at which the component absorbs and one at a reference wavelength where no absorption occurs. Fat measurement is based on the C=O stretching vibration of ester linkages at 1744.6 cm^{-1} (5.72 μm) and the CH stretching vibration at 2873 cm^{-1} (3.48 μm), protein measurement is based on the NH bending vibration at 1548.6 cm^{-1} (6.47μm) and lactose measurement is based on the C-O stretching vibration at 1043.1 cm^{-1} (9.61 μm)[11]. The wavelengths are selected by interposing narrow-band filters in the path of the IR beam, and the instruments are calibrated using a set of milk samples pre-analyzed using standard reference methods (Mojonnier for fat, Kjeldahl for protein and polarimetry for lactose). IR milk analyzers have tight specifications in terms of reproducibility and accuracy, having a standard deviation of the differences for accuracy (SDD_a) of less than 0.06% and a standard deviation of the differences for reproducibility (SDD_r) of less than 0.02%[12].

Both of these well-established methods predate the development of FTIR spectroscopy, which was a major advance in the field of IR spectroscopy. FTIR spectroscopy is based on interferometry and makes use of a beam-splitter to divide the IR radiation into two beams, where one beam is directed to a fixed mirror and the other beam is directed to a moving mirror (Figure 1.1). As the two beams recombine, they undergo constructive and destructive interference due to the path difference between the two mirrors, yielding an interferogram. Through the use of a fast Fourier transform algorithm, the time domain interferogram can be converted into the wavelength domain and ultimately into a conventional absorbance spectrum[1]. FTIR spectrometers have several advantages over dispersive IR instruments, including a dramatic improvement in the signal-to-noise ratio (S/N) obtained by multiplexing (simultaneous detection of all frequencies), reduction in scan time, higher energy throughput, superior resolution and wavelength accuracy obtained through the use of an internal reference laser. The latter advantage facilitates data manipulations such as spectral subtraction, addition and ratioing with a very high degree of accuracy[13]. The advancement of quantitative FTIR spectroscopy has been greatly assisted by the widespread implementation of increasingly powerful personal computers, which have facilitated the use of sophisticated multivariate analysis methods and software, including classical-least-squares (CLS), inverse-least-squares (ILS) and partial-least-squares (PLS) regression[2].

The renewed interest in IR spectroscopy has also been brought on by the greater versatility of FTIR spectrometers with regard to the sample handling techniques that may be employed. With conventional dispersive IR spectrometers, sample handling options for quantitative analysis were largely restricted to the use of narrow-pathlength transmission cells, which was a major limitation as they are difficult to load, flush and clean. Another drawback is that light scattering effects can make quantitation problematic in samples that are emulsions or dispersions[2]. Sample handling methodologies used in FTIR analysis include a variety of attenuated total reflectance (ATR) accessories (multiple- and single-bounce crystals and fiber optic probes), diffuse reflectance infrared Fourier transform (DRIFT) and photoacoustic spectroscopy (PAS) as well as new designs of conventional transmission flow-through cells[3]. The advantages associated with FTIR spectrometers and the new sample handling technologies available combined with a

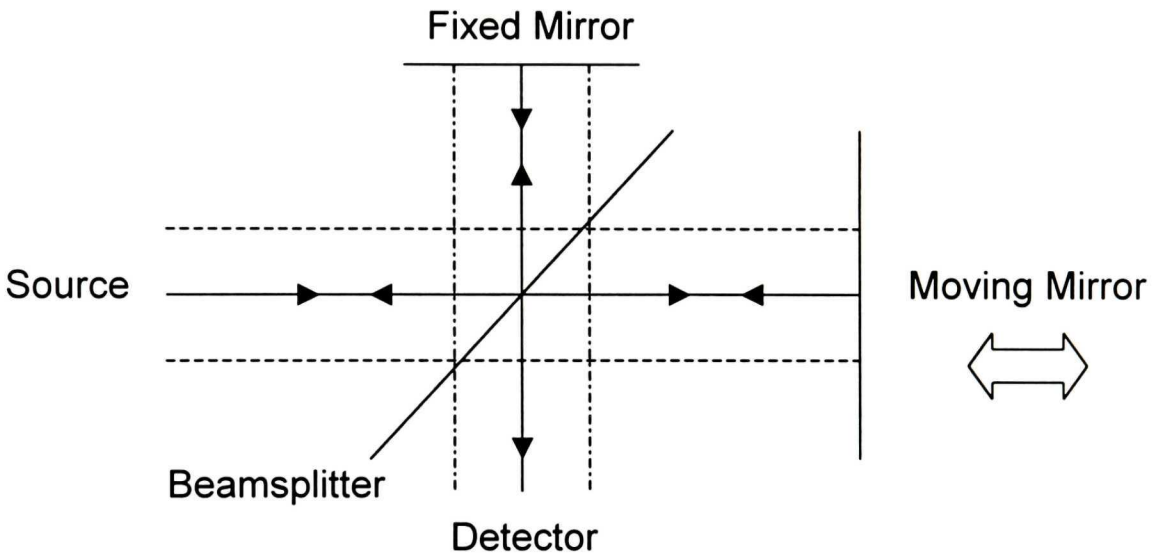

Figure 1.1. Schematic diagram of a Michelson interferometer. The IR radiation from the source is split into two beams by a beamsplitter and directed to the fixed and moving mirror. The two IR beams recombine at the beamsplitter and are directed to the sample and the detector (adapted from reference 2).

range of sophisticated multivariate analysis methods have increased the potential scope of quantitative mid-IR spectroscopy substantially. In the area of food analysis, FTIR spectroscopic methods for milk analysis, using a transmission flow-through cell, and *trans* content determination in fats and oils using a single-bounce ATR (SB-ATR) accessory were implemented as official methods in 1995 and 1999, respectively[14,15]. In addition, FTIR spectroscopic methods for the analysis of fats and oils, juices, alcoholic beverages, wines, jams, syrups, colas, chocolate, coffee, cheeses and meats have been published[16]. However, despite substantial research on analytical applications of FTIR spectroscopy in food analysis, progress has been limited in that only a few protocols have been implemented as routine methods of analysis. One notable example is the analysis of wines, for which a dedicated FTIR analyzer, the WineScan FT 120 (Foss A/S, Denmark), has recently been marketed[17].

1.2. RATIONALE AND OBJECTIVES OF THE RESEARCH

The research described in this thesis was undertaken to investigate SB-ATR/FTIR spectroscopy and 2D correlation spectroscopy in relation to quantitative analysis as these two recently developed techniques were considered to provide means of enhancing the utility of FTIR spectroscopy in food analysis. Following a discussion of the principles of these techniques and the reasons for their potential utility in food analysis in Chapter 2, Chapters 3 and 4 focus on examination of the feasibility of employing SB-ATR/FTIR spectroscopy for the quantitative analysis of aqueous systems, specifically the monitoring of lactose hydrolysis in milk and the analysis of distilled liquors and wines. These systems were chosen as a basis for evaluating the advantages and disadvantages of SB-ATR accessories in quantitative analysis as compared to the more commonly used transmission flow-through cells while also developing new analytical methodologies potentially of practical utility for the food industry. Although milk analysis by IR spectroscopy is a widely utilized AOAC official method[1], the transmission cells used in commercial IR milk analyzers limit their application in the analysis of other dairy products. These cells are assembled with CaF_2 windows because, unlike most IR window materials, CaF_2 is insoluble in water. However, the CaF_2 windows do not transmit a significant amount of IR radiation below 1110 cm^{-1}, thereby eliminating spectral

information important for the analysis of sugars and organic acids. Consequently, IR milk analyzers are not well suited for monitoring the enzymatic hydrolysis of lactose during the production of lactose-free and lactose-reduced milk, as this application requires the determination of low levels of lactose in the presence of its hydrolysis products, glucose and galactose. An SB-ATR accessory equipped with a ZnSe crystal that transmits IR radiation over the entire fingerprint region of the IR spectrum was considered to be a suitable alternative to a transmission cell for the monitoring of lactose hydrolysis, with additional advantages of convenience and simplicity. Thus the development of an SB-ATR/FTIR method for this application and an assessment of its analytical performance were undertaken, as described in Chapter 3 of this thesis. Further evaluation of the analytical performance of SB-ATR/FTIR spectroscopy was undertaken by developing analytical methodology for the analysis of distilled liquors and wines. This research, which is reported in Chapter 4, involved both a direct comparison of SB-ATR/FTIR spectroscopy with FT-NIR and transmission FTIR spectroscopy and the development of a multicomponent analysis for both major and minor constituents in wine to obtain data indicative of both the accuracy and the sensitivity of the SB-ATR technique.

The second aspect of the research described in this thesis concerns the use of generalized 2D correlation spectroscopy in the development of quantitative NIR analytical methods. The objective of this research was to develop an approach that would allow the analyst to take advantage of both the sample-handling versatility of NIR spectroscopy and the detailed information content of mid-IR spectra. Heterospectral 2D correlation spectroscopy (H2D-CS), which correlates data obtained for a set of samples by two different spectroscopic methods, has been extensively used for qualitative NIR band assignments[18,19]. It has also been suggested that H2D-CS be employed in quantitative analysis by NIR spectroscopy for the identification of suitable analytical wavelengths[20]; however, an investigation of this possibility has yet to be reported in the literature. In Chapter 5, the results of the first such investigation, involving a detailed H2D-CS analysis of the SB-ATR/FTIR and FT-NIR spectra of sugar solutions, are reported. This work led to the design and examination of a novel variant of this approach in which data obtained by high-pressure liquid chromatography (HPLC) and SB-ATR/FTIR spectroscopy were subjected to 2D correlation analysis, with the objective of

developing a simple, indirect means of coupling HPLC with FTIR detection. This final aspect of the research undertaken for this thesis is described in Chapter 6. Finally, Chapter 7 presents a summary of contributions to knowledge and general conclusions.

REFERENCES

1. van de Voort, F.R. and Ismail, A.A. (1991). Proximate analysis of foods by mid-FTIR spectroscopy, *Trends Food Sci.Technol.*, 2 (1), 13-17.

2. Ismail, A.A., van de Voort, F.R. and Sedman, J. (1997). Fourier transform infrared spectroscopy: Principles and applications. In: *Instrumental Methods in Food Analysis* (J.R.J. Paré and J.M.R. Bélanger eds., Elsevier, Amsterdam, The Netherlands), 93-139.

3. Wilson, R.H. (1990). Fourier transform mid-infrared spectroscopy for food analysis, *Trends Anal. Chem.*, 9 (4), 127-131.

4. Li-Chan, E.C.Y., Ismail, A.A., Sedman, J. and van de Voort, F.R. (2002) Vibrational spectroscopy of food and food products. In : *Handbook of Vibrational Spectroscopy* (J.M. Chalmers and P.R. Griffiths eds., John Wiley & Sons Ltd., Chichester, England), 3629-3662.

5. McClure, G.L. (1987). Quantitative analysis from the infrared spectrum. In: *Laboratory Methods in Vibrational Spectroscopy,* 3rd ed. (H.A. Willis, J.H. van der Maas and R.G.J. Miller eds., John Wiley & Sons Ltd., New York, NY), 145-199.

6. *Official Methods of Analysis of the Association of Official Analytical Chemists* (1975) 13th ed., AOAC, Arlington, VA, sec. 16.074-16.083.

7. *Official Methods and Recommended Practices of the American Oil Chemists' Society* (1989) 4th ed., American Oil Chemists' Society, Champaign, IL, Method Cd14-61.

8. 1995-1996 Additions and Revisions to the *Official Methods and Recommended Practices of the American Oil Chemists' Society* (1996) 4th ed., American Oil Chemists' Society, Champaign, IL.

9. Biggs, D.A. (1967) Milk analysis with the infrared milk analyzer, *J. Dairy Sci.*, 50 (5), 799-803.

10. Biggs, D.A. (1978) Instrumental infrared estimation of fat, protein, and lactose in milk: Collaborative study, *J. Assoc. Off. Anal. Chem.*, 61 (5), 1015-1023.

11. van de Voort, F.R., Kermasha, S., Smith, J.P., Mills, B.L. and Ng-Kwai-Hang, K.F. (1987) A study of the stability of record of performance milk samples for infrared milk analysis, *J. Dairy Sci.*, 70 (8), 1515-1523.

12. Biggs, D.A. (1979) Performance specifications for infrared milk analysis, *J. Assoc. Off. Anal. Chem.*, 62 (6), 1211-1214.

13. Griffiths, P.R. (1987) Mid-infrared Fourier transform spectrometry. In: *Laboratory Methods in Vibrational Spectroscopy*, 3rd ed. (H.A. Willis, J.H. van der Maas and R.G.J. Miller eds., John Wiley & Sons Ltd., New York, NY), 121-144.

14. *Official Methods of Analysis of the Association of Official Analytical Chemists* (1995) 16th ed., AOAC International, Arlington, VA, sec. 972.16.

15. *Official Methods and Recommended Practices of the American Oil Chemists' Society* (1999) 5th ed., American Oil Chemists' Society, Champaign, IL, Cd 14d-99.

16. Sedman, J., van de Voort, F.R. and Ismail, A.A. (1999) Attenuated total reflectance spectroscopy: Principles and applications in infrared analysis of food. In: *Spectral Methods in Food Analysis* (M.M. Mossoba ed., Marcel Decker Inc., New York, NY), 397-426.

17. Andersen, S.K., Hansen, P.W. and Andersen, H.V. (2002). Vibrational spectroscopy in the analysis of dairy products and wine. In: *Handbook of Vibrational Spectroscopy* (J.M. Chalmers and P.R. Griffiths eds., John Wiley & Sons Ltd., Chichester, England), 1-10.

18. McClure, W.F., Maeda, H., Dong, J., Liu, Y. and Ozaki, Y. (1996). Two-dimensional correlation of Fourier transform near-infrared and Fourier transform Raman spectra I: Mixtures of sugar and protein, *Appl. Spectrosc.*, 50 (4), 467-475.

19. Awichi, A., Tee, E.M., Srikanthan, G. and Zhao, W. (2002). Identification of overlapped near-infrared bands of glucose anomers using two-dimensional near-infrared and middle-infrared correlation spectroscopy, *Appl. Spectrosc.*, 56 (7), 897-901.

20. Barton II, F.E., Himmelsbach, D.S., Duckworth, J.H. and Smith, M.J. (1992). Two-dimensional vibration spectroscopy: Correlation of mid- and near-infrared regions, *Appl. Spectrosc.*, 46 (3), 420-429.

CHAPTER 2

LITERATURE REVIEW

2.1. INTRODUCTION

The work described in this thesis addresses the use of a novel sample handling technique, single-bounce attenuated total reflectance (SB-ATR) spectroscopy, as well as a new data analysis methodology, generalized two-dimensional (2D) correlation spectroscopy, for quantitative applications of Fourier transform infrared (FTIR) spectroscopy. This introduction first reviews sample handling methods used in FTIR spectroscopy that are pertinent to this thesis, including the theory of the transmission cell, attenuated total reflectance (ATR), photoacoustic spectroscopy (PAS) and diffuse reflectance infrared Fourier transform (DRIFT) sample-handling techniques. An overview of the applications of these techniques in quantitative analysis of foods will also be presented with a focus on the theory and all recent applications of SB-ATR spectroscopy. The second part consists of a review of the theory and applications of generalized 2D correlation spectroscopy. This review will include how to interpret 2D correlation synchronous and asynchronous maps, the spectral pretreatment methods commonly used in 2D correlation spectroscopy for quantitative applications and an introduction to heterospectral 2D correlation spectroscopy (H2D-CS).

2.2. SAMPLE HANDLING TECHNIQUES IN FTIR SPECTROSCOPY

2.2.1. Transmission FTIR Spectroscopy

2.2.1.1. Theory

The transmission mode is the most common and oldest mode of infrared (IR) sample analysis where the sample is placed in the optical path of the IR beam in a cell having a fixed pathlength[1]. The amount of light transmitted is inversely proportional to the concentration of the sample and the sample thickness, which can vary from meters for gas samples to microns for liquid samples[2]. The intensity of the incident beam is compared to the intensity transmitted by the sample:

$$I = I_o * 10^{-abc} \quad [2.1]$$

where, I_o is the intensity of the incident beam, a is the molar absorptivity, b is the path length and c is the concentration of the analyte. However, in addition to the light being absorbed by the sample, some light will be reflected and/or scattered, which may affect the measured intensity at the detector[3].

For aqueous samples longer pathlengths are undesirable because beyond a certain thickness, water absorbs all the IR radiation and, therefore, aqueous solutions are typically measured at small pathlengths of 0.015 to 0.040 mm (15-40 μm). A major limitation for emulsions and solids is that light scattering effects are a problem when particle dimensions are comparable to or exceed the wavelength of mid-IR radiation[4] and as such, particles must be reduced to < 3 μm prior to analysis. A further limitation which may be encountered is fringing, caused by the difference between the refractive index of the IR window material and that of the air space between them, which can cause underlying interferences throughout the spectral region[3]. Nevertheless, despite these apparent disadvantages, transmission still remains the preferred method for sample handling in FTIR spectroscopy.

Transmission cells can be demountable or sealed and Figure 2.1 presents an FTIR transmission flow through cell. Sealed transmission cells are better for quantitative applications because a fixed and stable pathlength is required to obtain reproducible results. If the sample is too viscous to inject or pump through a sealed cell an internal standard with a distinct absorption can be introduced into the sample to detect pathlength variations[4]. For solid samples, the sample can be ground to a particle size that is small enough to avoid light scattering effects and diluted with IR transparent material such as KBr, KCl or NaCl and then pressed to form a pellet and placed in the optical path of the IR instrument[1]. Common IR transparent materials tend to be highly water-soluble and are not suitable for the direct analysis of aqueous samples. An alternative procedure for analyzing samples containing moisture is to make a liquid dispersion using oils, such as mineral oil (Nujol) or paraffin oil. The emulsified sample is mixed into the liquid and squeezed between IR transparent plates. Both the pellet method and the dispersion method have the disadvantage of destroying the sample[3]. Therefore, for food applications, sampling by transmission mode employing FTIR spectroscopy has been limited to the analysis of liquids or solids dissolved in an aprotic solvent.

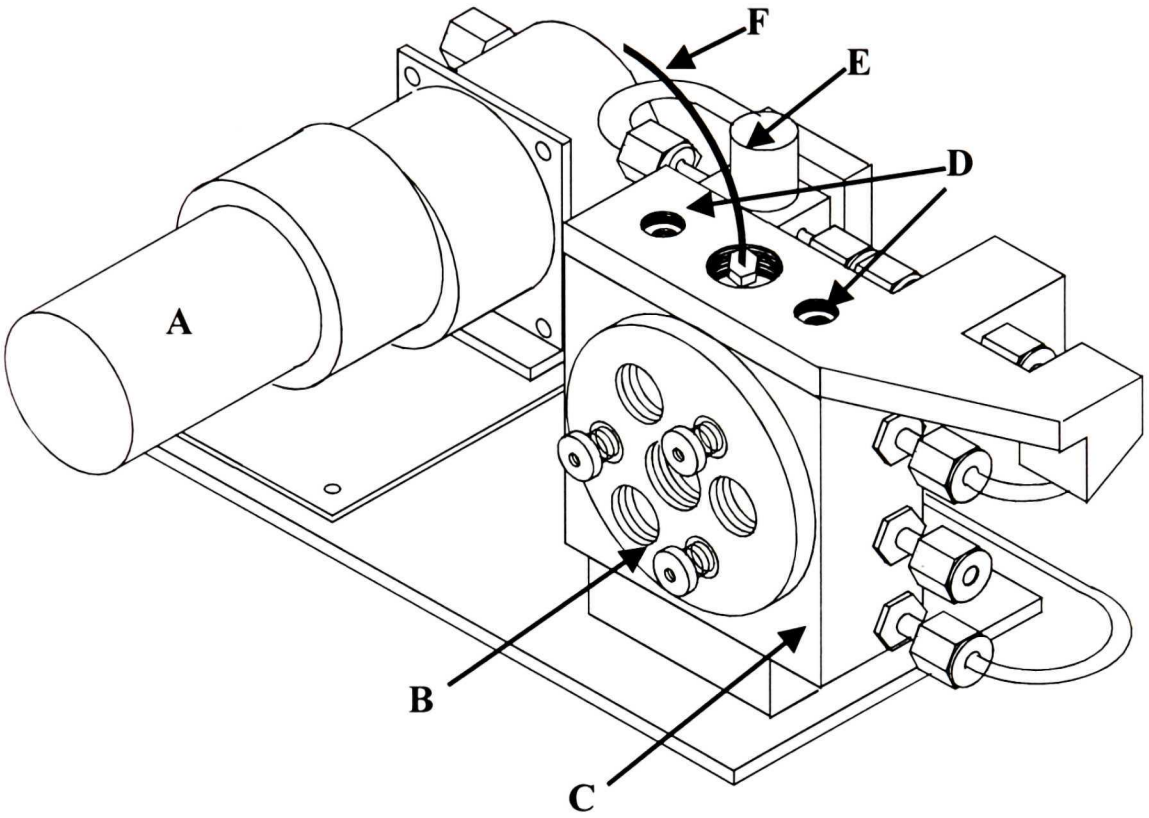

Figure 2.1. Schematic diagram of a transmission flow through cell: (A) micropump, (B) demountable cell insert (transmission cell), (C) cell block, (D) heat cartridges, (E) solenoid valve, (F) thermocouple. The accessory slides horizontally in order for the cell to move in and out of the path of the beam.

2.2.1.2. Applications

a) Milk Analysis, Wine Analysis and Dairy Products

Milk analysis by FTIR spectroscopy is an official method of the Association of Official Analytical Chemists (AOAC) for the determination of lactose, protein, fat and total solids in milk[5]. Other non-official methods have been developed for casein[6], water[7] and urea[8] determination. Typically, a 37 μm CaF_2 cell is used, and milk samples are heated to 40°C and homogenized prior to analysis. This allows the fat globules to be small enough in size and dispersed in the sample in order to avoid light scattering effects[9]. In high volume automated instruments (100-500 samples per hour), the transmission flow through cell is flushed with the next sample at extremely high pressure (150-200 kPa) and velocity (30 m/s), with the cell kept at a constant temperature, within ±0.1°C, to obtain reliable, stable and accurate measurements[10]. The pressure is maintained in the system during the whole analysis to avoid air bubbles forming in the cell. In the literature, other dairy products have been analyzed by transmission FTIR spectroscopy. A similar method to milk analysis was also developed for the determination of sucrose, lactose, total solids, and fat in chocolate milk by centrifuging out the cocoa particles prior to analysis[11]. Chen and Irudayaraj developed a cheese analysis method for fat and protein determination by using a microtome to slice the cheese samples to a thickness of 4, 8 or 16 μm[12]. The samples were attached to the surface of a silver chloride crystal for subsequent analysis by transmission FTIR spectroscopy. More recently, wine analysis has developed as a prominent FTIR spectroscopic application whereby typically 10 parameters or more are analyzed using instrumentation based on the FTIR milk analyzer described above[10].

b) Trans Determination and Edible Oil Analysis

In the original IR *trans* analysis method, samples were dissolved in carbon disulfide before recording their spectra in a fixed pathlength transmission cell[13]. This dilution procedure was necessary because the analysis of oils in their neat forms would require a cell pathlength of 0.01 mm or less due to the high absorptivity of the major absorption bands. With the development of FTIR spectrometers, however, analysis of oils in their neat forms is possible due to the higher optical throughput and linearity of the

deuterated triglycine sulfate (DTGS) detectors, commonly used in these type of instruments, which allows for somewhat longer pathlengths to be used (10-100 μm). In 1989, Sleeter and Matlock developed the first FTIR spectroscopic method for *trans* isomer determination in fats and oils measured in their neat forms, as neat methyl esters, employing peak area and peak height calibrations[14]. In 1992, Ulberth and Haider made a modification to Sleeter and Matlock's method by using spectral subtraction rather than peak area[15] whereby the spectrum of a *trans* fatty acid-free soy oil was subtracted from the spectra of all samples and calibration standards and a calibration developed based on the subtracted spectra. In addition, a similar method was developed for *trans* fatty acid determination in milk fat by subtracting the milk fat samples from methyl elaidate[16]. To evaluate the accuracy of the *trans* FTIR data, Ratnayake and Pelletier compared the reference method of the combined procedure of silver nitrate thin-layer chromatography and capillary gas chromatography (GC) with the FTIR method. It was found that values obtained by FTIR spectroscopy were ~16% lower[17], where the *trans* content in fats and oils is defined as % *trans* relative to a value of 100% trielaidin[4]. However, when the FTIR method is calibrated using fatty acid methyl esters (FAME) of partially hydrogenated vegetable oil instead of methyl elaidate, the calibration standard stated in the official method, the average difference between the methods was only 3% and consequently, this calibration approach was recommended.

The McGill IR group has done extensive work in edible oil analysis, typically using a 25–100 μm NaCl, KCl or CaF_2 demountable transmission flow through cell that is heated to 80°C to avoid fat crystallization during analysis[18]. Two *trans* analysis methods were developed using this type of sample handling accessory, both of which analyze the oils in their neat forms, without conversion of the oils into FAMEs. The first one is a procedure based on peak height measurements of spectra generated by ratioing the single beam spectrum of the sample against the single beam spectrum of a *trans*-free reference oil[19]. The other method does not use a peak height or ratioing procedure, but rather employs a partial-least-squares (PLS) calibration and prediction directly on the spectra of the oil samples[20]. De Greyt *et al.* employed the ratioing procedure described in the first method stated above for the determination of low levels of *trans* fatty acids in refined oils using a separate calibration curve for each type of oil[21]. Alonso *et al.* also

developed a method for determination of *trans* unsaturation in Spanish shortenings, without requiring to convert them into FAMEs, but by calibrating on pre-analyzed partially hydrogenated oil samples rather than trielaidin[22].

Other oil analysis methods developed by the McGill IR group using the same sample handling accessory include methods for *cis* content[20], free fatty acid determination[23], solid fat index[24], iodine value (IV)[25], saponification number (SN)[25], anisidine value (AV)[26], aldehydes[26] and peroxide value (PV)[27]. The PV method is based on a reaction of triphenylphosphine with the hydroperoxides in the oils to produce triphenylphosphine oxide, which gives a strongly absorbing band at 542 cm^{-1} used for PV quantitation. Several other methods were developed for edible oil analysis employing transmission FTIR spectroscopy and are listed in Table 2.1.

c) Total Fat Determination

Several methods have been developed for total fat determination in food products employing transmission FTIR spectroscopy. The first one, developed by Cronin and McKenzie, consisted of extracting fat from several food products with a chloroform methanol (2:1) solvent[39]. Subsequently, fat content was measured using the band area ratio of the ester carbonyl and that of an internal standard, methyl silate. In 1993, van de Voort *et al.* developed a method for total fat and moisture determination in mayonnaise and peanut butter using propanol as the extraction solvent and, subsequently, analyzing the extract in a 100 μm CaF_2 transmission cell[40]. Total fat and protein determination in meat by FTIR spectroscopy was done on meat samples, prepared by suspension in a 0.1N NaOH solution at 67°C and homogenized using a high-pressure valve homogenizer, prior to injection into a 37 μm CaF_2 heated (65°C) flow-through cell[41].

d) Beverages

Aside from milk and wine, other beverages have been analyzed by transmission FTIR spectroscopy. Among the first of these applications developed was for ethanol determination in alcoholic beverages and various publications describe methods for ethanol determination in distilled liquors, wines and beers using orthogonal or derivative functions to correct for water absorption[42-44] with dilution often required for beverages

Table 2.1: Edible oil analysis methods developed employing transmission FTIR spectroscopy.

Application	Reference	Description
Phospholipids	Nzai and Proctor[28]	Determination of phospholipids in vegetable oils by extracting and isolating phospholipids and using a microsyringe to load the extract into a salt plate cell.
Saturated, monounsaturated polyunsaturated	Guillen and Cabo[29]	Method to predict saturated, monounsaturated and polyunsaturated acyl groups in lards and edible oils by recording the FTIR spectrum of the film of the pure oil or lard between two KBr disks.
Moisture	Man and Mirghani[30]	Crude palm oils
PV	Setiowaty *et al.*[31]	Thermally oxidized palm olein
PV	Moh *et al.*[32]	Crude palm oil products
Free fatty acids	Man and Setiowaty[33]	Palm olein
AV	Man and Setiowaty[34]	Thermally oxidized palm olein
IV	Hendl *et al.*[35]	Vegetable oils, employing first derivative spectra.
Polyunsaturated fatty acids	Moya Moreno *et al.*[36]	Heating of culinary oils. Calibration equation based on different concentrations of methyl linoleate spiked into oil standards.
Oxidative stability	Guillen and Cabo[37]	Spectra of edible oils recorded in duplicate between two KBr disks.
Free fatty acids	Verleyen *et al.*[38]	Vegetable oils using a 25 μm transmission cell heated to 75°C.

having ethanol contents of >15% (v/v)[43]. Another approach used for ethanol and methanol determination in alcoholic beverages has been vapour-phase analysis, where the alcohols are volatilized inside a Pyrex glass reactor and subsequently transported into a 3.2 m long-path IR gas ZnSe transmission cell with a nitrogen carrier gas and measured[45]. In 1997, Sinnaeve *et al.* analyzed apple juice by transmission FTIR spectroscopy and successfully quantified malic acid, total sugars, glucose, fructose, sucrose and specific gravity using a 16 μm temperature stabilized transmission cell[46].

More recently, extensive work has been carried out on flow injection and sequential injection transmission FTIR analysis of beverages. Flow injection analysis involves carrying out an automated flow-through step prior to acquisition of the FTIR spectra. The first application involving IR detection coupled with flow injection analysis was investigated by Curran and Collier in the determination of an isocyanate moiety[47]. In food analysis, flow injection coupled with transmission FTIR spectroscopy was used in the determination of sucrose in fruit juices (orange juice, apple juice and sports drink)[48], caffeine in soft drinks[49] and caffeine in roasted and instant coffee samples[50]. In the case of fruit juice analysis, acetate buffer was used as the carrier solvent and samples were passed through an enzyme reactor containing β-fructosidase prior to FTIR spectral acquisition. For coffee analysis, caffeine was extracted by passing chloroform directly through a cartridge containing the sample prior to spectral acquisition and in the case of soft drinks, caffeine was extracted by passing the samples through a solid phase extraction column (C_{18}), again using chloroform as the eluent. In other studies caffeine quantitation in coffee and tea was carried out directly on chloroform extracts[51,52], without employing automated flow injection analysis. In other work, Ayora-Cañada used flow injection analysis/FTIR spectroscopy to quantify malic acid, tartaric acid and citric acid in juices and soft drinks using pH modulation to eliminate matrix effects[53]. Flow injection analysis was also employed for the determination of PV in edible oils on-line, without the need for manual sample manipulation[54].

Sequential injection is a form of flow injection analysis, which allows the automated and simultaneous mixing of calibration standards prior to spectral acquisition by FTIR spectroscopy. This allows the automated generation of calibration standards for multivariate calibration with different components and concentration values without

having to prepare them manually, which may be subject to human error[55]. Sequential injection FTIR spectrometry in food analysis has been applied to the determination of ethanol, glycerol, sugars and organic acids in wines[56], carbohydrates in beer[57] and sugars and organic acids in juices and soft drinks[55,58]. In the analysis of organic acids in juices and soft drinks, the sample was passed through a solid phase extraction column prior to FTIR analysis in order to separate the organic acids from the sugars[58].

e) Disposable IR Cards

The McGill IR group has proposed the utility of commercially available disposable polyethylene IR cards in the analysis of PV and *trans* fatty acid content in fats, margarine and oils[59,60] as the cards have the ability to absorb non-polar liquids into the polymer matrix by capillary action. In the case of PV determination, the cards were impregnated with the triphenylphosphine reagent so that the reaction between the hydroperoxides and the reagent could take place directly on the card. It was found that a peak height measurement of the triphenylphosphine oxide band at 542 cm^{-1}, as normally done with the transmission cell method, was not feasible with the cards because of fringing; however, the use of PLS regression allowed this interference to be compensated for. It was found that the card method could perform as well as conventional IR flow through cell methods in terms of analytical accuracy and precision[59]. In the case of *trans* determination in fats and margarine, all samples were melted by warming in a microwave prior to analysis. It was observed that the IR cards slowed the re-crystallization of fat, which allowed one to record the liquid state spectra of even relatively hard fats at room temperature. PLS calibrations were able to compensate for fringing in the calibration spectral region and the card results were comparable to the IR transmission cell method and within 0.8% of the official GC method. For margarine, results were also comparable to the transmission cell method with a reproducibility of within 1%[60]. Overall the disposable cards appear to be a simple and viable sample handling method for the quantitative analysis of fats and oils by transmission FTIR spectroscopy and also have the additional advantage of being archivable, however, the manufacture of these cards has been discontinued[61].

2.2.1.3. Conclusion

Transmission FTIR spectroscopy has been successful in the analysis of some liquid food products, namely, milk, oils and alcoholic beverages, but for viscous, solid and semi-solid food products, only methods involving lengthy extraction procedures and extensive sample preparation have been developed. Many of the methods developed have to deal with one or more of the inherent limitations of transmission FTIR spectroscopy, e.g., light scattering effects, fringing, particle size, cell pathlength and window material limitations. ATR spectroscopy provides a potential avenue by which some of these limitations can be addressed, especially in relation to aqueous systems.

2.2.2. Total Internal Reflection/ATR Spectroscopy

2.2.2.1. Theory

Total internal reflection spectroscopy, also referred to as ATR, was developed in the 1960's[2] and is based on total internal reflection of the IR beam in a high refractive index internal reflection element (IRE) or crystal. Internal reflection occurs when the angle of incidence of the IR light is above the critical angle of the IRE (Figure 2.2) and gives rise to an evanescent wave of IR light that emerges from the surface of the IRE material at each point of internal reflection. Portions of the evanescent wave are absorbed if a sample is placed on top of the IRE material, and the resulting attenuation of the evanescent wave produces an IR spectrum of the sample[4]. The intensity of the evanescent wave decays as it propagates away from the surface of the IRE material and the distance at which the intensity decays to 1/e of its value at the surface is defined as its depth of penetration[4]. As compared to the transmission method, the effective pathlength of an ATR accessory is usually very short and depends on a number of parameters including the refractive index of the IRE material, the refractive index of the sample material and the wavelength at which the sample is absorbing. The pathlength is calculated by multiplying the number of internal reflections by the depth of penetration (d_p), the latter determined by the following equation,

$$d_p = \lambda/\{2\pi n_1[\sin^2(\theta) - (n_2/n_1)^2]^{1/2}\} \quad [2.2]$$

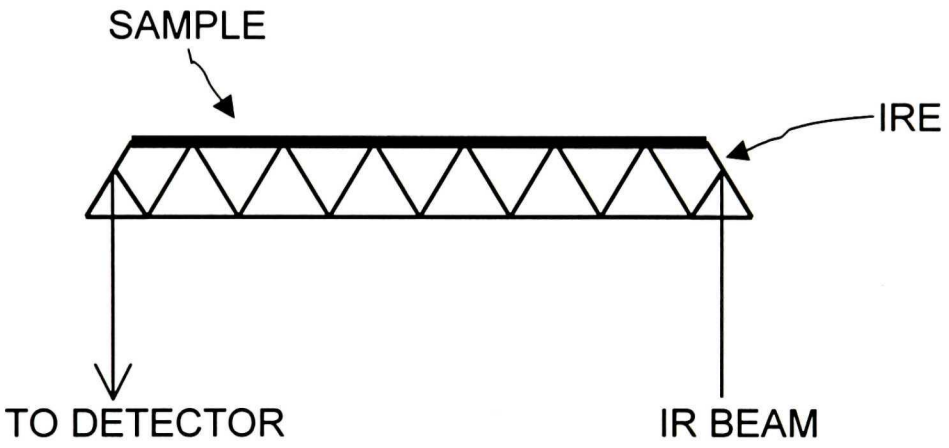

Figure 2.2. Schematic of a horizontal multiple-bounce attenuated total reflectance accessory (adapted from reference 62)

where λ is the wavelength of IR radiation, n_1 is the refractive index of the IRE material, n_2 is the refractive index of the sample and θ is the angle of which the IR radiation strikes the IRE interface[1]. Due to the variation of the depth of penetration in an ATR accessory, an ATR spectrum will differ from a conventional transmission spectrum in that the relative intensities of the bands will be different, with bands at the low frequency end of the spectrum being more intense. In addition, for the same reason, broad bands exhibit a noticeable broadening on the long wavelength side and consequently are shifted slightly to longer wavelengths[62].

The ATR method has several advantages over conventional transmission methods, such as the ability to adjust the pathlength by adjusting the angle of incidence or the number of internal reflections. The ATR method is particularly advantageous for analyzing aqueous solutions, the most obvious benefit being that it allows the sample to simply be applied onto the surface of the IRE material, rather than passing the sample through a transmission cell with a volume typically below <50 μL[62]. In addition, the short effective pathlength of the ATR method ensures that highly absorbing water bands are on scale, giving access to the entire spectral information of the sample[63]. IRE materials generally have a high refractive index so as to obtain a suitable critical angle necessary for internal reflection. The most common IRE materials are germanium and ZnSe[4], which are water insoluble and transmit IR radiation over the entire mid-IR absorption region.

Despite the advantages of the ATR method outlined above, there are still several limitations, the most important one being its short effective pathlength, which, while advantageous in some situations, can be disadvantageous when sensitivity is required. The maximum effective pathlength of most commercial ATR accessories is only in the order of 50 μm at 1000 cm^{-1} and 12.5 μm at 4000 cm^{-1} [62]. Since the depth of penetration is on the micrometer scale, only the spectrum of the surface of the sample will be recorded, requiring that the sample be homogeneous on this scale. In addition, any surface contamination of the IRE material will affect the spectrum of the sample, such as the migration and adherence of hydrophobic substances to the surface of some IRE materials resulting in cross contamination from the previous sample[18].

ATR accessories come in variety of forms including multiple-bounce ATR (MB-ATR) crystals, SB-ATR crystals, cylindrical internal reflectance cells for liquid

evaluation (CIRCLE) and ATR fiber-optic probes. MB-ATR accessories are the most common and consist of IREs that fit horizontally into an IR optical compartment. Commonly, the IRE sample application surface is located above the optical compartment so that the sample can be analyzed without disrupting the instrument purge. The samples are simply poured or spread on top of the crystal and an IR spectrum is recorded. It was found that MB-ATR accessories suffer a couple of drawbacks, the first being that it is difficult to obtain reproducible spectra of powdered and solid samples, where intimate contact between the sample and the IRE is required. Application of pressure onto the sample can be helpful; however, due to the size of the MB-ATR crystal it is difficult to obtain reproducible results required for quantitative analysis[3]. Another drawback is that it is difficult to obtain adequate temperature control of MB-ATR accessories, causing significant pathlength variability since the depth of penetration is dependent on the refractive indices of the IRE material and sample, which in turn are dependent on the temperature. Hence at first glance MB-ATR accessories appear to provide convenience and simplicity in terms of acquiring spectra, but in terms of quantitative applications, many of their potential benefits are largely lost.

In the last decade mid-IR ATR fiber-optic probes have been developed (Figure 2.3) which consist of two IR transmitting fiber-optic cables, about 1 to 10 m in length coupled to an IRE at one end. The IR beam is launched into one of the fiber optic cables and travels until it reaches the IRE immersed in the sample. The IR beam then propagates back through the other cable to reach the detector[64]. This system requires using a focusing cone to input the IR radiation into the input cable and a beam-expanding cone at the end of the return cable expands the IR beam before it reaches the detector[62]. The advantage of ATR fiber-optic probes is that the probe can be brought to the sample rather than the sample to the spectrometer, allowing in situ monitoring of production processes and rapid analysis of bulk materials[65]. However, the fiber optic probes suffer from the disadvantage that most commonly used fiber optic materials, such as silica or fluoride glass fibers, do not transmit mid-IR radiation below 2000 cm^{-1} [65]. Chalcogenide glass fibers have been successful in transmitting IR radiation to lower wavenumbers (down to 1000 cm^{-1}); however, poor optical throughput due to the attenuation that occurs in the cables and the inefficiency of coupling the IR beam to the chalcogenide fibers results in a

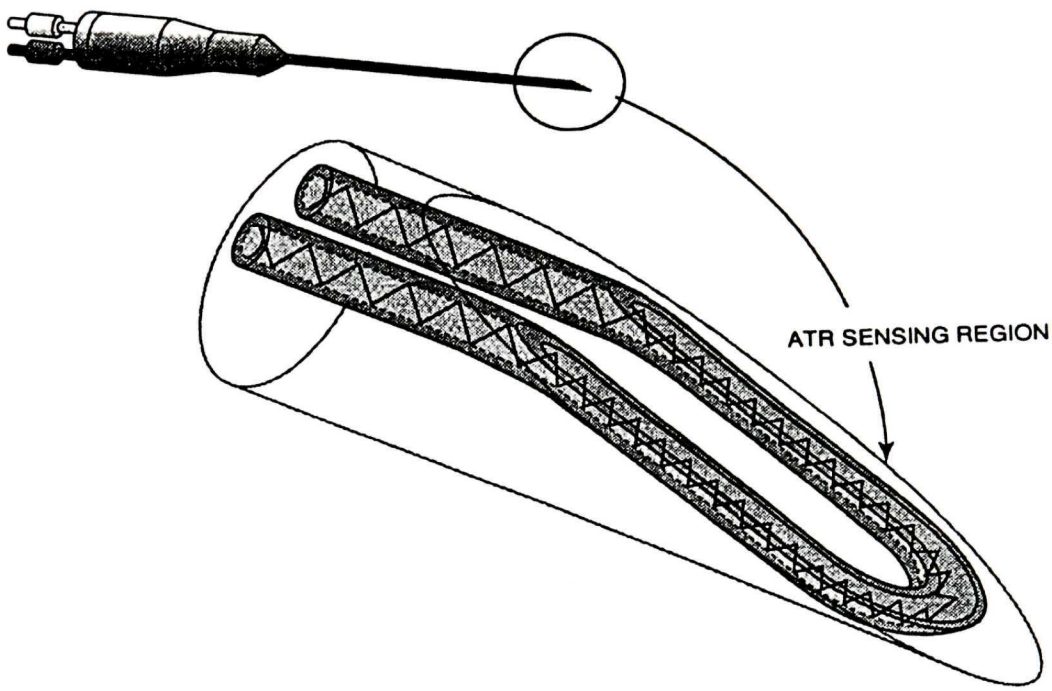

Figure 2.3. Schematic drawing of an ATR fiber-optic probe.

decreased signal-to-noise ratio (S/N) and analytical sensitivity[66].

SB-ATR, also known as single-reflection or single-pass ATR, has been available as long as the MB-ATR accessory[67] and its basic characteristics are illustrated in Figure 2.4. The improved S/N of spectrometers and optical design of SB-ATR accessories over the last 10 years have renewed interest in this accessory for quantitative analysis. The advantages of a single-bounce IRE includes very small sample size, ease of sample handling and cleaning of the crystal and, for solids analysis, low required clamping force[68]. Because of its small surface area, optical contact between the sample and the crystal is almost 100% for SB-ATR accessories, much higher than for MB-ATR accessories. Perhaps the most noteworthy reason for the recent interest in SB-ATR accessories is their novel optical design (Figure 2.4), which offers high optical throughput and sensitivity[69]. This is achieved by a single lens element that uses refraction and internal reflections to focus an image of the IR source onto the sample surface and re-focuses the image of the reflected light onto the spectrometer detector. This innovation has the overall effect of increasing the proportion of the IR energy interacting with the sample, which is ultimately used to produce the IR spectrum. In addition, by adding anti-reflection coatings to the entrance and exit facets of the ATR element, energy losses can be minimized[68]. Overall the SB-ATR accessory does not suffer from some of the common drawbacks of MB-ATR accessories, such as pathlength variability due to inadequate temperature control and crystal surface coverage, because of its very small surface area and optical design, making this accessory very promising for quantitative applications by FTIR spectroscopy.

2.2.2.2. Applications

a) Aqueous Systems

Although food applications using ATR spectroscopy were investigated soon after its development in the late 1960's[67], most of these applications were developed after low cost bench FTIR spectrometers were available on the market[62]. The most successful application of ATR/FTIR spectroscopy in quantitative food analysis is in the analysis of sugars in beverages, owing to its shorter effective pathlength and its ability to transmit IR

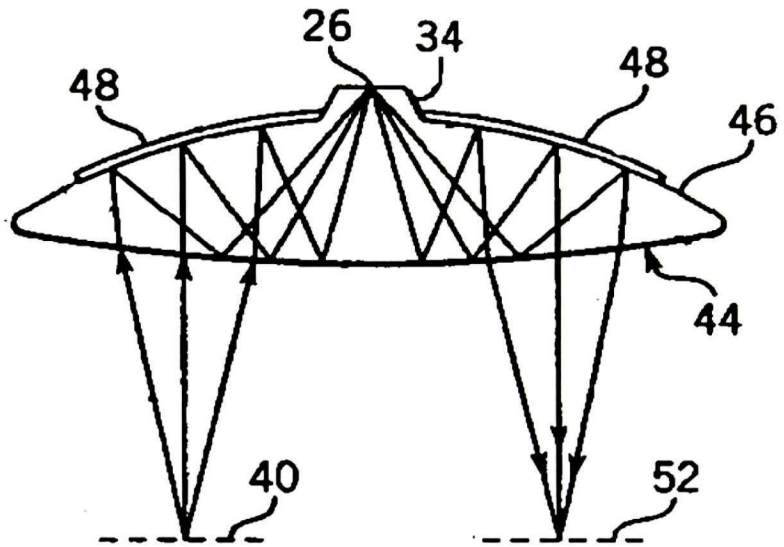

Figure 2.4. Depiction of the IRE of a SB-ATR accessory. Light from a focused image of the IR source at the image plane, 40, positioned beneath the left side of the IRE is focused at the sample surface, 26, and reflected light from the sample surface is focused again at image plane 52 positioned beneath the right side of the IRE. The single lens element IRE is defined by boundaries 26, 34, 46, 48 and 44 and is made up of an optically transparent material, typically ZnSe. Part of the surface of the IRE, 48, is coated with reflective material, such as aluminum. (adapted from reference 68)

radiation below 1000 cm^{-1}, a requirement for sugar analysis. One of the first reported studies was for the analysis of glucose in fruit juices and ethanol in alcoholic beverages employing a ZnSe ATR cell[70]. Absorption intensities at 1046 cm^{-1} and 1033 cm^{-1} were used for the quantitation of ethanol and glucose, respectively. Table 2.2 lists subsequent studies carried out on aqueous systems of sugars by ATR/FTIR spectroscopy. ATR methods have also been developed for other types of aqueous systems such as an MB-ATR method for the quantitation of vitamins B1, B2, B6 and niacin in glucose in aqueous solution. Quantitation of vitamins B2 and B6 was poor as it was difficult for PLS to extract spectral information for those components due to heavy overlapping of the bands in the spectral matrix[79]. A rapid ATR/FTIR method was also developed for the determination of caffeine in soft drinks employing a PLS calibration based on the CH stretching region (2800-3000 cm^{-1}) [80]. This method had the advantage of avoiding the extraction procedures required in alternate methods such as those employed in flow injection analysis and allowed caffeine quantitation in soft drinks at levels as low as 0.5 mg/100 mL. However, the values for caffeine obtained using this method were slightly higher when compared to the conventional ultraviolet (UV) spectrophotometric method.

The use of ATR fiber optic probes in the quantitative analysis of aqueous food systems has also been investigated by Kemsley *et al.* for the quantitation of alcohol in liqueurs[65]. Good quality spectra were obtained and calibrations could be developed employing the CH stretching region. Another study was conducted for the quantitative analysis of glucose, fructose and sucrose in sugar solutions using a sapphire fiber optic ATR accessory, also using the CH stretching region. The root mean square errors were calculated for an internal cross-validation using principal component regression (PCR) of gravimetrically prepared sugar solutions and good agreement was found between actual and predicted values, demonstrating the potential utility of fiber optics in process monitoring[64].

b) Syrups and Semi-Solids

The ATR method is particularly useful for viscous samples, such as syrups, that cannot be pumped through an IR flow through cell having a fixed pathlength. The first ATR/FTIR study of syrups addressed the determination of dextrose equivalent and dry

Table 2.2: Analysis of aqueous systems of sugars by ATR/FTIR spectroscopy.

Application	Reference	Description
Sugar cane juice	Cadet *et al.*[71]	Determination of sucrose in sugar cane juice employing PCR
Sugar cane juice	Cadet and Offman[72]	Determination of sucrose in sugar cane juice employing PCR. Results found to be more accurate than polarimetry.
Sugar cane juice	Cadet *et al.*[73]	Determination of sucrose, glucose, fructose, total sugars and reducing sugars in sugar cane juice employing PCR.
Sugar cane juice	Cadet[74]	Determination of sucrose, glucose, fructose, total sugars and reducing sugars in sugar cane juice employing PCR.
Sugar solutions and soft drinks	Kemsley *et al.*[75]	Determination of glucose, fructose and sucrose in sugar solutions employing a ZnSe CIRCLE™ cell. The calibration developed using ILS[a] performed better than CLS[a] and good agreement with reference HPLC[a] values was obtained.
Starch hydrolysis	Bellon-Maurel *et al.*[76]	Determination of glucose, maltose, maltotriose and maltodextrins employing PLS. Results met industrial specifications.
Juices and soft drinks	Rambla *et al.*[77]	Determination of sucrose, glucose, fructose and total sugar in juices (apple, orange and grape) and soft drinks employing PLS and first derivative to correct for baseline offset.
Juices and soft drinks	Guarrigues *et al.*[78]	Comparison of a ZnSe CIRCLE™ cell and an MB-ATR accessory in the determination of sugars in juices and soft drinks. It was found that the MB-ATR accessory had three times the analytical sensitivity of CIRCLE™ cells.

[a]abbreviations: Inverse-least-squares (ILS), classical-least-squares (CLS), high-pressure liquid chromatography (HPLC)

substance during on-line monitoring of the conversion of corn starch to corn syrup[81]. A subsequent study employed ATR/FTIR spectroscopy to determine dry substance (glucose, maltose and fructose) in glucose syrups after sample dilution (1 g/2 mL)[82] using a PLS calibration based on aqueous mixtures of glucose, fructose, maltose and sucrose from which the dry substance components could be determined with a precision of 3-5% (w/v). In another study, assessment of ATR fiber optic probes, using chalcogenide fibers, was investigated by Dimitri for the quantification of maltose, fructose, glucose, sucrose, water and total sugar in chocolate syrups using PLS regression[66].

Determination of fruit content and detection of adulteration in strawberry jam by ATR/FTIR spectroscopy was investigated by Wilson *et al.*[83], but the method was limited by water absorptions overlapping the 1725 cm^{-1} band used for fruit quantitation. In a later study, 36 jam samples were analyzed by ATR spectroscopy to classify jams according to their fruit content as "strawberry" or "nonstrawberry" [84] based and a PLS calibration correctly assigning 91% of the samples. A similar study was carried out on over 1000 fruit puree samples[85], whereby all the spectra were baseline corrected and area normalized prior to analysis to make spectra recorded with different IREs comparable. A PLS model was employed to detect adulterants in raspberry purees and to classify them based on whether they are raspberry or nonraspberry samples. The model correctly identified 95% of the purees and detected adulteration with sucrose at a level of 4% (w/w) and adulteration with apple and plum purees at a level of 20% (w/w). Other studies involving the detection of inverted cane sugar adulteration in honey and beet and cane sugar adulteration in maple syrups was also carried out using ATR/FTIR spectroscopy and PLS regression[86,87].

c) Solids

Several ATR studies were carried out on powders, but unlike aqueous and viscous samples, solid samples are difficult to analyze directly, without a dissolution step. The first such investigation using ATR/FTIR spectroscopy was carried out on protein and starch mixtures[88] where samples were prepared by mixing dry gluten and starch and casein and starch (dry mixtures) and then subsequently adding a gram of water per gram of sample to produce wet mixtures. The consistency of the samples varied from a moist

powder at high starch content to an elastic mass at high gluten content and the samples were spread evenly on the ATR crystal to ensure uniform coverage and application of a constant amount of pressure. Poor reproducibility was obtained, especially for the casein/starch mixtures owing to the large particle size of casein. In 1993, Dupuy *et al.* investigated quantitative analysis of sugar powders (glucose, fructose, sucrose) by ATR spectroscopy by impregnating the powders with an organic solvent (acetone), to increase optical contact after evaporation[89]. After carrying out a PLS calibration on the recorded spectra, the relative standard deviations (RSD) of the standard error of prediction (SEP) of sucrose, glucose and fructose were found to be 3.2%, 6.2% and 1.7% respectively[89].

Detection of adulterants and classification experiments have also been carried out on solid food products using ATR/FTIR spectroscopy. Discrimination of *Arabica* and *Robusta* instant coffees was carried out using principal component analysis (PCA) and linear discriminant analysis (LDA) of the principal component scores and resulted in correct classification of the coffee samples[90]. The samples were dissolved in distilled water at 50°C at a concentration of 30% (w/v) and the ATR/FTIR spectra recorded immediately upon application of the solution to the ATR crystal to avoid settling of the small insoluble fraction associated with the powders. Detection of adulteration (glucose, fructose and xylose) in instant coffees was also carried out using PCA and LDA[91] using the same procedure used for instant coffee classification, with 98% successful classification achieved. The carbohydrate profile was also successfully quantified using PLS. A study of ATR spectra of different meats using PCA and PLS has also been undertaken[92] whereby the meat samples were minced to generate more reproducible ATR spectra. Between samples, the ATR crystal was cleaned with 2% Triton X-100 solution, with the spectra baseline corrected and mean area normalized prior to analysis. It was reported that minced chicken, pork and turkey meats as well as fresh and frozen-thawed samples could be distinguished based on their characteristic ATR spectra. For quantitative analysis, PLS calibrations were derived for meat mixtures with standard deviation of the residuals being in the order of 13.8 and 14.8% (w/w) for pork and turkey, respectively.

d) Dairy and Confectionery Products

Milk is an emulsion containing fat globules of various sizes, which has presented a challenge for ATR/FTIR analysis of this product, which in transmission FTIR spectroscopy is overcome by on-line homogenization. The effect of fat globules in ATR/FTIR quantitative analysis was investigated by Kemsley *et al.* by examining the effect of fat globule size of cream on ATR/FTIR measurements[93]. A ZnSe ATR crystal was used and calibrated using sixteen cream samples with fat concentrations ranging between 0 and 48% (v/v), all ratioed against a water background spectrum. A plot of absorbance of the peak at 1744 cm^{-1} versus fat content was found to be non-linear and as a result, the author proposed using a non-linear calibration curve for samples having globules > 1 μm. In 1995, McQueen *et al.* assessed the feasibility of employing ATR/FTIR spectroscopy for protein, fat and moisture determination in 24 pre-analyzed cheese samples using PLS regression[94]. Cheese samples are particularly difficult to handle because they are inhomogeneous with respect to fat, with the diameter of fat globules varying on the order of several microns. Even after taking precautions of sampling from the center of the cheese and spreading the sample over the whole ATR crystal surface and carefully cleaning with 2% Triton X-100 solution, large variations in the signal strengths of the ATR/FTIR spectra were observed. This was attributed to the fact that some of the fat globules were of the same order of magnitude as the depth of penetration, giving poor PLS results for fat and protein with a correlation coefficient (R) of only 0.78 and 0.82, respectively. Moisture gave somewhat better results with an R value of 0.93 and the author concluded that analysis of cheeses by the ATR/FTIR method was quite limited, but may be improved if the cheese samples are homogenized prior to analysis, which, however, significantly complicates the procedure.

In 1992, van de Voort *et al.* developed a rapid FTIR quality control method for fat and moisture determination in butter employing an ATR sample handling accessory[95]. A calibration curve was prepared by recording the ATR/FTIR spectra of anhydrous butterfat and water mixtures in propanol and measuring the peak heights of the ester carbonyl and water (HOH bending) bands in the spectrum. The ATR crystal was cleaned thoroughly with Triton X-100 and hexane prior to analysis and sample spectra were ratioed against the spectrum of the solvent (propanol). Twenty butter samples that were

pre-analyzed by the Mojonnier method were dissolved in propanol, warmed to 40°C, applied to a heated ATR crystal (40°C) for spectral recording and predicted from the calibration curve. The results using the ATR/FTIR method were not significantly different from the results obtained by wet-chemical methods at the 1% level. The data were also reproducible with a standard deviation (SD) of 1.08 and 0.69% (w/w) for fat and water, respectively. The authors noted that fat adhering to the surface of the ZnSe ATR crystal can be a problem but could be overcome if a background spectrum of the solvent is taken before every sample and that overall the ATR/FTIR method provided a rapid and accurate means for analyzing butter. An ATR/FTIR method was also developed for fat and solids determination in sweetened condensed milk using a germanium crystal which is less prone to fat adherence, an effect that is problematic with the use of ZnSe crystals[96]. This type of viscous and difficult to handle product can be handled quite readily by ATR, however, due to variability in the homogeneity of the samples, all samples were homogenized at 65°C using a polytron mixer prior to analysis. Twenty pre-analyzed samples of sweetened condensed milk covering the range of 6.78-8.43 and 61.44-74.5% (w/w) for fat and solids, respectively, were used to calibrate the instrument and a PLS calibration using 3700-2900 cm^{-1}, 2100-1877 cm^{-1}, 1768-1793 cm^{-1} and 1180-884 cm^{-1} as spectral regions was developed. Validation of the calibration employing 30 pre-analyzed sweetened condensed milk samples gave an RSD of 1.10% and 0.74% for fat and solids, respectively. This method offered a simple means of monitoring the fat and solids content for quality control application purposes during manufacture of sweetened condensed milk. Belton *et al.*, 1988, examined the potential utility of ATR/FTIR spectroscopy for the analysis of fat in molten chocolate and cocoa liquor[97]. However, solid samples clamped onto the surface of the ZnSe ATR crystal did not yield reproducible results as crystal coverage and applied pressure could not be kept constant.

e) Edible Oils and Fats

Edible oils and melted fats can be considered as viscous liquid samples and have been investigated by ATR/FTIR techniques. The first reported study using ATR/FTIR spectroscopy for quantitative analysis of fats and oils was in the estimation of *trans* content in margarines[98]. Samples were applied directly onto the ATR crystal, avoiding

the need for dissolution in organic solvents, and it was found that *trans* content could be determined to within 2%; however, an internal peak ratioing method was employed to overcome non-uniformity of crystal coverage. In 1996, Mossoba *et al.*[99] developed an ATR/FTIR method for total *trans* content in neat hydrogenated oils using the spectral ratioing method originally described by Sedman *et al.*[19], substituting soybean oil as the reference oil for triolein used in the original method. This method was simple, requiring only that the samples be poured onto the ATR crystal and scanned and the limit of quantitation was found to be 1% for isolated *trans* isomers in samples covering a range of 5% to 30% *trans* fatty acid content.

Numerous methods were developed for the quantitation of total unsaturation (IV), free fatty acids, SN (average molecular weight), saturated fatty acids, monounsaturated fatty acids and polyunsaturated fatty acids in fats and oils employing ATR/FTIR spectroscopy. In addition, numerous methods were also developed for the authentication and detection of adulteration in edible oils. These methods are summarized in Table 2.3.

f) SB-ATR Applications

The applications discussed above were investigated employing horizontal MB-ATR accessories, unless otherwise indicated. Recently, there have been a few studies undertaken employing SB-ATR accessories, due to the renewed interest in this accessory and some of the advantages it offers. The most successful application of SB-ATR spectroscopy in food analysis has been the determination of *trans* fatty acids in food lipids. The first study of this kind was conducted for *trans* determination in fat extracted from 18 different food products[110] whereby the food samples were digested in 6N HCl and the digest extracted with ether and petroleum ether and then dried to yield the fat sample. The fat samples were then converted to their respective FAMEs, using the standard AOAC method 969.33. For SB-ATR analysis, only 50 μL of the FAME samples was required for analysis on the ZnSe crystal and refined, bleached and deodorized soybean oil was used as the reference oil for spectral ratioing. The calibration was based on mixtures of *trans* isomers of octadecenoate in methyl oleate covering a range of 0.592% to 54.15% *trans* fatty acids. The results were compared to the reference GC method and for food products containing higher *trans* levels (>5%), the methods were

Table 2.3: Analysis of fats and edible oils by ATR/FTIR spectroscopy.

Application	Reference	Description
Total unsaturation	Afran and Newberry[100]	Determination of total unsaturation in edible oils employing peak height ratios of the olefinic and aliphatic CH stretching bands.
IV and SN	van de Voort *et al.*[101]	Determination of IV and SN employing PLS. Difficulty in obtaining reproducible spectra because of temperature effects was reported, causing baseline curvature. A correction factor based on the ratio of the intensity of the carbonyl absorption band of triolein was used to correct for this problem
Free fatty acids	Ismail *et al.*[23]	Determination of free fatty acids in fats and oils employing 40° ZnSe ATR plate to increase effective pathlength. For thermally stressed and oxidized oils, free fatty acids were extracted by 1% KOH/MeOH solvent prior to analysis. Non-linear calibration equations were used on the absorption band at 1711 cm^{-1}. ATR could measure free fatty acid content to a level of 0.2%.
Free fatty acids	Bertran *et al.*[102]	Determination of free fatty acids in olive oils employing two PLS calibrations, one for the concentration range of 0.1% to 0.5% and another for 0.5% to 2.1% free fatty acids. By using standard normal variate pretreatment to the spectral data prior to PLS calibration and analysis, the same calibration could be used for thermally stressed oils. Overall, fatty acid content could be measured down to 0.1%.
Saturated, monounsaturated, polyunsaturated fatty acids	Ripoche and Guillard[103]	Determination of fatty acids in pork fat employing chloroform and methanol (2:1) as an extraction solvent and PLS based on GC reference values. Good agreement with GC values was obtained. The amount of palmitic acid, stearic acid, oleic acid and linoleic acid were also well estimated using ATR.

Table 2.3: Analysis of fats and edible oils by ATR/FTIR spectroscopy.

Application	Reference	Description
Citrus oils	Shulz *et al.* [104]	Determination of limonene, myrcene, α-pinene, β-pinene, sabinene, γ-terpinene, optical rotation and aldehydes in citrus oils employing PLS.
Authentication of vegetable oils	Lai *et al.* [105]	Authentication of vegetable oils employing PCA. 100% classification achieved.
Adulteration in extra virgin olive oil	Lai *et al.* [106]	Quantification of adulterants, refined olive oil and walnut oil, in extra virgin olive oil employing PLS.
Classification of oils, butter and margarines	Safar *et al.* [107]	Classification of oils, butter and margarines employing PCA algorithm based on degree of esterification and unsaturation.
Classification of butter and margarine	Dupuy *et al.* [108]	Classification of butter and margarine employing PCA. For ATR studies, good clustering of margarine and butter samples was obtained. However, poor reproducibility was obtained when spreading fat samples directly onto the ATR crystal. For fiber-optic probe studies, chalcogenide fibers were used with a ZnSe ATR crystal and PCA was able to distinguish samples of oils of sunflower origin from peanut and olive oils.
Adulteration of extra virgin olive oil	Yang and Irudayaraj [109]	Method of detection of adulteration of extra virgin olive oil with olive pomace oil employing PLS. An SEP of 3.28% was obtained.

comparable; however there was a significant discrepancy for low *trans* levels (<5%), with relative differences of above 30%. The authors cited that a probable source of error is from the use of only one reference oil for spectral ratioing of all food samples, which is insufficient. Furthermore, the bleaching and deodorizing process does not eliminate completely the *trans* containing isomers in the reference oil, thereby causing *trans* values in the SB-ATR method to be lower than GC values, especially for low *trans* containing food products. Finally, another source of error is to assume that absorption of *trans* double bonds in food products is the same as in octadecenoate, while in reality absorptivities of other *trans* triglycerides are different. The authors concluded that more work needs to be done to develop a viable method for *trans* analysis of food products by SB-ATR spectroscopy. A second study using SB-ATR spectroscopy was conducted for *trans* fatty acid determination in hydrogenated vegetable oils[111]. This time the analysis was carried out on the neat hydrogenated oils premelted and analyzed at 65°C, using suitable reference oils for background spectral recording. The authors cited that the advantage of the SB-ATR method is that it requires less test material and precision and accuracy were significantly improved. The RSD between 5 labs was 1.62% for 39.12 % *trans* fatty acids and 18.97% for 1.95% *trans* fatty acids. At present, the SB-ATR method for *trans* determination described above has been adopted as American Oil Chemists' Society (AOCS) and AOAC official methods[112,113]. However, the method is limited to *trans* levels greater than 5%[114] and has an analysis time of less than 5 minutes per sample.

The McGill IR group extended the SB-ATR method for *trans* analysis to allow simultaneous determination of IV number[115]. Calibration models were developed using PLS regression and compared to the standard AOCS method for SB-ATR *trans* analysis, which uses a calibration equation based on the spectra ratioed against a suitable reference oil. Good agreement was obtained between the GC method, PLS method and AOCS method for *trans* analysis and between the GC method and SB-ATR method for IV determination. The authors stated that the SB-ATR accessory proved to be amenable to precise temperature control owing to the small surface area of the ATR crystal.

SB-ATR spectroscopy in combination with cluster analysis and PCA was used to discriminate between phenolic extracts of different wine cultivars[116]. Phenolic extracts

were obtained by solid phase extraction of the wine samples and subsequent elution of the phenols with methanol and the extracts allowed to dry on the SB-ATR crystal for spectral recording. Only 1 μL of the extract was required to cover the ATR crystal and almost complete discrimination of all cultivars investigated was achieved. SB-ATR spectroscopy was also used in the analysis of white wine polysaccharide extracts[117] and by employing PCA and canonical correlation analysis, SB-ATR/FTIR spectroscopy was able to identify the wine making process involved (must clarification versus maceration) based on the type of wine polysaccharides present. Furthermore, a calibration equation was developed using PLS regression for mannose determination in the polysaccharide extracts[117].

The first study of proteins using SB-ATR/FTIR spectroscopy has been for monitoring changes in the amide bands of lysozyme during lyophilization[118]. The advantage of using a germanium SB-ATR accessory is that water structure changes during lyophilization could be monitored spectrally without any signal saturation effects. The accessory was equipped with the ability to cool the sample in a controlled manner using liquid nitrogen. It was found that the amide I band shifts to a higher frequency during water loss and conversely, the amide II band shifts to a lower frequency and broadens. Overall it was found that lysozyme is not affected by the stress of freezing and drying under vacuum. SB-ATR/FTIR spectroscopy has also been used to carry out protein secondary structure analysis directly in H_2O, without the need for D_2O exchange[119]. A 10-20 μL sample of protein solution is deposited on the surface of a germanium SB-ATR crystal and allowed to dry by blowing a stream of N_2 gas over a Teflon block to dehydrate the sample. The spectrum of the resulting gel is recorded, thereby eliminating the need for H_2O subtraction. This method successfully predicted α-helical and β-sheet content to a level comparable to methods using transmission FTIR and MB-ATR/FTIR spectroscopy but with superior reproducibility. The improved predictions were likely due to the inclusion of a greater number of spectral regions, which can be acquired using the SB-ATR technique, enabling the simultaneous observation of amide III and amide A and B bands[120]. Finally, SB-ATR/FTIR spectroscopy has been used to assess lipid:protein and detergent:protein ratios during membrane-protein crystallization[121]. Using a diamond SB-ATR accessory, rapid screening of small aliquots

of samples was carried out and it was found that the ability to predict lipid:protein ratio was accurate down to a level of five molecules of lipid per molecule of 300 kDa protein. Detergent concentrations were found to be accurate well below detergent concentrations used in crystallization trials.

2.2.2.3. Conclusion

The development of MB-ATR, CIRCLE and fiber optic ATR sampling accessories coupled to FTIR spectrometers has provided a new avenue of quantitative analysis of aqueous and viscous solutions, particularly those containing sugars. Quantitative analysis of solids is still problematic due to the lack of reproducibility, even when pressure is applied to the sample to improve contact with the ATR crystal surface. Quantitative analysis of dairy products has also some promise but has been limited by variation in fat globule size, fat absorption or non-homogeneity of fat in the sample. Quantitative analysis of fats and oils by ATR/FTIR spectroscopy has been relatively successful as they are not dispersions; however in the case of ZnSe ATR crystals, fat adherence to the crystal can be a problem[96] and for fats, heating the accessory avoids crystallization, but it is difficult to obtain adequate temperature control for quantitative applications[101,108]. In addition, MB-ATR is limited in terms of on-line analysis due to the large size and inherent difficulties associated with rinsing and cleaning the crystal surface. ATR fiber optic probes, although appearing to be more amenable to on-line analysis, have poor optical throughput which limits their ability to provide sufficiently accurate and reproducible results.

Although SB-ATR/FTIR spectroscopy has only recently come to the forefront and despite the limited number of applications developed thus far, there are already some clear advantages of this accessory for quantitative analysis as compared to conventional transmission cells and other ATR sampling methods. This is largely due to the high optical throughput of these accessories and their small surface area, the latter requiring only very small volumes of sample to be analyzed and facilitating cleaning and reloading. In addition, the small crystal size allows good temperature and hence pathlength control, which often results in better reproducibility as compared to conventional sample handling methods. Finally, as seen with the wine extracts, SB-ATR spectroscopy is potentially

amenable to analysis of solids as more reproducible spectra of solid samples can be obtained. Overall this method appears promising for quantitative analysis of food systems as it offers good reproducibility and ease of sample handling.

2.2.3. Photoacoustic Spectroscopy

2.2.3.1. Theory

The photoacoustic effect, the detection of light absorption using sound, was first described by Alexander Graham Bell over 100 years ago but has seen only limited IR application over the last few decades[122]. For PAS analysis, a sample is placed in a cell containing a microphone and covered with an IR transparent window, which traps a volume of inert gas (e.g., helium) between the sample and the window (Figure 2.5)[2]. When IR radiation is absorbed by the sample, it heats up the sample and the surrounding inert gas, causing it to expand. The expansion produces a pressure wave, which can effectively be considered a sound wave, which propagates through the surrounding gas in the cell and is picked up by the microphone[123]. The microphone then converts the sound into an electrical signal and the plot of the signal versus the optical path difference yields an interferogram, which is Fourier transformed to produce a conventional IR spectrum[1].

Quantitative analysis using PAS depends on a number of factors and is a function of the incident energy, absorption coefficient, surface morphology and thermal diffusivity. Furthermore, thermal diffusivity is a complex function that depends on the thermal conductivity, density, specific heat and modulation frequency of the IR beam. Even with the many complications, a linear relationship between the PAS signal and the concentration of constituents of interest can be obtained[2]. For homogeneous samples, the depth at which the PAS signal arises depends on the thermal diffusivity and frequency of IR radiation, according to the following relationship:

$$L = (D/\pi F)^{1/2} \quad [2.3]$$

where L is the sampling depth (thermal diffusion length) in cm, D is the sample thermal diffusivity in cm^2/s and F is the frequency of modulation of radiation[1]. In this way, PAS is similar to ATR in that the sampling depth depends on the wavenumber[88] and that the PAS response will only originate from the sample within the thermal diffusion length.

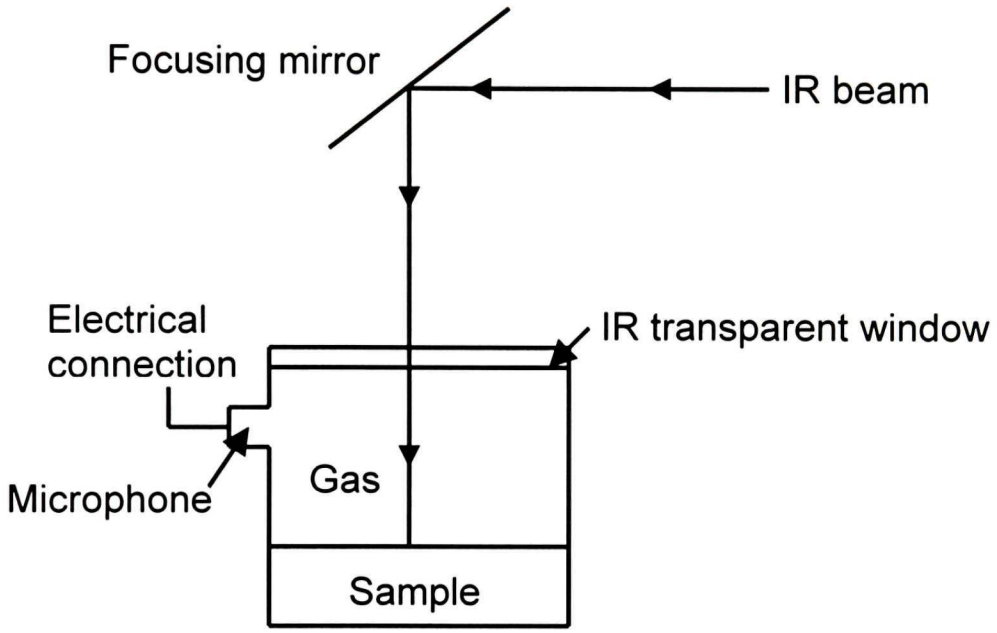

Figure 2.5. A diagram of a PAS accessory (adapted from reference 1).

Typically for FTIR spectrometers, the sampling depth is between 20 and 200 μm [3], with PAS spectra being broader than transmission or ATR spectra due to the functional relationship between the PAS intensity and the amount of light absorbed[88]. There are a couple of major drawbacks to carrying out quantitative analysis by PAS. If the radiation is absorbed so strongly that the pathlength is smaller than the thermal diffusion length, then photoacoustic saturation sets in, where the PAS signal becomes independent of the concentration[2] and this can result in a non-linear response in the PAS signal[124]. Although there are several approaches to correct for a non-linear response, such as the linearization procedure developed by Poulet *et al.*[125], when the signal saturation is significant, these corrections do not perform well[124]. Another limitation is that PAS is sensitive to surface morphology and unless powdered samples are packed reproducibly and are homogeneous on a centimeter scale, the results will be significantly affected[124]. What is attractive about PAS is that in theory it can be used to analyze any kind of sample, it is non-destructive and does not require any sample preparation[1], making it possible to analyze solid and opaque samples[126]. The reality is that the technique has a poor S/N relative to transmission and ATR techniques because the efficiency of energy transfer (absorbance to sound) is poor[3] and therefore PAS is a relatively insensitive technique. In addition, any IR active vapour (e.g., water vapour) will give rise to strong photoacoustic signals, requiring that the sample be very dry during analysis[1]. Finally, the photoacoustic signal is dependent on several factors, such as incident energy, absorption coefficient, surface morphology and thermal diffusivity, which, in part, are sample dependent[2].

2.2.3.2. Applications

The first investigation of a PAS/FTIR application in food analysis was on protein and starch mixtures[88]. As with the ATR investigation, PAS spectra were taken of the dry mixtures and wetted mixtures with all PAS spectra ratioed against finely powdered carbon black. Poor PAS spectra of the wetted mixtures were obtained due to saturation effects. For dry mixtures, the starch spectral contributions also exhibited saturation and phase effects; however, dilution of the dry mixtures with KBr proved to be a means of overcoming this problem and good correlation and linear plots were obtained for protein and starch content. Similar studies were carried out on chocolate and cocoa liquor[97] in

their molten state. It was found that the best results were obtained after a thermal equilibration of 5 minutes, with PAS spectra being broader than conventional transmission cell and ATR spectra. Fat analysis in chocolate samples was carried out using the carbonyl stretching band at 1744 cm^{-1} and a linear relationship was established between the reciprocal of PAS intensity and the fat concentration. An R value of 0.98 was obtained and demonstrated the possibility of PAS/FTIR for the quantitative determination of fat. PAS was also evaluated for the determination of the major components, starch, protein and fat, in single pea seeds[127]. In model mixtures, the PAS signal was linear over the entire range of protein concentration, but not starch. For actual pea seeds, PLS was employed instead of a univariate regression in order to model the complexity of the pea seed matrix. Good correlations between chemical and predicted values were obtained with R values of 0.84, 0.97 and 0.98 for protein, starch and fat, respectively. Ootake and Kokot investigated using PAS to discriminate between glutinous and non-glutinous rice[128], however; water vapour problems in the regions 1400 to 1900 cm^{-1} and 3500 to 3900 cm^{-1} as well as particle size variability influenced the PAS spectra. Nevertheless, they were able to obtain 96% correct classification when the spectral region between 1400 and 800 cm^{-1} was employed.

The determination of total *trans* fatty acid content in margarine was investigated using FTIR spectroscopy equipped with an optothermal window (OW), a variant of PAS[129]. In the OW method, the sample is placed on a sapphire disc and heat generated by the sample after irradiation diffuses into the sapphire disc, causing it to expand. The expansion of the disc generates an acoustic wave, which is detected by a ceramic piezoelectric detector or a thermistor[124]. This method is easier to use compared to conventional PAS, because of the open cell architecture. Margarine samples were converted to their FAMEs and dissolved in hexane prior to analysis and calibration curves were prepared using methyl elaidate and methyl oleate. This method resulted in a relative error of 2% with good reproducibility. A similar study was carried out on aqueous solutions of lactose and corn starch gels[130] and linear plots with a limit of detection (LOD) of 0.19 and 0.6% (w/w) for lactose and starch, respectively, were obtained. OW has also been used to determine sunflower and safflower adulterants in

extra-virgin olive oil[131] with limits of detection of 6.0 and 4.5% (w/w) for detecting safflower and sunflower oil, respectively.

Recently, there have been several qualitative PAS/FTIR studies of food samples. The first one involved the determination of the optimal parameters for PAS/FTIR measurements on soybean oil, butter and lard[132]. It was found that scanning at a lower speed (2.5 Hz) using 256 scans at a resolution of 4 cm^{-1} produced good quality soybean and lard spectra, however; good quality butter spectra could not be obtained due to its high moisture content (14.8% (w/w)). In another study, wrapped cheddar cheese slices were examined by step-scan PAS/FTIR[133], which eliminates the relationship of frequency of IR radiation and depth of penetration into the samples to obtain the same depth of penetration at all frequencies. The cheese samples were kept in a dessicator overnight to minimize the effect of moisture and PAS depth-profiling studies indicated that there is a diffusion of cheese components into the package during storage. Other PAS/FTIR studies reported include detection of olive pomace oil adulteration in extra virgin olive oil[109], monitoring of the oxidation of potato chips at 80°C[134], depth profiling studies and characterization of beef and pork[135], monitoring of chemical changes in lard, peanut butter, mayonnaise and whipped topping upon heating[136] and particle size estimation in sucrose powders[137]. In all of the above studies, good PAS spectra were obtained for dry samples, but moisture was a problem for samples such as whipped topping and mayonnaise.

2.2.3.3. Conclusions

FTIR/PAS could provide an alternative for the quantitative analysis of dry solid samples; however, limitations due to sample morphology and PAS saturation effects, especially from moisture, restrict its use substantially. Although PAS can be used to obtain relatively good quality spectra for depth-profiling, it does not appear to have general applicability for quantitative food analysis.

2.2.4. DRIFT Spectroscopy

2.2.4.1. Theory

DRIFT spectroscopy has some of the potential advantages of PAS, but like PAS, most advantages are not realized. This is a reflectance technique particularly suitable for powders and solids, where the incident IR radiation is scattered in all directions, which, with the proper optical setup, is picked up by a detector[138]. Figure 2.6 illustrates a typical DRIFT accessory. To obtain good spectra for quantitative analysis that obeys Beer's law, the spectra must undergo a Kubelka-Munk transform. The reflectance, R_∞, is related to the concentration of the sample by the following equation,

$$F(R_\infty) = (1- R_\infty)^2/ 2 R_\infty = K/s \quad [2.4]$$

where K is the molar absorption coefficient and s is the scattering coefficient. The scattering coefficient depends on the particle size and packing of the material and must be strictly controlled for quantitative analysis applications[2]. This relationship also becomes non-linear at high concentrations, often requiring the dilution of the sample with a non-absorbing powder such as KBr or KCl. Typically, sample concentrations in the diluent are 1-5% and the alkali halide powders are also used to record background spectra[138]. Highly absorbing species and large particulates lead to the Reststrahlen effect, which leads to the distortion or the inversion of the absorption bands[2]. On the other hand, fine powders (less than 40 μm) with a consistent particle size leads to high internal scattering, which is favorable for very low concentration of species in powdered samples[2,138].

A disadvantage of the DRIFT method is that the amount of energy diffusely reflected is very low and as a result, longer data collection times are required to obtain an adequate S/N. Optical throughput is also relatively poor, somewhere between 10-15%[138], and for quantitative analysis applications, samples must be ground into a powder with a small enough (typically below 80 μm) and consistent particle size and diluted in an alkali halide powder[2,138]. The grinding procedure may induce chemical changes in the sample, although less than in the preparation of a KBr pellet or Nujol mull[138]. Samples must also be kept dry to minimize the Reststrahlen effects due to high absorption from water.

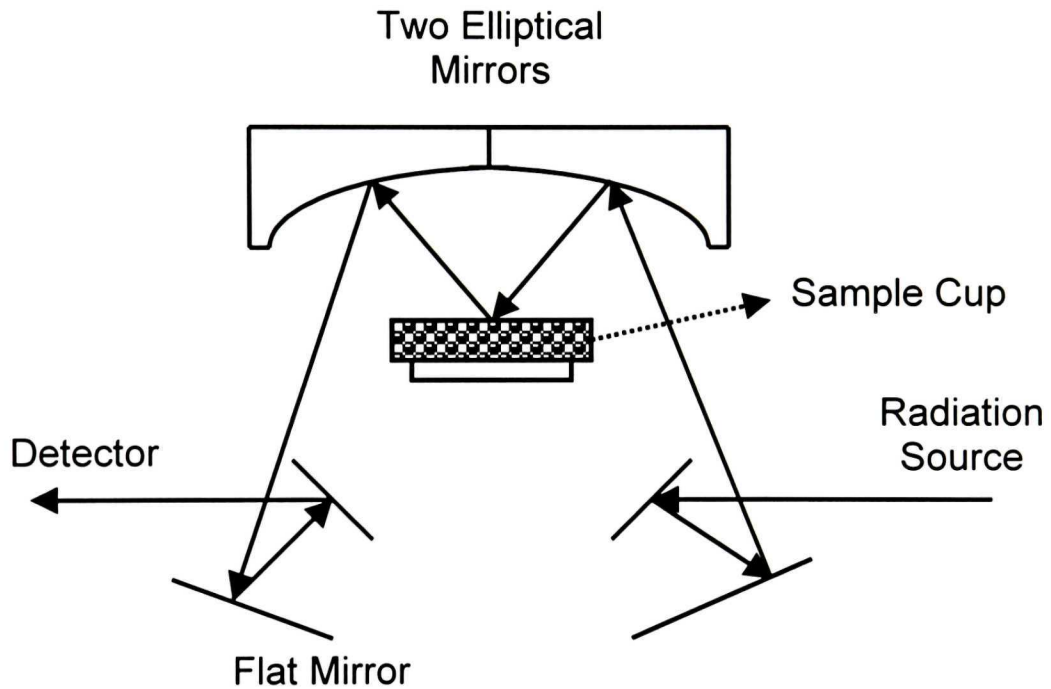

Figure 2.6. Schematic diagram of the "Collector" DRIFT spectroscopy cell showing four flat mirrors, two elliptical mirrors, and the blocker to help eliminate specular reflected radiation with the path of radiation indicated (adapted from reference 138).

2.2.4.2. Applications

DRIFT spectroscopy was carried out for the determination of fruit content in jam[83] where the samples were dissolved in water, filtered and dried in an oven, after which 5 mm diameter samples were cut for DRIFT analysis. DRIFT spectra were seriously distorted and not suitable for quantitative analysis, but could act as identifiers for various fruit types, as their spectra were reproducible. Another study later attempted to verify the applicability of DRIFT spectroscopy in the classification of jams using PCA and discriminant analysis (DA)[84]. By adjusting the geometry of the instrument, few artifacts were observed and all jams were classified correctly as being strawberry or non-strawberry.

DRIFT spectroscopy has also been used in the discrimination of *Arabica* and *Robusta* coffee beans[139], which were ground, mixed with equal amounts of KBr and pounded with a pestle to obtain a fine powder. Although the authors reported difficulty in loading the sample cup reproducibly, this problem could be corrected for by carrying out a baseline correction and peak area normalization procedure. Discrimination based on PCA followed by DA was successful and based in part on differences in lipid content of the beans. A similar study was carried out for the discrimination between *Arabica* and *Robusta* instant coffees[90], as well as, between pure coffee and coffee adulterated with glucose, starch or chicory[91]. The use of artificial neural networks resulted in correct classification of all samples.

Reeves and Zapf used DRIFT spectroscopy to discriminate between various food powders, such as buttermilk, cheeses, dehydrated onion, dehydrated milk-egg powders, wheat flours, powdered cheese seasoning and powdered ranch seasoning employing PCA and Mahalanobis distances[140]. Estimation of particle size distribution of sucrose powder using DRIFT spectroscopy was also investigated[137] by placing sugar separated using sieves in a cup of 10 mm in diameter and 2.3 mm in depth. Samples were analyzed with and without dilution with KBr and PLS was employed to predict particle size content. It was found that despite the presence of Reststrahlen bands in the spectra of the undiluted samples, better results were obtained than with diluted samples. Finally, DRIFT spectroscopy has also been used to detect cocoa butter adulterated with vegetable fats at the 10 and 20% levels[141].

2.2.4.3. Conclusion

The DRIFT spectroscopic method is good in qualitative studies of powders, but quantitative analysis of foods proved to be unsuccessful and DRIFT spectroscopy was, rather, delegated to classification and particle size studies. Grinding of the sample to achieve uniform particle size is not always feasible in the analysis of some food samples and moisture, a major component in most food samples, causes distortion of the bands due to Reststrahlen effects. The difficulty of obtaining reproducible spectra because of sampling considerations also makes the use of this sample-handling technique not feasible for quantitative analysis applications by FTIR spectroscopy.

2.3. 2D CORRELATION SPECTROSCOPY

Multidimensional correlation techniques, such as, 2D correlation spectroscopy, were first extensively used in nuclear magnetic resonance (NMR) spectroscopy about 30 years ago and since then, have been applied mostly to NMR and other resonance spectroscopic methods[142,143]. However in 1986, Noda proposed a 2D correlation method for IR spectroscopy, known as 2D IR spectroscopy[144]. The basic concept is similar to 2D NMR spectroscopy; however, it requires the use of different experimental procedures, as the vibrational relaxation rates are an order of magnitude faster than the spin relaxation rates in NMR[145]. In the experimental approach for 2D IR spectroscopy, an external perturbation is applied to the sample and the time-dependent molecular response of the sample is measured by an IR detector.

Initially, 2D IR spectroscopy was limited to simple sinusoidal spectral intensity variations in order to employ the original data analysis scheme. In 1993, Noda developed a generalized 2D correlation algorithm that is designed to handle signals as an arbitrary function of time or any other physical variable[146]. This allowed the application of 2D correlation spectroscopy to be universal and applicable, not only to IR, but to any type of spectroscopic study. Since the development of generalized 2D correlation spectroscopy, 2D correlation analysis has been employed in a wide range of applications, such as NIR band assignments, polymer studies, concentration dependent studies, protein structure studies and temperature dependent studies[147-151]. Finally, a variant of generalized 2D correlation spectroscopy, H2D-CS, which correlates data from two different

spectroscopic methods has been developed and has provided insight into NIR band assignments[142] and has the potential to improve NIR quantitative analysis applications[152]. In this section, the theory and applications of generalized 2D correlation spectroscopy will be reviewed, as well as applications of the up and coming H2D-CS approach to 2D correlation analysis.

2.3.1. Theory of 2D Correlation Spectroscopy

The concept of 2D IR correlation spectroscopy was originally based on an extension of dynamic IR spectroscopy for rheo-optical studies of polymers[144-146, 148]. In dynamic IR spectroscopy, variations are induced by an external perturbation applied to the sample to induce re-orientations of dipole-transition moments. The rates of re-orientation of functional groups depend on the submolecular environment and IR spectra collected while molecular re-orientations take place are termed dynamic IR spectra and can reveal intensity variations, wavenumber shifts and sometimes changes in directional absorbances, known as dichroism[145]. The external perturbation can be mechanical, electrical, chemical, magnetic, optical or thermal; however, the algorithm for 2D IR spectroscopy was initially based on sinusoidal perturbations that resulted in time–dependent changes in IR dichroism[144,145,148]. Figure 2.7 illustrates the general conceptual scheme used to generate 2D IR correlation spectra and a full description of the algorithm is presented in Appendix A.

To generate IR correlation spectra, the in-phase (synchronous) and quadrature (asynchronous) components of the cross correlation function with their respective correlation intensity values are plotted as a function of two independent wavenumbers. These dynamic IR correlation spectra can be represented as synchronous and asynchronous 2D contour maps; their interpretation will be explained in detail later (Section 2.3.2). The development of a more generalized 2D algorithm has dramatically widened its range of application and utility as the generalized 2D correlation algorithm allows the external perturbation not only to be sinusoidal, but of various physical origins, such as thermal, mechanical, electrical, acoustical, or chemical. The resulting intensity fluctuations can be a function not only of time but temperature, pressure, electrical field strength and even concentration[153]. Furthermore, the extension of this method to other

types of spectroscopic studies is straightforward. Figure 2.8 illustrates the scheme for obtaining generalized 2D correlation spectra and a full description of the algorithm is presented in Appendix B.

The computation of generalized 2D correlation spectra can be simplified by considering the dynamic spectra as a matrix, **M**, with dimensions of w × s, where w is the number of wavenumbers and s is the number of samples. Therefore, every row of the matrix can be viewed as a vector of the spectral absorbance changes at a given wavenumber. To obtain a matrix of synchronous spectra, the matrix **M** is multiplied by its transpose $\mathbf{M}^T$. The resulting synchronous matrix is called a covariance matrix, **Z**, which is a square matrix with dimensions of w × w

$$\mathbf{Z} = 1/(s-1)\mathbf{M}\mathbf{M}^T \quad [2.5]$$

where s is the number of samples. Therefore **Z** will reveal the similarities and dissimilarities, representing the in-phase relationships, between a pair of wavenumbers ν_1 and ν_2. The matrix **Z** holds all the characteristics of a synchronous spectrum and can be considered as correlation coefficients of dynamic spectral vectors of a spectral matrix[142,154,155].

To obtain the asynchronous spectrum, **R**, the dynamic vectors of the sample matrix must be correlated with the orthogonalized dynamic vectors of the Hilbert transform matrix, **H**, so that

$$\mathbf{R} = 1/(s-1)\mathbf{M}^T\mathbf{H}\mathbf{M} \quad [2.6]$$

Therefore, **R** will reveal non-linear (out-of-phase) relationships between a pair of wavenumbers ν_1 and ν_2. The matrix **R** holds all the characteristics of an asynchronous spectrum[142,154,155]. The Hilbert transform matrix, **H**, is defined as

$$\mathbf{H}_{jk} = 0 \text{ if } j = k$$

$$\mathbf{H}_{jk} = 1/((k-j)*\pi) \text{ if } j \neq k \quad [2.7]$$

where j and k are the number of columns and rows in the matrix. Smaller numbers appear at the corners of the Hilbert transform matrix and the diagonal positions have the value of

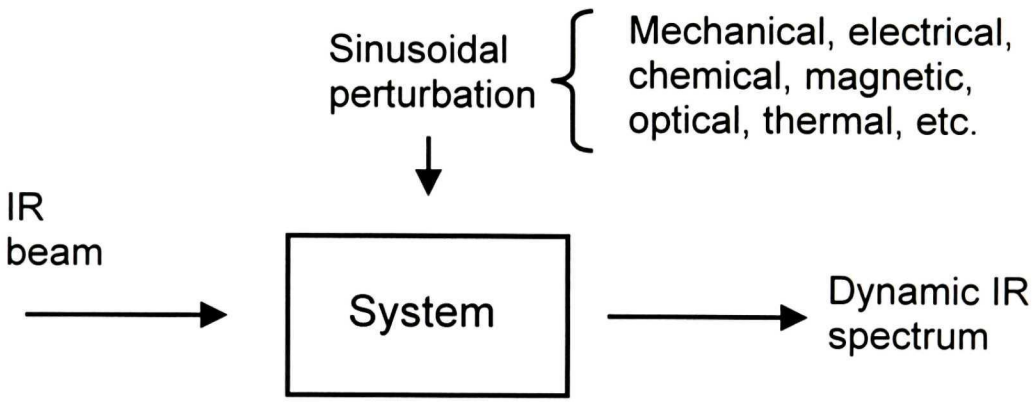

Figure 2.7. General conceptual scheme to obtain a 2D IR correlation spectrum (adapted from reference 146).

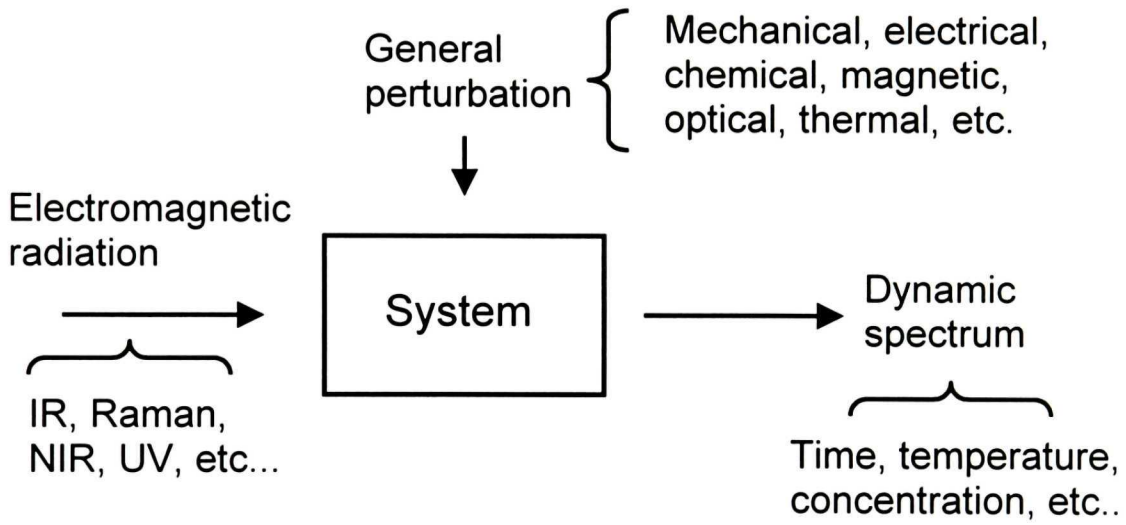

Figure 2.8. General conceptual scheme for generalized 2D correlation spectroscopy (adapted from reference 146).

zero. Below is an example of a Hilbert transform matrix with four columns and four rows:

0	$1/\pi$	$1/2\pi$	$1/3\pi$
$-1/\pi$	0	$1/\pi$	$1/2\pi$
$-1/2\pi$	$-1/\pi$	0	$1/\pi$
$-1/3\pi$	$-1/2\pi$	$-1/\pi$	0

2.3.2. 2D Contour Map Representation of Dynamic Spectra

To help interpret the 2D correlation spectral data, a 2D contour map representation is commonly used. For illustration purposes, a simulation of 4 peaks changing in intensity over a correlation period, *T*, is used. Five spectra are employed to generate synchronous and asynchronous 2D contour maps. Figure 2.9 shows a series of synthetic spectra where peaks A and C are increasing simultaneously from spectrum 1→5 and peaks B and D are decreasing simultaneously from spectrum 2→5 but remain constant from spectrum 1→2. Figure 2.10 shows the synchronous 2D contour map of the dynamic spectra, reflecting the intensity changes occurring in Figure 2.9. Since the spectral variables in Figure 2.10 are identical ($\nu_1 = \nu_2$), the synchronous 2D correlation map is symmetric with respect to the diagonal line. Peaks that appear on the diagonal line are known as autopeaks and represent regions of the dynamic spectrum that are changing over the correlation period. The correlation peaks that are located off the diagonal line are known as cross peaks and they represent the simultaneous spectral intensity changes occurring at two different wavenumbers. The correlation can be positive, represented by solid lines, or negative, represented by broken lines. A positive correlation means that the spectral intensity variations at both wavenumbers are occurring in the same direction, while a negative correlation indicates that the intensity changes are occurring in opposite directions. For example, in the simulation there is a positive correlation between peaks A and C at 1450 and 1250 cm^{-1}, respectively, and between peaks B and D at 1350 and 1150 cm^{-1}, respectively. Note that although peaks B and D are decreasing in intensity throughout the correlation period, there is a positive correlation between both peaks, because their intensities are changing in the same direction, simultaneously. There is a

negative correlation in Figure 2.10 between peaks A and B as well as A and D and between peaks C and B as well as C and D because their intensity changes are simultaneous, but in opposite directions. The synchronous 2D correlation map gives useful information about which bands, and therefore which functional groups, behave in the same way during the correlation period and accordingly indicates which bands are associated with one another.

Figure 2.11 is the asynchronous 2D correlation map generated from the spectral intensity changes in Figure 2.9, which represents changes in spectral intensity between two wavenumbers, ν_1 and ν_2, that are not simultaneous, i.e. out-of-phase with one another. This information is useful, as it tells which functional groups are not associated with one another with regards to the perturbation induced spectral intensity changes. Therefore if bands that overlap with one another are from two different types of molecules, they may respond differently to the induced external perturbation and hence be resolved. The asynchronous 2D correlation map may reveal if the bands are from different sources. In Figure 2.11, there are no autopeaks along the diagonal, but cross peaks are found at the off-diagonal position. A cross peak is observed between peaks A and B as well as A and D and between peaks C and B as well as C and D. A positive asynchronous cross peak indicates that the intensity change at ν_1 occurs before ν_2, if a corresponding cross peak in the synchronous 2D correlation map is positive. If the synchronous cross peak is negative, the reverse is true. Since the synchronous cross peaks between A and B as well as A and D are negative, this indicates that spectral intensity changes in A occur before B and D, which is as expected since peaks B and D only decrease in the third spectrum of the correlation period. Therefore the spectral intensity changes in A are not associated with those in bands B and C. As can be seen from the simulation, the asynchronous 2D correlation map is a powerful tool to elucidate spectral information at the molecular level.

2.3.3. Three-Dimensional (3D) Representation of 2D Correlation Spectra

2D contour maps can be represented as a 3D image, where the third axis represents the changes in correlation intensity. Figure 2.12 is a 3D representation of the

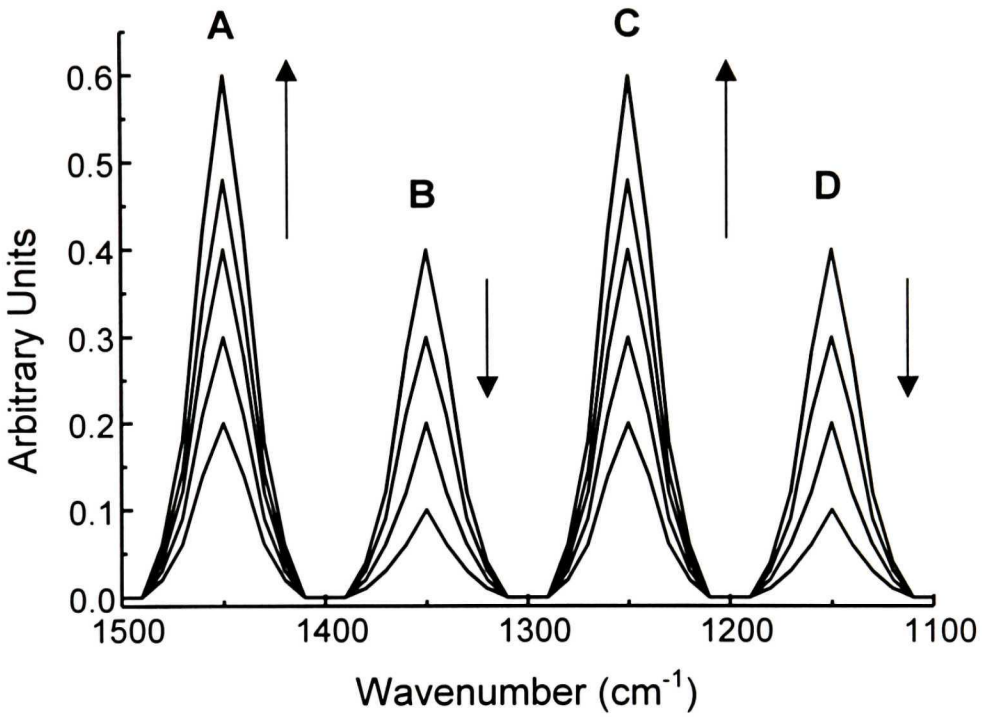

Figure 2.9. Simulation of 4 spectral peaks changing in intensity.

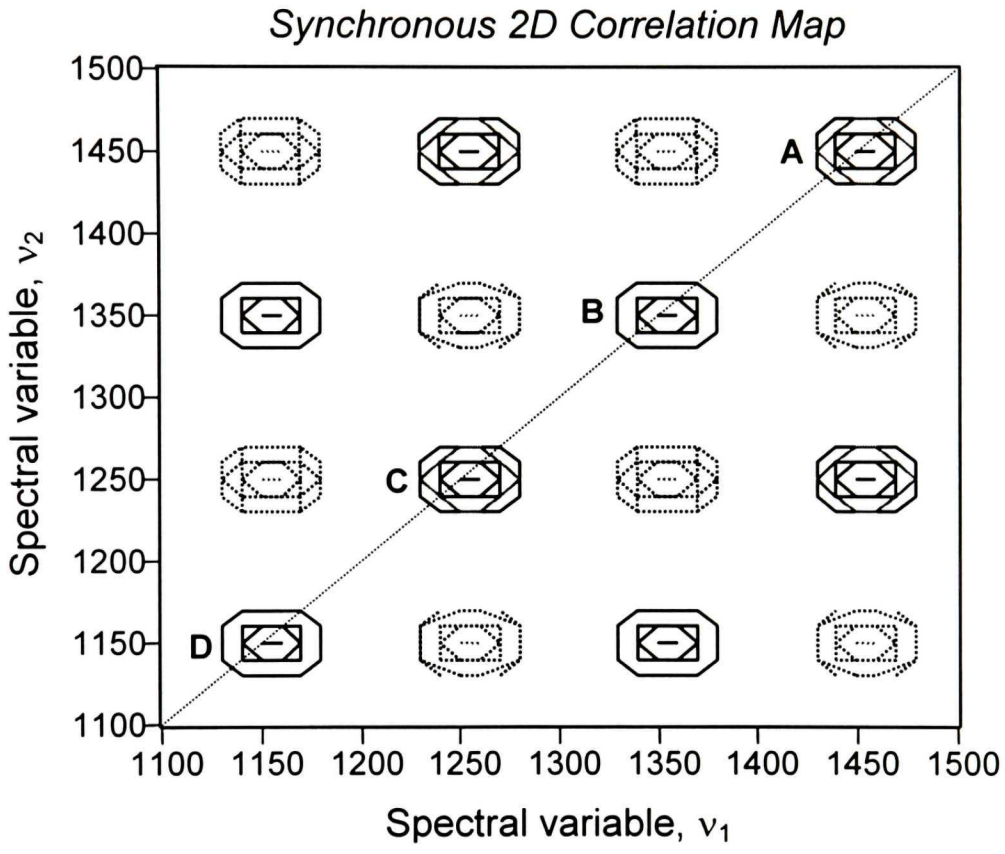

Figure 2.10. Synchronous 2D contour map constructed from the spectra in Figure 2.9. The solid lines represent positive correlation intensity, while the broken lines represent negative correlation intensity.

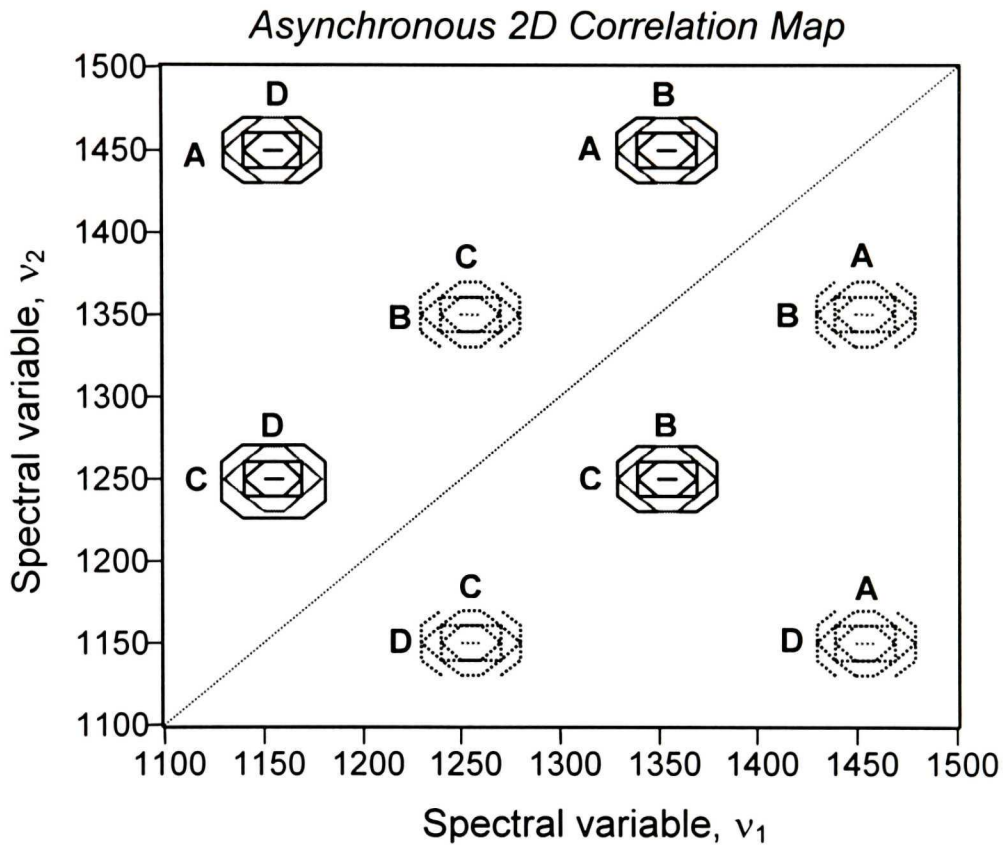

Figure 2.11. Asynchronous 2D contour map constructed from the spectra in Figure 2.9. The solid lines represent positive correlation intensity, while the broken lines represent negative correlation intensity.

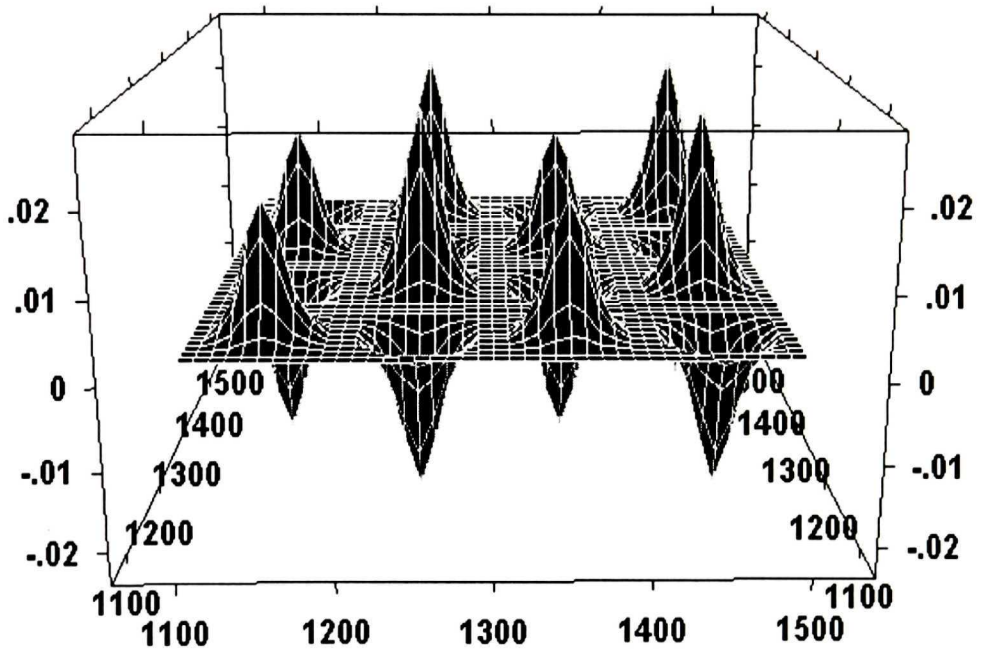

Figure 2.12. 3D representation of the synchronous 2D contour map.

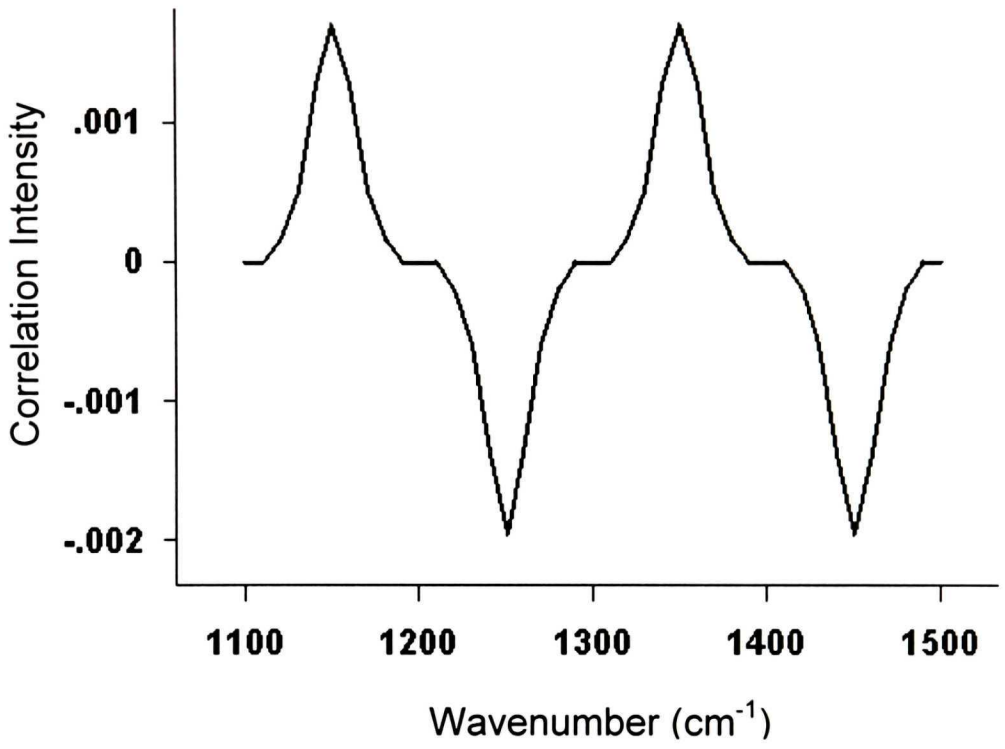

Figure 2.13. Slice spectrum at 1150 cm^{-1} generated from the synchronous 2D contour map.

synchronous 2D contour map generated from the simulation above. From the 3D map, a slice spectrum can be obtained by holding one of the spectral variables at a constant wavenumber and plotting the correlation intensity at that wavenumber with all the wavenumbers of the second variable. Figure 2.13 is a slice spectrum of the peak at 1150 cm^{-1}. The slice spectrum makes it easy to visualize the correlation of one peak with another, and the strength of the correlation can be assessed from the height of the peak. In Figure 2.13, we can clearly see that the peak at 1150 cm^{-1} correlates well with itself (autopeak) at 1150 cm^{-1} and with the peak at 1350 cm^{-1}. Conversely, there is a negative correlation with peaks at 1250 and 1450 cm^{-1}. Accordingly, the slice spectrum provides a good way to visualize the 2D correlation of spectral intensity changes occurring during the correlation period.

2.3.4. Pretreatment Methods

Sometimes it is necessary to pretreat the spectral data, aside from mean centering (Appendix B), prior to 2D correlation analysis because of spectral noise or fluctuation from other sources[155]. Spectral pretreatment is especially important in concentration perturbed systems, where small differences in sample spectra can affect the analysis data. The most common form of spectral pretreatment is auto-scaling. For a matrix, **A**, with dimensions of w × s, where w is the number of wavenumbers and s is the number of samples, auto-scaling is defined as

$$A'_{ws} = (A_{ws} - m_s) / s_s \quad [2.8]$$

where A' represents the auto-scaled matrix of absorbance data and m_s and s_s are the mean and standard deviation of the s^{th} column, respectively. By auto-scaling spectra, the variances of all the rows of the data matrix are equalized and the spectra are transformed into shapes that are visually very different from the original spectral shapes[156]. In 2001, Sasic and Ozaki used auto-scaling as a spectral pretreatment prior to employing generalized 2D IR correlation analysis, and named it statistical 2D correlation spectroscopy[157]. This method was employed in the study of a synthetic model system of polystyrene (PS) and poly(2,6-dimethyl-1,4-phenylene ether) (PPE) and in the study of concentration perturbed milk samples. It was found that auto-scaling was useful in the synthetic model system as the pure component spectra of PS and PPE had very different

intensities. In the case of milk samples, however, auto-scaling had no noticeable effect as the spectra of different milk samples are similar.

In 2001, Sasic *et al.* investigated using mean normalization as a method of spectral pretreatment for the study of mixtures of PS and PPE[155]. The two bands of PS and PPE are heavily overlapped with one another, with PPE having a much larger absorption coefficient. Without spectral pretreatment, the intensity of all the wavenumber points in the synchronous 2D correlation spectrum decrease with a decrease in PPE, despite an increase in PS. This trend was also observed with the mean centered data and therefore does not give a proper portrayal of the concentration dynamics. Mean normalization is defined as dividing each element of the matrix, A_{ws}, by the column mean, m_s:

$$A''_{ws} = (A_{ws} / m_s) \quad [2.9]$$

where A'' represents the mean normalized matrix of absorbance data. After mean normalization, the absorbance values at each wavenumber are normalized, giving equal statistical weight to each wavenumber point[158]. For the asynchronous 2D correlation spectrum, mean normalization had the effect of eliminating the asynchronous spectrum as the scalar product of the orthogonal vectors after mean normalization comes close to zero because of equalization of the rate of spectral intensity changes.

2.3.5. Applications of 2D Correlation Spectroscopy

2.3.5.1. Polymers

The first application of 2D IR spectroscopy was in the study of solution-cast thin films of atactic PS[144]. After exposure of this film to a tensile strain, the IR spectra were recorded at different time intervals and the set of dynamic spectra used to generate synchronous and asynchronous 2D correlation spectra of the sample. It was shown that different functional groups of the polymer showed different time-dependent behaviours, particularly the backbone and side groups. The second application of 2D IR correlation spectroscopy was in the study of mixtures of atactic PS and low-density polyethylene[148]. An oscillatory tensile strain was applied to the polymer blend and the time dependent IR spectra recorded. The synchronous and asynchronous 2D correlation spectra were calculated and revealed that the molecular orientations of PS and polyethylene under

tensile strain were independent of one another. Both applications illustrated that 2D IR spectroscopy provided enhanced resolution and could reveal information that is not obtainable from observing the one-dimensional (1D) spectra alone. Subsequently, studies were carried out on a number of polymers, such as atactic poly(methyl methacrylate)[159], miscible blends of atactic PS and poly(vinyl methyl ether)[160], PPE and PS[161], atactic PS plasticized with toluene[160], atactic PS plasticized with dioctyl phthalate[159], linear low density polyethylene[162], blends of high density and low density polyethylenes[163], isotactic polypropylene[164], poly(3-hydroxybutyrate)[165] and immiscible blends of atactic PS and amorphous Teflon[166]. These initial studies were all carried out by applying a mechanical strain to the sample. With the development of generalized 2D correlation spectroscopy, 2D IR studies of polymers were extended to the examination of the effect of temperature on polymer structure. Jung *et al.* recorded FTIR spectra of Langmuir-Blodgett films of poly(*tert*-butyl methacrylate) from 26 to 136°C. The synchronous and asynchronous 2D correlation maps were generated to determine the transition temperature of this glass material, as well as to investigate the re-orientation of the polymer chain[167,168].

2.3.5.2. Proteins

2D IR correlation spectroscopy of human skin stratum corneum[145] and human hair keratin[157] proteins provided new information about the secondary structure changes in protein conformation during mechanical perturbation. With the development of generalized 2D correlation spectroscopy, temperature dependent studies of proteins were carried out by Noda *et al.* 1996, using a simple model system of N-methylacetamide (NMA), a polyamide[169]. The association and dissociation of the hydrogen bonding of the amide groups of NMA produce bands at different frequencies in the amide I, II and III regions. 2D IR spectroscopy was used to correlate bands between the different amide regions, to resolve different overlapping bands in each amide region and to draw conclusions about the dissociation of hydrogen bonding of NMA as it is heated. This study asserted the potential utility of 2D IR correlation spectroscopy in the analysis of secondary structure and unfolding of proteins, which is dependent on the association and dissociation of hydrogen bonding of the amide groups. In 2000, Ismoyo *et al.* used 2D IR correlation spectroscopy to examine secondary structure changes in the avidin-biotin

complex when the protein is heated from 25 to 95°C[170]. The FTIR spectra underwent Fourier self-deconvolution (FSD) prior to analysis to obtain very sharp and well-resolved cross peaks in the synchronous and asynchronous 2D contour maps. The asynchronous map of the avidin-biotin complex revealed that the unfolding of the β-sheet structures preceded the unfolding of the α-helical structures when unfolding was induced by a temperature increase. Other studies of protein secondary structure by 2D IR correlation spectroscopy include thermal induced studies for cro-v55C[171], CMP kinases[172], aggregation of cytochrome c[173], β-hairpins[174] and human serum albumin[175], pH induced studies for hydrogen bonding of side chains of human serum albumin[176], concentration induced studies for β-lactoglobulin[177] and human serum albumin[175], hydrogen-deuterium exchange studies for human serum albumin[178] and myoglobin[179], secondary structure changes induced by adsorption of β-lactoglobulin to an ATR crystal surface[177] and the study of the secondary structure of 22 different proteins[180].

In addition to the secondary structure studies carried out on mid-IR spectra, there have been near-infrared (NIR) studies of proteins using 2D IR correlation spectroscopy. In 1996, Liu *et al.* also used NMA as a model system for generalized 2D IR correlation studies of proteins and 2D correlation of the NIR spectra provided information about the dissociation of the NMA oligomers during heating from changes in the first and second overtones of the N-H stretching vibrational modes[181]. A similar study was undertaken with another polyamide, nylon 12[182]. The first studies on actual proteins were done on temperature- and pH-induced perturbation of NIR spectra of ovalbumin and serum albumin, respectively[183]. Examination of the NIR 2D correlation maps of thermally induced changes in ovalbumin revealed that the hydration of ovalbumin occurs before protein unfolding and is likely required to facilitate the unfolding process. For serum albumin, an increase in pH produces significant changes in the environment of the amide groups, providing evidence for the unfolding of the secondary structure of serum albumin. In a later publication, the study of pH-dependent structural changes of ovalbumin by 2D IR correlation spectroscopy revealed that the structure of ovalbumin changes significantly as the pH decreases and is likely to take on a molten globule state below a pH of 2.6[184].

2.3.5.3. NIR Band Assignment Studies

Besides NIR studies of proteins, many other NIR studies using generalized 2D IR correlation spectroscopy were undertaken over the past 7 years, many dealing with NIR band assignments. The first of these studies involved the identification of two separate bands arising from the first overtone of the OH stretching mode of oleyl alcohol[153,185]. Upon heating, the dimers and trimers of the associated molecules of oleyl alcohol, dissociate into monomeric species. Different bands were assigned to oleyl alcohol, including the dimer (1462 nm) and two bands at 1405 and 1410 nm ascribed to rotational isomerism of the free OH group. In addition, this study suggested for the first time that the relationship between the first and second overtone of the OH stretching mode can be used to establish band assignments of rather complicated spectral regions of the NIR spectrum. In 1998, Czarnecki *et al.* conducted a similar study on the thermal dissociation of *sec*-butanol, where three band assignments were given for the first overtone of the OH stretching mode for the monomer[147]. A new band at 1527 nm was assigned to the first overtone of the OHO bending mode of cyclic polymers of *sec*-butanol. Similar studies were carried out on octan-1-ol[186], butan-1-(ol-d)[187], 2-methylpropan-2-(ol-d)[187], oleic acid[188] and octanoic acid[189].

Another application of 2D IR correlation spectroscopy for NIR band assignments involved the examination of the concentration-induced spectral variations of fat and protein in milk. In 1998, Wang *et al.* were able to assign NIR bands of protein and fat in milk using 2D IR correlation spectroscopy[149]. In 2000, Czarnik-Matusewicz *et al.* did a similar study by pretreating the spectral data first, using multiplicative scatter correction and smoothing[190]. From the synchronous and asynchronous 2D correlation maps, they found bands for fat and protein that could not be identified using second derivative or chemometric analysis of the spectra and, in addition, they found bands associated with free water and hydrated water at 1419 and 1485 nm, respectively[190,142].

2.3.5.4. Other Applications

There are numerous other applications of 2D correlation spectroscopy, many of which involve the application of the generalized 2D correlation algorithm to other types of spectroscopic methods. To name a few examples, generalized 2D correlation

spectroscopy has been employed in IR studies of molecular structure and orientation of ferroelectric liquid crystals with a naphthalene ring[191], the air/water interface of a monolayer film of 1,2-dipalmitoyl-sn-glycero-3-phosphocholine[192], acid and base titrations of malic acid and succinic acid[193], melting behaviour of microbial polyhydroxyalkanoates[194] and xylene isomerization on H-MFI zeolite[195], in NIR/UV studies of chicken meats during cold storage[196], in gel permeation chromatography studies of octyltriethoxysilane sol-gel polymerization process[197] and in Raman spectroscopic studies of non-oxidative photodegradation of β-carotene[198].

2.3.6. H2D-CS Studies

H2D-CS is an increasingly popular correlation technique, which is a variant of generalized 2D correlation spectroscopy that correlates data from two different spectroscopic methods. This method is particularly useful when information in one region of the electromagnetic spectrum can help to unravel information in another, such as in the assignment of NIR bands, which are difficult to interpret, using well defined bands in the mid-IR spectrum. The first set of H2D-CS data was obtained from the angle X-ray scattering and IR dichroism measurements of dynamically strained block copolymer films[199]. The molecular level re-orientations of the polymer were correlated with the structural re-orientations observed in the X-ray scattering pattern. The first noteworthy H2D-CS application for NIR band assignment was carried out by Barton *et al.* (1992) employing H2D-CS on DRIFT/FTIR and NIR spectra of forages in order to determine NIR wavelength information[152]. The author proposed that the NIR bands identified by H2D-CS can help explain why certain wavenumbers are selected for chemometric calibration models and could be used to assign bands employed in calibrations. H2D-CS was also used in the correlation of temperature-dependent IR and Raman spectral variations of NMA[200] and bands in the amide regions in the Raman spectrum could be assigned to oligomers and dimers of NMA. In 1996, McClure *et al.* carried out a 2D NIR-Raman study of mixtures of lysozyme and sugar in water[201] where the sugar and protein bands that are well assigned in the Raman spectrum were used to identify corresponding bands in the NIR spectrum. The authors used NIR slice spectra generated from the bands for protein or sugar in the Raman spectrum to assign particular bands in the NIR region to

sugar and protein and also proposed H2D-CS could help explain why certain wavenumbers are selected in chemometric calibration models. Other H2D-CS studies reported include NIR-Raman studies of partial miscibility of poly(methyl methacrylate) and poly(4-vinyl phenol) blends[202] and poly(methyl methacrylate) and atactic PS immiscible blends[203], IR-Raman studies of β-lactoglobulin[204] and of 22 proteins[205], Raman-circular dichroism studies of 22 proteins[205] and NIR-mid-IR studies of oligomerization of bis(hydroxyethylterephthalate)[206], nylon 12[207], lignins[208], rice[209], hard red winter and spring wheats[210] and glucose anomers[211]. In the latter study, well defined bands of α and β anomers in the mid-IR spectrum were correlated with the NIR spectrum in the combination region (2410 to 2222 nm) to identify bands assignable to α (2299 nm) and β (2381 and 2353 nm) anomers in the NIR spectrum. Overall this new approach to 2D correlation spectroscopy is very promising for gaining qualitative information about spectra of different regions of the electromagnetic spectrum and could possibly be used to assign NIR bands or wavelengths for quantitative analysis purposes as proposed by Barton *et al.* and McClure *et al.*

2.3.7. Conclusion

Despite the numerous applications published employing generalized 2D correlation spectroscopy, this new data analysis technique is still in its infancy and this field is growing with new variants of this method recently developed, including statistical 2D correlation[157], sample-sample 2D correlation[154,188] and H2D-CS. The latter is particularly interesting to the NIR spectroscopist as it can provide more in-depth information about the nature of the bands and regions employed in chemometric calibration models. Overall, this field is very promising in aiding in spectral interpretation and can provide interesting new applications for quantitative and qualitative analysis by FTIR and FT-NIR spectroscopy.

REFERENCES

1. Smith, B.C. (1996) Choosing the right sampling technique. In: *Fundamentals of Fourier Transform Infrared Spectroscopy* (CRC Press, Boca Raton, FL) 87-137.

2. Harrick Science Corporation (1987) *Optical Spectroscopy: Sampling Techniques Manual.*

3. Belton, P.S. and Wilson R.H. (1990) Infrared sampling methods. In: *Perspectives in Modern Chemical Spectroscopy* (D.L. Andrews ed., Springer-Verlag, Berlin, Germany) 67-86.

4. Ismail, A.A., van de Voort, F.R. and Sedman, J. (1997) Fourier transform infrared spectroscopy: Principles and applications. In: *Instrumental Methods in Food Analysis* (J.R.J. Paré and J.M.R. Bélanger eds., Elsevier, Amsterdam, The Netherlands) 93-139.

5. *Official Methods of Analysis of the Association of Official Analytical Chemists* (1995) 16th ed., AOAC International, Arlington, VA, sec. 972.16.

6. Hewavitharana, A.K. and van Brakel, B. (1997). Fourier transform infrared spectrometric method for the rapid determination of casein in raw milk, *Analyst*, 122, 701-704.

7. Hop, E., Luinge, H.J. and Van Hemert, H. (1993). Quantitative analysis of water in milk by FT-IR spectrometry, *Appl. Spectrosc.*, 47 (8), 1180-1182.

8. Hansen, P.W. (1998). Urea determination in milk using Fourier transform infrared spectroscopy and multivariate calibration, *Milchwissenschaft*, 53 (5), 251-255.

9. Van de Voort, F.R., Sedman, J., Emo, G. and Ismail, A.A. (1992). Assessment of Fourier transform infrared analysis of milk, *J. AOAC Int.*, 75 (5), 780-785.

10. Andersen, S.K., Hansen, P.W. and Andersen, H.V. (2002). Vibrational spectroscopy in the analysis of dairy products and wine. In: *Handbook of Vibrational Spectroscopy* (J.M. Chalmers and P.R. Griffiths eds., John Wiley & Sons Ltd., Chichester, England), 1-10.

11. Cocciardi, R.A., Ismail, A.A., van de Voort, F.R. and Sedman, J. (2002). A rapid Fourier transform infrared quality control method for the determination of lactose, sucrose, fat and total solids in chocolate milk, *Milchwissenschaft*, 57 (2), 90-93.

12. Chen, M. and Irudayaraj, J. (1998) Sampling technique for cheese analysis by FTIR spectroscopy, *J. Food Sci.* 63 (1) 96-99.

13. Firestone, D. and LaBouliere, P. (1965) Determination of isolated *trans* isomers by infrared spectrophotometry, *J. Am. Oil Chem. Soc.*, 48, 437-443.

14. Sleeter, R.T. and Matlock, M. G. (1989) Automated quantitative analysis of isolated (nonconjugated) *trans* isomers using Fourier transform infrared spectroscopy incorporating improvements in the procedure, *J. Am. Oil Chem. Soc.*, 66 (1) 121-127.

15. Ulberth, F. and Haider, H.J. (1992) Determination of low level *trans* unsaturation in fats by Fourier transform infrared spectroscopy, *J. Food Sci.*, 57 (6), 1444-1447.

16. Ulberth, F. and Henninger, M. (1994). Quantitation of *trans* fatty acids in milk fat using spectroscopic and chromatographic methods, *J. Dairy Res.*, 61 517-527.

17. Ratnayake, W.M.N. and Pelletier, G. (1996). Methyl esters from a partially hydrogenated vegetable oil is a better infrared external standard than methyl elaidate for the measurement of total *trans* content, *J. Am. Oil Chem. Soc.*, 73, 1165-1169.

18. Sedman, J., van de Voort, F.R. and Ismail, A.A. (1997) Application of Fourier transform infrared spectroscopy in edible oil analysis. In: *New Techniques and Applications in Lipid Analysis* (R.E. McDonald and M.M. Mossoba eds., AOCS Press, Champaign, IL), 283-324.

19. Sedman, J., van de Voort, F.R. and Ismail, A.A. (1997) Upgrading the AOCS infrared *trans* method for analysis of neat fats and oils by Fourier transform infrared spectroscopy, *J. Am. Oil Chem. Soc.*, 74 907-913.

20. van de Voort, F.R., Ismail, A.A. and Sedman, J. (1995) A rapid, automated method for the determination of *cis* and *trans* content of fats and oils by Fourier transform infrared spectroscopy, *J. Am. Oil Chem. Soc.*, 72, 873-880.

21. De Greyt, W., Kint, A., Kellens, M. and Huyghebaert, A. (1998). Determination of low *trans* levels in refined oils by Fourier transform infrared spectroscopy, *J. Am. Oil Chem. Soc.*, 75 (2) 115-118.

22. Alonso, L., Fraga, M.J., Juarez, M. and Carmona, P. (2002). Fatty acid composition of Spanish shortenings with special emphasis on *trans* unsaturation content as determined by Fourier transform infrared spectroscopy and gas chromatography, *J. Am. Oil Chem. Soc.*, 79 (1) 1-6.

23. Ismail, A.A., van de Voort, F.R., Emo, G. and Sedman, J. (1993). Rapid quantitative determination of free fatty acids in fats and oils by Fourier transform infrared spectroscopy, *J. Am. Oil Chem. Soc.*, 70 (4), 335-341.

24. van de Voort, F.R., Memon, K.P., Sedman, J. and Ismail, A.A. (1996) Determination of solid fat index by Fourier transform infrared spectroscopy, *J. Am. Oil Chem. Soc.*, 73 (4), 411-416.

25. Sedman, J., van de Voort, F.R., Ismail, A.A. and Maes, P. (1998). Industrial validation of Fourier transform infrared *trans* and iodine value analyses of fats and oils, *J. Am. Oil Chem. Soc.*, 75 (1), 33-39.

26. Dubois, J., van de Voort, F.R., Sedman, J., Ismail, A.A. and Ramaswamy, H.R. (1996). Quantitative Fourier transform infrared analysis for anisidine value and aldehydes in thermally stressed oils, *J. Am. Oil Chem. Soc.*, 73 (6), 787-794.

27. Ma, K., van de Voort, F.R., Sedman, J. and Ismail, A.A. (1997). Stoichiometric determination of hydroperoxides in fats and oils by Fourier transform infrared spectroscopy, *J. Am. Oil Chem. Soc.*, 74 (8), 897-906.

28. Nzai, J.M. and Proctor, A. (1998). Determination of phospholipids in vegetable oil by Fourier transform infrared spectroscopy, *J. Am. Oil Chem. Soc.*, 75 (10), 1281-1289.

29. Guillen, M.D. and Cabo, N. (1997). Characterization of edible oils and lard by Fourier transform infrared spectroscopy. Relationaships between composition and frequency of concrete bands in the fingerprint region, *J. Am. Oil Chem. Soc.*, 74 (10), 1281-1286.

30. Man, Y.B. Che and Mirghani, M.E.S. (2000). Rapid method for determining moisture content in crude palm oil by Fourier transform infrared spectroscopy, *J. Am. Oil Chem. Soc.*, 77 (6), 631-637.

31. Setiowaty, G., Man, Y.B. Che, Jinap, S. and Moh, M.H. (2000). Quantitative determination of peroxide value in thermally oxidized palm olein by Fourier transform infrared spectroscopy, *Phytochem. Anal.*, 11 (2), 74-78.

32. Moh, M.H., Tang, T.S., Man, Y.B. Che and Lai, O.M. (1999). Rapid determination of peroxide value in crude palm oil products using Fourier transform infrared spectroscopy, *J. Food Lipids*, 6 (4), 261-270.

33. Man, Y.B. and Setiowaty, G. (1999). Application of Fourier transform infrared spectroscopy to determine free fatty acid contents in palm olein, *Food Chem.*, 66 (1), 109-114.

34. Man, Y.B. and Setiowaty, G. (1999). Determination of anisidine value in thermally oxidized palm olein by Fourier transform infrared spectroscopy, *J. Am. Oil Chem. Soc.*, 76 (2), 243-247.

35. Hendl, O., Howell, J.A., Lowery, J. and Jones, W. (2001). A rapid and simple method for the determination of iodine values using derivative Fourier transform infrared measurements, *Anal. Chim. Acta*, 427, 75-81.

36. Moya Moreno, M.C.M., Mendoza Olivares, D., Amezquita Lopez, F.J., Gimeno Adelantado, J.V. and Bosch Reig, F. (1999). Analytical evaluation of polyunsaturated fatty acids degradation during thermal oxidation of edible oils by Fourier transform infrared spectroscopy, *Talanta*, 50, 269-275.

37. Guillen, M.D. and Cabo, N. (1999). Usefulness of the frequency data of the Fourier transform infrared spectra to evaluate the degree of oxidation of edible oils, *J. Agric. Food Chem.*, 47, 709-719.

38. Verleyen, T., Verhe, R., Cano, A., Huyghebaert, A. and De Greyt, W. (2001). Influence of triacylglycerol characteristics on the determination of free fatty acids in vegetable oils by Fourier transform infrared spectroscopy, *J. Am. Oil Chem. Soc.*, 78 (10), 981-984.

39. Cronin, D.A. and McKenzie, K. (1990) A rapid method for the determination of fat in foodstuffs by infrared spectrometry, *Food Chem.*, 35, 39-49.

40. van de Voort, F.R., Sedman, J. and Ismail, A.A. (1993) A rapid FTIR quality-control method for determining fat and moisture in high-fat products, *Food Chem.*, 48, 213-221.

41. Dion, B., Ruzbie, M., van de Voort, F.R., Ismail, A.A. and Blais, J.S. (1994) Determination of protein and fat in meat by transmission Fourier transform infrared spectrometry, *Analyst*, 119 1765-1771.

42. Lopez-Mahia, P., Simal Gandara, J. and Paseiro-Losada, P. (1992). Validation of ethanol determination in alcoholic beverages by infrared spectrophotometry using orthogonal and derivative functions to correct for water absorption, *Vibr. Spectrosc.*, 3, 133-138.

43. Gallignani, M., Garrigues, S. and de la Guardia, M. (1994). Derivative Fourier transform infrared spectrometric determination of ethanol in alcoholic beverages, *Anal. Chim. Acta*, 287, 275-283.

44. Gallignani, M., Garrigues, S. and de la Guardia, M. (1994). Derivative Fourier transform infrared spectrometric determination of ethanol in beers, *Analyst*, 119, 1773-1778.

45. Perez-Ponce, A., Rambla, F.J., Garrigues, J.M., Garrigues, S. and de la Guardia, M. (1998). Partial-least-squares Fourier transform infrared spectrometric determination of methanol and ethanol by vapour-phase generation, *Analyst*, 123, 1253-1258.

46. Sinnaeve, G., Dardenne, P., Agneessens, R., Lateur, M. and Hallet, A. (1997). Quantitative analysis of raw apple juices using near infrared, Fourier-transform near infrared and Fourier-transform infrared instruments: A comparison of their analytical performances, *J. Near Infrared Spectrosc.*, 5, 1-17.

47. Curran, D.J. and Collier, W.G. (1985). Determination of phenyl isocyanate in flow-injection system with infrared spectrometric detection, *Anal. Chim. Acta*, 177, 259-262.

48. Kellner, R., Lendl, B., Wells, I. and Worsfold, P.J. (1997). Comparison of univariate and multivariate strategies for the determination of sucrose in fruit juices by automated flow injection analysis with Fourier transform infrared detection, *Appl. Spectrosc.*, 51 (2), 227-235.

49. Daghbouche, Y., Garrigues, S., Vidal, M.T. and de la Guardia, M. (1997). Flow injection Fourier transform infrared determination of caffeine in soft drinks, *Anal. Chem.*, 69 (6), 1086-1091.

50. Bouhsain, Z., Garrigues, J.M., Garrigues, S. and de la Guardia, M. (1999). Flow injection Fourier transform infrared determination of caffeine in coffee, *Vibr. Spectrosc.*, 21, 143-150.

51. Garrigues, J.M., Bouhsain, Z., Garrigues, S. and de la Guardia, M. (2000). Fourier transform infrared determination of caffeine in roasted coffee samples, *Fresenius J. Anal. Chem.*, 366, 319-322.

52. Ohnsmann, J., Quintas, G., Garrigues, S. and de la Guardia, M. (2002). Determination of caffeine in tea samples by Fourier transform infrared spectroscopy, *Anal. Bioanal. Chem.*, 374 (3), 561-565.

53. Ayora-Cañada, M.J. and Lendl, B. (2000). Sheath-flow Fourier transform infrared spectrometry for the simultaneous determination of citric, malic and tartaric acids in soft drinks, *Anal. Chim. Acta*, 417, 41-50.

54. Ruiz, A., Ayora-Cañada, M.J. and Lendl, B. (2001). A rapid method for peroxide value determination in edible oils based on flow analysis with Fourier transform infrared spectroscopic detection, *Analyst*, 126, 242-246.

55. Schindler, R., Watkins, M., Vonach, R., Lendl, B. and Kellner, R. (1998). Automated multivariate calibration in sequential injection-Fourier transform infrared spectroscopy for sugar analysis, *Anal. Chem.*, 70 (2), 226-231.

56. Schindler, R., Vonach, R., Lendl, B. and Kellner, R. (1998). A rapid automated method for wine analysis based upon sequential injection (SI)-FTIR spectrometry, *Fresenius J. Anal. Chem.*, 362, 130-136.

57. Haberkorn, M., Hinsmann, P. and Lendl, B. (2002). A mid-IR flow-through sensor for direct monitoring of enzyme catalysed reactions. Case study: Measurement of carbohydrates in beer, *Analyst*, 127, 109-113.

58. LeThanh, H. and Lendl, B. (2000)., Sequential injection Fourier transform infrared spectroscopy for the simultaneous determination of organic acids and sugars in soft drinks employing automated solid phase extraction, *Anal. Chim. Acta*, 422, 63-69.

59. Ma, K., van de Voort, F.R., Ismail, A.A. and Sedman, J. (1998). Quantitative determination of hydroperoxides by Fourier transform infrared spectroscopy with a disposable infrared card, *J. Am. Oil Chem. Soc.*, 75 (9), 1095-1101.

60. Ma, K., van de Voort, F.R., Sedman, J. and Ismail, A.A. (1999). Trans fatty acid determination in fats and margarine by Fourier transform infrared spectroscopy using a disposable infrared card, *J. Am. Oil Chem. Soc.*, 76 (12), 1399-1404.

61. Russin, T., van de Voort, F.R. and Sedman, J. (2003). Novel method for rapid monitoring of lipid oxidation by FTIR spectroscopy using disposable infrared cards, *J. Am. Oil Chem. Soc.*, In Press.

62. Sedman, J., van de Voort, F.R. and Ismail, A.A. (1999) Attenuated total reflectance spectroscopy: Principles and applications in infrared analysis of food. In: *Spectral Methods in Food Analysis* (M.M. Mossoba ed., Marcel Decker Inc., New York, NY), 397-426.

63. van de Voort, F.R. and Ismail, A.A. (1991) Proximate analysis of foods by mid-FTIR spectroscopy, *Trends Food Sci.Technol.*, 2 (1) 13-17.

64. Kemsley, E.K., Wilson, R.H., Poulter, G. and Day, L.L. (1993). Quantitative analysis of sugar solutions using a novel fiber-optic-based sapphire ATR accessory, *Appl. Spectrosc.*, 47 (10), 1651-1654.

65. Kemsley, E.K., Wilson, R.H. and Belton, P.S. (1992). Potential of Fourier transform infrared spectroscopy and fiber optics for process control, *J. Agric. Food Chem.*, 40, 435-438.

66. Dimitri-Hakim, A. (2000). Quantitative analysis of sugars in confectionary products by Fourier transform infrared spectroscopy: Development of analytical methodology using a mid-infrared fiber optic probe and investigation of the effects of sugar-water interactions in model systems. Ph.D. Thesis, McGill University.

67. Cameron, A.G. (1967). An assessment of the potential application of the method of attenuated total reflectance (ATR) infrared qualitative analysis of food materials, *J. Food Technol.*, 2, 223-232.

68. Brierley, P.R. (1999). Imaging stage for Fourier transform infrared spectrometer, *U.S. Patent* 5,965,889.

69. Stanek, Z. (1999). Analysis of combinatorial chemistry media with a single-reflection HATR accessory, *Am. Lab.*, 22-26.

70. Heisz, O. (1989). Fourier-transform infrared spectrometry in food analysis, *Labor Praxis*, 13 (5), 402-404.

71. Cadet, F., Bertrand, D., Robert, P., Maillot, J., Dieudonne, J. and Rouch, C. (1991). Quantitative determination of sugarcane sucrose by multidimensional statistical analysis of its mid-infrared attenuated total reflectance spectra, *Appl. Spectrosc.*, 45 (2), 166-172.

72. Cadet, F. and Offmann, B. (1997). Direct spectroscopic sucrose determination of raw sugar cane juices, *J. Agric. Food Chem.*, 45, 166-171.

73. Cadet, F., Robert, C. and Offmann, B. (1997). Simultaneous determination of sugars by multivariate analysis applied to mid-infrared spectra of biological samples, *Appl. Spectrosc.*, 51 (3), 369-375.

74. Cadet, F. (1999). Measurement of sugar content by multidimensional analysis and mid-infrared spectroscopy, *Talanta*, 48, 867-875.

75. Kemsley, E.K., Zhuo, L., Hammouri, M.K. and Wilson, R.H. (1992). Quantitative analysis of sugar solutions using infrared spectroscopy, *Food Chem.*, 44, 299-304.

76. Bellon-Maurel, V., Vallat, C. and Goffinet, D. (1995). Quantitative analysis of individual sugars during starch hydrolysis by FTIR/ATR spectrometry. Part I: Multivariate calibration study-repeatability and reproducibility, *Appl. Spectrosc.*, 49 (5), 556-562.

77. Rambla, F.J., Garrigues, S., Ferrer, N. and de la Guardia, M. (1998). Simple partial least squares-attenuated total reflectance Fourier transform infrared spectrometric method for the determination of sugars in fruit juices and soft drinks using aqueous standards, *Analyst*, 123, 277-281.

78. Garrigues, S., Rambla, F.J. and de la Guardia, M. (1998). Comparative study of reflectance cells for PLS-FTIR determination of sugars in soft drinks, *Fresenius J. Anal. Chem.*, 362, 137-140.

79. Wojciechowski, C., Dupuy, N., Ta, C.D., Huvenne, J.P. and Legrand, P. (1998). Quantitative analysis of water-soluble vitamins by ATR-FTIR spectroscopy, *Food Chem.*, 63 (1), 133-140.

80. Paradkar, M.M. and Irudayaraj, J. (2002). Rapid determination of caffeine content in soft drinks using FTIR-ATR spectroscopy, *Food Chem.*, 78, 261-266.

81. Fuller, M.P., Gary, M.C. and Stanek, Z. (1990). An FTIR liquid analyzer, *Am. Lab.*, 22, 58-69.

82. De Lene Mirouze, F., Boulou, J.C., Dupuy, N., Meurens, M., Huvenne, J.P. and Legrand, P. (1993). Quantitative analysis of glucose syrups by ATR/FT-IR spectroscopy, *Appl. Spectrosc.*, 47 (8), 1187-1191.

83. Wilson, R.H., Slack, P.T., Appleton, G.P., Sun, L. and Belton, P.S. (1993). Determination of the fruit content of jam using Fourier transform infrared spectroscopy, *Food Chem.*, 47, 303-308.

84. Defernez, M. and Wilson, R.H. (1995). Mid-infrared spectroscopy and chemometrics for determining the type of fruit used in jam, *J. Sci. Food Agric.*, 67, 461-467.

85. Kemsley, E.K., Holland, J.K., Defernez, M. and Wilson, R.H. (1996). Detection of adulteration of raspberry purees using infrared spectroscopy and chemometrics, *J. Agric. Food Chem.* 44, 3864-3870.

86. Sivakesava, S. and Irudayaraj, J. (2001). Prediction of inverted cane sugar adulteration of honey by Fourier transform infrared spectroscopy, *J. Food Sci.*, 66 (7), 972-978.

87. Paradkar, M.M., Sivakesava, S. and Irudayaraj, J. (2002). Discrimination and classification of adulterants in maple syrup with the use of infrared spectroscopic techniques, *J. Sci. Food Agric.*, 82 (5), 497-504.

88. Belton, P.S., Saffa, A.M. and Wilson, R.H. (1987). Use of Fourier transform infrared spectroscopy for quantitative analysis: A comparative study of different detection methods, *Analyst*, 112, 1117-1120.

89. Dupuy, N., Meurens, M., Sombert, B., Legrand, P. and Huvenne, J.P. (1993). Multivariate determination of sugar powders by attenuated total reflectance infrared spectroscopy, *Appl. Spectrosc.*, 47 (4), 452-457.

90. Briandet, R., Kemsley, E.K., and Wilson, R.H. (1996). Discrimination of *Arabica* and *Robusta* in instant coffee by Fourier transform infrared spectroscopy and chemometrics, *J. Agric. Food Chem.*, 44, 170-174.

91. Briandet, R., Kemsley, E.K. and Wilson, R.H. (1996). Approaches to adulteration detection in instant coffees using infrared spectroscopy and chemometrics, *J. Sci. Food Agric.*, 71, 359-366.

92. Al-Jowder, O., Kemsley, E.K. and Wilson, R.H. (1997). Mid-infrared spectroscopy and authenticity problems in selected meats: a feasibility study, *Food Chem.*, 59, 195-201.

93. Kemsley, E.K., Appleton, G.P. and Wilson, R.H. (1994). Quantitative analysis of emulsions using attenuated total reflectance (ATR), *Spectrochim. Acta*, 50A (7), 1235-1242.

94. McQueen, D.H., Wilson, R., Kinnunen, A. and Jensen, E.P. (1995). Comparison of two infrared spectroscopic methods for cheese analysis, *Talanta*, 42, 2007-2015.

95. van de Voort, F.R., Sedman, J. and Emo, G. (1992) A rapid FTIR quality control method for fat and moisture determination in butter, *Food Res. Int.*, 25, 193-198.

96. Nathier-Dufour, N., Sedman, J. and van de Voort, F.R. (1995) A rapid ATR/FTIR quality control method for the determination of fat and solids in sweetened condensed milk, *Milchwissenschaft*, 50, 462-466.

97. Belton, P.S., Saffa, A.M., Wilson, R.H. and Ince, A.D. (1988) The potential of Fourier transform infrared spectroscopy for the analysis of confectionary products, *Food Chem.*, 28, 53-61.

98. Belton, P.S., Wilson, R.H., Sadeghi-Jorabchi, H and Peers, K.E. (1988) A rapid method for the estimation of isolated *trans* double bonds in oils and fats by using Fourier transform infrared spectroscopy combined with attenuated total reflectance, *Lebensm.-Wiss. U.-Technol.*, 21 (3), 153-157.

99. Mossoba, M.M., Yurawecz, M.P. and McDonald, R.E. (1996) Rapid determination of the total *trans* content of neat hydrogenated oils by attenuated total reflection spectroscopy, *J. Am. Oil Chem. Soc.*, 73 (8), 1003-1009.

100. Afran, A. and Newberry, J.E. (1991). Analysis of the degree of unsaturation in edible oils by Fourier transform-infrared/attenuated total reflectance spectroscopy, *Spectrosc. Int.*, 3, 39.

101. van de Voort, F.R., Sedman, J., Emo, G. and Ismail, A.A. (1992). Rapid and direct iodine value and saponification number determination of fats and oils by attenuated total reflectance/Fourier transform infrared spectroscopy, *J. Am. Oil Chem. Soc.*, 69 (11), 1118-1123.

102. Bertran, E., Blanco, M., Coello, J., Iturriaga, H., Maspoch, S. and Montoliu, I. (1999). Determination of olive oil free fatty acid by Fourier transform infrared spectroscopy, *J. Am. Oil Chem. Soc.*, 76 (5), 611-616.

103. Ripoche, A. and Guillard, A.S. (2001). Determination of fatty acid composition of pork fat by Fourier transform infrared spectroscopy, *Meat Sci.*, 58, 299-304.

104. Schulz, H., Schrader, B., Quilitzsch, R. and Steuer, B. (2002). Quantitative analysis of various citrus oils by ATR/FTIR and NIR-FT Raman spectroscopy, *Appl. Spectrosc.*, 56 (1), 117-124.

105. Lai, Y.W., Kemsley, E.K. and Wilson, R.H. (1994). Potential of Fourier transform infrared spectroscopy for the authentication of vegetable oils, *J. Agric. Food Chem.*, 42, 1154-1159.

106. Lai, Y.W., Kemsley, E.K. and Wilson, R.H. (1995). Quantitative analysis of potential adulterants of extra virgin olive oil using infrared spectroscopy, *Food Chem.*, 53, 95-98.

107. Safar, M., Bertrand, D., Robert, P., Devaux, M.F. and Genot, C. (1994). Characterization of edible oils, butters and margarines by Fourier transform infrared spectroscopy with attenuated total reflectance, *J. Am. Oil Chem. Soc.*, 71 (4), 371-377.

108. Dupuy, N., Duponchel, L., Huvenne, J.P., Sombret, B. and Legrand, P. (1996). Classification of edible fats and oils by principal component analysis of Fourier transform infrared spectra, *Food Chem.*, 57 (2), 245-251.

109. Yang, H. and Irudayaraj, J. (2001). Comparison of near-infrared, Fourier transform-infrared, and Fourier transform-Raman methods for determining olive pomace oil adulteration in extra virgin olive oil, *J. Am. Oil Chem. Soc.*, 78 (9) 889-895.

110. Ali, L.H., Angyal, G., Weaver, C.M., Rader, J.I. and Mossoba, M.M. (1996). Determination of total *trans* fatty acids in foods: Comparison of capillary-column gas chromatography and single-bounce horizontal attenuated total reflection infrared spectroscopy, *J. Am. Oil Chem. Soc.*, 73 (12), 1699-1705.

111. Adam, M., Chew, M., Wasserman, S., McCollum, A., McDonald, R.E. and Mossoba, M.M. (1998). Determination of *trans* fatty acids in hydrogenated vegetable oils by attenuated total reflection infrared spectroscopy: Two limited collaborative studies, *J. Am. Oil Chem. Soc.*, 75 (3), 353-358.

112. *Official Methods and Recommended Practices of the American Oil Chemists' Society* (1999) 5th ed., American Oil Chemists' Society, Champaign, IL, Cd 14d-99.

113. *Official Methods of Analysis of the Association of Official Analytical Chemists* (2000) 17th ed., AOAC International, Arlington, VA, sec. 2000.10.

114. Mossoba, M.M., Adam, M. and Lee, T. (2001). Rapid determination of total *trans* fat content – an attenuated total reflection infrared spectroscopy international collaborative study, *J. AOAC Int.*, 84 (4), 1144-1150

115. Sedman, J., van de Voort, F.R. and Ismail, A. (2000). Simultaneous determination of iodine value and *trans* content of fats and oils by single-bounce horizontal attenuated total reflectance Fourier transform infrared spectroscopy, *J. Am. Oil Chem. Soc.*, 77 (4), 399-403.

116. Edelmann, A., Diewok, J., Schuster, K.C. and Lendl, B. (2001). Rapid method for the discrimination of red wine cultivars based on mid-infrared spectroscopy of phenolic wine extracts, *J. Agric. Food Chem.*, 49, 1139-1145.

117. Coimbra, M.A., Goncalves, F., Barros, A.S. and Delgadillo, I. (2002). Fourier transform infrared spectroscopy and chemometric analysis of white wine polysaccharide extracts, *J. Agric. Food Chem.*, 50, 3405-3411.

118. Remmele, R.L. and Stushnoff, C. (1994). Low-temperature IR spectroscopy reveals four stages of water loss during lyophilization of hen egg white lysozyme, *Biopolymers*, 34, 365-370.

119. Smith, B.M., Oswald, L. and Franzen, S. (2002). Single-pass attenuated total reflection Fourier transform infrared spectroscopy for the prediction of protein secondary structure, *Anal. Chem.*, 74, 3386-3391.

120. Smith, B.M. and Franzen, S. (2002). Single-pass attenuated total reflection Fourier transform infrared spectroscopy for the analysis of proteins in H_2O solution, *Anal. Chem.*, 74, 4076-4080.

121. DaCosta, C.J.B. and Baenziger, J.E. (2003). A rapid method for assessing lipid:protein and detergent:protein ratios in membrane-protein crystallization, *Acta Cryst.*, D59, 77-83.

122. Rosencwaig, A. (1980) *Photoacoustics and Photoacoustic Spectroscopy* (P.J. Elving and J.D. Winefordner eds., John Wiley& Sons, New York, NY).

123. Scotter, C.N.G. (1997) Non-destructive spectroscopic techniques for the measurement of food quality, *Trends Food Sci.Technol.*, 8, 285-291.

124. McQueen, D.H., Wilson, R.H. and Kinnunen, A. (1995). Near and mid-infrared photoacoustic analysis of principal components of foodstuffs, *Trends Anal. Chem.*, 14 (10), 482-492.

125. Poulet, P., Chambron, J. and Unterreiner, R. (1980). Quantitative photoacoustic spectroscopy applied to thermally thick samples, *J. Appl. Phys.*, 51, 1738-1742.

126. Belton, P.S. and Tanner, S.F. (1983) Determination of the moisture content of starch using near infrared photoacoustic spectroscopy, *Analyst*, 108, 591-596.

127. Letzelter, N.S., Wilson, R.H., Jones, A.D. and Sinnaeve, G. (1995) Quantitative determination of the composition of individual pea seeds by Fourier transform infrared photoacoustic spectroscopy, *J. Sci. Food Agric.*, 67 239-245.

128. Ootake, Y. and Kokot, S. (1998). Discrimination between glutinous and non-glutinous rice by vibrational spectroscopy. I: Comparison of FT-NIR DRIFT, PAS and Raman spectroscopy, *J. Near Infrared Spectrosc.*, 6, 241-249.

129. Favier, J.P., Bicanic, D., van de Bovenkamp, P., Chirtoc, M. and Helander, P. (1996). Detection of total *Trans* fatty acids content in margarine: An

intercomparison study of GLC, GLC + TLC, FT-IR, and optothermal window (open photoacoustic cell), *Anal. Chem.*, 68 (5), 729-733.

130. Favier, J.P., Bicanic, D., Doka, O., Chirtoc, M. and Helander, P. (1997). Optothermal detection of infrared radiation-induced absorption in aqueous solutions of carbohydrates: Lactose and corn starch, *J. Agric. Food Chem.*, 45, 777-780.

131. Favier, J.P., Bicanic, J., Cozijnsen, B., van Veldhuizen, M. and Helander, P. (1998). CO_2 laser infrared optothermal spectroscopy for quantitative adulteration studies in binary mixtures of extra-virgin olive oil, *J. Am. Oil Chem. Soc.*, 75 (3), 359-362.

132. Yang, H. and Irudayaraj, J. (2000). Characterization of semisolid fats and edible oils by Fourier transform infrared photoacoustic spectroscopy, *J. Am. Oil Chem. Soc.*, 77 (3), 291-295.

133. Irudayaraj, J. and Yang, H. (2000). Analysis of cheese using step-scan Fourier transform infrared photoacoustic spectroscopy, *Appl. Spectrosc.*, 54 (4), 595-600.

134. Sivakesava, S. and Irudayaraj, J. (2000). Analysis of potato chips using FTIR photoacoustic spectroscopy, *J. Sci. Food Agric.*, 80, 1805-1810.

135. Yang, H. and Irudayaraj, J. (2001). Characterization of beef and pork using Fourier-transform infrared photoacoustic spectroscopy, *Lebensm.-Wiss. U.-Technol.*, 34, 402-409.

136. Irudayaraj, J., Sivakesave, S., Kamath, S. and Yang, H. (2001). Monitoring chemical changes in some foods using Fourier transform photoacoustic spectroscopy, *J. Food Sci.*, 66 (9), 1416-1421.

137. Hong, Y. and Irudayaraj, J. (1999). Estimation of particle size by DRIFTS and FTIR-PAS, *Particulate Sci. Technol.*, 17, 269-282.

138. Culler, S.R. (1993). Diffuse reflectance infrared spectroscopy: Sampling techniques for qualitative/quantitative analysis of solids. *In: Practical Sampling Techniques for Infrared Analysis* (P.B. Coleman ed., CRC Press, New York, NY), 93-106.

139. Kemsley, E.K., Ruault, S. and Wilson, R.H. (1995). Discrimination between *Coffea arabica* and *Coffea canephora* variant *robusta* beans using infrared spectroscopy, *Food Chem.*, 54, 321-326.

140. Reeves, J.B. and Zapf, C.M. (1998). Mid-infrared diffuse reflectance spectroscopy for discriminant analysis of food ingredients, *J. Agric. Food Chem.*, 46, 3614-3622.

141. Goodacre, R. and Anklam, E. (2001). Fourier transform infrared spectroscopy and chemometrics as a tool for the rapid detection of other vegetable fats mixed in cocoa butter, *J. Am. Oil Chem. Soc.*, 78 (10), 993-1000.

142. Ozaki, Y., Sasic, S., Tanaka, T. and Noda, I. (2001). Two-dimensional correlation spectroscopy: Principle and recent theoretical development, *Bull.Chem. Soc. Jpn.*, 74, 1-17.

143. Aue, W.P., Bartholdi, E. and Ernst, R.R. (1976). Two-dimensional spectroscopy. Application to nuclear magnetic resonance, *J. Chem Phys.*, 64, 2229.

144. Noda, I. (1986). *Bull. Am. Phys. Soc.*, 31, 520.

145. Noda, I. (1990). Two-dimensional infrared (2D IR) spectroscopy: Theory and applications, *Appl. Spectrosc.*, 44 (4), 550-561.

146. Noda, I. (1993). Generalized two-dimensional correlation method applicable to infrared, Raman, and other types of spectroscopy, *Appl. Spectrosc.*, 47 (9), 1329-1336.

147. Czarnecki, M.A., Maeda, H., Ozaki, Y., Suzuki, M. and Iwahashi, M. (1998). Resolution enhancement and band assignments for the first overtone of OH stretching mode of butanols by two-dimensional near-infrared correlation spectroscopy. Part I: *sec*-Butanol, *Appl. Spectrosc.*, 52 (7), 994-1000.

148. Noda, I. (1989). Two-dimensional infrared spectroscopy, *J. Am. Chem. Soc.*, 111, 8116-8118.

149. Wang, Y., Tsenkova, R., Amari, M., Terada, F., Hayashi, T., Abe, A. and Ozaki, Y. (1998). Potential of two-dimensional correlation spectroscopy in analyses of NIR spectra of biological fluids. I. Two-dimensional correlation analysis of protein and fat concentration-dependent spectral variations of milk, *Analusis*, 26 (4), M64-M69.

150. Ozaki, Y., Murayama, K. and Wang, Y. (1999). Application of two-dimensional near-infrared correlation spectroscopy to protein research, *Vibr. Spectrosc.*, 20, 127-132.

151. Ozaki, Y., Liu, Y. and Noda, I. (1997). Two-dimensional infrared and near-infrared correlation spectroscopy: Applications to studies of temperature-dependent spectral variations of self-associated molecules, *Appl. Spectrosc.*, 51 (4), 526-535.

152. Barton II, F.E., Himmelsbach, D.S., Duckworth, J.H. and Smith, M.J. (1992). Two-dimensional vibration spectroscopy: Correlation of mid- and near-infrared regions, *Appl. Spectrosc.*, 46 (3) 420-429.

153. Ozaki, Y. and Noda, I. (1996). Potential of generalized two-dimensional correlation spectroscopy in the near infrared region, *J. Near Infrared Spectrosc.*, 4, 85-99.

154. Sasic, S., Muszynski, A. and Ozaki, Y. (2000). A new possibility of the generalized two-dimensional correlation spectroscopy. 1. Sample-sample correlation spectroscopy, *J. Phys. Chem. A*, 104, 6380-6387.

155. Sasic, S., Muszynski, A. and Ozaki, Y. (2001). New insight into the mathematical background of generalized two-dimensional correlation spectroscopy and the influence of mean normalization pretreatment on two-dimensional correlation spectra, *Appl. Spectrosc.*, 55 (3), 343-349.

156. Ozaki, Y., Sasic, S. and Jiang, H.J. (2001). How can we unravel complicated near infrared spectra? –Recent progress in spectral analysis methods for resolution enhancement and band assignments in the near infrared region, *J. Near Infrared Spectrosc.*, 9, 63-95.

157. Sasic, S. and Ozaki, Y. (2001). Statistical two-dimensional correlation spectroscopy: Its theory and applications to sets of vibrational spectra, *Anal. Chem.*, 73 (10), 2294-2301.

158. Sasic, S. and Ozaki, Y. (2001). Comparison of principal component analysis and generalized two-dimensional correlation spectroscopy: Spectral analysis of synthetic model system and near-infrared spectra of milk, *Appl. Spectrosc.*, 55 (1), 29-38.

159. Noda, I., Dowrey, E. and Marcott, C. (1990). Two-dimensional infrared (2D IR) analysis of poly(methyl methacrylate), *Polym. Prepr.*, 31 (1), 576-577.

160. Noda, I., Dowrey, E. and Marcott, C. (1993). Recent developments in two-dimensional infrared (2D IR) correlation spectroscopy, *Appl. Spectrosc.*, 47 (9), 1317-1323.

161. Palmer, R.A., Gregoriou, V.G. and Chao, J.L. (1992). Dynamic rheooptical characterization of polymer films using step-scan FT-IR, *Polym. Prepr.*,33 (1), 1222.

162. Stein, R.S., Satkowski, M. and Noda, I. (1992). The nature of the crystral/amorphous interface in polyethylene and its blends. In: *Polymer Blends, Solutions and Interfaces* (I. Noda and D.N. Rubingh eds., Elsevier, New York, NY), 109-131.

163. Gregoriou, V.G., Chao, J.L., Toriumi, H., Marcott, C., Noda, I. and Palmer, R.A. (1992). Time-resolved vibrational spectroscopy of liquid crystals and polymer films using step-scan 2D FT-IR, *Proc. SPIE*, 1575, 209-210.

164. Palmer, R.A., Manning, C.J., Rzepiela, J.A., Widder, J.M., Thomas, P.J., Chao, J.L., Marcott, C. and Noda, I. (1989). Application of step-scan interferometry to dynamic infrared spectroscopy, *Proc. SPIE*, 1145, 277-279.

165. Noda, I., Dowrey, E. and Marcott, C. (1991). Dynamic linear dichroism of polymers, *Polym. Prepr.*, 32 (3), 671-672.

166. Marcott, C., Dowrey, A.E. and Noda, I. (1994). Dynamic two-dimensional IR spectroscopy, *Anal. Chem.*, 66, 1065A-1075A.

167. Jung, Y.M., Shin, H.S., Czarnick-Matusewiscz, B., Noda, I. and Kim, S.B. (2002). Characterization of transition temperatures of a Langmuir-Blodgett film of poly(*tert*-butyl methacrylate) by two-dimensional correlation spectroscopy and principal component analysis, *Appl. Spectrosc.*, 56 (12), 1568-1574.

168. Shin, H.S., Jung, Y.M., Chang, T., Ozaki, Y. and Kim, S.B. (2002). Characterization of β-transition of poly(*tert*-butyl methacrylate) thin films by two-dimensional infrared correlation spectral analysis, *Vibr. Spectrosc.*, 29 (1-2), 73-77.

169. Noda, I., Liu, Y. and Ozaki, Y. (1996). Two-dimensional correlation spectroscopy study of temperature-dependent spectral variations of *N*-methylacetamide in the pure liquid state. 1. Two-dimensional infrared analysis, *J. Phys. Chem.*, 100, 8665-8673.

170. Ismoyo, F., Wang, Y. and Ismail, A.A. (2000). Examination of the effect of heating on the secondary structure of avidin and avidin-biotin complex by resolution-enhanced 2D infrared correlation spectroscopy, *Appl. Spectrosc.*, 54 (7), 939-947.

171. Heinz, F., Mantsch, H.H. and Schultz, C.P. (2000). Sequential unfolding events in proteins monitored by 2D correlation analysis of FTIR spectra, *AIP Conference Proceedings*, 503, 95-102.

172. Schultz, C.P., Barzu, O. and Mantsch, H.H. (2000). Two-dimensional infrared correlation analysis of protein unfolding: Use of spectral simulations to validate structural changes during thermal denaturation of bacterial CMP kinases, *Appl. Spectrosc.*, 54 (7), 931-938.

173. Paquet, M.J., Laviolette, M., Pezolet, M. and Auger, M. (2001). Two-dimensional infrared correlation spectroscopy study of the aggregation of cytochrome c in the presence of dimyristoylphosphatidylglycerol, *Biophys. J.*, 81 (1), 305-312.

174. Lee, J. and Shin, S. (2002). Two-dimensional correlation analysis of peptide unfolding: Molecular dynamics simulations of β hairpins, *J. Phys. Chem. B*, 106 (34), 8796-8802.

175. Wu, Y., Murayama, K., Czarnick-Matusewiscz, B. and Ozaki, Y. (2002). Two-dimensional attenuated total reflection/infrared correlation spectroscopy studies on concentration and heat-induced structural changes of human serum albumin in aqueous solutions, *Appl. Spectrosc.*, 56 (9), 1186-1193.

176. Murayama, K., Wu, Y., Czarnick-Matusewicz, B. and Ozaki, Y. (2001). Two-dimensional/attenuated total reflection infrared correlation spectroscopy studies on secondary structural changes in human serum albumin aqueous solutions: pH-Dependent structural changes in the secondary structures and in the hydrogen bondings of side chains, *J. Phys. Chem. B*, 105 (20), 4763-4769.

177. Czarnick-Matusewicz, B. Murayama K., Wu, Y. and Ozaki, Y. (2000). Two-dimensional attenuated total reflection/infrared correlation spectroscopy of adsorption-induced and concentration-dependent spectral variations of β-lactoglobulin in aqueous solutions, *J. of Phys. Chem. B,* 104 (32), 7803-7811.

178. Wu, Y., Murayama, K. and Ozaki, Y. (2001). Two-dimensional infrared spectroscopy and principal component analysis studies of the secondary structure and kinetics of hydrogen-deuterium exchange of human serum albumin, *J. Phys. Chem. B*, 105 (26), 6251-6259.

179. Nabet, A. and Pézolet, M. (1997). Two-dimensional FT-IR spectroscopy: A powerful method to study the secondary structure of proteins using H-D exchange, *Appl. Spectrosc.*, 51 (4), 466-469.

180. Pancoska, P., Kubelka, J. and Keiderling, T.A. (1999). Novel use of a static modification of two-dimensional correlation analysis. Part I: Comparison of the secondary structure sensivity of electronic circular dichroism, FT-IR, and Raman spectra of proteins, *Appl. Spectrosc.*, 53 (6), 655-665.

181. Liu, Y., Ozaki, Y. and Noda, I. (1996). Two-dimensional Fourier-transform near-infrared correlation spectroscopy study of dissociation of hydrogen-bonded *N*-methylacetamide in the pure liquid state, *J. Phys. Chem.*, 100 (18), 7326-7332.

182. Ozaki, Y., Liu, Y. and Noda, I. (1997). Two-dimensional near-infrared correlation spectroscopy study of premelting behavior of nylon 12, *Macromolecules*, 30 (8), 2391-2399.

183. Ozaki, Y., Murayama, K. and Wang, Y. (1999). Application of two-dimensional near-infrared correlation spectroscopy to protein research, *Vibr. Spectrosc.*, 20, 127-132.

184. Murayama, K. and Ozaki, Y. (2002). Two-dimensional near-IR correlation spectroscopy study of molten globule-like state of ovalbumin in acidic pH region: Simultaneous changes in hydration and secondary structure, *Biopolymers*, 67 (6), 394-405.

185. Ozaki, Y., Liu, Y. and Noda, I. (1997). Two-dimensional infrared and near-infrared correlation spectroscopy: Applications to studies of temperature-dependent spectral variations of self-associated molecules, *Appl. Spectrosc.*, 51 (4), 526-535.

186. Czarnecki, M.A. (2000). Two-dimensional correlation analysis of the second overtone of the ν(OH) mode of octan-1-ol in the pure liquid phase, *Appl. Spectrosc.*, 54 (12), 1767-1770.

187. Czarnecki, M.A., Czarnick-Matusewicz, B., Ozaki, Y. and Iwahashi, M. (2000) Resolution enhancement and band assignments for the first overtone of OH(D) stretching modes of butanols by two-dimensional near-infrared correlation spectroscopy. 3. Thermal dynamics of hydrogen bonding in butan-1-(ol-d) and 2-methylpropan-2-(ol-d) in the pure liquid states, *J. Phys. Chem. A*, 104 (21), 4906-4911.

188. Sasic, S., Muszynski, A. and Ozaki, Y. (2000). A new possibility of the generalized two-dimensional correlation spectroscopy. 2. Sample-sample and wavenumber-wavenumber correlations of temperature-dependent near-infrared of oleic acid in the pure liquid state, *J. Phys. Chem. A*, 104 (27), 6388-6394.

189. Czarnecki, M.A. (2002). Near-infrared spectroscopic study of self-association of octanoic acid, *Chem. Phys. Lett.*, 368, (1,2), 115-120.

190. Czarnik-Matusewicz, B., Murayama, K., Tsenkova, R. and Ozaki, Y. (1999). Analysis of near-infrared spectra of complicated biological fluids by two-dimensional correlation spectroscopy: Protein and fat concentration-dependent spectral changes of milk, *Appl. Spectrosc.*, 53, 1582-1594.

191. Nagasaki, Y. and Ozaki, Y. (2000). A polarized infrared spectroscopic study on electric-field-induced layer rotation of ferroelectric liquid crystal mixtures with ultrashort pitch, *Phys. Chem. Chem. Phys.*, 2 (13), 3037-3042.

192. Elmore, D. and Dluhy, R.A. (2000). Pressure-dependent changes in the infrared C-H vibrations of monolayer films at the air/water interface revealed by two-dimensional infrared correlation spectroscopy, *Appl. Spectrosc.*, 54 (7), 956-962.

193. Ayora-Cañada, M.J. and Lendl, B. (2000). Study of acid-base titration of succinic and malic acid in aqueous solution by two-dimensional FTIR correlation spectroscopy, *Vibr. Spectrosc.*, 24 (2), 297-306.

194. Wu, Q., Tian, G., Sun, S., Noda, I. and Chen, G. (2001). Study of microbial polyhydroxyalkanoates using two-dimensional Fourier-transform infrared correlation spectroscopy, *J. Appl. Polym. Sci.*, 82 (4), 934-940.

195. Thibault-Starzyk, F., Vimont, A. and Gilson, J. (2001). 2D correlation IR spectroscopy of xylene isomerization on H-MFI zeolite, *Stud. Surf. Sci. Catal.*, 135, 1828-1836.

196. Liu, Y. and Chen, Y. (2000). Two-dimensional correlation spectroscopy study of visible and near-infrared spectral variations of chicken meats in cold storage, *Appl. Spectrosc.*, 54 (10), 1458-1470.

197. Izawa, K, Ogasawara, T., Masuda, H., Okabayashi, H. and Noda, I. (2002). Two-dimensional correlation gel permeation chromatography study of octyltriethoxysilane sol-gel polymerization process, *Macromolecules*, 35 (1), 92-96.

198. Noda, I. And Marcott, C. (2002). Two-dimensional Raman (2D Raman) correlation spectroscopy study of non-oxidative photodegradation of β-carotene, *J. Phys. Chem. A*, 106 (14), 3371-3376.

199. Noda, I. (1990). Two-dimensional correlation approach to the dynamic rheooptical characterization of polymers, *Chemtracts-Macromol. Chem.*, 1 (2), 89-105.

200. Noda, I., Liu, Y. and Ozaki, Y. (1996). Two-dimensional correlation spectroscopy study of temperature-dependent spectral variations of *N*-methylacetamide in the pure liquid state. 2. Two-dimensional Raman and infrared-Raman heterospectral analysis, *J. Phys. Chem.*, 100, 8674-8680.

201. McClure, W.F., Maeda, H., Dong, J., Liu, Y. and Ozaki, Y. (1996). Two-dimensional correlation of Fourier transform near-infrared and Fourier transform Raman spectra I: Mixtures of sugar and protein, *Appl. Spectrosc.*, 50 (4), 467-475.

202. Ren, Y., Matsushita, A., Matsukawa, K., Inoue, H., Minami, Y., Noda, I. and Ozaki, Y. (2000). Two-dimensional Raman and Raman-near infrared heterospectral correlation spectroscopy studies of the specific interaction in partially miscible blends of poly(methyl methacrylate) and poly(4-vinyl phenol). In: *Two-Dimensional Correlation Spectroscopy* (Y. Ozaki and I. Noda eds., American Institute of Physics, College Park, MD), 250.

203. Matsushita, A., Ren, Y., Matsukawa, K., Inoue, H., Minami, Y., Noda, I. and Ozaki, Y. (2000). Two-dimensional Fourier-transform Raman and near-infrared correlation spectroscopy studies of poly(methyl methacrylate) blends 1. Immiscible blends of poly(methyl methacrylate) and atactic polystyrene, *Appl. Spectrosc.*, 54 (2), 171-180.

204. Jung, Y.M., Czarnik-Matusewicz, B. and Ozaki, Y. (2000). An IR vs. Raman 2D heterospectral correlation study of the secondary structure of β-lactoglobulin in aqueous solutions, *AIP Conference Proceedings,* 503, 275-278.

205. Kubelka, J., Pancoska, P. and Keiderling, T.A. (1999). Novel use of a static modification of two-dimensional correlation analysis. Part II: hetero-spectral correlations of protein Raman, FT-IR, and circular dichroism spectra, *Appl. Spectrosc.*, 53 (6), 666-671.

206. Amari, T. and Ozaki, Y. (2002). Generalized two-dimensional attenuated total reflection/infrared and near-infrared correlation spectroscopy studies of real-time monitoring of the oligomerization of bis(hydroxyethyl terephthalate), *Macromolecules*, 35, 8020-8028.

207. Czarnecki, M.A., Wu, P. and Siesler, H.W. (1998). 2D FT-NIR and FT-IR correlation analysis of temperature-induced changes of nylon 12, *Chem. Phys. Lett.*, 283 (5,6), 326-332.

208. Barton II, F.E. and Himmelsbach, D.S. (1993). Two-dimensional vibrational spectroscopy II: Correlation of the absorptions of lignins in the mid- and near-infrared, *Appl. Spectrosc.*, 47 (11), 1920-1925.

209. Barton II, F.E., Himmelsbach, D.S., McClung, A.M. and Champagne, E.L. (2002). Two-dimensional vibration spectroscopy of rice quality and cooking, *Cereal Chem.*, 79 (1), 143-147.

210. Barton II, F.E., Himmelsbach, D.S. and Archibald, D.D. (1996). Two-dimensional vibrational spectroscopy V: Correlation of mid- and near-infrared of hard red winter and spring wheats, *J. Near Infrared Spectrosc.*, 4, 139-152.

211. Awichi, A., Tee, E. M., Srikanthan, G. and Zhao, W. (2002). Identification of overlapped near-infrared bands of glucose anomers using two-dimensional near-infrared and middle-infrared correlation spectroscopy, *Appl. Spectrosc.*, 56 (7), 897-901.

CHAPTER 3

MONITORING OF LACTOSE HYDROLYSIS IN MILK BY SINGLE-BOUNCE ATTENUATED TOTAL REFLECTANCE FOURIER TRANSFORM INFRARED SPECTROSCOPY

3.1. ABSTRACT

A Fourier transform infrared (FTIR) method for monitoring the hydrolysis of lactose in milk has been developed based on the use of a single-bounce attenuated total reflectance (SB-ATR) accessory. Preliminary work indicated that the SB-ATR accessory was suitable for the analysis of sugars in milk and the trace by-products produced by transgalactosylation were determined to be unlikely to interfere with calibration development. Calibration standards were formulated by mixing milk and Lacteeze® (99% lactose-free) gravimetrically with lactose, glucose, galactose and distilled water to introduce matrix variability. The spectra of the formulated calibration standards were recorded and partial-least-squares regression (PLS) was used to derive a calibration relating the spectral information to the sugar concentrations of the standards, calculated from gravimetric and high-pressure liquid chromatography (HPLC) data. Lactose in milk was hydrolyzed at 4°C using β-galactosidase obtained from *Kluyveromyces lactis*, with samples taken for FTIR and HPLC analysis at selected times over 48 hours. The concentrations of lactose, glucose and galactose were predicted for the FTIR analyzed samples using the PLS calibration model and compared to HPLC results yielding standard errors of prediction (SEP) of 0.20, 0.13 and 0.10% (w/v) for lactose, glucose and galactose respectively. The results indicate that the SB-ATR FTIR method is highly accurate and could serve as a convenient means by which to monitor lactose hydrolysis in the manufacture of lactose-reduced milk.

3.2. INTRODUCTION

Milk analysis is one of the earliest and most important applications of quantitative infrared (IR) spectroscopy in the domain of food analysis and today both herd management and milk payment are heavily reliant on centralized laboratories using IR instruments for the determination of of fat, protein and lactose[1], with dairy plants using

them for quality control applications[2]. Filter-based instruments, such as the MilkoScan[3,4], were originally employed and instrumentation changed relatively little until van de Voort *et al.* demonstrated that milk analysis could be carried out by Fourier transform infrared (FTIR) spectroscopy with the same degree of accuracy[5]. The use of FTIR spectrometers for milk analysis was approved by the Association of Official Analytical Chemists (AOAC) International in 1995[6], following an international collaborative study[7], and FTIR milk analyzers are currently on the market. The capability of FTIR spectrometers to record all wavelengths simultaneously has facilitated the development of new IR-based methods for the analysis of other dairy products such as the development of an FTIR spectroscopic method for the analysis of fat and total solids in sweetened condensed milk[8] and the development of a rapid FTIR quality control method for the determination of lactose, sucrose, fat and total solids in chocolate milk[9] for use in a production environment.

Lactose-reduced and lactose-free milk are produced by treating milk with β-galactosidase, usually from *Kluyveromyces lactis*, to convert lactose into its respective monosaccharides, glucose and galactose. The progress of the enzymatic reaction is sensitive to temperature as well as the initial concentration of the enzyme[10], and transgalactosylation can produce disaccharides other than lactose as well as some trisaccharides and higher oligosaccharides[11-13], the oligosaccharides reaching levels of up to 5% of the initial lactose concentration[13]. A simple means of monitoring the reaction as it progresses would allow for improved control and optimization of the process. Determination of lactose in milk has been made by a variety of means, including high-pressure liquid chromatography (HPLC)[11], paper chromatography with colorimetric detection[14-16], enzyme kits[17] and freezing point cryoscopy[18,19]. These methods are tedious and time-consuming, with the exception of the cryoscopic method which has the disadvantage that the production of oligosaccharides during the hydrolysis reaction interferes with the analysis[20]. Although conventional filter-based IR milk analysis equipment is capable of measuring lactose in milk, these measurements become meaningless in monitoring lactose hydrolysis as the main products, glucose and galactose have similar spectral signatures and cannot be differentiated from lactose. However, newer FTIR milk analysis instrumentation, with its higher resolution and access to all

wavelengths in the mid-IR region, could potentially be useful for this application. Hansen *et al.* investigated the use of a MilkoScan FT120 spectrometer to monitor the lactose hydrolysis process but without actually calibrating the instrument and giving quantitative numbers[10]. The standard operational configuration of these analyzers uses a high-pressure homogenizer/pump to deliver the sample to a thermostated (40°C) 37-μm CaF_2 flow cell[21,22], which may make this approach problematic because; (a) homogenization and heating of the sample being analyzed would disrupt the normal progress of the enzymatic reaction being monitored and (b) the spectral analysis of sugar mixtures is problematic with CaF_2 windows as their transmission cut-off eliminates some of the sugar spectral information that allows one sugar to be differentiated from another. A potential means of overcoming these limitations to FTIR analysis of the lactose hydrolysis process could be the use of a single-bounce attenuated total reflectance (SB-ATR) accessory equipped with a ZnSe crystal, which transmits IR radiation down to a much lower frequency. This paper reports on the development of a practical quantitative SB-ATR method for monitoring the progress of the enzymatic reaction used in the production of lactose-reduced milk.

3.3. EXPERIMENTAL

3.3.1. Chemicals and Reagents

D(+)-Galactose, α-D(+)-glucose and α-lactose monohydrate were obtained from Sigma (St. Louis, MO). Skim milk, whole milk (3.25%), and Lacteeze® (99% lactose-free milk), skim and 2%, were obtained from Natrel (Saint-Laurent, QC). Validase Yeast Lactase, a *K. lactis* β-galactosidase enzyme with an activity of 50,000 ONPGU/g was obtained from Valley Research Inc. (South Bend, IN). All other reagents used were of analytical grade and obtained from Fisher Scientific (Montreal, QC).

3.3.2. Instrumentation

3.3.2.1. FTIR Spectroscopy

FTIR spectra were recorded using an ABB Bomem (Québec City, QC) MB-150 spectrometer equipped with a temperature-controlled (Watlow System Integrators,

Decorah, IA) ZnSe SB-ATR accessory (Harrick, Ossining, NY). The temperature of the ZnSe crystal was maintained at 30 ± 0.1°C to minimize spectral variability associated with changes in room temperature. All spectra were collected by co-addition of 64 scans at a resolution of 8 cm^{-1}. Between each analysis, the ATR crystal was wiped with a tissue soaked in detergent, rinsed with deionized water and wiped dry with a lint-free tissue. A background single-beam spectrum of the dry clean ZnSe crystal was taken prior to loading each sample, followed by collecting the spectrum of the sample, and storing the absorbance spectra used for calibration development and sample analysis to disk. The spectrometer was kept purged with dry air by a Balston air drier (Lexington, MA) to avoid spectral contributions from atmospheric water vapour and carbon dioxide. For the qualitative FTIR spectral comparison of oligosaccharides obtained from lactose hydrolyzed in milk and Lacteeze by HPLC fractionation, the IR spectra were recorded (32 scans @ 4 cm^{-1}) on a Biorad, Excalibur Series, FTIR spectrometer (Cambridge, MA) equipped with a Pike ZnSe SB-ATR accessory (Pike Technologies, Madison, WI) requiring only 10 μL of sample.

3.3.2.2. HPLC

HPLC analysis was carried out using a Waters (Millipore, Milford, MA) HPLC system with a 600E system controller, a U 6K injection and a R401 differential refractometer detector. The HPLC system was controlled by Millenium 2010 computer software (Millipore, Milford, MA). An ION-300 polymeric cation exchange column (Transgenomic Inc., San José, CA) was used with a mobile phase of 0.02 N H_2SO_4, a flowrate of 0.4 mL/min and a column temperature of 30 ± 0.1°C, capable of separating glucose from galactose as well as separating monosaccharides from disaccharides and trisaccharides.

3.3.3. Calibration

3.3.3.1. FTIR Analysis

A set of 26 calibration standards (Table 3.1) was prepared by blending whole milk with Lacteeze and adding lactose, glucose, galactose and distilled water in various ratios

to provide variability for all of the constituents of interest. HPLC provided the reference values for the milks used to formulate the calibration standards and the final composition of the standards is given in Table 3.2. The FTIR absorbance spectra of the standards were used to develop a partial-least-squares (PLS) calibration to quantitate total lactose, glucose and galactose using Turbo Quant software (Nicolet Instruments, Madison, WI). The correlation, variance and pure component spectra generated from the PLS software package were used to select regions in developing and optimizing the calibration model for each component. The optimal number of factors used for each component was determined from the minimum point on the predicted residual error sum of squares (PRESS) plot. The overall suitability of the calibration model ultimately developed was assessed by calculating the mean difference and standard deviation of the differences for accuracy (MD_a and SDD_a, respectively) between the leave-one-out cross-validation predictions and the actual gravimetric and HPLC determined values of the calibration standards.

3.3.3.2. HPLC Analysis

The HPLC was calibrated using 6 individual solutions of glucose, galactose and lactose ranging from 0.01 to 2.00% (w/v) prepared in distilled water. The calibration was validated using triplicate injections of 3 solutions of intermediate concentrations of each of the three sugars (Table 3.3). In order to carry out HPLC analysis of milk samples, 0.3 mL of the sample was first deproteinated and clarified using 1.2 mL of a mixture of a 1.8% (w/v) solution of $Ba(OH)_2 \bullet 8H_2O$ and a 2% (w/v) solution of $ZnSO_4 \bullet 7H_2O$ according to the method described by Nakanishi *et al.*[23], centrifuged and the supernatant filtered through a 0.45-μm nylon filter prior to HPLC injection. The efficacy of milk analysis by HPLC was evaluated by standard addition of lactose to milk at levels of 0.05, 0.5 and 2% (w/v) and the results for lactose recovery are listed in Table 3.4.

Table 3.1: Preparation of calibration matrix for PLS regression

Standard	Whole Milk (mL)	Skim Milk (mL)	2% Lacteeze (mL)	Skim Lacteeze (mL)	Lactose (g)	Glucose (g)	Galactose (g)	Water (mL)
1	100.0	-	-	-	-	-	-	-
2	-	100	-	-	-	-	-	-
3	-	-	100	-	-	-	-	-
4	50.0	-	-	50	-	-	-	-
5	100.0	-	-	-	0.5007	1.0008	0.4009	-
6	-	100	-	-	0.2001	0.2006	2.0005	-
7	100.0	-	-	-	-	2.5007	0.1003	-
8	-	100	-	-	0.1001	2.7003	1.4001	-
9	100	-	-	-	-	0.8006	2.6005	-
10	50	-	-	-	-	1.2005	0.801	50
11	-	75	-	-	-	1.7001	1.0005	25
12	-	50	-	-	-	0.1076	0.1031	50
13	60	-	40	-	-	-	0.8002	-
14	-	40	60	-	0.3011	-	1.5003	-
15	-	20	-	80	-	1.0038	-	-
16	-	20	30	-	-	-	-	50
17	20	-	-	20	-	-	0.5001	60
18	-	10	40	-	-	1.0003	0.5011	50
19	-	-	100	-	0.1504	0.3	-	-
20	-	-	-	100	-	0.7005	0.5011	-
21	-	-	100	-	0.3	0.3001	-	-
22	-	-	-	100	1.505	0.1031	-	-
23	-	-	100	-	3.008	-	-	-
24	100	-	-	-	-	-	3.0009	-
25	-	100	-	-	-	3.001	-	-
26	-	-	50	-	-	1.2507	1.25	50

Table 3.2: Carbohydrate composition of standards used for calibration

Sample	Lactose (%w/v)	Glucose (%w/v)	Galactose (%w/v)
1	5.01	0	0
2	5.01	0	0
3	0.23	2.31	2.4
4	2.62	1.16	1.2
5	5.51	1	0.4
6	5.21	0.2	2
7	5.01	2.5	0.1
8	5.11	2.7	1.4
9	5.01	0.8	2.6
10	2.51	1.2	0.8
11	3.76	1.7	1
12	2.51	0.11	0.1
13	3.1	0.92	1.76
14	2.45	1.39	2.94
15	1.19	2.85	1.92
16	1.07	0.69	0.72
17	1.05	0.46	0.98
18	0.59	1.92	1.46
19	0.38	2.61	2.4
20	0.23	3.01	2.9
21	0.53	2.61	2.4
22	1.74	2.41	2.4
23	3.24	2.31	2.4
24	5.01	0	3
25	5.01	3	0
26	0.12	2.41	2.45

Table 3.3: Mean and standard deviation (SD) for triplicate HPLC analyses of validation samples for lactose, glucose and galactose at 0.05, 0.50 and 2.00% (w/v).

Component	0.05% (w/v)		0.50% (w/v)		2.00% (w/v)	
	Mean	SD	Mean	SD	Mean	SD
Lactose	0.016	0.001	0.497	0.001	2.033	0.004
Glucose	0.027	0.001	0.517	0.019	1.917	0.089
Galactose	0.022	0	0.517	0.023	1.939	0.091

Table 3.4: Average lactose recovery for duplicate HPLC analyses of milk spiked with lactose.

Sample	Amount spiked (%w/v)	HPLC recovery (%w/v)
1	0.05	0.01
2	0.50	0.42
3	2.00	2.06

3.3.4. Milk Hydrolysis and Fractionation

A sample of 2% milk was analyzed by HPLC and then subjected to lactose hydrolysis by β-galactosidase (100 μL in 100 mL of milk) at 4°C. Aliquots were taken at various times over a 48-h period and immediately analyzed by FTIR spectroscopy and deproteinized for HPLC analysis. These runs were carried out in duplicate. Samples of the β-galactosidase treated milk and Lacteeze were deproteinized, and centrifuged and their supernatants frozen. Prior to HPLC fractionation, these samples were freeze-dried and reconstituted in 500 μL of distilled water in order to concentrate them. The di- and trisaccharide fractions were separated and collected using an ION-300 polymeric cation exchange column and re-injected to confirm their purity. After neutralization (pH 7) by addition of NaOH, the fractions were freeze-dried and reconstituted in 20 μL of distilled water for collection of their SB-ATR/FTIR spectra.

3.4. RESULTS AND DISCUSSION

3.4.1. General Considerations

Preliminary FTIR studies with milk, enzyme-treated milk, Lacteeze and sugar solutions indicated that good-quality, reproducible spectra could be obtained with the use of the ZnSe SB-ATR accessory. Of particular importance for the present work is that the bands in the sugar absorption region of 1200-800 cm^{-1} were clearly observed, whereas spectra recorded with a transmission cell equipped with ZnSe windows are affected by fringing[24] and CaF_2 windows transmit little energy in this region[24]. Only one drop of sample was required for analysis, the accessory was simple to load and clean. Because of the small surface area of the SB-ATR crystal, temperature control was excellent, which is critical for quantitative analysis owing to the dependence of the effective pathlength on the refractive index of the crystal and the sample and thus on the temperature[24].

Figure 3.1 presents typical SB-ATR/FTIR spectra obtained for lactose, glucose and galactose over the 1200-950 cm^{-1} region, illustrating the spectroscopic similarity of these sugars. Because of their spectral similarity as well as spectral contributions from fat and/or protein present in milk, advanced multivariate methods such as PLS are deemed the most appropriate for calibration development, as has been reported in other FTIR quantitative studies of milk[5] and sugar-containing beverages[25,26]. The development of a

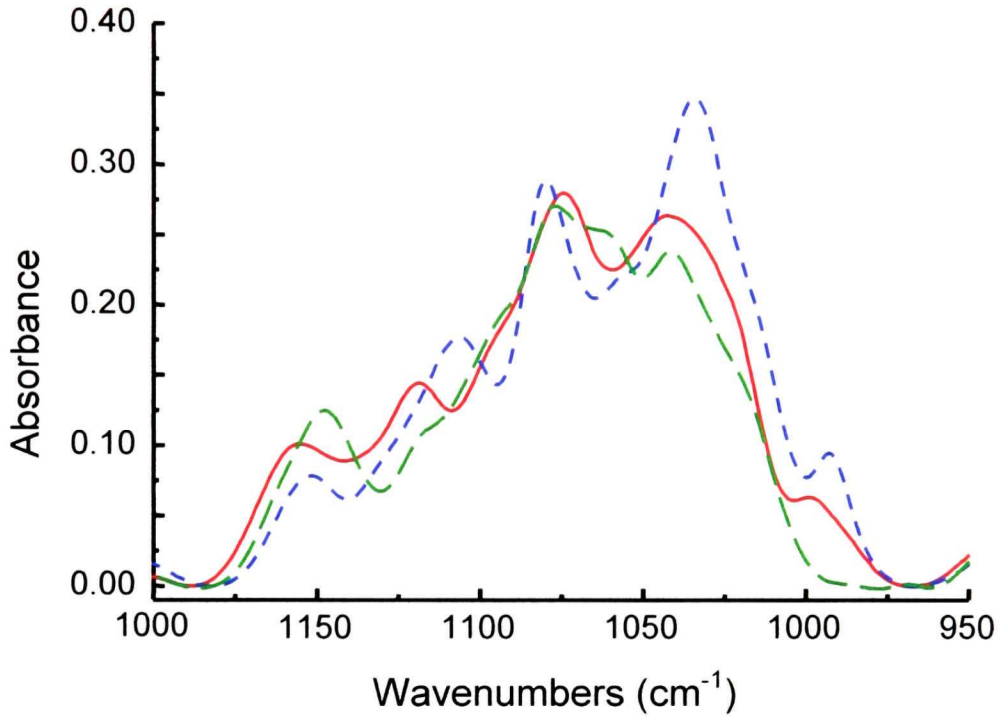

Figure 3.1. Spectra of 5% (w/v) aqueous solutions of lactose (——), glucose (- - -) and galactose (— — -). The spectrum of water has been subtracted from each spectrum.

robust PLS calibration model requires that the concentrations of the constituents being analyzed for be defined and known and that any other constituents that may be present (e.g., fat and protein) have to be represented in the calibration standards over the range of variability in the samples to be analyzed, although their concentrations need not be known[27]. Hence in order to develop a calibration suitable for the analysis of lactose, glucose and galactose in milk undergoing lactose hydrolysis a calibration set consisting of solutions of these sugars is an inadequate spectral representation of the milk matrix. The development of a representative set of standards in this case is a complex undertaking, requiring that milks be prepared in which fat, protein and sugars all vary substantively, with the sugar composition being accurately known.

To assess whether the FTIR method is able to track the sugar concentration changes during lactose hydrolysis, it is necessary to compare the FTIR data to those obtained by a reference method, HPLC being the method chosen. The HPLC system was calibrated using lactose, glucose and galactose standards and Table 3.3 presents the statistics of subsequent triplicate analyses of sugar standards. The ability of the HPLC system to analyze for the three sugars in milk was evaluated by standard addition of lactose to a milk sample and typical recovery data are presented in Table 3.4. Based on these results, it was concluded that the HPLC procedure devised provided a suitable means to pre-analyze milks used for FTIR calibration and to validate the FTIR method.

During lactose hydrolysis by β-galactosidase, some disaccharides as well as higher oligosaccharides may be produced by transgalactosylation. It should be noted that the column employed does not separate lactose from other disaccharides and hence the lactose concentration values in actuality represent total disaccharides. Thus, the commercial 99% lactose-free milk, Lacteeze, used in formulating the calibration standards could include these constituents, and they might also be produced when laboratory lactose hydrolysis in milk is carried out using *K. lactis* β-galactosidase. These oligosaccharide by-products could interfere with calibration development as they absorb IR radiation in the same region as lactose, glucose and galactose. However, this problem can be overcome if the by-products in the calibration standards formulated from Lacteeze are equivalent to those found in the samples to be analyzed as PLS can then compensate for this source of interference. Hence, Lacteeze and the enzyme-treated milk samples

were analyzed by HPLC to separate and isolate the di- and trisaccharide by-products. The HPLC chromatogram illustrated in Figure 3.2 indicates that only small amounts of di- and trisaccharides are present, confirming the observations obtained in other studies[11,12,28]. The di- and trisaccharide fractions were collected and concentrated for FTIR spectral analysis and comparison. As the amounts ultimately collected were minute, an SB-ATR accessory that requires only 10 µl of sample was used for this analysis. Figures 3.3.a and 3.3.b illustrate the spectra of the di- and trisaccharide fractions obtained by HPLC analysis of the enzyme-treated milk samples and Lacteeze as well as the difference spectra produced when the respective spectra are subtracted from each other. The trisaccharide fractions isolated from the enzyme-treated milk samples and Lacteeze are spectrally similar, their subtraction producing largely spectral noise. In the case of the disaccharide fractions, a small shoulder at 1021 cm^{-1} in the spectrum of the enzyme-treated milk fraction is absent in the spectrum of the Lacteeze fraction, which is clearly noticeable when their spectra are subtracted from one another. Comparison of this spectrum with that of a 2.5% (w/v) lactose solution after subtracting out the water spectrum (Figure 3.4) confirmed that the disaccharide in the enzyme-treated milk sample is not lactose and is some undefined transgalactosylation disaccharide by-product. However, it was concluded that in practical terms, this minor product could be regarded as insignificant.

3.4.2. Calibration and Lactose Hydrolysis Monitoring

Calibration standards were prepared by blending HPLC pre-analyzed skim milk and/or whole milk with Lacteeze, these products representing the input process raw materials and end product, respectively. Then these blends were spiked gravimetrically with varying amounts of glucose, galactose, lactose and water so as to introduce variability that is representative of a lactose hydrolysis run (Tables 3.1 and 3.2). The variance and correlation spectra generated from the spectra of these standards, based on the spectral region between 1300 and 800 cm^{-1} was selected for development of a PLS calibration. The calibration was iteratively optimized by refining the regions and baseline selections using the PRESS test to minimize the standard error of prediction (SEP) and further evaluated by performing a leave-one-out cross-validation. Ultimately, the region

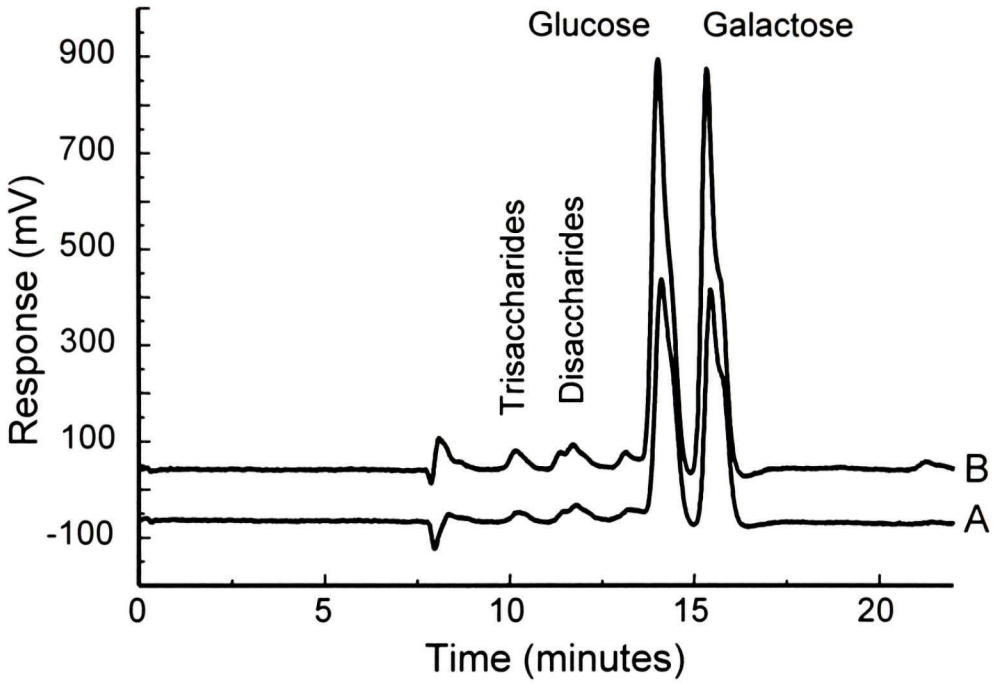

Figure 3.2. HPLC chromatograms of (A) Lacteeze and (B) enzyme-treated milk sample using an ION-300 polymeric cation exchange column.

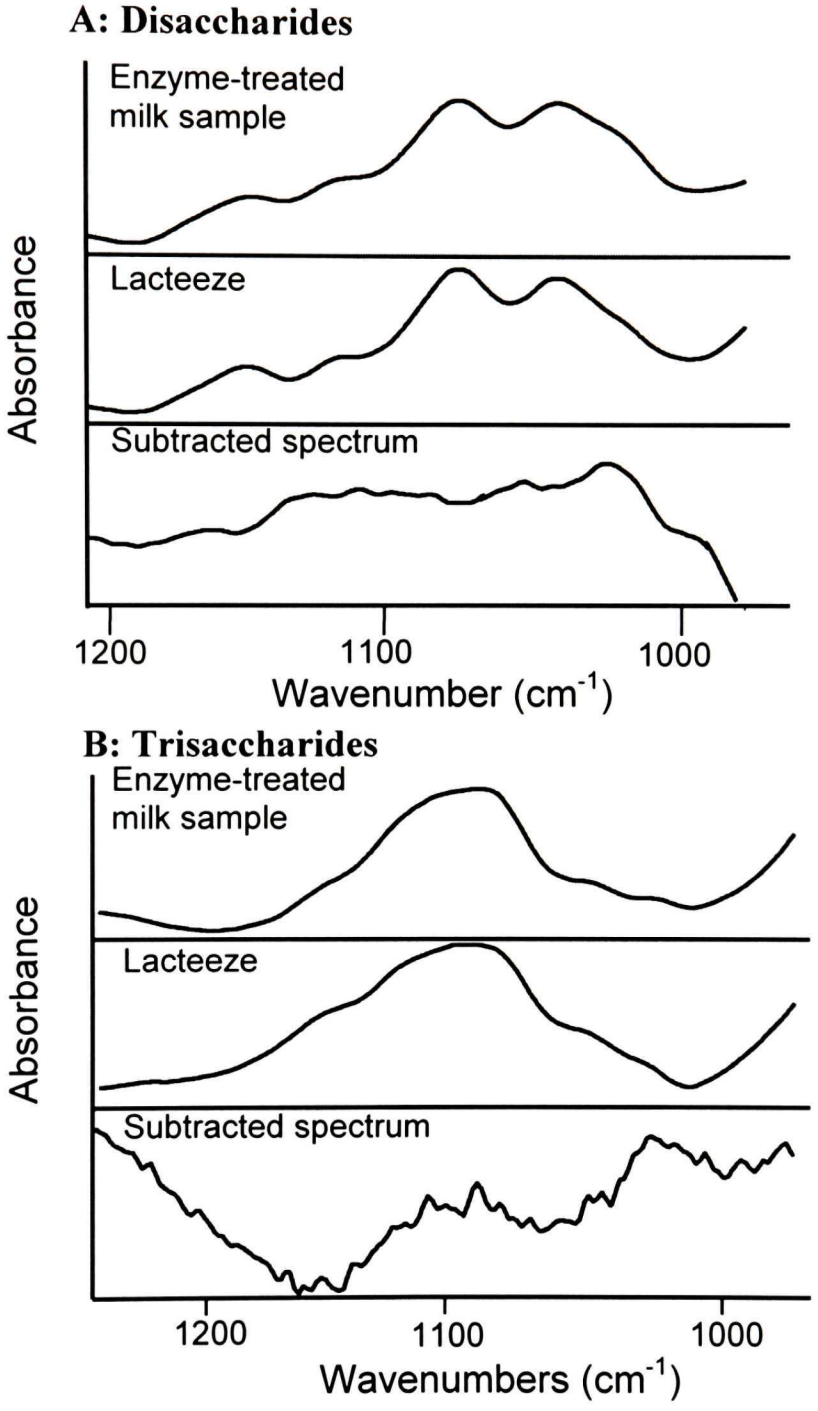

Figure 3.3. FTIR spectra of enzyme-treated milk sample, Lacteeze and their spectra subtracted from one another of the disaccharide (A) and trisaccharide (B) HPLC fractions.

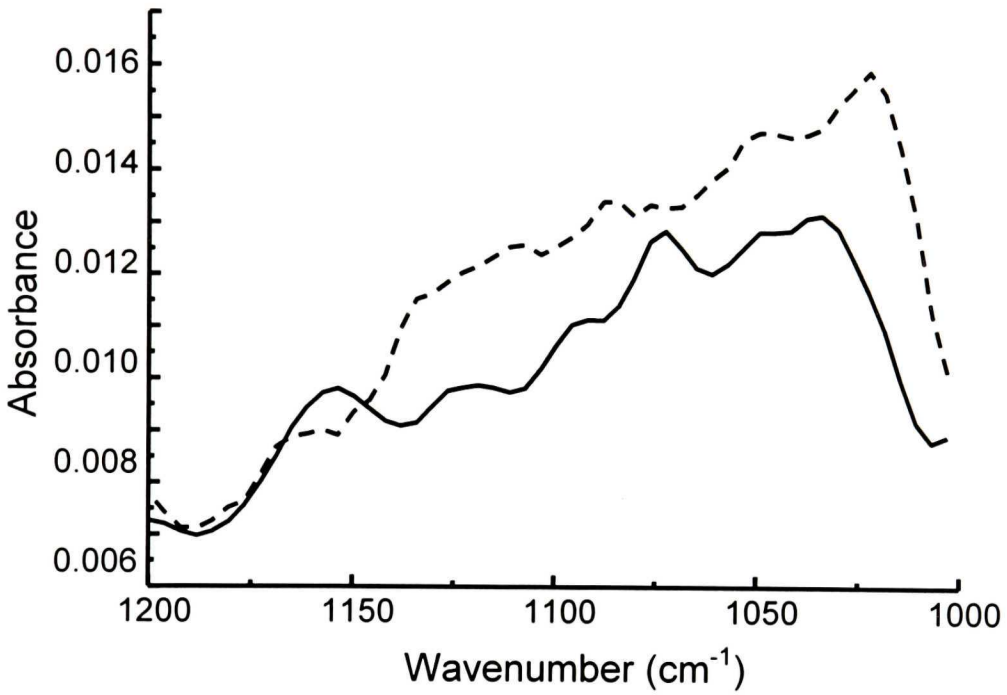

Figure 3.4. Comparison of SB-ATR/FTIR spectrum of 2.5% (w/v) lactose (——) subtracted from water with the subtracted spectrum in Figure 3.3.a (- - -) illustrating that they are different.

between 1203.4 and 971.9 cm^{-1}, with a single-point baseline at 1484.9 cm^{-1} was selected for the final calibration. Table 3.5 presents the statistical performance of the final PLS calibration in terms of linear regression equations and their respective MD_a and SDD_a for the predictions obtained for glucose, galactose and lactose. This data indicates that the calibration model is able to track the changes in concentration of the three sugars of interest in standards representative of milk samples undergoing lactose hydrolysis.

Two hydrolysis runs were carried out over a period of 48 h, with samples being taken at selected time intervals and analyzed by HPLC and SB-ATR/FTIR spectroscopy. The FTIR spectra were processed through the PLS calibration devised to quantitate the sugar contents in the sample. A plot of the changes in sugar concentration, as determined by FTIR spectroscopy, as a function of time is presented in Figure 3.5. This plot shows a loss of lactose and a concurrent rise in glucose and galactose, following a similar profile as the HPLC data. After ~8 h, 85-90% of the initial lactose has been hydrolyzed and a slight decrease in glucose concentration is subsequently observed, indicating the possible formation of additional disaccharide transgalactosylation products, a fact noted by Mozaffar *et al.* when *K. lactis* β-galactosidase is used[16]. Figure 3.6 presents the representative HPLC reference method sugar analysis results plotted against the FTIR data, illustrating a linear relationship between the methods. The respective linear regression equations for the two hydrolysis runs carried out are presented in Table 3.6.

Overall, SEPs of ~0.2% (w/v) for lactose and of ~0.08-0.17% (w/v) for the monosaccharides were obtained. In general, the small MD_a values indicate that there is little overall discrepancy between the FTIR and HPLC data. There is more potential for discrepancies between the methods early on in the reaction as the enzymatic reaction is stopped in samples set aside for HPLC analysis by the deproteination step, but not in samples analyzed by the FTIR method. The magnitude of this effect may be estimated from Figure 3.7, a plot of ln [Absorbance] vs time. Given that the FTIR scan time is in the order of 100 seconds and that the rate constant calculated from the plot in Figure 3.7. is 4.31×10^{-3} min^{-1}, this effect would be a significant source of error for the first 15 min of the reaction process, but quickly drops to within the error of prediction thereafter. In practical terms, this should not be an issue as the progress of the reaction is what is of interest rather than absolute sugar concentrations at the beginning of the process.

Table 3.5: Linear regression equations, correlation coefficients (R), SEP, MD_a and SDD_a for the cross-validation data.

Component	Equation	R	SEP (% w/v)	MD_a (% w/v)	SDD_a (% w/v)
Lactose	Y = 0.016 + 0.996X	0.999	0.076	0.01	0.08
Glucose	Y = 0.003 + 0.998X	0.996	0.051	0.00	0.05
Galactose	Y = 0.020 + 0.988X	0.995	0.104	0.00	0.10

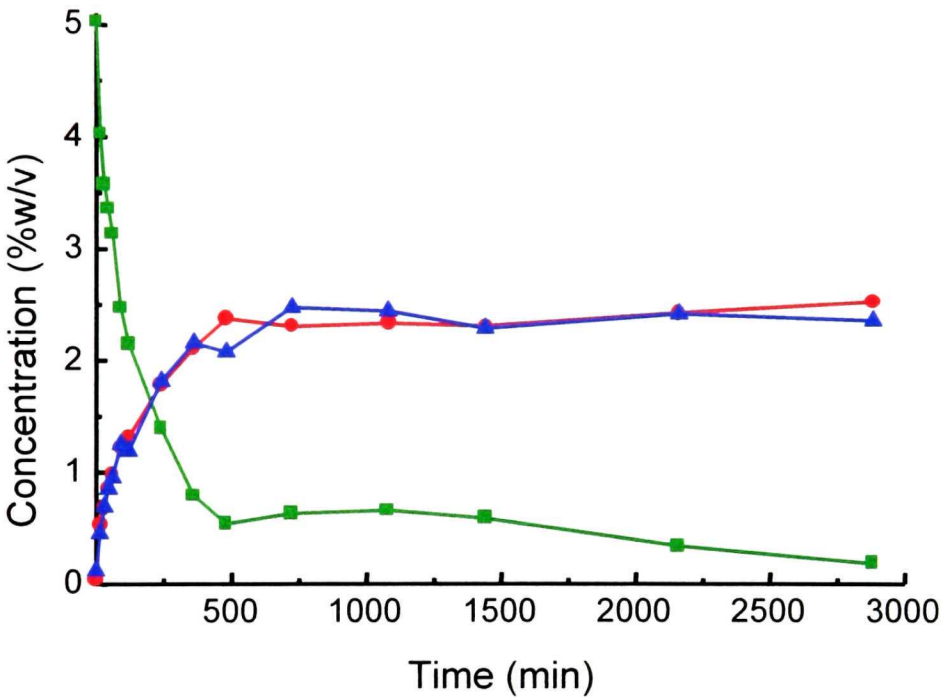

Figure 3.5. Changes in lactose (—■—), glucose (—●—) and galactose (—▲—) concentrations as predicted from the FTIR/PLS calibration during a 48-h lactose hydrolysis in milk reaction at 4°C.

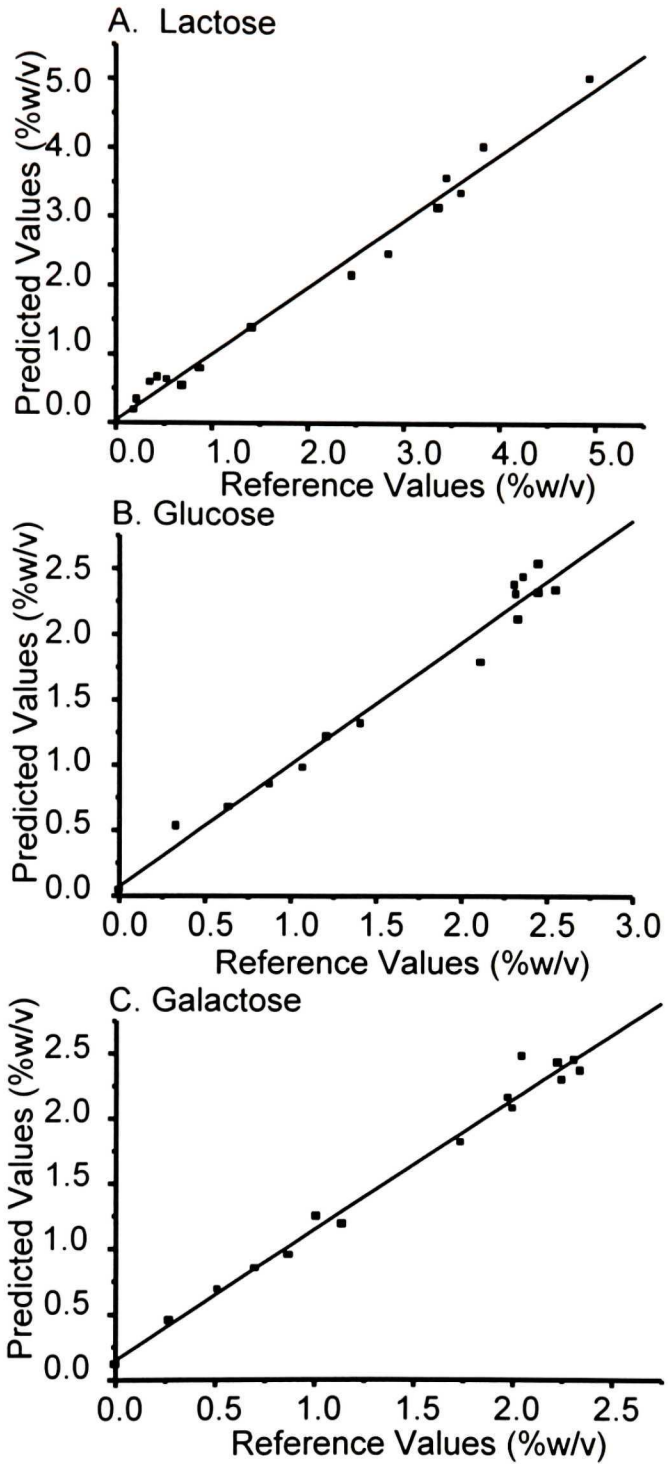

Figure 3.6. Plot of FTIR/PLS predicted values against HPLC values for the concentrations of lactose (A), glucose (B) and galactose (C) during a 48-h lactose hydrolysis in milk reaction at 4°C.

Table 3.6: Linear regression equations, correlation coefficients (R), SEP, MD_a and SDD_a for FTIR/PLS data compared to reference HPLC data for two 48-h lactose hydrolysis runs at 4°C.

Run	Component	Equation	R	SEP (%w/v)	MD_a (%w/v)	SDD_a (%w/v)
1	**Lactose**	Y = 0.035 + 0.971X	0.992	0.202	-0.02	0.20
	Glucose	Y = 0.069 + 0.935X	0.989	0.130	-0.04	0.14
	Galactose	Y = 0.149 + 0.998X	0.993	0.104	0.15	0.10
2	**Lactose**	Y = 0.136 + 1.02X	0.993	0.210	-0.18	0.21
	Glucose	Y = -0.097 + 0.932X	0.982	0.163	0.21	0.17
	Galactose	Y = 0.134 + 0.956X	0.996	0.075	-0.07	0.08

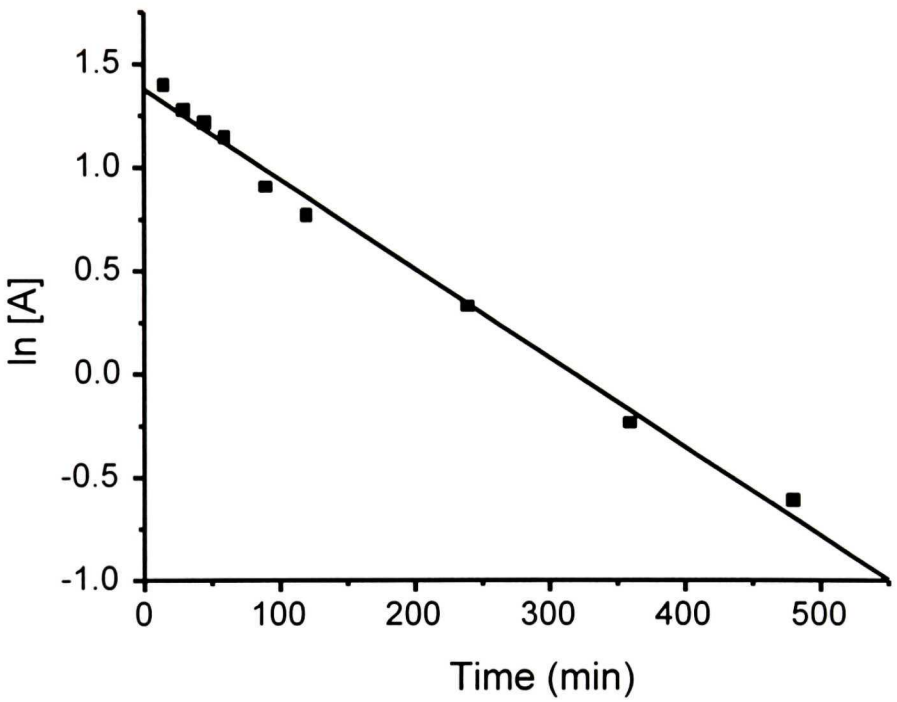

Figure 3.7. Plot of ln [A] versus time, where [A] is the concentration of lactose, for the first nine time points of a lactose hydrolysis reaction in milk at 4°C.

Overall, the SB-ATR/FTIR method would be appropriate to monitor the lactose hydrolysis process up to a level of about 95-98% lactose reduction given that the error of prediction is in the order of 0.1-0.2% (w/v) which corresponds to 2-4 % of the initial lactose concentration.

3.5. CONCLUSION

The use of an SB-ATR accessory has facilitated the development of a quantitative FTIR method which allows one to conveniently and rapidly monitor the hydrolysis of lactose in milk, overcoming a variety of limitations associated with conventional FTIR transmission analysis. The methodology is particularly well suited for at-line industrial process analysis and provides simple tracking data for an ongoing process in about two minutes. Although the calibration procedure presented here is fairly complicated, once a robust calibration has been developed and implemented, the analysis is straightforward. It is possible that a more accurate calibration can be developed by employing an HPLC reference method that can separate lactose from other disaccharides, such as using amide bonded columns[11], and as such a calibration can be developed to monitor 99% lactose reduction. A somewhat less accurate calibration could be also be derived from simpler sugar/skim milk powder/water mixtures[29]. As a quality control tracking tool, the reaction's progress is the key determinant as opposed to obtaining exact sugar concentration values. With the development of dedicated software, including an appropriate operator interface and direct data output, this SB-ATR/FTIR method could be a very useful tool for monitoring the production of lactose-reduced milk. This also would result in time and cost savings as the hydrolysis process could be optimized and the end of the reaction readily determined so that a new batch of milk can be started. The successful development of this method also indicates that the quantitative analysis of other aqueous beverages by SB-ATR/FTIR spectroscopy may be viable.

REFERENCES

1. Biggs, D.A. (1972). Precision and accuracy of infrared milk analysis, *J. Assoc. Off. Anal. Chem.*, 55, 488-497.

2. Agnet, Y. (1998). Fourier transform infrared spectroscopy: A new concept for milk and milk product analysis, *Bull. Int. Dairy Fed*, 332, 58-68.

3. van de Voort, F.R. (1980). Evaluation of Milkoscan 104 infrared milk analyzer, *J. Assoc. Off. Anal. Chem.*, 63 (5), 973-980.

4. Sjaunja, L.O. and Andersson, I. (1985). Laboratory experiments with a new infrared (IR) milk analyzer, the Milko-Scan 605, *Acta Agric. Scand.*, 35, 345-352.

5. van de Voort, F.R., Sedman, J., Emo, G. and Ismail, A.A. (1992). Assessment of Fourier transform infrared analysis of milk, *J. AOAC Int.*, 75, 780-785.

6. *Official Methods of Analysis of the Association of Official Analytical Chemists* (1995) 16th ed., AOAC International, Arlington, VA, sec. 972.16.

7. Lanher, B.S. (1996). Evaluation of Aegys MI 600 Fourier transform infrared milk analyzer for analysis of fat, protein, lactose, and solids nonfat: A compilation of eight independent studies, *J. AOAC Int.*, 79 (6), 1388-1399.

8. Nathier-Dufour, N., Sedman, J. and van de Voort, F.R. (1995). A rapid ATR/FTIR quality control method for the determination of fat and solids in sweetened condensed milk, *Milchwissenschaft*, 50, 462-466.

9. Cocciardi, R.A., Ismail, A.A., van de Voort, F.R. and Sedman, J. (2002). A rapid Fourier transform infrared quality control method for the determination of lactose, sucrose, fat and total solids in chocolate milk, *Milchwissenschaft*, 57, 90-93.

10. Hansen, P.W., van Brackel, A.S., Garman, J. and Norgaard, L. (1999). Detection of specific sugars in dairy process samples using multivariate curve resolution, *J. Dairy Sci.*, 82, 1351-1360.

11. Indyk, H.E., Edwards, M.J. and Woollard, D.C. (1996). High performance liquid chromatographic analysis of lactose-hydrolysed milk, *Food Chem.*, 57, 575-580.

12. Boon, M.A., Janssen, A.E.M. and van't Riet, K. (2000). Effect of temperature and enzyme origin on the enzymatic synthesis of oligosaccharides, *Enzyme Microb. Technol.*, 26, 271-281.

13. Burvall, A., Asp N.-G. and Dahlqvist, A. (1979). Oligosaccharide formation during hydrolysis of lactose with *Saccharomyces lactis* lactase (Maxilact®): Part 1 – quantitative aspects, *Food Chem.*, 4, 243-250.

14. Dubois, M., Gilles, K., Hamilton, J.K., Rebers, P.A. and Smith, F. (1951). A colorimetric method for the determination of sugars, *Nature*, 168 (4265), 167.

15. Greenberg, N.A. and Mahoney, R.R. (1983). Formation of oligosaccharides by β-galactosidase from *Streptococcus thermophilus*, *Food Chem.*, 10, 195-204.

16. Mozaffar, Z., Nakanishi, K. and Matsuno, R. (1985). Formation of oligosaccharides during hydrolysis of lactose in milk using β-galactosidase from *Bacillus circulans*, *J. Food Sci.*, 50, 1602-1605.

17. Kleyn, D.H. and Trout, J.R. (1984). Enzymatic-ultraviolet method for measuring lactose in milk: Collaborative study, *J. Assoc. Off. Anal. Chem.*, 67 (3), 637-640.

18. Ramet, J.P., Novak, P., Evers, P.A. and Nijpels, H.H. (1979). Application de la cryométrie à la mesure de l'hydrolyse enzymatique du lactose, *Le Lait*, 59, 46-55.

19. Nijpels, H.H., Evers, P.A., Novak, P. and Ramet, J.P. (1980). Application of cryoscopy for the measurement of enzymatic hydrolysis of lactose, *J. Food Sci.*, 45 (6), 1684-1687.

20. Jeon, I.J. and Saunders, S.R. (1986). Effect of oligosaccharide formation on the cryoscopic measurements of enzymatic hydrolysis of lactose in dairy products, *J. Food Sci.*, 51 (1), 245-246.

21. Biggs, D.A. (1979). Infrared estimation of fat, protein, and lactose in milk: Evaluation of Multispec instrument, *J. Assoc. Off. Anal. Chem.*, 62, 1202-1210.

22. Smith, E.B., Barbano, D.M., Lynch J.M. and Fleming, J.R. (1993). Performance of homogenizers in infrared milk analyzers: A survey, *J. AOAC Int.*, 76, 1033-1041.

23. Nakanishi, K., Matsuno, R., Torii, R., Yamamoto, K. and Kamikubo, T. (1983). Properties of immobilized β-galactosidase from *Bacillus circulans*, *Enzyme Microb. Technol.*, 5, 115.

24. Ismail, A.A., van de Voort, F.R. and Sedman, J. (1997). Fourier transform infrared spectroscopy: Principles and applications. In: *Instrumental Methods in Food Analysis* (J.R.J. Paré and J.M.R. Bélanger eds., Elsevier, Amsterdam, Netherlands), 93-139.

25. Dupuy, N., Meurens, M., Sombret, B., Legrand, P. and Huvenne, J.P. (1992). Determination of sugars and organic acids in fruit juices by FT mid-IR investigation of dry extract, *Appl. Spectrosc.*, 46 (5), 860-863.

26. Rambla, F.J., Garrigues, S., Ferrer, N. and de la Guardia, M. (1998). Simple partial-least-squares attenuated total reflectance Fourier transform infrared spectrometric method for the determination of sugars in fruit juices and soft drinks using aqueous standards, *Analyst*, 123, 277-281.

27. Haaland, D.M. and Thomas, E.V. (1988). Partial-least-squares methods for spectral analyses. 1. Relation to other quantitative calibration methods and the extraction of qualitative information, *Anal. Chem.*, 60, 1193-1201.

28. Jeon, I.J. and Mantha, V.R. (1985). High performance liquid chromatography analysis of oligosaccharides formed during β-galactosidase action on lactose, *J. Dairy Sci.*, 68, 581-588.

29. van de Voort, F.R., Elkashef, A.A. and Blais, J.S. (1991). Interlaboratory assessment of dry calibration milk powders for calibrating infrared milk analyzers, *J. Assoc. Off. Anal. Chem.*, 74, 772-779.

BRIDGE

In the previous chapter, SB-ATR/FTIR spectroscopy was investigated for the quantitative analysis of lactose, glucose and galactose in milk during the enzymatic hydrolysis of lactose with β-galactosidase. It was found that SB-ATR/FTIR spectroscopy was suitable for this application. To further assess the feasibility of using SB-ATR/FTIR spectroscopy for quantitative analysis applications, it is necessary to compare this novel method to conventional FT-NIR and FTIR methods in multicomponent analysis. In the following chapter, SB-ATR/FTIR spectroscopy is compared to transmission FT-NIR and FTIR spectroscopy in the quantitative analysis of distilled liquors and wines.

CHAPTER 4

INVESTIGATION OF THE POTENTIAL UTILITY OF SINGLE-BOUNCE ATTENUATED TOTAL REFLECTANCE FOURIER TRANSFORM INFRARED SPECTROSCOPY IN THE ANALYSIS OF DISTILLED LIQUORS AND WINES

4.1 ABSTRACT

A new Fourier transform infrared (FTIR) spectroscopic method based on single-bounce attenuated total reflectance (SB-ATR) spectroscopy was developed for the analysis of distilled liquors and wines. For distilled liquors, a partial-least-squares (PLS) calibration based on the SB-ATR/FTIR spectra of mixtures of ethanol and distilled water was developed. The standard deviation of the differences for accuracy (SDD_a) for alcohol determination for twelve pre-analyzed samples of different distilled liquors was 0.142% (v/v) as compared to 0.163% (v/v) using Fourier transform near-infrared (FT-NIR) spectroscopy. The potential utility of SB-ATR/FTIR spectroscopy for the analysis of wines was initially evaluated based on a comparison with FT-NIR spectroscopy and FTIR spectroscopy using a flow-through transmission cell. PLS calibrations were developed for each of the three techniques using a set of 28 wine samples pre-analyzed for alcohol, total reducing sugars, total acidity and pH. The leave-one-out cross-validation statistics revealed that SB-ATR/FTIR spectroscopy performed better than FT-NIR spectroscopy and comparably to transmission FTIR spectroscopy. A PLS calibration for the prediction of 11 different components and parameters in wines (alcohol, glycerol, fructose, total reducing sugars, tartaric acid, citric acid, malic acid, lactic acid, total acidity, volatile acids and total SO_2) by SB-ATR/FTIR spectroscopy was subsequently developed by employing 72 pre-analyzed wine samples as calibration standards and validated using an independent set of 77 pre-analyzed wine samples. Good correlations between the reference and predicted values for the validation set were obtained for all components and parameters except citric acid, volatile acids and total SO_2. The results of this study demonstrate the suitability of SB-ATR/FTIR spectroscopy for the routine analysis of distilled liquors and wines.

4.2 INTRODUCTION

Spirits are largely alcohol/water mixtures with only minor levels of added or developed constituents present. Wines, on the other hand, can have a complex provenance and their quality can depend on volatile constituents, such as ethanol and aromatic substances and nonvolatile compounds (e.g., sugars, organic acids, tannins, nitrogen compounds and mineral matter)[1]. Historically, wines have been regionalized and certified, the European Union having particularly strict rules regarding the authenticity of wines, especially in regards to fraudulent practices such as adulteration[2]. As a consequence, whereas the analysis for alcohol in spirits and wines is routine for industrial quality control and government regulatory purposes, more detailed analysis for minor constituents in wines is also commonplace[3,4]. Such analyses tend to be tedious and the availability of a simple and rapid means of obtaining most of the relevant information using a single method of analysis would clearly be desirable.

Near-infrared (NIR) spectroscopy might be considered a likely candidate to meet this demand as it is a well-established technique for multicomponent analysis of agricultural and food products[5]. Its utility for the analysis of alcohol in wines was initially demonstrated using filter-based NIR reflectance spectrometers, employing wavelengths of 2270, 2230, 2180 and 1778 nm[6]. Since then, NIR spectroscopic methods have also been developed for the analysis of alcohol in spirits using transmission measurements[7,8] and flow injection analysis[9], for monitoring alcohol and sugars during wine fermentation[3] and for analyzing alcohol, sugars and glycerol in botrytized-grape sweet wines using filter-based reflectance spectrometers[10]. Overall, these studies suggest that although NIR spectroscopy is an adequate analytical tool for predicting the alcohol content in wines and spirits, it is limited in its ability to analyze other wine components. For example, although NIR methods for the determination of sugar content have been developed for sweet wines[10], the major NIR absorption bands of sugars are highly overlapped by the OH stretching and deformation combination bands of water, making the measurement of sugars imprecise below 30 g/L[11].

Although mid-IR spectroscopy has generally found much less practical application than NIR spectroscopy in the analysis of agricultural and food products, it has been successfully employed in the analysis of alcohol in alcoholic beverages[12,13] and has

recently been shown to be a suitable technique for the multicomponent analysis of wines with the use of Fourier transform infrared (FTIR) instrumentation[14-16]. A dedicated FTIR wine analyzer, which has been developed by Foss Electric (Denmark) based on the design of the Foss FTIR milk analyzer, can be calibrated using representative wine samples, pre-analyzed by standard chemical, colorimetric, enzymatic and chromatographic methods. Patz *et al.*[14] employed a Foss wine analyzer to analyze for alcohol, tartaric acid, malic acid, lactic acid, total acidity, pH, volatile acidity, reducing sugars, fructose, glucose, total SO_2, total phenols and glycerol. The calibration and test sets comprised 165 wine samples, and because the concentration ranges for glycerol and volatile acidity in these samples were too narrow, standards prepared in water were added to the calibration set to expand the wine data. The authors reported that results were acceptable for all parameters except total SO_2 and total phenols. Dubernet and Dubernet[15] used the same instrument to analyze for alcohol, reducing sugars, total acidity, pH, malic acid, tartaric acid, lactic acid, total phenols, volatile acidity, CO_2, glycerol, gluconic acid and saccharose content in 200,000 wine samples. These authors reported that not all wines could be analyzed using the same calibration due to matrix effects and therefore developed separate calibrations for dry and sweet wines as well as for wine musts. Because calibration development may require the accurate analysis of several hundred representative wines for multiple components, which is clearly a major undertaking, Schindler *et al.*[4] investigated the alternative of developing infrared (IR) wine calibrations based on model solutions of nine common components as a substitute for pre-analyzed wines. However, when these calibrations were applied to the analysis of wine samples, only limited agreement was obtained between the IR-predicted values for organic acids and sugars and results obtained by high-pressure liquid chromatography (HPLC).

At present, FTIR wine analysis is basically restricted to proprietary commercial instrumentation dedicated to this application. The sample handling accessory integrated into these systems incorporates a temperature-controlled flow-through transmission cell equipped with CaF_2 windows and having a fixed pathlength of ~50 μm. Despite this short pathlength, which is required to limit the overwhelming IR absorptions of water[16], products containing high levels of alcohol and/or sugar would require dilution prior to analysis in order to keep the major absorption bands of these components on scale. The

present work was undertaken to develop FTIR analytical methodology that utilizes a more versatile single-bounce attenuated total reflectance (SB-ATR) sample handling accessory and a standard benchtop FTIR spectrometer, thereby reducing the cost of implementing FTIR wine analysis. The advantages of the SB-ATR accessory include ease of use, high-energy throughput[17], and amenability to precise temperature control. Furthermore, the SB-ATR accessory provides access to much more spectral information than the transmission cell employed in commercial FTIR wine analyzers. This advantage is a result of its inherent short pathlength, with even the intense absorptions of water being on scale, as well as because the transmission cut-off of the ATR crystal (commonly ZnSe) occurs at a much lower-frequency than that of CaF_2 windows. These inherent advantages, which were exploited in previous work in our laboratory for the quantitative analysis of sugars during lactose hydrolysis in milk[18], make the SB-ATR accessory a versatile alternative to the transmission cell. As such, all kinds of alcoholic beverages can be analyzed easily, without the need for sample dilution and complex cell maintenance protocols.

Based on the above considerations, a structured examination of the potential utility of SB-ATR/FTIR spectroscopy in the analysis of alcoholic beverages, specifically wines and spirits, was undertaken. In the first part of the study, alcohol determination in spirits, which are relatively simple matrices, was assessed. Subsequently, a comparative evaluation of SB-ATR/FTIR spectroscopy relative to Fourier transform near-infrared (FT-NIR) and FTIR transmission methods for the analysis of wines was carried out. Finally, the simultaneous determination of 11 constituents in wines by SB-ATR/FTIR spectroscopy was investigated

4.3. EXPERIMENTAL

4.3.1 Samples, Chemicals and Reagents

Anhydrous alcohol (ethanol) was obtained from Commercial Alcohols Inc. (Brampton, ON) and 12 distilled liquor samples (rum, gin, vodka, brandy, scotch and whisky) were obtained from local liquor stores. A total of 177 pre-analyzed wine samples were obtained courtesy of the central laboratory of the Société des alcools du Québec (SAQ). The products included red and white, dry, semi-sweet and sweet wines

from a wide variety of countries including Italy, France, Spain, USA, South Africa, Germany, Canada and Australia. All reagents were obtained from Fisher Scientific (Montreal, QC) and were of analytical grade.

4.3.2. Instrumentation

4.3.2.1. FTIR Analysis

All quantitative IR analyses were carried out using an ABB Bomem (Québec City, QC) MB-150 dual-range [NIR/mid-IR] FTIR spectrometer equipped with a deuterated triglycine sulfate (DTGS) detector. The spectrometer was purged with dry air by a Balston air drier (Lexington, MA) to avoid spectral contributions from atmospheric water vapour and carbon dioxide. SB-ATR spectra were recorded with the use of a Harrick (Ossining, NY) ZnSe accessory equipped with a temperature controller (Watlow System Integrators, Decorah, IA). During sample analysis, the SB-ATR crystal was covered with a glass microscope slide to avoid any alcohol evaporation during spectral recording and the sample temperature was maintained at 30 ± 0.1°C to minimize spectral changes due to temperature variation. For purposes of comparison, FT-NIR and FTIR analyses were carried out with a 1000-μm quartz cell and a 50-μm CaF_2 cell, respectively, both thermostated at 30 ± 0.1°C using an Omega temperature controller (Omega Engineering, Stamford, CT). Spectral collection parameters for FT-NIR, FTIR transmission and SB-ATR analysis were 16, 32 and 32 co-added scans at resolutions of 16, 8 and 8 cm^{-1}, respectively. In all cases, a background single beam spectrum was taken prior to loading each sample, followed by collecting the spectrum of the sample and storing the resulting absorbance spectra used for calibration development and sample analysis to disk.

4.3.2.2. HPLC Analysis

HPLC analysis of 149 wines for glycerol, fructose and organic acids (citric acid, malic acid, tartaric acid and lactic acid) was carried out employing a Hewlett-Packard 1050 HPLC system, equipped with an ultraviolet (UV) detector set to 192 nm. Separation was carried out isocratically on a 7.8 mm × 300 mm Rezex ROA-Organic Acid column manufactured by Phenomenex Inc. (Torrance, CA) using 0.0025 N sulfuric acid at a flow

rate of 0.5 mL/min and a column temperature of 52 ± 0.1°C. The HPLC was calibrated based on 8 standard aqueous solutions of the components ranging from 0.1 to 10 g/L for organic acids and 0.1-100 g/L for glycerol and fructose. Calibrations for all components were found to be linear. The instrument was calibrated once but validated daily by triplicate injections of three standards of intermediate concentrations to verify the calibration's stability throughout the analysis period. The possibility of interference during analysis from other wine components was investigated by injecting each calibration standard and wine sample a second time at a detector wavelength of 240 nm and the ratio of the peak heights between the samples and standards were compared. For all components, the ratios were virtually identical, confirming that there was no interference.

4.3.3. Calibration Development

For spirits, 15 calibration standards were prepared by blending anhydrous ethanol with distilled water to cover a range of 25-75% (v/v) alcohol, and the validation set comprised 12 distilled liquor samples. Both standards and validation samples were analyzed using an Anton Paar Density Meter (Graz, Austria) according to the Association of Official Analytical Chemists (AOAC) method 982.10[19]. For wines, an initial set of 28 samples, pre-analyzed for basic wine parameters such as alcohol content, pH, total acidity and total reducing sugars, was used for comparing the utility of the SB-ATR method to more conventional FT-NIR and FTIR transmission methods. A second set of 149 wines, pre-analyzed for alcohol content, total acidity, total reducing sugars, total SO_2 and volatile acidity, was analyzed by HPLC for fructose, glycerol, and malic, citric, tartaric and lactic acid content. This larger set of wines was used to assess the feasibility of using the SB-ATR accessory for multi-component analysis of wines, with 72 of the wines used for calibration and 77 used as validation samples.

All calibrations were developed by applying partial-least-squares (PLS) using Omnic Turbo Quant Analyst software (Nicolet Instrument, Madison, WI). The correlation, variance and pure component spectra generated from the PLS software package were used to select regions in developing and optimizing the calibration model for each component. The optimal number of factors used for each component was

determined from the minimum point on the predicted residual error sum of squares (PRESS) plot. The overall suitability of the calibration model ultimately developed was assessed by calculating the mean difference and standard deviation of the differences for accuracy (MD_a and SDD_a, respectively) between the leave-one-out cross-validation predictions and values obtained by the reference method(s).

4.4 RESULTS AND DISCUSSION

4.4.1 Distilled Liquor Analysis

Although there are many ways of measuring alcohol in distilled liquors, the most commonly used official methods are those involving physical measurements[19-22]. NIR[7-9] and mid-IR[12,13] transmission methods have also been investigated and developed, with NIR methods dominating. Due to the simplicity of the distilled liquor matrix, the NIR spectra of distilled liquors exhibit some fairly well defined combination and first overtone bands of the O-H, C-H and C-O stretching and bending vibrational frequencies of ethanol[8], while the mid-IR spectra exhibit two strong bands at 1046 and 1086 cm^{-1} due to the fundamental C-O stretching vibrations (Figure 4.1). Since transmission-based FT-NIR spectroscopy for the determination of alcohol in distilled liquors has been shown to work well[7,8], it was used as a basis of comparison in the evaluation of an SB-ATR method. Given that a variety of IR methods were being developed and compared in this study, PLS was chosen as the preferred calibration approach because of its versatility and ability to compensate for unidentified sources of interference from other compounds as well as allowing information from all or portions of the spectra to be used[23]. The spectra of ethanol/distilled water mixtures were used to develop PLS calibrations for the FT-NIR transmission and SB-ATR procedures. The spectral regions ultimately used to derive the PLS calibrations and the leave-one-out cross-validation linear regression equations and their attendant standard error of prediction (SEP) are presented in Table 4.1.

The PLS calibrations were used to evaluate the alcohol content of 12 distilled liquors representing a variety of products. The predicted alcohol contents were compared to the results obtained using the Anton Paar density meter in terms of MD_a and SDD_a (Table 4.2); however, regression was not performed as there was inadequate variability in the alcohol content (ranging from 40 to 41% (v/v)) to produce valid regression data. The

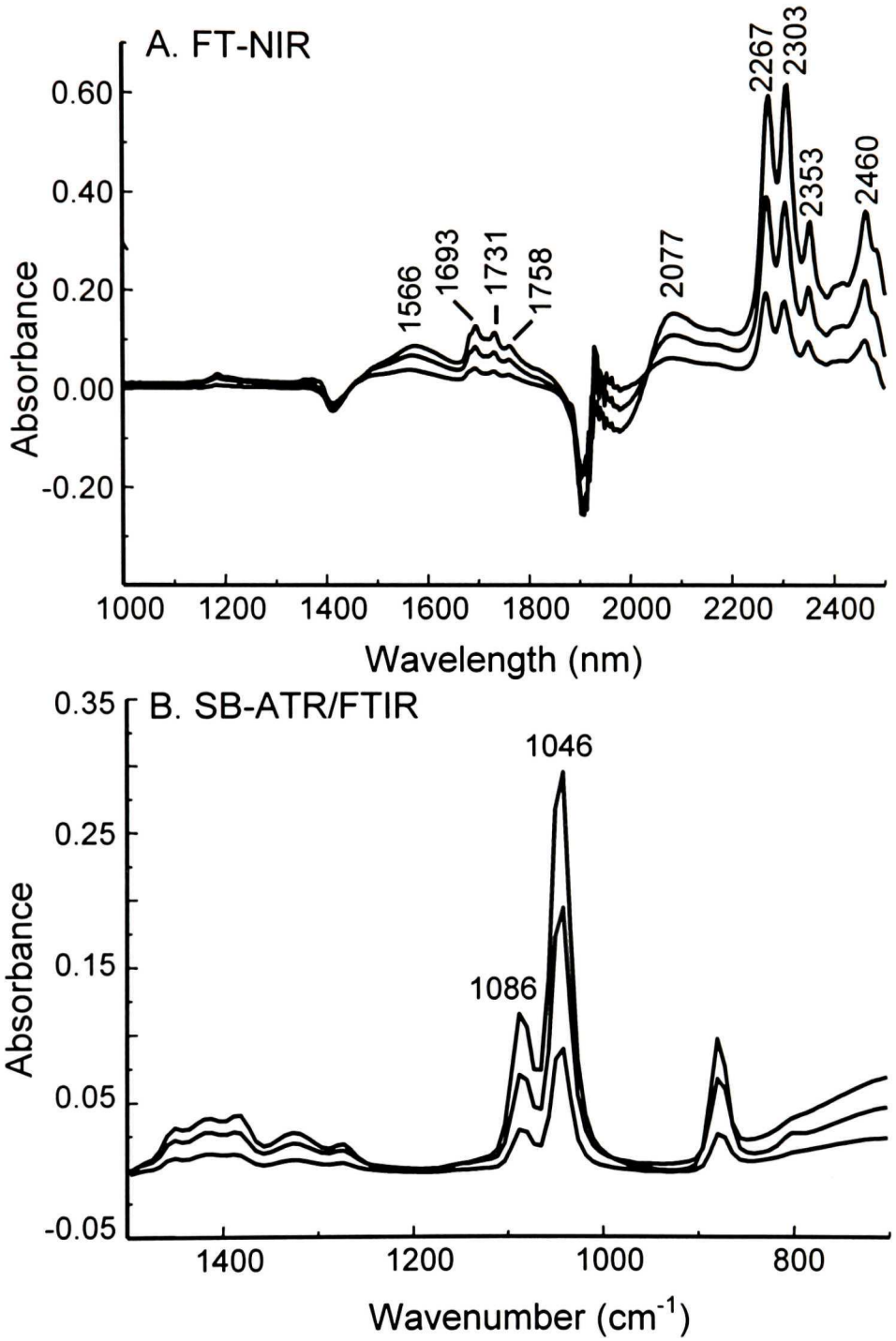

Figure 4.1. FT-NIR (A) and SB-ATR/FTIR (B) spectra of 20, 40 and 60% (v/v) solutions of ethanol after subtraction of water absorptions.

Table 4.1: Spectral regions, linear regression equations and regression statistics of the leave-one-out cross-validation for PLS calibrations derived for the FT-NIR and SB-ATR/FTIR methods for alcohol determination in spirits.

Method	Region employed	Equation	R	SEP (% v/v)
FT-NIR	2368-2207 nm	Y = -0.002 + 1.000X	0.999	0.065
SB-ATR	1183-987 cm^{-1}	Y = 0.000 + 1.000X	1.000	0.080

Table 4.2: MD_a and SDD_a for the PLS FT-NIR and SB-ATR/FTIR predictions relative to reference densitometric values.

Method	MD_a (% v/v)	SDD_a (% v/v)
FT-NIR	0.03	0.163
SB-ATR	0.02	0.142

MD_a and SDD_a data indicate that the alcohol content of the distilled liquor products investigated could be predicted to within 0.17% (v/v) of the density meter values, with no significant bias indicated between the reference and IR methods and no significant difference existing between the NIR and SB-ATR methods. To further verify that the calibrations could respond to substantive changes in the alcohol content in the products investigated, they were randomly spiked with water and absolute alcohol to provide a wider range of alcohol content (35-45% (v/v)). A highly linear response to alcohol content was obtained, and the MD_a and SDD_a of the predictions for these samples were similar to those for the unspiked samples.

These results indicate that the SB-ATR/FTIR method is readily able to quantify alcohol content in spirits to a similar, if not higher, degree of accuracy than the FT-NIR procedure. The results are also comparable to those reported in publications on both NIR[7-9] and mid-IR[12,13] methods for the analysis of distilled liquors. With respect to the previous mid-IR methods, which were based on the use of transmission cells, the SB-ATR procedure has the advantage that sample dilution is not required.

4.4.2. Comparison of FT-NIR, FTIR and SB-ATR/FTIR Methods for Wine Analysis

A preliminary comparative feasibility study was carried out by developing PLS calibrations for four parameters (alcohol content, total reducing sugars, total acidity and pH) in wines by using transmission FTIR and FT-NIR as well as SB-ATR/FTIR spectra of 28 pre-analyzed wine samples. The spectral regions employed in the optimized PLS calibration models for alcohol, total reducing sugar, total acidity and pH are presented in Table 4.3. Table 4.4 summarizes the leave-one-out cross-validation results in terms of the linear regression equations relating the predicted values to the values obtained by the reference methods, together with the corresponding correlation coefficients (R) and standard errors of prediction (SEP) as well as the values of MD_a and SDD_a. The FT-NIR cross-validation data indicated poor agreement between the predicted and reference method values for all the components except alcohol. Better overall agreement between the predicted and reference method values was obtained with both the transmission FTIR and SB-ATR/FTIR calibrations. Again, the best results were obtained for alcohol, while the results for reducing sugars, total acidity and pH are very much in line with what has

been reported in the literature for FTIR wine analysis using a transmission cell[14,15]. The performance of the SB-ATR calibrations is generally comparable to that obtained with the conventional transmission cell, despite the much shorter effective pathlength of the SB-ATR accessory, and is in fact superior in the case of reducing sugars. This is likely due to the lower transmission cutoff of the ZnSe crystal as compared to CaF_2 windows, through which the transmission of IR energy declines rapidly between 1110 and 1000 cm^{-1}, where the strongest absorption bands for sugars and alcohol are found[11]. In addition, owing to the short effective pathlength of the SB-ATR accessory, all the spectral information in the regions where water absorbs is available, and the CH stretching (3000-2800 cm^{-1}) and carbonyl stretching bands (1800-1600 cm^{-1}) are on scale. Figure 4.2 illustrates the "pure component" spectra generated by the Turbo Quant Analyst software, each of which corresponds to the first loading spectrum in a PLS calibration for the component in question. The "pure component" spectra reveal that there is significantly less spectral information available in the transmission cell spectra. This is especially the case for total acidity, where the region between 1750 and 1600 cm^{-1} is totally "blanked out" due to off-scale water absorptions, while the SB-ATR spectra exhibit the characteristic carbonyl stretching absorption of carboxylic acids. Overall, based on these initial comparative results, SB-ATR/FTIR spectroscopy appears to have the potential to serve as a means by which multicomponent analysis of wines can be carried out.

4.4.3. Multicomponent Wine Analysis by SB-ATR/FTIR Spectroscopy

Winemakers, enologists and governments have an interest in a variety of components and parameters that affect the quality of wine, are indicative of adulteration or provenance, or affect revenue. In Quebec, the SAQ routinely analyzes wines from around the world for alcohol, reducing sugars, total acidity, volatile acidity and SO_2 and provided 149 pre-analyzed wine samples for this study. This information was supplemented by carrying out HPLC analysis of these wines to provide additional quantitative data on individual acids (citric, tartaric, malic and lactic) as well as fructose and glycerol. The combined data provided information for a total of 11 components and parameters for which PLS calibrations were developed, using about half of the samples as standards with the balance serving as an independent validation set.

Table 4.3: Regions employed in FTIR and SB-ATR/FTIR PLS regressions.

Component	FT-NIR regions (nm)	FTIR regions (cm^{-1})	SB-ATR regions (cm^{-1})
Alcohol	2368-2207	1000-1500	850-1500
Reducing sugar	1851-1666	1108-1500	956.7-1500
			3000-2800
Total acidity	2368-2207	1108.3-1500	1108.3-1500
		1700-1800	1700-1800
pH	1851-1389	1000-1500	956.7-1500
			3000-2800

Table 4.4: Cross-validation results for FT-NIR, FTIR and SB-ATR/FTIR PLS calibration models for alcohol (% v/v), reducing sugar (g/L), total acidity (g/L H_2SO_4) and pH of 28 wine samples.

Method	Component	Equation	R	SEP	MD_a	SDD_a
FT-NIR	Alcohol	Y = 0.231 + 0.982X	0.991	0.110	0.00	0.109
FTIR	Alcohol	Y = 0.059 + 0.996X	0.991	0.111	0.01	0.109
SB-ATR	Alcohol	Y = 0.061 + 0.995X	0.993	0.102	0.00	0.100
FT-NIR	Reducing Sugar	Y = 1.479 + 0.341X	0.500	0.764	-0.04	1.123
FTIR	Reducing Sugar	Y = 0.946 + 0.584X	0.735	0.697	-0.01	0.863
SB-ATR	Reducing Sugar	Y = 0.605 + 0.711X	0.837	0.613	-0.06	0.707
FT-NIR	Total Acidity	Y = 2.874 + 0.152X	0.270	0.167	0.00	0.304
FTIR	Total Acidity	Y = 0.453 + 0.863X	0.882	0.142	-0.01	0.146
SB-ATR	Total Acidity	Y = 1.164 + 0.656X	0.787	0.156	0.00	0.189
FT-NIR	pH	Y = 2.107 + 0.390X	0.548	0.202	0.01	0.283
FTIR	pH	Y = 1.213 + 0.654X	0.706	0.222	0.02	0.246
SB-ATR	pH	Y = 1.416 + 0.582X	0.713	0.190	-0.01	0.230

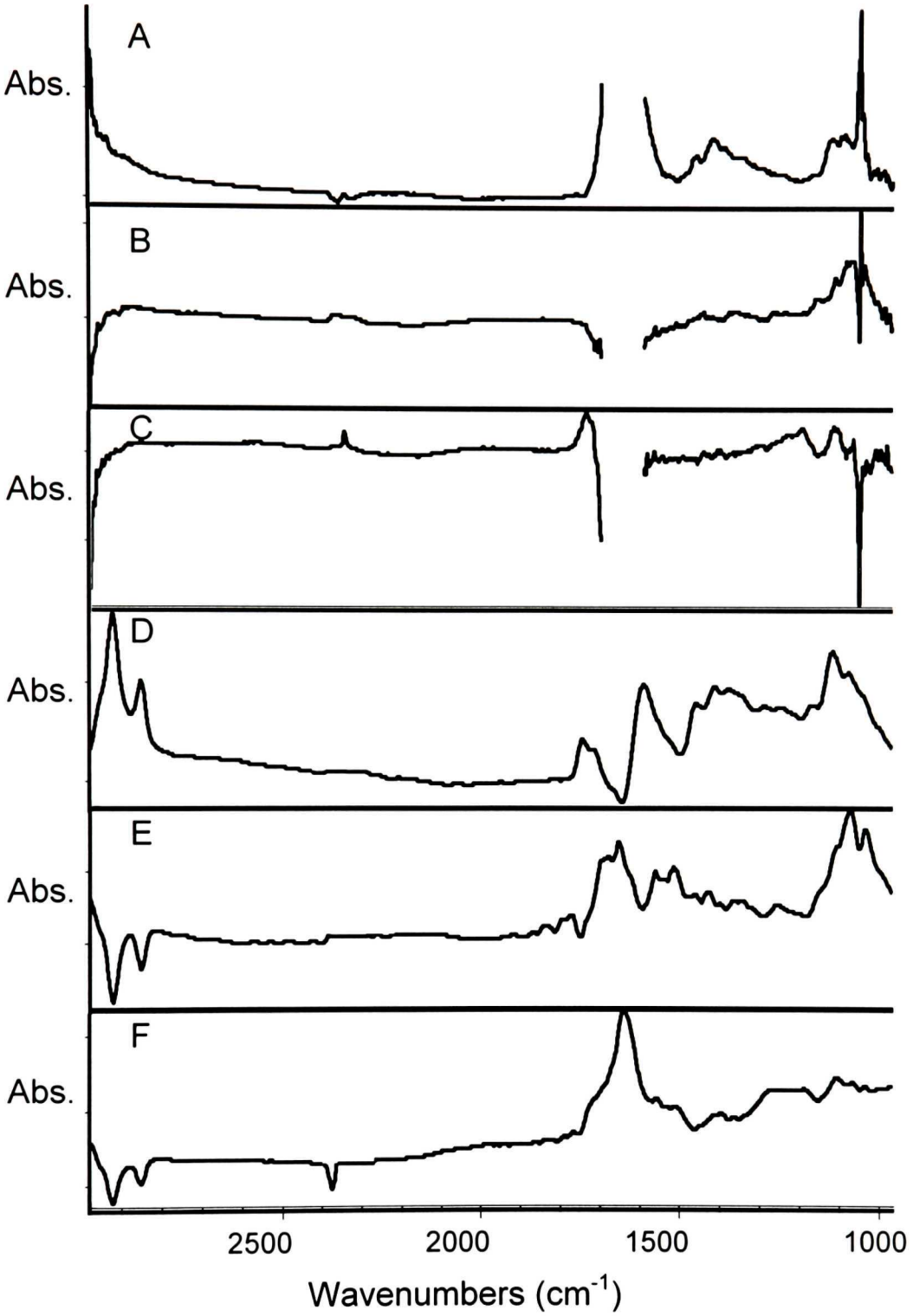

Figure 4.2. PLS pure component spectra derived for (A) pH, (B) total reducing sugar and (C) total acidity from FTIR transmission spectra and for (D) pH, (E) total reducing sugar and (F) total acidity from SB-ATR spectra.

In developing the PLS calibration models, five broad spectral regions were initially selected by examining the "pure component" spectra. The optimal spectral region or combination of spectral regions for the prediction of each of the 11 parameters was chosen by evaluating the cross-validation statistics. The regions ultimately selected are summarized in Table 4.5. The optimized calibration models were validated by comparing the PLS-predicted values for the 77 pre-analyzed wines in the validation set to the reference method values. Figures 4.3-4.6 present plots of the predicted vs. actual (i.e., reference) values for alcohol, reducing sugars, glycerol and organic acids, respectively. Table 4.6 summarizes the data obtained for all 11 parameters, including the ranges of the values spanned by the validation set and the linear regression equations relating the PLS predicted values to the reference method values and R, SEP, MD_a and SDD_a values. For purposes of comparison, the SEP and SDD_a values reported by Patz *et al.*[14] and Dubernet and Dubernet[15], respectively, for FTIR wine analysis using a Foss wine analyzer are also included in Table 4.6.

The predicted values for the parameters evaluated in the initial trial (alcohol, reducing sugars and total acidity) corresponded well to the reference method values for the validation samples. For alcohol and reducing sugars, as well as fructose, R values of >0.99 were obtained. It may be noted in Figures 4.3 and 4.4 that the validation set was uniformly distributed over the entire range of alcohol content, while for sugars, most of the wines were dry with only a few of them being semi-sweet or sweet. An attempt was made to develop PLS calibration models for the prediction of these two components in wines based simply on mixtures of ethanol, glycerol, fructose and glucose as calibration standards. However, large biases were obtained when wines were analyzed using these calibrations, indicating that these simple calibration standards did not adequately model the spectra of wines. This finding is consistent with results obtained by Schindler *et al.*[4] in their investigation of a calibration set consisting of model solutions as an alternative to pre-analyzed wines.

Satisfactory agreement between the FTIR predicted and reference values was also obtained for glycerol (Figure 4.5), a component present in wines as a fermentation by-product[24], and for the individual organic acids (Figure 4.6), with the exception of citric acid. Better results were obtained for total acidity (R = 0.925) than for the individual

Table 4.5: Regions employed in the PLS regression for multicomponent analysis of wines by SB-ATR/FTIR spectroscopy.

Component	Region (cm^{-1})				
	1500–850	1500– 957	1500 – 1108	1801 – 1500	3000 - 2800
Alcohol	+	-	-	-	-
Fructose	-	+	-	-	+
Citric acid	+	-	-	+	+
Tartaric acid	+	-	-	+	+
Malic acid	-	-	+	+	-
Glycerol	+	-	-	+	-
Lactic acid	+	-	-	+	-
Red. sugar	-	+	-	-	+
Vol. acidity	-	+	-	+	-
Tot. acidity	-	-	+	+	-
Total SO_2	+	-	-	-	-

Table 4.6: Linear regression equations relating PLS predictions to the reference values for the validation samples (n=77) ranked in terms of decreasing R value with comparison of SEP and SDD_a to data published from studies using a CaF_2 transmission flow-through cell.

Component	Range of Concentration	Equation	R	SEP	SEP[a]	MD_a	SDD_a	SDD_a[b]
Alcohol[c]	7.3-17.0% (v/v)	Y = -0.235 + 1.020X	0.997	0.099	0.21	0.01	0.101	0.08
Reducing sugar[c]	1.3-116.6 g/L	Y = -0.729 + 0.970X	0.992	2.180	0.86	-0.94	2.231	2.41
Fructose	0-64.48 g/L	Y = -0.179 + 1.040X	0.987	1.606	0.62	-0.08	1.630	-
Total acidity[c]	2.7-6.3 g/L (H_2SO_4)	Y = 0.172 + 0.906X	0.925	0.178	0.13	-0.17	0.182	0.07
Lactic acid	0.03-3.47 g/L	Y = 0.366 + 0.821X	0.901	0.291	0.20	0.12	0.317	0.30
Glycerol	2.07-15.53 g/L	Y = 2.136 + 0.796X	0.864	0.824	0.49	0.84	0.894	1.315
Malic acid	0-4.54 g/L	Y = 0.498 + 0.700X	0.768	0.651	0.16	0.26	0.727	0.12
Tartaric acid	0.43-3.81 g/L	Y = 0.432 + 0.764X	0.709	0.388	0.38	-0.09	0.404	0.11
Volatile acidity	0.21-0.83 g/L (H_2SO_4)	Y = 0.281 + 0.472X	0.625	0.105	0.071	0.04	0.14	0.022
Total SO_2	0-250 ppm	Y = 54.27 + 0.307X	0.569	21.1	17	-5.9	38.8	-
Citric acid	0-3.37 g/L	Y = 0.126 + 0.081X	0.384	0.104	-	-0.11	0.497	-

[a]SEP values from Patz *et al.*[14]
[b]SDD_a values from Dubernet and Dubernet[15]
[c]Parameters evaluated in the SB-ATR feasibility trial.

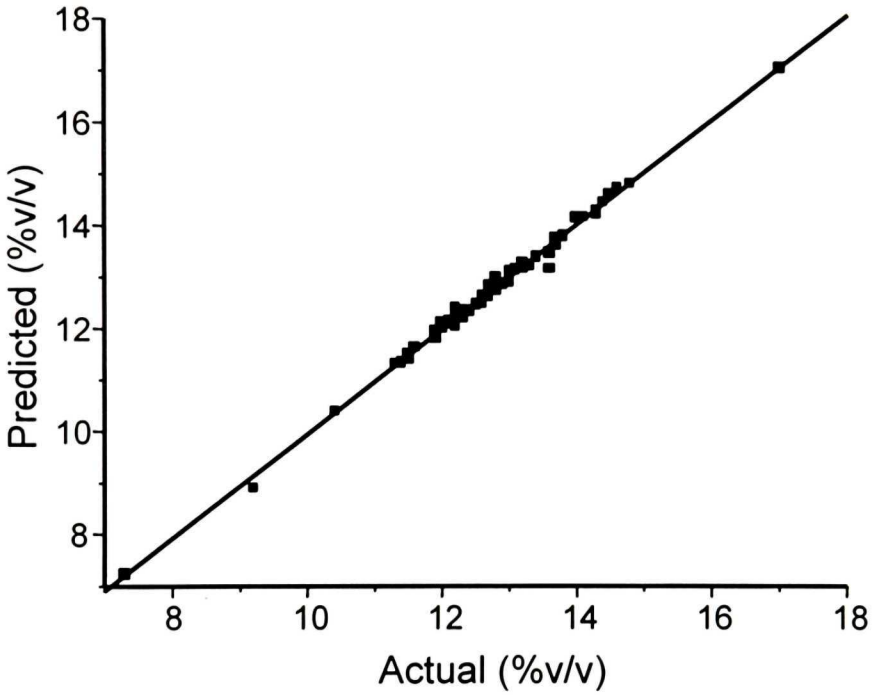

Figure 4.3. Plot of predicted vs actual percent alcohol for the validation set (R= 0.997, SEP = 0.09% (v/v)).

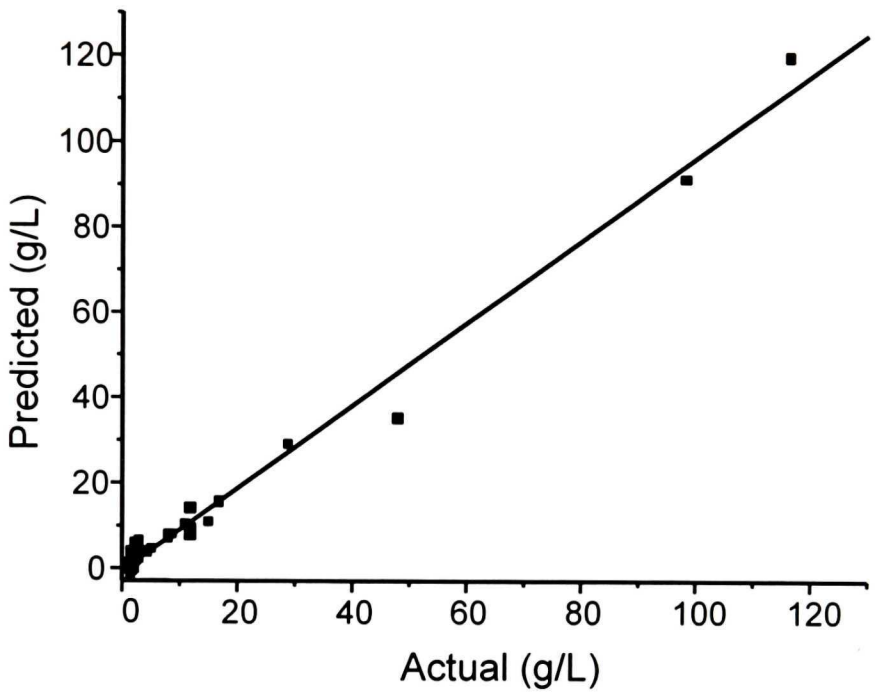

Figure 4.4. Plot of predicted vs actual total reducing sugar for the validation set (R= 0.992, SEP = 2.18 g/L).

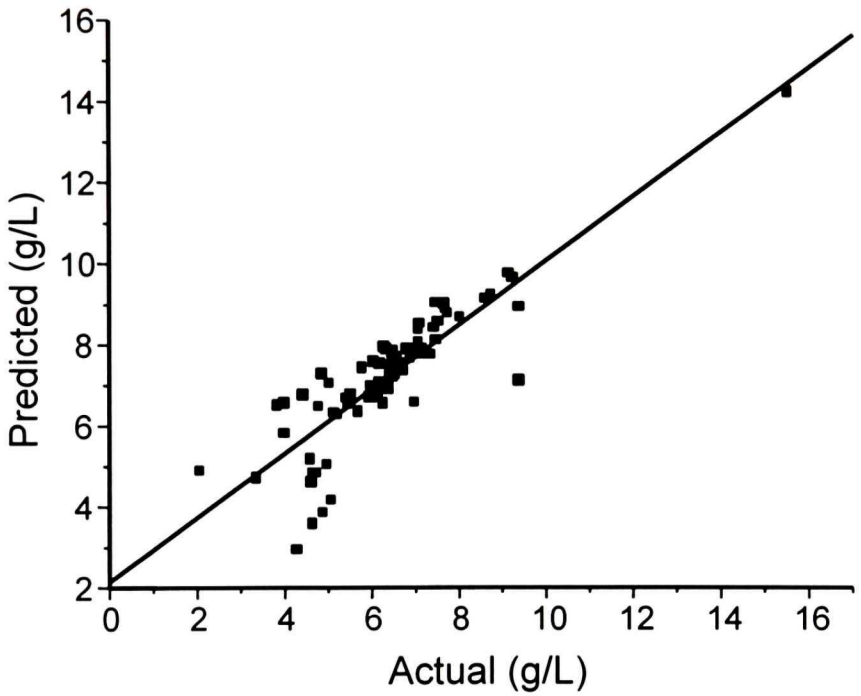

Figure 4.5. Plot of predicted vs actual glycerol content for the validation set (R= 0.864, SEP = 0.824 g/L).

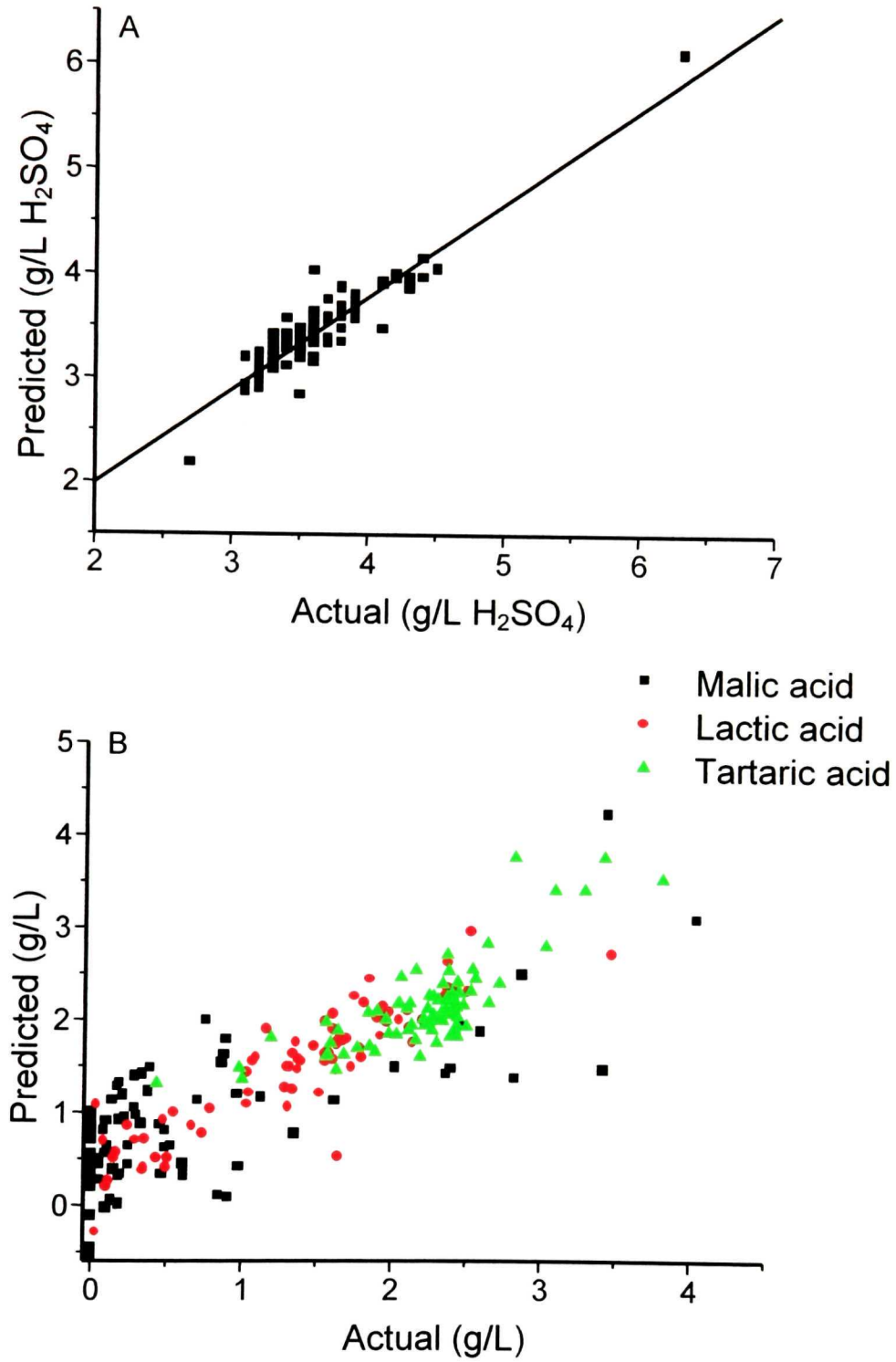

Figure 4.6. Plot of predicted vs actual total acidity (R= 0.925, SEP = 0.178 g/L H_2SO_4) (A) and malic acid (R = 0.768, SEP = 0.651 g/L), lactic acid (R = 0.901, SEP = 0.291 g/L) and tartaric acid (R = 0.709, SEP = 0.388 g/L) content (B) for the validation set.

organic acids, which may be attributed to differences in the precision of the reference methods as well as to possible inadequacy of the FTIR method in differentiating among the various organic acids. The poor results for citric acid are due to its very low concentration, as naturally occurring levels in wine are typically below 0.1 g/L[24] and very few of the samples available for this study contained >0.30 g/L. However, citric acid is sometimes added to wines to increase the total acidity content or to prevent casse, an incipient souring in certain wines caused by an excess of metallic salts, which results in cloudiness and an off-taste[24]. For these types of samples, if citric acid information is required, spiking known amounts of citric acid into wines to model in variability and response into the calibration can be carried out.

In addition to citric acid, volatile acidity and total SO_2 were poorly predicted. Volatile acidity levels were too low and spanned too narrow a range of concentration (0.2–0.8 g/L H_2SO_4) to develop an adequate calibration, while total SO_2, present at the ppm level in wines, does not produce an adequate signal to calibrate on at concentrations of <100 ppm[14] and its spectrum is complicated by its multiple ionic states which are sensitive to the sample matrix pH[15].

A detailed comparison between the SEP and SDD_a values obtained in this study and the values from the literature tabulated in Table 4.6 would not be informative. This is because the analytical performance achieved for each component is highly dependent on the precision of the reference method used to analyze the calibration and validation samples and the number and types of wine samples used in the calibration and validation sets. However, overall, the data in Table 4.6 indicate that the SB-ATR/FTIR results are comparable to those obtained in studies using a commercial FTIR wine analyzer equipped with a CaF_2 flow-through cell[14,15] (Table 4.6). Taken together with the results in Table 4.4 for the SB-ATR accessory and a 50-μm CaF_2 transmission cell, which can be directly compared since they are based on the same set of samples and reference values, it may be concluded that SB-ATR/FTIR spectroscopy can provide comparable sensitivity to commercial FTIR wine analyzers, capable of measuring concentrations of components at levels of >0.1 g/L[14,15].

4.5 CONCLUSION

This study has demonstrated the suitability of SB-ATR/FTIR spectroscopy for the analysis of distilled liquors and wines. The determination of alcohol in distilled liquors is a simple analytical procedure, and calibration can be performed using a small set of ethanol/distilled water mixtures as standards. In contrast, multicomponent wine analysis is a complex undertaking, requiring a very careful selection of the wines used as calibration standards to represent the population of interest and substantial investment in quality reference method analyses. This drawback pertains equally to commercially available FTIR wine analyzers[14,15]. In this context, the use of gravimetrically prepared solutions containing the pure components of interest as calibration standards would clearly be advantageous. However, an investigation of this possibility in the present work indicated that such an approach was not viable owing to the complexity of the wine matrix.

As an alternative to the transmission cell employed in FTIR wine analyzers, the SB-ATR accessory yielded comparable analytical performance. In addition it provided a very simple means of sample handling, as only a drop of sample is required to cover the surface of the ATR crystal for analysis and is readily rinsed and wiped off, ready for the next analysis. It also provides a means of analyzing a wide range of alcoholic beverages, including products high in alcohol and/or sugar content without any need for prior dilution of the sample. The proven suitability of an SB-ATR accessory for wine analysis makes it possible to readily implement FTIR wine analysis methodology on a standard benchtop FTIR spectrometer, furnishing a less costly alternative to the purchase of a dedicated analyzer. Furthermore, the standard SB-ATR accessory can be adapted to a flow-through configuration to accommodate high-volume analytical applications in distilleries, wineries, and commercial and regulatory laboratories.

ACKNOWLEDGEMENTS

The authors would like to thank the SAQ for so generously providing the wine samples and some of the reference analyses for this work. Financial support for this work by Thermal-Lube Inc. is gratefully acknowledged.

REFERENCES

1. Macrae, R., ed. (1993) *Encyclopedia of Food Science, Food Technology and Nutrition* (Academic Press, San Diego, CA), 4921-4941.

2. Fauhl, C. and Wittkowski, R. (2000). Oenological influences on the D/H ratios of wine ethanol, *J. Agric. Food Chem.*, 48, 3979-3984.

3. Davenel, A., Grenier, P., Foch, B., Bouvier, J.C., Verlaque, P. and Pourcin, J. (1991). Filter, Fourier transform infrared, and areometry, for following alcoholic fermentation in wines, *J. Food Sci.*, 56 (6) 1635-1638.

4. Schindler, R., Vonach, R., Lendl, B. and Kellner, R. (1998). A rapid automated method for wine analysis based upon sequential injection (SI)-FTIR spectrometry, *Fresenius J. Anal. Chem.*, 362, 130-136.

5. Li-Chan, E.C.Y., Ismail, A.A., Sedman, J. and van de Voort, F.R. (2002). Vibrational spectroscopy of food and food products. In : *Handbook of Vibrational Spectroscopy* (J.M. Chalmers and P.R. Griffiths eds., John Wiley & Sons Ltd., Chichester, England), 3629-3662.

6. Cabanis, M.T., Cabanis, J.C., Raffy, J., Peyronnenche, M., Viotte, O. and Leboeuf, J.P. (1983). L'Infralyzer 400: une détermination automatique du titre alcoolmétrique des vins, *Rev. Fr. OENO.*, 89, 75-79.

7. van den Berg, F.W.J., van Osenbruggen, W.A. and Smilde, A.K. (1997). Process analytical chemistry in the distillation industry using near-infrared spectroscopy, *Process Control Qual.*, 9, 51-57.

8. Gallignani, M., Garrigues, S. and de la Guardia, M. (1993). Direct determination of ethanol in all types of alcoholic beverages by near-infrared derivative spectrometry, *Analyst*, 118, 1167-1173.

9. Tipparat, P., Lapanantnoppakhum, S., Jakmunee, J. and Grudpan, K. (2001). Determination of ethanol in liquor by near-infrared spectrophotometry with flow injection, *Talanta*, 53, 1199-1204.

10. Garcia-Jares, C.M. and Medina, B. (1997). Application of multivariate calibration to the simultaneous routine determination of ethanol, glycerol, fructose, glucose and total residual sugars in botrytized-grape sweet wines by means of near-infrared reflectance spectroscopy, *Fresenius J. Anal. Chem.*, 357, 86-91.

11. Bouvier, J.C. (2001). Réflexion sur l'analyse oenologique par spectrométrie infrarouge, *Rev. Fr. OENO.*, 191, 16-17.

12. Mahia, P.L., Gandara, J.S. and Losada, P.P. (1992). Validation of ethanol determination in alcoholic beverages by infrared spectrophotometry using orthogonal and derivative functions to correct for water absorption, *Vibr. Spectrosc.*, 3, 133-138.

13. Gallignani, M., Garrigues, S. and de la Guardia, M. (1994). Derivative Fourier transform infrared spectrometric determination of ethanol in alcoholic beverages, *Anal. Chim. Acta*, 287, 275-283.

14. Patz, C.D., David, A., Thente, K., Kurbel, P. and Dietrich, H. (1999). Wine analysis with FTIR spectrometry, *Vitic. Enol. Sci.*, 54 (2-3) 80-87.

15. Dubernet, M. and Dubernet, M. (2000). Utilisation de l'analyse infrarouge à transformée de Fourier pour l'analyse oenologique de routine, *Rev. Fr. OENO.*, 181, 10-13.

16. Andersen, S.T., Hansen, P.W. and Andersen, H.V. (2002). Vibrational spectroscopy in the analysis of dairy products and wine. In: *Hanbook of Vibrational Spectroscopy* (J.M. Chalmers and P.R. Griffiths eds., John Wiley & Sons Ltd, Chichester, England), 1-10.

17. Brierley, P.R. (1999). Imaging stage for Fourier transform infrared spectrometer, *U.S. Patent* 5,965,889.

18. Cocciardi, R.A., van de Voort, F.R., Sedman, J. and Ismail, A.A. Monitoring of lactose hydrolysis in milk by single-bounce attenuated total reflectance Fourier transform infrared spectroscopy. To be submitted.

19. *Official Methods of Analysis of the Association of Official Analytical Chemists* (1995) 16th ed., AOAC International, Arlington, VA, sec. 982.10.

20. *Official Methods of Analysis of the Association of Official Analytical Chemists* (1995) 16th ed., AOAC International, Arlington, VA, sec. 942.06.

21. *Official Methods of Analysis of the Association of Official Analytical Chemists* (1995) 16th ed., AOAC International, Arlington, VA, sec. 950.04.

22. *Official Methods of Analysis of the Association of Official Analytical Chemists* (1995) 16th ed., AOAC International, Arlington, VA, sec. 957.03.

23. Haaland, D.M. and Thomas, E.V. (1988). Partial-least-squares methods for spectral analyses. 1. Relation to other quantitative calibration methods and the extraction of qualitative information, *Anal. Chem.*, 60, 1193-1201.

24. Amerine, M.A., Berg, H.W., Kunkee, R.E., Ough, C.S., Singleton, V.L. and Webb, A.D. (1980). Legal Restrictions on wine making. In: *The Technology of Wine Making*, 4th ed. (The Avi Publishing Company Inc., Westport, CO), 715-755.

BRIDGE

In Chapters 3 and 4, the feasibility of using SB-ATR/FTIR spectroscopy in quantitative analysis applications was assessed. It was found that this method performed comparably to the transmission FTIR method for the analysis of wines; however, the SB-ATR accessory offered the advantages of versatility and ease of sample handling. Another potential alternative is to use FT-NIR spectroscopy, a method more commonly used for quantitative analysis because of sample-handling considerations. One drawback of FT-NIR analysis is that NIR bands are broad, poorly defined and highly overlapped. In the case of sugar analysis, it is difficult to differentiate spectrally one sugar from another from their NIR spectra. Among the findings of the research presented in Chapters 3 and 4 was the capability of SB-ATR/FTIR spectroscopy for the quantitative multicomponent analysis of sugars. This capability is due to the excellent quality of SB-ATR spectra in the 1200-950 cm^{-1} region, in which sugars exhibit intense and characteristic spectral profiles that allow them to be differentiated from each other. In the next chapter, the resolving power of H2D-CS will be employed to make use of the information content of the SB-ATR/FTIR spectra of sugar solutions to identify potentially suitable NIR wavelengths for the development of MLR calibrations for the determination of individual sugars in sugar solutions.

CHAPTER 5

HETEROSPECTRAL TWO-DIMENSIONAL CORRELATION SPECTROSCOPY OF FOURIER SELF-DECONVOLVED FOURIER TRANSFORM NEAR-INFRARED AND FOURIER TRANSFORM MID-INFRARED SPECTRA OF SUGAR SOLUTIONS

5.1 ABSTRACT

The mid- and near-infrared (mid-IR and NIR) spectra of aqueous solutions of glucose and fructose, fructose and galactose, and glucose and galactose were recorded and analyzed by heterospectral two-dimensional (2D) correlation spectroscopy (H2D-CS) to determine characteristic NIR wavelengths for each sugar. Fourier self-deconvolution (FSD) was applied to the NIR spectra prior to H2D-CS analysis to help resolve the strongly overlapping sugar absorptions. Both 2D contour maps and 2D slice spectra were examined to identify the positions of correlation peaks, representing parallel intensity changes in the mid-IR and NIR spectra with changes in the concentrations of the sugars. Two regions of the NIR spectrum were investigated, the first combination region between 1850 and 2500 nm and the first overtone region between 1350 and 1850 nm. Examination of the H2D-CS data indicated absorption by glucose at 1673, 1692, 1710, 1750, 1780, 2230, 2282, 2324 and 2337 nm, by fructose at 1686, 1701, 1721, 1736, 2098, 2258 and 2278 nm and by galactose at 1589, 1671, 1750, 1811, 1826, 2141, 2263, 2306, 2336, 2368 and 2395 nm. The wavelengths identified by H2D-CS were then used to develop multiple linear regression (MLR) calibrations for the quantitative analysis of mixtures of the three sugars in solution. This approach gave comparable results to MLR calibrations based on wavelengths selected by examination of the 1^{st} and 2^{nd} derivative spectra of solutions of the individual sugars and superior results to partial-least-squares (PLS) regression employing the first combination region of the NIR spectra.

5.2 INTRODUCTION

Near-infrared (NIR) spectroscopy is a widely used instrumental method for the compositional analysis of food products largely due to its speed and its capability to simultaneously determine multiple components without the need for solvents or

reagents[1]. Although mid-IR spectroscopy shares many of these advantages, NIR spectroscopy has a substantial advantage in terms of ease of sample handling because it allows for longer pathlengths and the use of glass/quartz cells or optical fibers for process control applications[2]. From the standpoint of calibration development, however, mid-IR spectroscopy has the advantage that distinctive bands can be associated to different functional groups and constituents of interest, whereas NIR spectra are difficult to interpret, consisting largely of broad bands that are the superposition of various combinations and overtones of the fundamental vibrational modes that give rise to mid-IR absorption bands. Furthermore, in complex matrices multiple components can interact, making the NIR spectrum very complicated[3]. As a result, quantitative analysis by NIR spectroscopy has relied heavily on the use of chemometric techniques to relate subtle spectral variations to changes in concentration of a particular component in the sample matrix, resulting in the need for a large number of calibration standards to construct a calibration model. Calibration development is generally a time-consuming, iterative process as the selection of wavelengths or spectral regions to be used for calibration is generally done empirically[4].

The drawbacks described above may be exemplified by NIR analysis of sugars in solutions, such as beverages, where the low absorptivity of sugars and the strong overlap of individual sugar absorptions as well as their extensive overlap with water absorptions make calibration particularly difficult[5,6]. Although the analysis of sugars in fruit juices and botrytized-grape sweet wines by NIR spectroscopy has been successfully carried out[2,7-9], the further development of quantitative NIR spectroscopic methods of sugar analysis would benefit from a better understanding of the NIR spectra of sugars and more precise band assignments.

In 1993, Robert *et al.* employed canonical correlation analysis to study carbohydrate absorptions in the mid-IR and NIR spectral regions and identify NIR wavelengths characteristic to individual carbohydrates[10]. Also, in 1993, Noda introduced generalized two-dimensional (2D) correlation spectroscopy, a technique capable of extracting information not available from a one-dimensional (1D) spectrum[11]. In the 2D correlation approach, the spectral data are spread over the second dimension, simplifying the visualisation of complex overlapping bands and enhancing spectral resolution[12].

Synchronous and asynchronous spectra, generated by perturbation-induced dynamic fluctuations represent in- and out-of-phase variations, respectively, which can assist in the assignment of two correlated bands to the same origin. Over the past decade, a wide range of applications of this technique have been reported, including heterospectral 2D correlation (H2D-CS) studies, where the data from two different spectroscopic methods are correlated[13]. H2D-CS has been used extensively for band assignments and spectral interpretation of polymers[14-17], proteins[18-20], forages[21], lignins[22], rice[23], hard red winter and spring wheats[24], sugar and lysozyme mixtures[25] and glucose anomers[26]. H2D-CS studies are especially powerful in unraveling NIR spectral information by correlating it to well-defined bands in other types of spectra. For example, Barton *et al.* used H2D-CS between IR and NIR spectra to determine the most probable source of NIR signals in forages[21]. McClure *et al.* carried out Raman-NIR H2D-CS on mixtures of sugar and lysozyme[25], where bands clearly assigned in the Raman spectra were used to identify bands in the NIR spectra that are attributable to sugar or protein, respectively. Awichi *et al.* also employed IR-NIR H2D-CS to identify glucose α and β anomer bands in the combination region of the NIR spectrum[26]. In this paper, H2D-CS was applied to the mid-IR and NIR spectra of aqueous mixtures of glucose, fructose and galactose with the objective of identifying specific wavelengths in the NIR region that are characteristic of the individual sugars. These wavelengths were subsequently employed in the development of multiple linear regression (MLR) calibrations for the quantitative analysis of ternary sugar solutions.

5.3 EXPERIMENTAL

5.3.1. Samples, Chemicals and Reagents

D-Galactose, D-fructose and α-D-glucose were obtained from Sigma-Aldrich (Milwaukee, WI). All other reagents used were of analytical grade and obtained from Fisher Scientific (Montreal, QC). Binary aqueous solutions of glucose/galactose, glucose/fructose and fructose/galactose having a total sugar concentration of 20% (w/w) were prepared for H2D-CS analysis. Ternary aqueous solutions of the same sugars having a total sugar concentration of 20% (w/w) were prepared according to a 16-point

mixture design (Figure 5.1) so as to statistically maximize the information content for MLR and partial-least-squares (PLS) regression analysis[27].

5.3.2. Instrumentation

Fourier transform mid-infrared (FTIR) and near-infrared (FT-NIR) spectra of sugar solutions were recorded using an ABB Bomem (Québec City, QC) MB-150 dual-range (NIR/mid-IR) FTIR spectrometer. The spectrometer was purged with dry air from a Balston air drier (Lexington, MA) to avoid spectral contributions from atmospheric water vapour and carbon dioxide. For FT-NIR analysis, a 500 μm quartz transmission cell was used and spectra were recorded from 2850-800 nm with a resolution of 4 nm and ratioed against an open-beam background spectrum. For FTIR analysis, a ZnSe single-bounce attenuated total reflectance (SB-ATR) accessory (Harrick, Ossining, NY) was used and spectra were recorded from 4000-400 cm^{-1} at a resolution of 4 cm^{-1} and ratioed against a background single beam spectrum of the dry clean ZnSe crystal recorded prior to loading each sample. The transmission cell and ZnSe crystal were maintained at 30 ± 0.1°C using Omega (Omega Engineering, Stamford, CT) and Watlow (Watlow System Integrators, Decorah, IA) temperature controllers, respectively, to minimize spectral variability associated with changes in ambient temperature.

5.3.3. Spectral Analysis

FTIR and FT-NIR spectra of binary sugar solutions were correlated by H2D-CS, a type of generalized 2D correlation spectroscopy described in detail elsewhere[11,28,29], using KG2D software (written by Dr. Y. Wang). This software generates 2D contour maps derived from three-dimensional (3D) spectral space. Fourier self-deconvolution (FSD) was employed to enhance the resolution[30] of the FT-NIR spectra prior to H2D-CS analysis and was carried out by employing Gplot software (written by D. Moffett) with a k factor of 2 and a bandwidth of 17 cm^{-1}. The contour maps and slice spectra obtained by H2D-CS were examined to select wavelengths for use in MLR calibrations. A second set of wavelengths was obtained by examining the 1st and 2nd derivatives of the FT-NIR spectra of 20% (w/w) fructose, glucose and galactose aqueous solutions, after subtraction of the spectral contributions of water. The 1st and 2nd derivatives were computed using

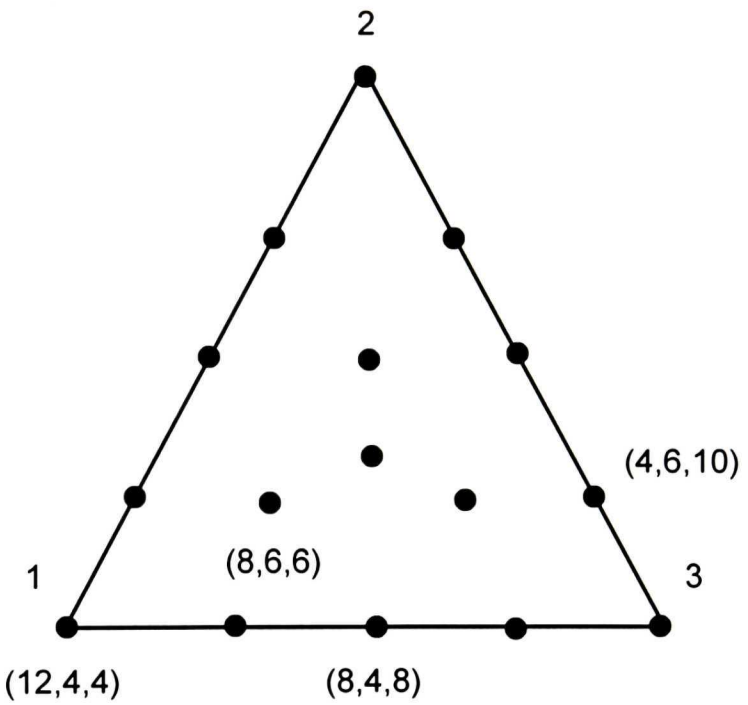

Figure 5.1. Optimal mixture design for a 3 component system (adapted from reference 27).

the Savitzky-Golay algorithm available in the GRAMS/386 software package (Galactic Industries Co., Salem, NH) and the positions of the residual 1st and 2nd derivative peaks were selected as wavelengths for use in MLR calibrations.

5.3.4. Development and Comparison of FT-NIR Calibrations

The utility of H2D-CS analysis as a tool for wavelength selection in the development of MLR-based NIR calibrations was evaluated by comparison with a conventional MLR calibration approach as well as PLS regression. The overall experimental design is outlined in Figure 5.2. All calibrations were developed using 16 ternary mixtures of sugar solutions (Figure 5.1) as calibration standards.

MLR calibration was carried out using the Statgraphics statistical software package (STSC Inc., Rockville, MD) and employing the raw FT-NIR spectra of the calibration standards. The wavelengths selected by H2D-CS or derivative spectroscopy were subjected to backward stepwise variable selection (BSVS)[31], a method commonly used for wavelength selection for MLR. The performance of the MLR calibrations developed was evaluated by computing the standard deviation of the differences for accuracy (SDD_a) between the actual (gravimetric) and fitted values. PLS analyses were carried out using the Omnic Turbo Quant Analyst software package (Nicolet Instruments, Madison, WI). PLS calibrations were developed using the 2050-2400 nm and 1480-1850 nm regions in the raw and 1st and 2nd derivative NIR spectra. The SDD_a for each component was calculated from the leave-one-out cross-validation data obtained using the optimal number of factors determined from the corresponding predicted residual error sum of squares (PRESS) plot. In order to compare the performances of the various calibration approaches, an F-test using the variances (s^2) between the actual and predicted values and a confidence interval of $\alpha = 0.05$ was employed.

5.4. RESULTS AND DISCUSSION

5.4.1. Spectral Analysis of Sugars

In order to employ mid-IR spectral information of sugars to gain a better understanding of their NIR spectra using H2D-CS, mid-IR wavelengths characteristic of the constituents of interest need to be selected. In the mid-IR spectrum, the region

between 1200 and 950 cm^{-1} provides the most intense and characteristic absorptions of sugars, assigned to coupled C-O and C-C stretching vibrations[32]. Figure 5.3 presents the SB-ATR/FTIR spectra of 20% (w/w) solutions of glucose, fructose and galactose, illustrating that although their bands over the 1200-950 cm^{-1} region are highly overlapped, each sugar has a distinct spectral profile that differentiates it from the others. Table 5.1 lists the principal peaks associated with the three sugars, which were subsequently used in the H2D-CS analysis to identify corresponding wavelengths in the NIR region for each sugar.

The most intense bands in the NIR spectra of carbohydrates occur in the first combination region (1850-2500 nm), containing bands due to C-H stretching + C-H deformation (2280-2500 nm) and O-H stretching + O-H deformation (1850-2280 nm), and the first overtone region, containing the first C-H stretching (1650-1850 nm) and first O-H stretching (1350-1650 nm) overtones[33]. In aqueous solution, however, two strong water absorption bands at 1450 and 1940 nm effectively blank out sugar spectral features from 1350 to 1480 nm and from 1850 to 2000 nm, respectively. Figures 5.4 and 5.5 show the remaining portions of the first combination and first overtone regions, respectively, of the NIR spectra of glucose, galactose and fructose aqueous solutions (20% (w/w)), with the spectrum of water subtracted out. The NIR spectral profiles of glucose, galactose and fructose are very similar, with bands at 2110, 2273, 2330, 1560, 1740 and 1690 nm. The resolution of the spectra can be enhanced through the use of FSD or by computing their 1^{st} and 2^{nd} derivatives. As illustrated in Figure 5.6, when these transforms are carried out on the spectrum of a 20% (w/w) fructose solution, they reveal an additional peak at 2258 nm not evident in the raw absorbance spectrum. Because FSD of the 20% (w/w) solutions of glucose, fructose and galactose provided additional characteristic bands for each sugar, H2D-CS analysis was carried out on the FSD rather than the raw FT-NIR spectra.

5.4.2. H2D-CS Analysis

An H2D-CS examination of the spectra of the binary sugar solutions was carried out over the 1200-950 cm^{-1} region of the mid-IR spectra relative to the first combination and first overtone regions in the FSD/FT-NIR spectra. In each of the three series of binary solutions examined (fructose/galactose, fructose/glucose and glucose/galactose),

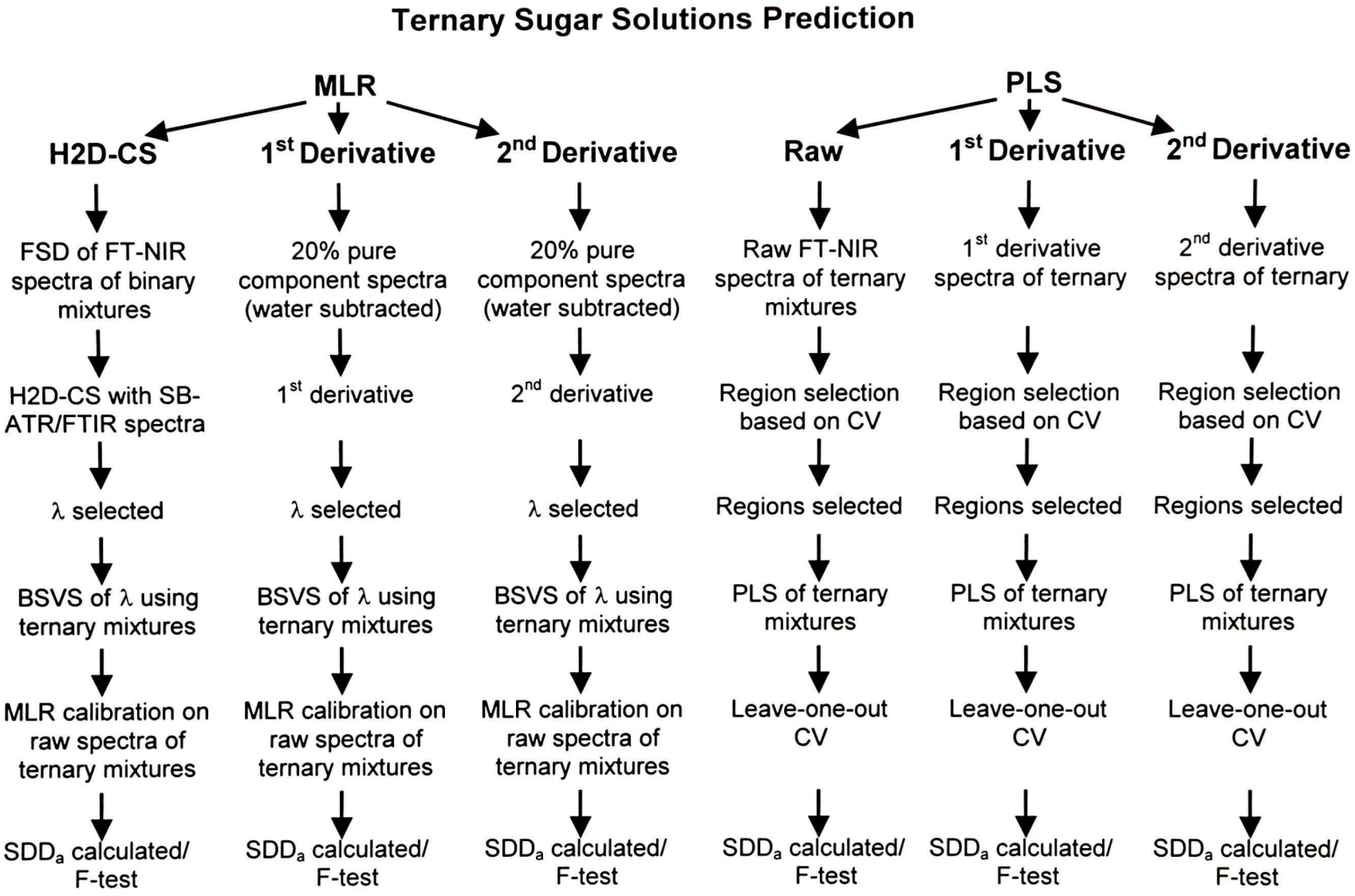

Figure 5.2. Schematic diagram of experimental design (CV = cross-validation)

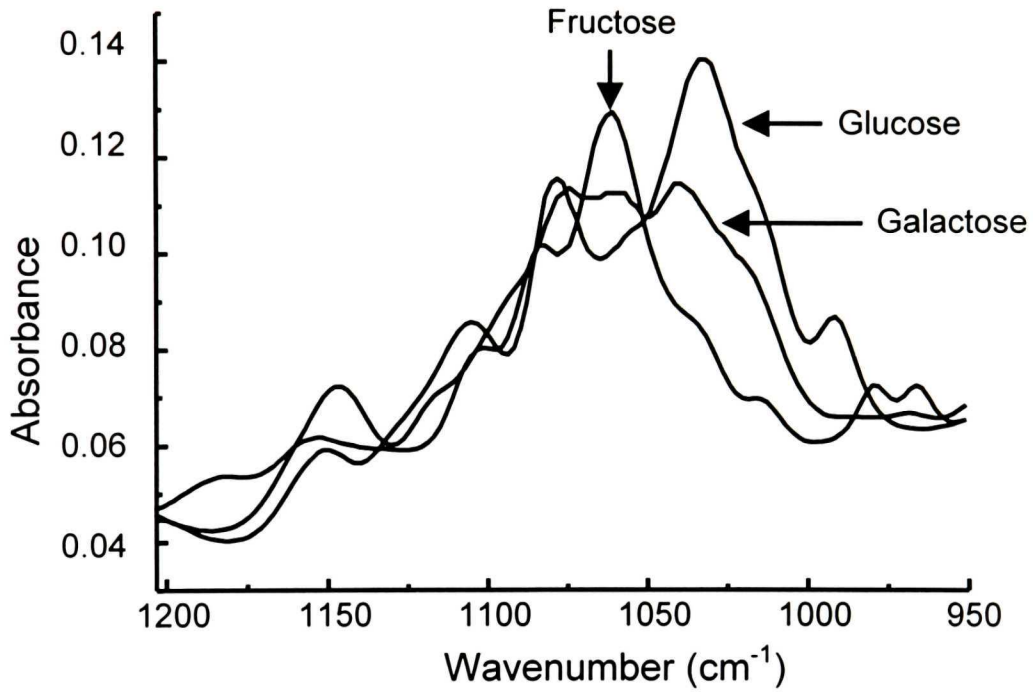

Figure 5.3. SB-ATR/FTIR spectra of 20% (w/w) solutions of glucose, fructose and galactose, with the water spectrum subtracted out, between 1200 and 950 cm^{-1}.

Table 5.1: Mid-IR absorption frequencies of glucose, fructose and galactose between 1200 and 950 cm^{-1}.

Sugar	Absorption frequency (cm^{-1})
Glucose	1150, 1105, 1078, 1032, 992
Fructose	1182, 1153, 1101, 1082, 1062, 1016, 979, 966
Galactose	1147, 1075, 1060, 1040, 986, 969

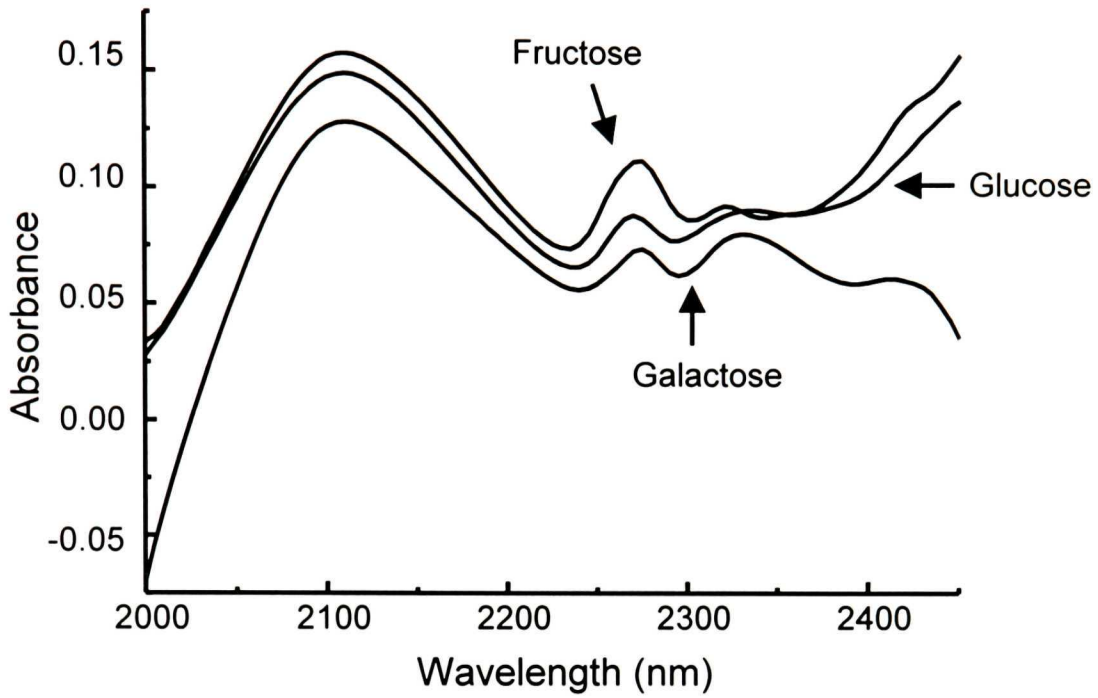

Figure 5.4. FT-NIR spectra of 20% (w/w) solutions of glucose, galactose and fructose, with the water spectrum subtracted out, in the first combination region.

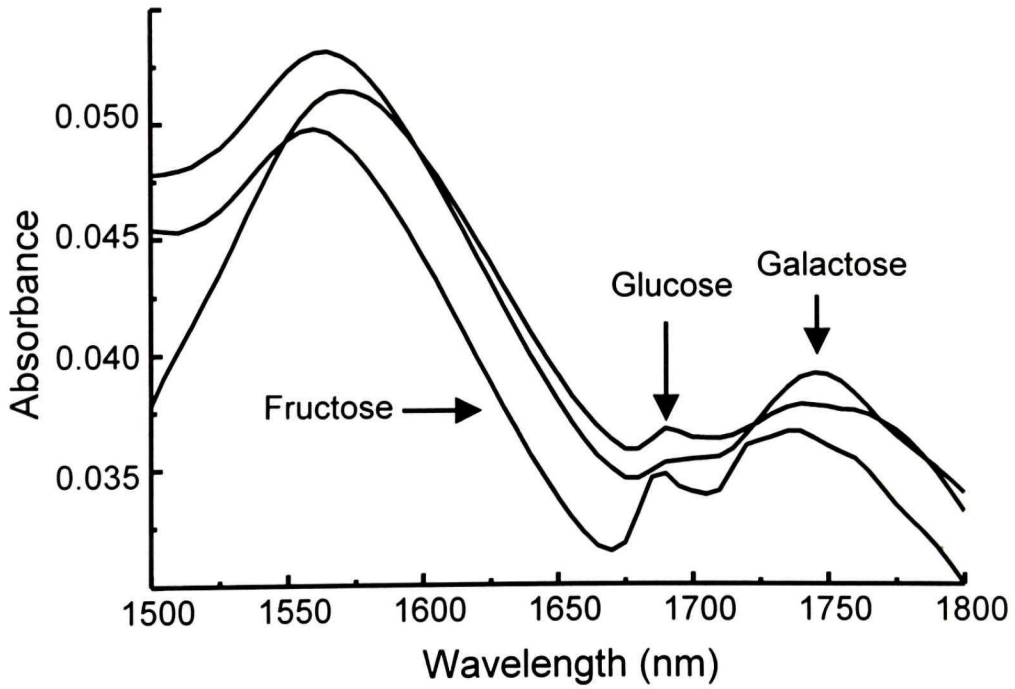

Figure 5.5. FT-NIR spectra of 20% (w/w) solutions of glucose, galactose and fructose, with the water spectrum subtracted out, in the first overtone region.

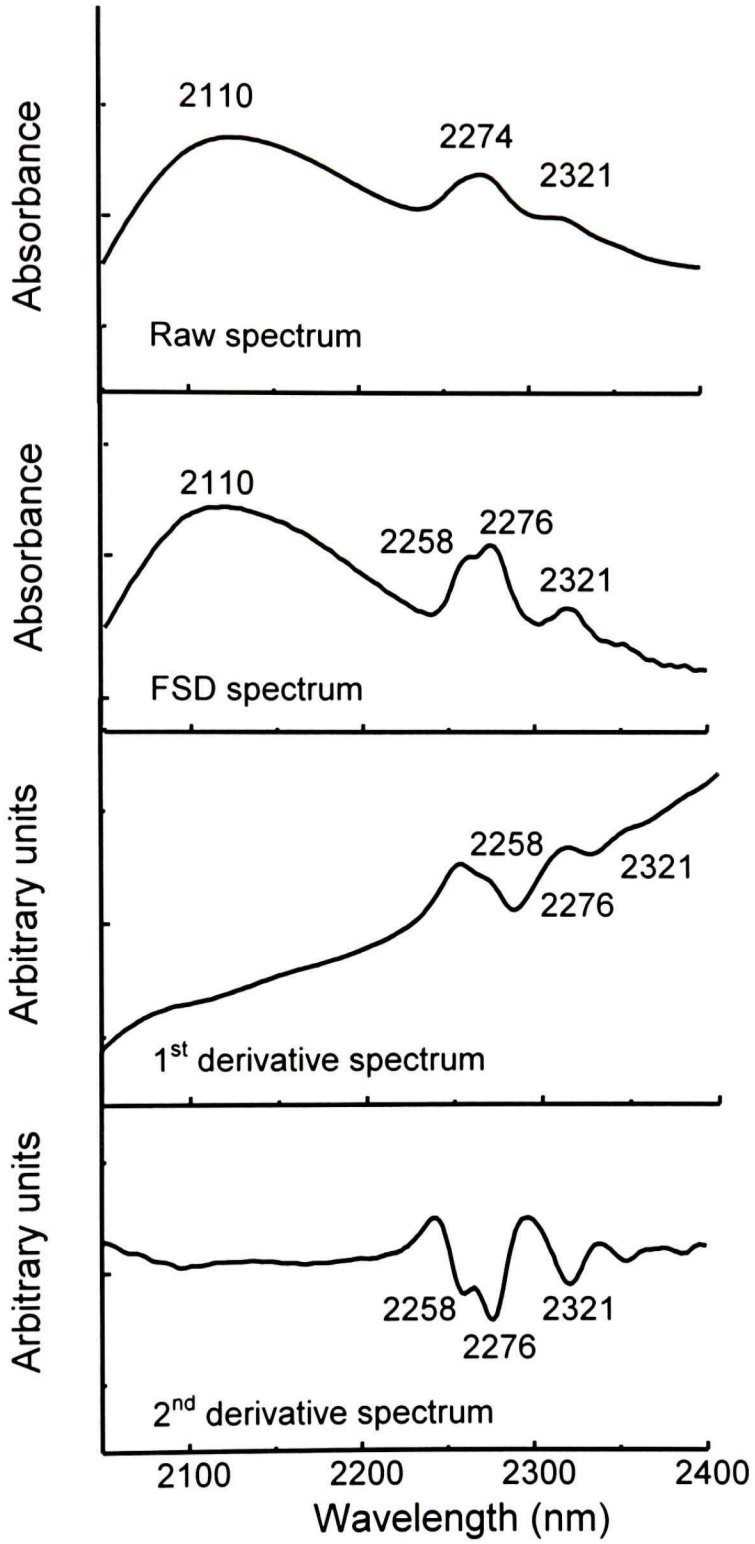

Figure 5.6. Raw, FSD, 1st and 2nd derivative FT-NIR spectra of a 20% (w/w) fructose solution, with the water spectrum subtracted out, in the first combination region.

the concentration of one sugar increased while the other decreased, with the total sugar concentration was maintained at 20% (w/w). Figures 5.7-5.9 show the H2D-CS contour maps generated for fructose/galactose, fructose/glucose and glucose/galactose solutions, respectively, using the first combination region; the 2400-2500 nm and 2000-2050 nm ranges have been omitted from the map as they did not contain any significant spectral information. The corresponding H2D-CS synchronous correlation maps for the first overtone region are illustrated in Figures 5.10-5.12, respectively. The appearance of a contour on a map, termed a cross peak, indicates a positive correlation between the mid-IR and FSD-NIR spectra if the countour lines are solid, i.e. that the spectral intensity changes are from the same component, while a broken contour line indicates that the spectral intensity changes are from the increase in concentration of one component and the decrease in concentration of the other. Figure 5.7 reveals a positive correlation between the mid-IR band at 1062 cm^{-1}, corresponding to fructose, and NIR absorption at wavelengths of 2098, 2258 and 2278 nm, as well as a positive correlation between the mid-IR band at 1147 cm^{-1}, corresponding to galactose, and NIR absorption at wavelengths of 2306, 2336 and 2368 nm. Tables 5.2-5.4 summarize the cross peaks for the three sets of binary solutions. A cross peak associated with a particular component in the H2D-CS maps for both of the sets of solutions containing that component may be regarded as a "characteristic" wavelength for that component in relation to the analysis of mixtures of glucose, fructose and galactose. On the other hand, a cross peak associated with a particular component in the H2D-CS map for one of the sets of solutions containing that component but not in the other indicates that the absorption of that component at that wavelength is predominant only in the presence of one of the two sugars. Thus, although "characteristic" wavelengths were found for fructose and glucose from the H2D correlations, there were no wavelengths at which galactose absorption was predominant in the H2D correlations for both the fructose/galactose and glucose/galactose solutions. This may indicate that there is less characteristic spectral information available for galactose in the NIR spectra of mixtures of glucose, fructose and galactose.

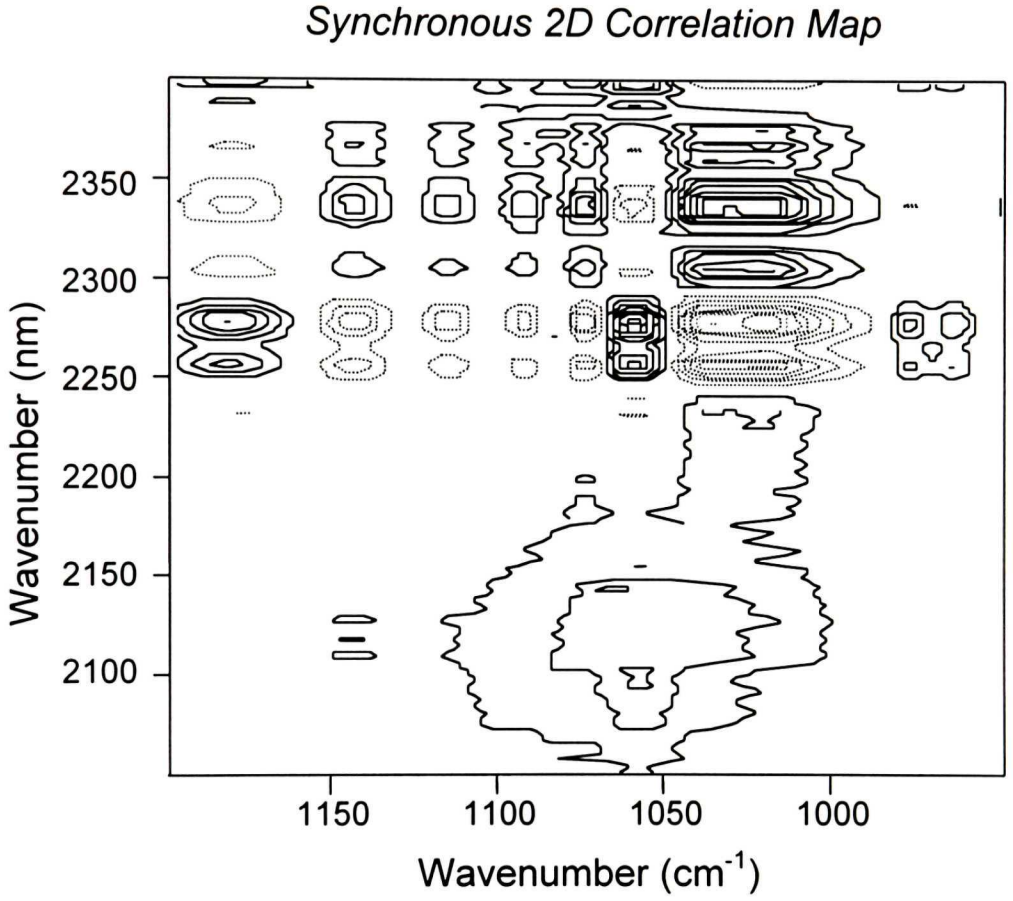

Figure 5.7. Synchronous H2D-CS contour map for fructose/galactose solutions obtained by correlation of the first combination region in the FT-NIR spectra to the 1200-950 cm^{-1} region in the mid-IR spectra.

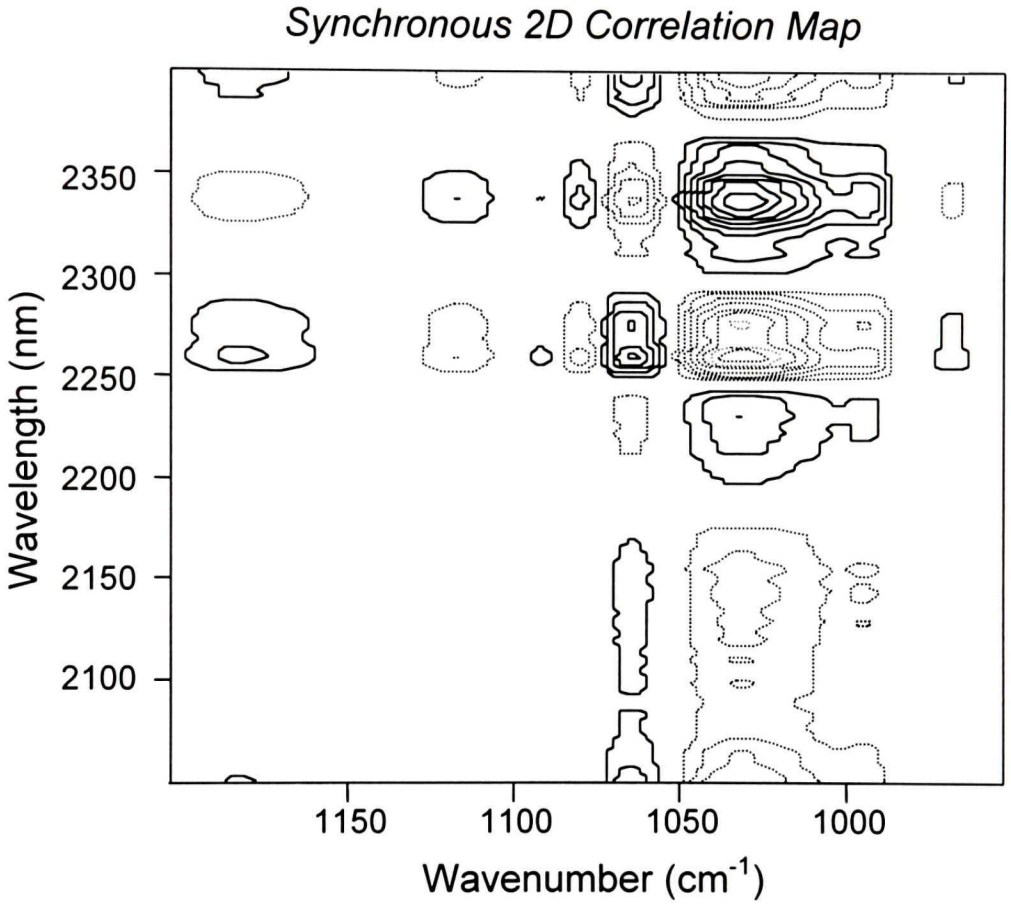

Figure 5.8. Synchronous H2D-CS contour map for fructose/glucose solutions obtained by correlation of the first combination region in the FT-NIR spectra to the 1200-950 cm^{-1} region in the mid-IR spectra.

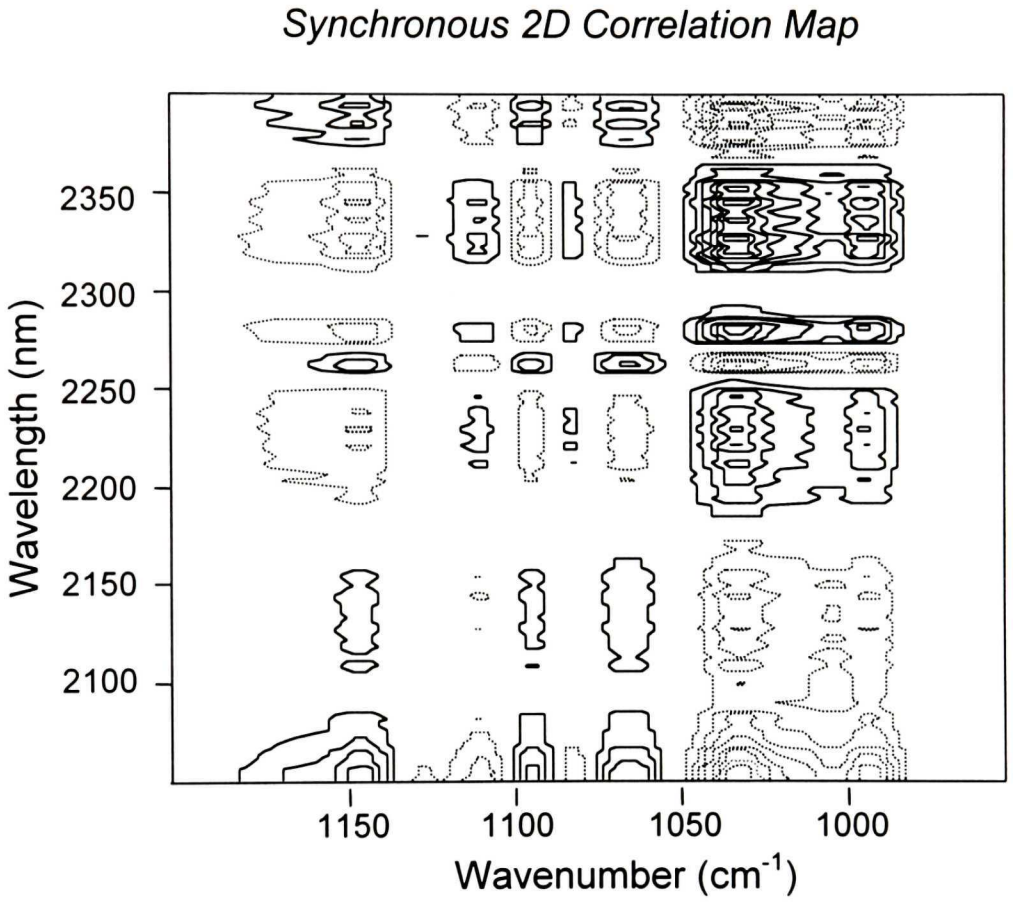

Figure 5.9. Synchronous H2D-CS contour map for glucose/galactose solutions obtained by correlation of the first combination region in the FT-NIR spectra to the 1200-950 cm^{-1} region in the mid-IR spectra.

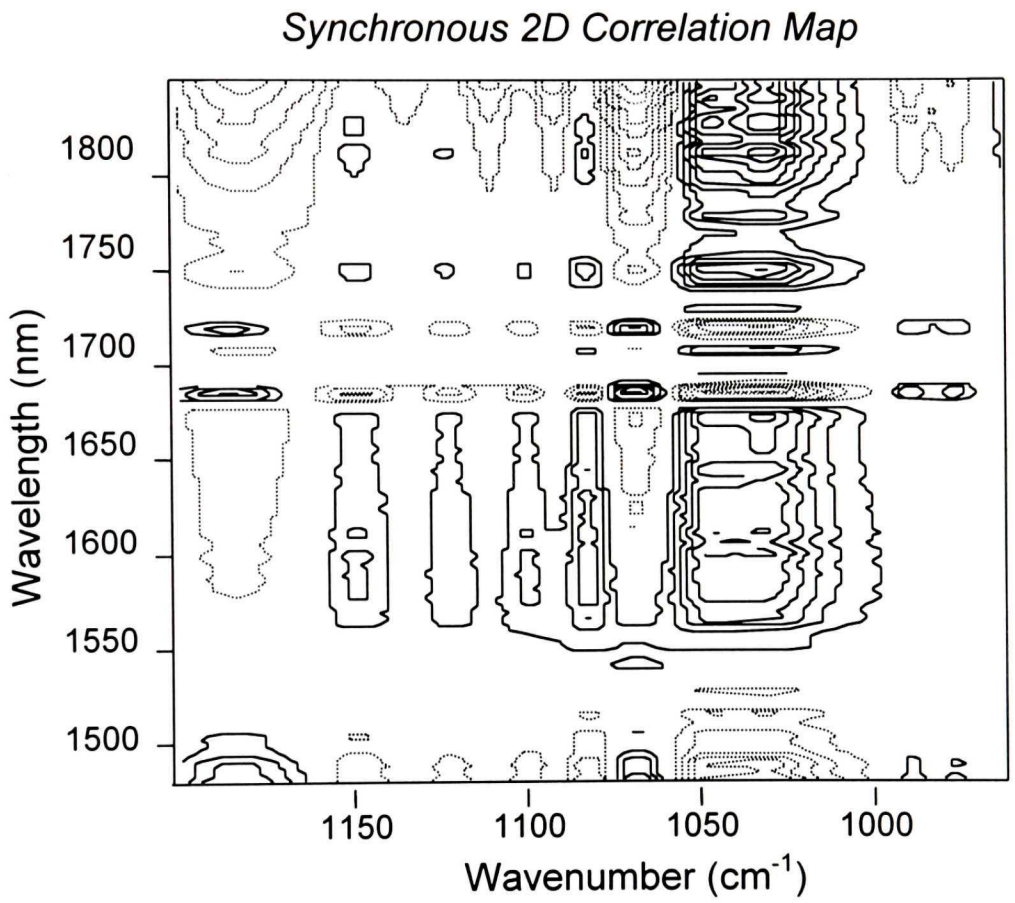

Figure 5.10. Synchronous H2D-CS contour map for fructose/galactose solutions obtained by correlation of the first overtone region in the FT-NIR spectra to the 1200-950 cm^{-1} region in the mid-IR spectra.

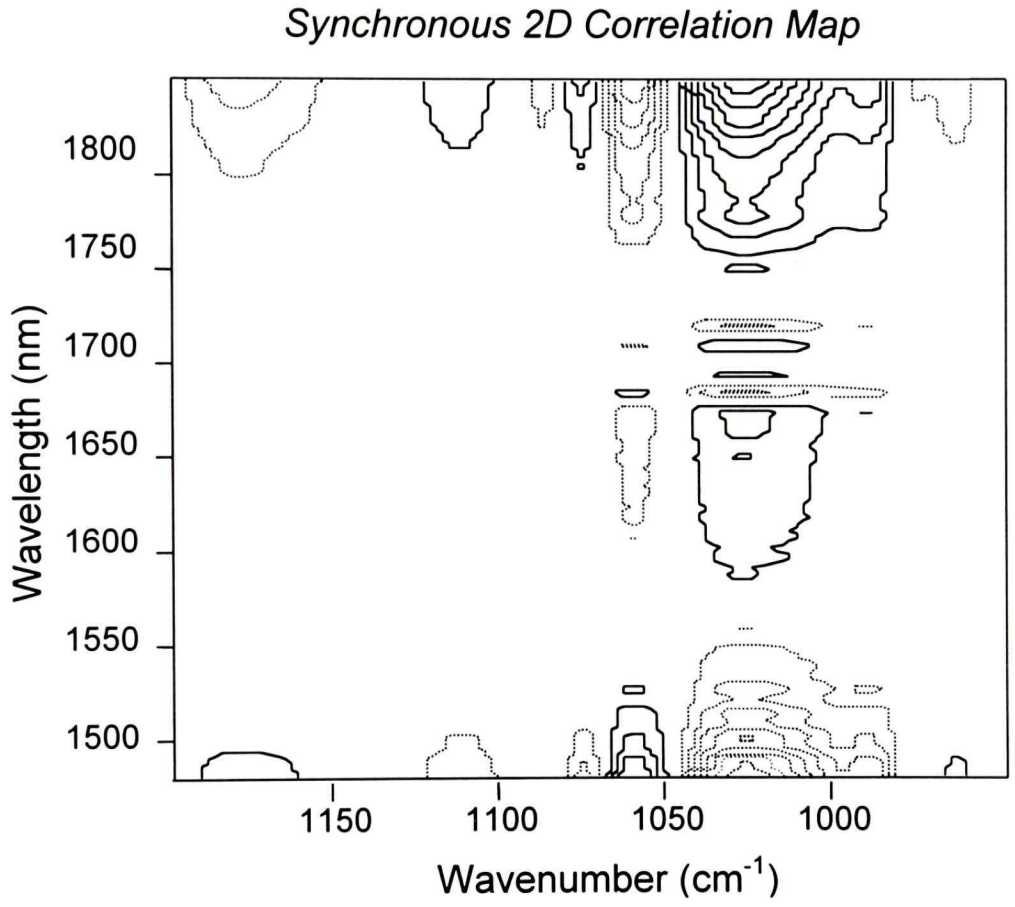

Figure 5.11. Synchronous H2D-CS contour map for fructose/glucose solutions obtained by correlation of the first overtone region in the FT-NIR spectra to the 1200-950 cm^{-1} region in the mid-IR spectra.

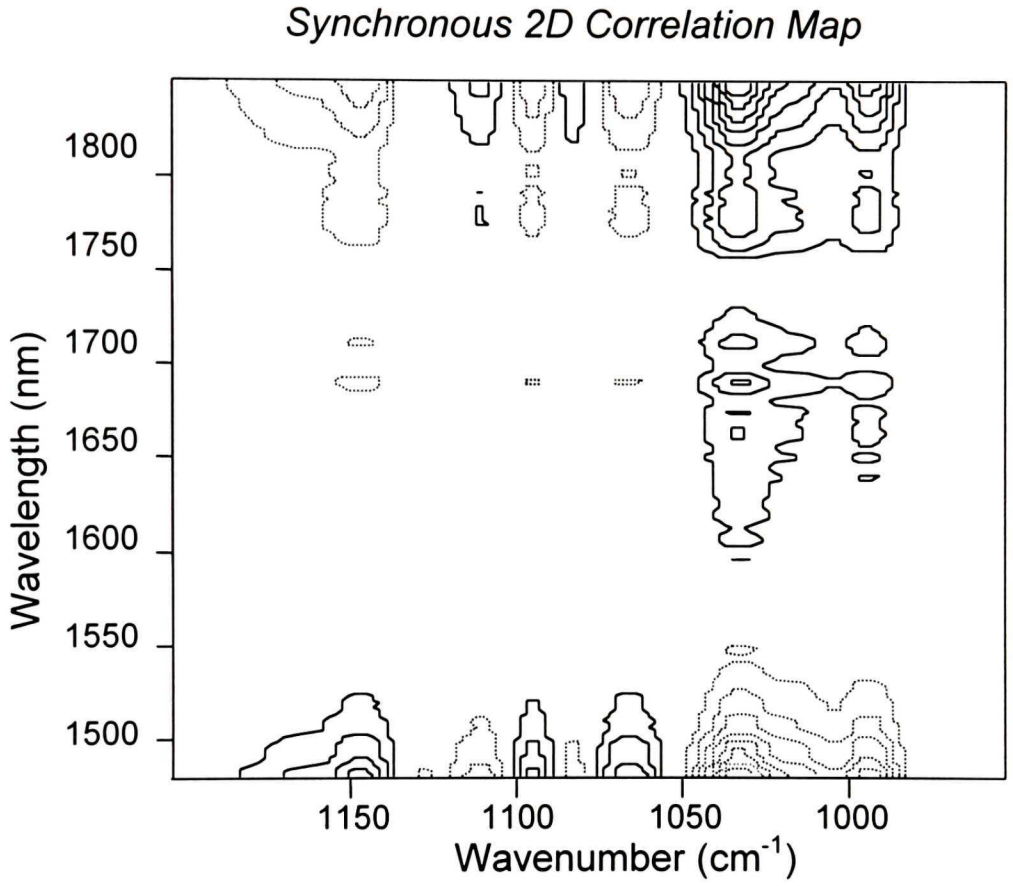

Figure 5.12. Synchronous H2D-CS contour map for glucose/galactose solutions obtained by correlation of the first overtone region in the FT-NIR spectra to the 1200-950 cm^{-1} region in the mid-IR spectra.

Table 5.2 : Signs of H2D-CS peaks for fructose/galactose solutions[a].

λ NIR (nm)	1062 cm^{-1} (fructose)	1147 cm^{-1} (galactose)
1589	-	+
1671	-	+
1686	+	-
1721	+	-
1750	-	+
1811	-	+
1826	-	+
2098	+	-
2258	+	-
2278	+	-
2306	-	+
2336	-	+
2368	-	+

[a]A positive (+) sign indicates that the mid-IR and FSD-NIR bands are from the same sugar, a negative (-) sign means that the two bands are of different origin.

Table 5.3: Signs of H2D-CS peaks for fructose/glucose solutions[a].

λ NIR (nm)	1062 cm^{-1} (fructose)	1032 cm^{-1} (glucose)
1673	-	+
1686	+	-
1692	-	+
1701	+	-
1710	-	+
1721	+	-
1736	+	-
1750	-	+
1780	-	+
2098	+	-
2230	-	+
2258	+	-
2278	+	-
2337	-	+

[a]A positive (+) sign indicates that the mid-IR and FSD-NIR bands are from the same sugar, a negative (-) sign means that the two bands are of different origin.

Table 5.4: Signs of H2D-CS peaks for glucose/galactose solutions[a].

λ NIR (nm)	1147 cm^{-1} (galactose)	1032 cm^{-1} (glucose)
1692	-	+
1710	-	+
1780	-	+
2141	+	-
2230	-	+
2263	+	-
2282	-	+
2324	-	+
2337	-	+
2395	+	-

[a]A positive (+) sign indicates that the mid-IR and FSD-NIR bands are from the same sugar, a negative (-) sign means that the two bands are of different origin.

Although 2D correlation contour maps representing 3D spectral space can be used to assign peaks, 2D slices of the contour map provide more readily interpretable information about the relationships between a band in one spectrum and multiple bands in another. Thus, slice spectra were generated to show the correlation between absorption at a particular wavenumber in the mid-IR region and NIR absorption at all wavelengths on the contour map. Figure 5.13 presents a slice spectrum illustrating the correlation between the band at 1062 cm^{-1} in the mid-IR spectrum and the FSD/FT-NIR spectra, providing a more conventional and interpretable spectral representation of the cross peaks for fructose at 2098, 2258 and 2278 nm shown in the 2D correlation map in Figure 5.7.

5.4.3. MLR and PLS Calibration and Analysis

The NIR wavelengths identified for each sugar from H2D-CS analysis of the binary solutions were used to develop MLR calibrations based on the spectra of 16 ternary sugar solutions, recorded in duplicate. As is commonly done in the development of MLR calibrations, stepwise variable selection was applied to select optimal combinations of wavelengths; although the use of genetic algorithms for this purpose has recently been demonstrated[34], this alternative approach was not investigated in the present work. Table 5.5 lists the wavelengths obtained for the determination of each sugar by application of BSVS. The performance of the resulting MLR calibrations was assessed on the basis of the agreement between the fitted and actual (gravimetric) values, expressed in terms of SDD_a, yielding values of 0.26, 0.20 and 0.35% (w/w) for glucose, fructose and galactose, respectively (Table 5.6). The poorer results for galactose are consistent with their being less spectral information specific to this component as indicated by the H2D-CS study.

For comparative purposes, MLR calibrations were also developed by applying BSVS to wavelengths selected by examination of the 1st and 2nd derivative spectra of solutions of the individual sugars, and the sets of wavelengths obtained in this manner are also listed in Table 5.5. Overall, these wavelengths are also in the H2D-CS-derived wavelength sets, whereas the wavelengths highlighted in bold in Table 5.5 are additional wavelengths present only in the H2D-CS derived wavelength sets. Thus, the H2D-CS wavelength selection approach allowed additional relevant spectral information to be

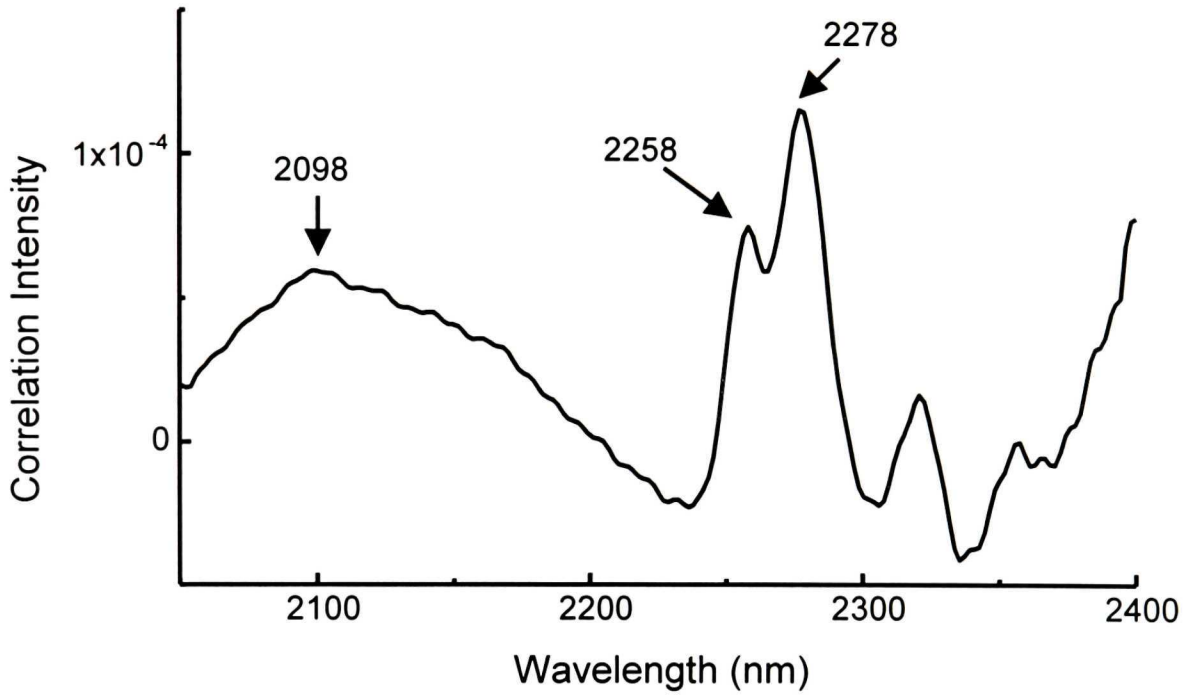

Figure 5.13. H2D-CS slice spectrum showing correlation between the first combination region in the FT-NIR spectra of fructose/galactose solutions and mid-IR absorption at 1062 cm^{-1} characteristic of fructose.

Table 5.5: Wavelengths (nm) selected by examination of 2nd derivative spectra and H2D-CS after BSVS for MLR calibrations for the prediction of glucose, fructose and galactose. Wavelengths in bold are those produced by H2D-CS that were not identified by derivative spectroscopy.

λ	Glucose		Fructose		Galactose	
	2nd deriv.	H2D-CS	2nd deriv.	H2D-CS	2nd deriv.	H2D-CS
λ_1		**1589**				**1589**
λ_2				1686	1690	1686
λ_3				1710		
λ_4				1721		
λ_5	1738	1736	1738	1736	1739	1736
λ_6	1779	1780	1779		1779	1780
λ_7		**1811**				
λ_8						**1826**
λ_9			2092			
λ_{10}		**2141**		**2141**		**2141**
λ_{11}	2258	2258				
λ_{12}	2267		2267		2267	2263
λ_{13}	2276	2282	2276	2282	2276	2282
λ_{14}		**2306**		**2306**		**2306**
λ_{15}	2323	2324	2323	2324		

utilized in the development of the MLR calibrations. In addition, this approach provides the capability of taking into account interactions of the components in the sample matrix that result in shifting of band positions as compared to the spectra of the respective pure components[12]. However, in a detailed examination of the FTIR spectra of pure sugar solutions as a function of concentration[35], no such band shifts were observed over the concentration range employed in the present work, owing to the predominance of sugar-water interactions over sugar-sugar interactions. Thus, this advantage of the H2D-CS approach would not have a significant role in the present study. This can explain why the F-test results in Table 5.6 indicate that the MLR calibrations based on wavelength selection using the derivative spectra of pure solutions of individual sugars performed comparably to those based on the H2D-CS wavelength selection technique.

For further comparison, the raw and 1st and 2nd derivative spectra of the ternary sugar solutions were employed to develop PLS calibrations. Use of the first overtone region, the first combination region and both the first overtone and the first combination regions was investigated and it was found that employing the combination region only (2050-2400 nm) gave the best results. The SDD_a values derived from leave-one-out cross-validation of the various PLS calibrations employing the combination region are included in Table 5.6. Based on the F-test results, the MLR calibrations were superior, in general, to the PLS calibrations. In another study on aqueous ternary sugar solutions of glucose, fructose and sucrose, Rambla *et al.*[2] compared individual wavelength equations based on the pure component solutions and PLS of the ternary solutions and found that PLS gave better results. However, the superior performance of PLS in that study is expected because the individual wavelength equations did not take into account underlying absorptions from the other sugar components.

5.5 CONCLUSION

Correlation of the FSD/FT-NIR and FTIR spectra of aqueous glucose/galactose, glucose/fructose and fructose/galactose solutions by H2D-CS provided information on the NIR spectral characteristics of each sugar that was not available from conventional raw and 1st and 2nd derivative 1D spectra. This additional information was exploited in wavelength selection for the development of MLR calibrations for the quantitative

Table 5.6: SDD_a between actual and predicted values and F-ratios of MLR regressions based on 1st and 2nd derivative selected wavelengths and PLS regressions as compared to MLR regressions based on H2D-CS selected wavelengths.

Method	Glucose (%w/w)		Fructose (%w/w)		Galactose (%w/w)	
	SDD_a	F-ratio[a]	SDD_a	F-ratio[a]	SDD_a	F-ratio[a]
MLR (H2D-CS)	0.258	-	0.203	-	0.351	-
MLR (1st derivative)	0.303	1.38	0.270	1.76	0.427	1.48
MLR (2nd derivative)	0.338	1.71	0.223	1.20	0.392	1.25
PLS (raw spectrum)	0.378	2.14	0.264	1.68	0.801	5.22
PLS (1st derivative)	0.380	2.17	0.293	2.07	0.559	2.54
PLS (2nd derivative)	0.338	1.72	0.324	2.54	0.508	2.10

[a]F-ratio (n = 32, degrees of freedom, d.f. = 2 and a confidence level of $\alpha = 0.05$) based on the ratio of the variances of the differences between the actual and predicted values. The critical F value is 1.84.

analysis of ternary aqueous solutions of glucose, fructose and galactose. MLR calibrations employing H2D-CS derived wavelengths performed comparably to BSVS MLR derivative selected wavelengths and better overall to PLS methods of wavelength region selection and calibration. The use of binary sugar solutions for H2D-CS analysis was the simplest model system that could be employed to interpret the spectra of sugar solutions and to select appropriate wavelengths. For the purpose of this study, this model was considered adequate as the principal interactions involved were sugar-water interactions as the total sugar concentration was 20% (w/w). However, in theory, an additional advantage of H2D-CS is its ability to provide information on intermolecular interactions and as such, H2D-CS could be a powerful tool in assigning wavelengths for calibration and significantly improving calibration models. In the future, this approach can be extended to include H2D-CS analysis of ternary and higher mixtures of components and to sugars in soft drinks and juices.

REFERENCES

1. Dull, G.G. and Giangiacomo, R. (1984). Determination of individual simple sugars in aqueous solution by near infrared spectrophotometry, *J. Food Sci.*, 49, 1601-1603.

2. Rambla, F.J., Garrigues, S. and de la Guardia, M. (1997). PLS-NIR determination of total sugar, glucose, fructose and sucrose in aqueous solutions of fruit juices, *Anal. Chim. Acta*, 344, 41-53.

3. Sasic, S. and Ozaki, Y. (2000). Band assignment of near-infrared spectra of milk by use of partial-least-squares regression, *Appl. Spectrosc.*, 54 (9), 1327-1338.

4. Wilson, R.H. (1990). Fourier transform mid-infrared spectroscopy for food analysis, *Trends Anal. Chem,* 9 (4), 127-131.

5. Giangiacomo, R., Magee, J.B., Birth G.S. and Dull, G.G. (1981). Predicting concentrations of individual sugars in dry mixtures by near-infrared reflectance spectroscopy, *J. Food Sci.,* 46, 531-534.

6. Dumoulin, E.D., Bernard, A.P. and Guerain, J.T. (1987). Determination of sugar and ethanol content in aqueous products of molasses distilleries by near infrared spectrophotometry, *J. Food Sci.,* 52 (3), 626-630.

7. Giangiacomo, R. and Dull, G.G. (1986). Near infrared spectrophotometric determination of individual sugars in aqueous mixtures, *J. Food Sci.,* 51 (3), 679-683.

8. Sinnaeve, G., Dardenne, P. and Agneessens, R. (1997). Quantitative analysis of raw apple juices using near infrared, Fourier-transform near infrared and Fourier-transform infrared instruments: A comparison of their analytical performances, *J. Near Infrared Spectrosc.*, 5, 1-17.

9. Garcia-Jares, C.M. and Medina, B. (1997). Application of multivariate calibration to the simultaneous routine determination of ethanol, glycerol, fructose, glucose and total residual sugars in botrytized-grape sweet wines by means of near-infrared reflectance spectroscopy, *Fresenius J. Anal. Chem,*. 357, 86-91.

10. Robert, P., Devaux, M.F., Qannari, A. and Safar, M. (1993). Mid and near infrared study of carbohydrates by canonical correlation analysis, *J. Near Infrared Spectrosc.*, 1, 99-108.

11. Noda, I. (1993). Generalized two-dimensional correlation method applicable to infrared, Raman, and other types of spectroscopy, *Appl. Spectrosc.*, 47 (9), 1329-1336.

12. Ozaki, Y. and Noda, I. (1996). Potential of generalized two-dimensional correlation spectroscopy in the near infrared region, *J. Near Infrared Spectrosc.*, 4, 85-99.

13. Ozaki, Y., Sasic, S., Tanaka, T. and Noda, I. (2001). Two-dimensional correlation spectroscopy: Principle and recent theoretical development, *Bull. Chem. Soc. Jpn.*, 74, 1-17.

14. Ren, Y., Matsushita, A., Matsukawa, K., Inoue, H., Minami, Y., Noda, I. and Ozaki, Y. (2000). Two-dimensional Raman and Raman-near infrared heterospectral correlation spectroscopy studies of the specific interaction in partially miscible blends of poly(methyl methacrylate) and poly(4-vinyl phenol). In: *Two-Dimensional Correlation Spectroscopy* (Y. Ozaki and I. Noda eds., American Institute of Physics, College Park, MD), 250.

15. Matsushita, A., Ren, Y., Matsukawa, K., Inoue, H., Minami, Y., Noda, I. and Ozaki, Y. (2000). Two-dimensional Fourier-transform Raman and near-infrared correlation spectroscopy studies of poly(methyl methacrylate) blends 1. Immiscible blends of poly(methyl methacrylate) and atactic polystyrene, *Appl. Spectrosc.*, 54 (2), 171-180.

16. Czarnecki, M. A., Wu, P. and Siesler, H.W. (1998). 2D FT-NIR and FT-IR correlation analysis of temperature-induced changes of nylon 12, *Chem. Phys. Lett.*, 283 (5,6), 326-332.

17. Amari, T. and Ozaki, Y. (2002). Generalized two-dimensional attenuated total reflection/infrared and near-infrared correlation spectroscopy studies of real-time monitoring of the oligomerization of bis(hydroxyethyl terephthalate), *Macromolecules*, 35, 8020-8028.

18. Noda, I., Liu, Y. and Ozaki, Y. (1996). Two-dimensional correlation spectroscopy study of temperature-dependent spectral variations of *N*-methylacetamide in the pure liquid state. 2. Two-dimensional Raman and infrared-Raman heterospectral analysis, *J. Phys. Chem.*, 100, 8674-8680.

19. Jung, Y.M., Czarnik-Matusewicz, B. and Ozaki, Y. (2000). An IR vs. Raman 2D heterospectral correlation study of the secondary structure of β-lactoglobulin in aqueous solutions, *AIP Conference Proceedings,* 503, 275-278.

20. Kubelka, J., Pancoska, P. and Keiderling, T.A. (1999). Novel use of a static modification of two-dimensional correlation analysis. Part II: Hetero-spectral correlations of protein Raman, FT-IR, and circular dichroism spectra, *Appl. Spectrosc.*, 53 (6), 666-671.

21. Barton II, F.E., Himmelsbach, D.S., Duckworth, J.H. and Smith, M.J. (1992). Two-dimensional vibration spectroscopy: Correlation of mid- and near-infrared regions, *Appl. Spectrosc.*, 46 (3), 420-429.

22. Barton II, F.E. and Himmelsbach, D.S. (1993). Two-dimensional vibrational spectroscopy II: Correlation of the absorptions of lignins in the mid- and near-infrared, *Appl. Spectrosc.*, 47 (11), 1920-1925.

23. Barton II, F.E., Himmelsbach, D.S., McClung, A.M. and Champagne, E.L. (2002). Two-dimensional vibration spectroscopy of rice quality and cooking, *Cereal Chem.*, 79 (1), 143-147.

24. Barton II, F.E., Himmelsbach, D.S. and Archibald, D.D. (1996). Two-dimensional vibrational spectroscopy V: Correlation of mid- and near-infrared of hard red winter and spring wheats, *J. Near Infrared Spectrosc.*, 4, 139-152.

25. McClure, W.F., Maeda, H., Dong, J., Liu, Y. and Ozaki, Y. (1996). Two-dimensional correlation of Fourier transform near-infrared and Fourier transform Raman spectra I: Mixtures of sugar and protein, *Appl. Spectrosc.*, 50 (4), 467-475.

26. Awichi, A., Tee, E.M., Srikanthan, G. and Zhao, W. (2002). Identification of overlapped near-infrared bands of glucose anomers using two-dimensional near-infrared and middle-infrared correlation spectroscopy, *Appl. Spectrosc.*, 56 (7), 897-901.

27. Haaland, D.M. and Thomas, E.V. (1988). Partial-least-squares methods for spectral analyses. 1. Relation to other quantitative calibration methods and the extraction of qualitative information, *Anal. Chem.*, 60 (11), 1193-1202.

28. Noda, I. (1990). Two-dimensional infrared (2D IR) spectroscopy: Theory and applications, *Appl. Spectrosc.*, 44 (4), 550-561.

29. Noda, I., Dowrey, A.E. and Marcott, C. (1993). Recent developments in two-dimensional infrared (2D IR) correlation spectroscopy, *Appl. Spectrosc.*, 47 (9), 1317-1323.

30. Kauppinen, J.K., Moffatt, D.J., Cameron, D.G. and Mantsch, H.H. (1981). Fourier self-deconvolution: A method for resolving intrinsically overlapped bands, *Appl. Spectrosc.*, 35 (3), 271-276.

31. Osborne, B.G. and Fearn, T. (1986). Near infrared data handling and calibration by multiple linear regression. In: *Near Infrared Spectroscopy in Food Analysis* (Longman Scientific and Technical, Essex, UK), 86-103.

32. Mathlouthi, M. and Koenig, J.L. (1986). Vibrational spectra of carbohydrates, *Adv. Carbohyd. Chem. Biochem.*, 44, 7-89.

33. Robert, C. and Cadet, F. (1998). Analysis of near-infrared spectra of some carbohydrates, *Appl. Spectrosc. Rev.*, 33 (3), 253-266.

34. Broadhurst, D., Goodacre, R., Jones, A., Rowland, J.J. and Kell, J.B. (1997). Genetic algorithms as a method for variable selection in multiple linear regression and partial least squares regression, with applications to pyrolysis mass spectrometry, *Anal. Chim. Acta*, 348, 71-86.

35. Dimitri-Hakim, A. (2000). Quantitative analysis of sugars in confectionary products by Fourier transform infrared spectroscopy: Development of analytical methodology using a mid-infrared fiber optic probe and investigation of the effects of sugar-water interactions in model systems. Ph.D. Thesis, McGill University.

BRIDGE

In Chapter 5, H2D-CS was used to identify wavelengths in the NIR spectrum characteristic to each sugar using the well resolved bands of sugars in the mid-IR spectrum. In principle, H2D-CS can be extended to include 2D correlations between FTIR spectra and HPLC chromatograms, termed spectroscopic/chromatographic 2D correlation (SC2D-C). In theory, well resolved HPLC peaks of different components in a complex matrix can be correlated to overlapping peaks in their respective FTIR spectra in order to elucidate the IR spectrum of each component. In Chapter 4, SB-ATR/FTIR spectroscopy was used for multi-component analysis of wines, an ideal type of sample to be used to investigate the feasibility of using the SC2D-C approach in identifying HPLC peaks. In the following chapter, an investigation of SC2D-C of the HPLC chromatograms and SB-ATR/FTIR spectra of wines will be described. This study was undertaken to explore the potential utility of this approach for HPLC peak identification.

CHAPTER 6

COMPOUND IDENTIFICATION BY TWO-DIMENSIONAL CORRELATION OF HIGH-PRESSURE LIQUID CHROMATOGRAMS WITH SINGLE-BOUNCE ATTENUATED TOTAL REFLECTANCE FOURIER TRANSFORM INFRARED SPECTRA USING WINES AS A MODEL SYSTEM

6.1 ABSTRACT

The possibility of employing spectroscopic/chromatographic two-dimensional correlation (SC2D-C) analysis for the identification of chromatographic peaks was investigated using wines as a model system. Chromatograms obtained by high-pressure liquid chromatography (HPLC) of wine samples were correlated with the single-bounce attenuated total reflectance (SB-ATR) Fourier transform infrared (FTIR) spectra of the samples by SC2D-C. From the SC2D-C map, infrared (IR) slice spectra corresponding to each of the chromatographic peaks were generated and were subsequently transformed to ATR-corrected spectra to allow them to be matched against the transmission spectra in an IR spectral library. In the first stage of this work, a dry red wine was spiked with glucose, fructose and sucrose in different amounts to generate 15 samples for subsequent SC2D-C analysis. The IR slice spectra generated from SC2D-C analysis were identified by a search of an IR spectral library consisting of 404 spectra, including the spectra of aqueous solutions of each of the pure sugars. Correct classifications with spectral matches of 78.93, 91.18 and 91.40% for glucose, fructose and sucrose, respectively, were obtained by a search employing the spectral region between 1500 and 750 cm^{-1}. In a subsequent study, samples of 7 different wines were spiked with different amounts of sucrose and were pooled with the unspiked samples to generate a data set of 14 samples for SC2D-C analysis. The slice spectrum corresponding to the HPLC peak for sucrose was correctly identified by a search of the IR spectral library with a spectral match of 93.85%. Finally, SC2D-C analysis was applied to the HPLC chromatograms and SB-ATR/FTIR spectra of 149 wine samples. Library searches of the slice spectra corresponding to the major HPLC peaks correctly identified ethanol but not glucose and fructose due to collinearity effects nor glycerol and organic acids due to insufficient variability in the concentrations of these components within this set of wine samples.

This study has shown that SC2D-C analysis is a workable method for identifying the origin of HPLC peaks without the need for isolation of the eluted compounds, provided there is sufficient random variability of their concentrations in the samples analyzed.

6.2 INTRODUCTION

Infrared (IR) spectroscopy is a well-established technique for the identification of compounds. Since the IR spectrum of a compound is one of its most characteristic physical properties and may be considered its "fingerprint" [1], unknowns can be identified by matching their spectra against those in a database, termed a spectral library. IR spectral libraries containing the spectra of more than 10,000 chemical compounds are commercially available, and libraries have also been developed specifically for identification of polymers[2] and food ingredients[3], forensic analysis using attenuated total reflectance (ATR) spectra[4] and authentication of pharmaceuticals using near-infrared (NIR) spectra[5], as well as many other applications. Traditionally, the compounds of interest are isolated before IR measurements are performed[6], a tedious and time-consuming process if the compound is part of a complex mixture. This requirement has been eliminated by interfacing a Fourier transform infrared (FTIR) spectrometer equipped with a flow cell to gas chromatography, high-pressure liquid chromatography (HPLC), supercritical fluid extraction and, more recently, capillary electrophoresis systems[7]. However, the use of an FTIR spectrometer as a detector imposes certain limitations on these various separation techniques. For example, HPLC-FTIR suffers from the drawback that the IR opacity of the mobile phase becomes a problem, particularly if the mobile phase is aqueous[8], which seriously reduces the sensitivity of the method. To overcome this problem, the use of mobile-phase elimination methods or deuterated mobile phases has been reported[8]; however, both of these approaches are unsatisfactory as they are costly and present serious limitations. Recently, an HPLC-FTIR system employing a mercury-cadmium-telluride (MCT) detector and a low wave pass filter has been developed to allow for on-line FTIR detection without the need for solvent elimination[9]. This optical setup improves analytical sensitivity, albeit with a reduction of the multiplexing advantage as a portion of the mid-IR spectral region is no longer available. However, the on-line HPLC-FTIR approach suffers from several

drawbacks. First, the short time for spectral IR recording under these dynamic conditions (typically under 5 s) requires the use of MCT detectors to obtain good signal-to-noise ratio (S/N) as commonly employed deuterated triglycine sulfate (DTGS) detectors require more time for signal averaging. These detectors require cooling with liquid nitrogen, increasing the complexity and cost of the instrument. Secondly, HPLC-FTIR is restricted to isocratic mobile phases instead of gradient elution as spectral subtraction of the mobile phase absorption bands is virtually impossible when the composition of the eluent is changing[8]. Finally, the choice of mobile phase is also restricted by the requirement that the IR-transparent window material needs to be insoluble in the mobile phase used, which can be problematic as most IR-transparent windows are water soluble, and water-insoluble CaF_2 windows are soluble when the mobile phase is slightly acidic[10]. However, recently developed diamond-coated ATR accessories can circumvent this problem[11].

An alternative means of employing FTIR spectroscopy to identify compounds separated by HPLC may be proposed based on the application of the principles of two-dimensional (2D) correlation spectroscopy. Since the introduction of generalized 2D correlation spectroscopy by Noda in 1993[12], a wide range of applications have been reported, including the study of molecular changes in polymer blends[13,14] and proteins[15-18] under thermal perturbation, studies of NIR bands of alcohols[19], proteins and fat in milk[20] and heterospectral 2D correlation (H2D-CS) studies, where the data from two different spectroscopic methods are correlated[21]. To date, there have been H2D-CS studies between X-ray diffraction and IR dichroism[22], IR and NIR[23-25], IR and Raman[26], NIR and Raman[27] and Raman and circular dichroism data[28]. In theory, the H2D-CS approach can be extended to include correlations between spectroscopic and HPLC (or other chromatographic) data, termed spectroscopic/chromatographic 2D correlation (SC2D-C) analysis. This thereby allows identification of chromatographic peaks without the need to isolate the eluted compound and avoids the inherent difficulties and limitations associated with HPLC-FTIR. The rationale of this proposed alternative is summarized in Figure 6.1.

Wine is an example of a complex matrix that has been analyzed by on-line HPLC-FTIR using either a transmission flow cell[10] or a multiple-bounce diamond ATR (MB-ATR) accessory[11]. In previous work, in which we employed FTIR spectroscopy in

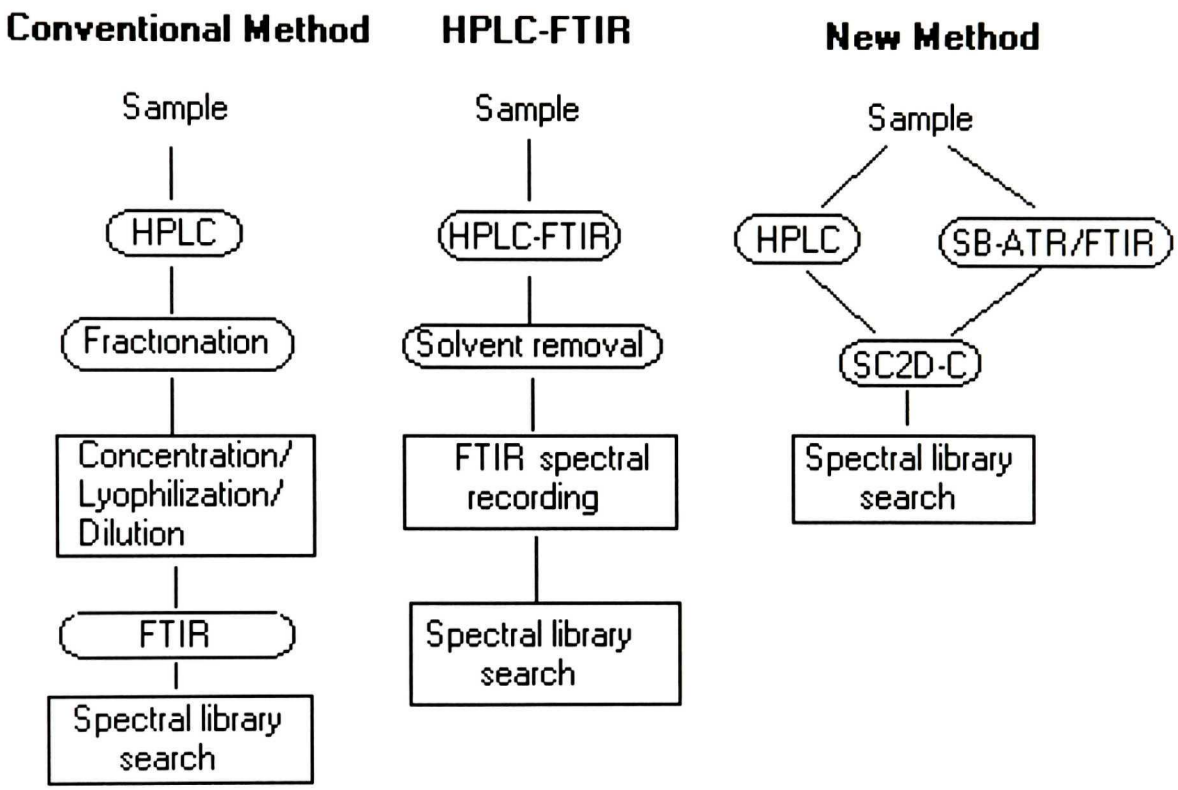

Figure 6.1. Conventional and HPLC-FTIR methods versus new proposed method for compound identification using SC2D-C.

conjunction with multivariate analysis methods to simultaneously determine 11 components and parameters in wines[29], we acquired HPLC and FTIR data for a large set of wine samples of different types and geographic origins. Thus, these wines were selected as a model system for the investigation of SC2D-C analysis. Preliminary investigations were performed with small numbers of wine samples spiked with sugars to establish the feasibility of the SC2D-C approach. Subsequently, SC2D-C analysis relating FTIR spectra and HPLC chromatograms of 149 wines was carried out to determine if this technique could be employed to identify wine constituents.

6.3 EXPERIMENTAL

6.3.1. Instrumentation

6.3.1.1. FTIR Analysis

FTIR analysis was carried out using an ABB Bomem (Québec City, QC) MB-150 spectrometer equipped with a temperature-controlled (Watlow System Integrators, Decorah, IA) ZnSe single-bounce ATR (SB-ATR) accessory (Harrick, Ossining, NY). The spectrometer was purged with dry air from a Balston air drier (Lexington, MA) to avoid spectral contributions from atmospheric water vapour and carbon dioxide. The temperature of the ZnSe crystal was maintained at 30 ± 0.1°C to minimize spectral variability associated with changes in room temperature. Prior to the loading of each sample onto the ATR crystal, the crystal was rinsed with deionized water and wiped dry with a lint-free tissue and a new background spectrum was collected. Wine samples were covered with a microscope slide during spectral recording to avoid evaporation. All spectra were collected by co-addition of 16 scans at a resolution of 8 cm^{-1}.

6.3.1.2. HPLC Analysis

HPLC analysis was carried out using a Beckman Coulter HPLC system (Fullerton, CA) equipped with a diode array detector, set at 192 nm, an autosampler and a solvent module. The HPLC system was controlled by Beckman System Gold v. 8.1 software (Fullerton, CA). An ION-300 polymeric cation exchange column (Transgenomic Inc., San José, CA) was used with a mobile phase of 0.0025 N H_2SO_4, a

flow rate of 0.5 mL/min and a column temperature of 20 ± 0.1°C to separate the wine components isocratically.

6.3.2. Sample Preparation

D-Fructose, α-D-glucose and sucrose were obtained from Sigma (St. Louis, MO). All other reagents used were of analytical grade and obtained from Fisher Scientific (Montreal, QC). Two sets of samples were prepared. The first set consisted of 15 samples of a dry red wine spiked with varying amounts of D-fructose, α-D-glucose and sucrose (Table 6.1) The second set consisted of a red/white/rosé selection of 14 dry wines, purchased locally, which were split, with half being spiked with varying amounts of sucrose (1, 2, 5, 10, 15, 20 and 50 g/L) and the other half left unspiked. A third set of samples comprised 149 wine samples collected for an earlier study[29].

6.3.3. SC2D-C Analysis

HPLC chromatograms and FTIR spectra of the three sets of wine samples were correlated by generalized 2D correlation spectroscopy, a method described in detail elsewhere[12], using KG2D software (written by Dr. Y. Wang). This software generates 2D contour maps derived from three-dimensional (3D) spectral space. For the analysis of the large sample set (149 samples), the KG2D matrix routines were implemented in Microsoft Excel™, owing to the 20 sample limit associated with the KG2D software. Mean centering of the data was performed by selecting this data pretreatment option in the KG2D software; other types of data pretreatment (mean normalization and auto-scaling) were carried out in Microsoft Excel™.

6.3.4. IR Spectral Library Search

For each chromatographic peak, a cross-sectional slice of the synchronous 2D contour map at the corresponding retention time, termed a slice spectrum, was generated. In principle, the slice spectrum should represent the IR spectrum of the compound eluted with that retention time, allowing for its identification by an IR spectral library search. Because the slice spectra were generated from spectral data acquired with the use

Table 6.1: Spiked carbohydrate concentrations of wine samples used in the first experiment employing SC2D-C analysis.

Sample #	Sucrose (g/L)	Glucose (g/L)	Fructose (g/L)
1	-	-	-
2	5	-	-
3	20	-	-
4	1	5	20
5	10	50	1
6	100	1	5
7	-	50	50
8	50	20	10
9	-	80	-
10	-	-	80
11	80	-	-
12	30	30	30
13	40	10	60
14	2	40	2
15	7	2	40

of an SB-ATR accessory, which produces different relative band intensities from those in transmission spectra, the slice spectra were transformed using the ATR correction provided in Omnic v. 4.1a software (Nicolet Instrument Corp., Madison, WI) to allow them to be compared to transmission spectra in an IR spectral library. The slice spectra were then matched against a library containing 404 IR spectra of different compounds. This library included the sample library spectra provided with the Omnic software from the Aldrich Condensed Phase, Georgia State Crime Lab, and Sigma Biological Sample libraries together with the ATR-corrected SB-ATR spectra of ethanol, glycerol, and 50 g/L aqueous solutions of glucose, fructose, sucrose, lactose, galactose, and citric, malic, tartaric and lactic acids. To match the resolution of the spectra in the library, the SB-ATR spectra were recorded at a resolution of 8 cm^{-1} and, for the aqueous solutions, the water spectrum was subtracted out to give the spectrum of the pure component. The library search was based on the spectral region between 1500 and 750 cm^{-1}, which contains most of the relevant spectral information, employing the "correlation" algorithm included in the Omnic software. This algorithm is similar to the Euclidean distance algorithm except that the unknown and library spectra are mean centered before the vector dot products are calculated, which removes any effect of baseline offset in the unknown spectrum.

6.3.5. Data Pretreatment

Mean centering of the FTIR spectral and HPLC data was performed prior to all SC2D-C analyses. This form of data pretreatment eliminates invariant spectral or chromatographic features in a data set[30]. For an $i \times j$ spectral or chromatographic data matrix, where i is the number of measurement frequencies or retention times, respectively, and j is the number of samples, mean centering involves subtracting the column mean, m_j, from each element of the matrix, A_{ij}:

$$A'_{ij} = (A_{ij} - m_j) \quad [6.1]$$

where A' represents the mean centered matrix of absorbance data.

For the analysis of the large data set of wines, two other types of pretreatment methods, auto-scaling and mean normalization, were carried out on the FTIR spectral data in Microsoft Excel™. Auto-scaling is defined as

$$A''_{ij} = (A_{ij} - m_j) / s_j \quad [6.2]$$

where A'' represents the auto-scaled matrix of absorbance data, and s_j is the standard deviation of the j^{th} column. By auto-scaling spectra, the variances of all the rows of the data matrix are equalized and the spectra are transformed into shapes that are visually very different from the original spectral shapes[31]. The other spectral pretreatment method employed was mean normalization, which entails dividing each element of the matrix, A_{ij}, by the column mean, m_j,:

$$A'''_{ij} = (A_{ij} / m_j) \quad [6.3]$$

where A''' represents the mean normalized matrix of absorbance data. After mean normalization, the absorbance values at each wavenumber are normalized giving equal statistical weight to each wavenumber point[32].

6.4. RESULTS AND DISCUSSION

6.4.1. Analysis of Spiked Wines

In the first experiment, a dry red wine was spiked with various concentrations of glucose, fructose and sucrose. Figure 6.2 illustrates a representative HPLC chromatogram for sample #12 (Table 6.1), which contains equal amounts of added glucose, fructose and sucrose, with retention times of 13.25, 14.92 and 10.77 min, respectively. Despite the multitude of constituents in wines, the chromatogram of the unspiked wine showed no significant interferences, except that glucose was not completely separated from tartaric acid (retention time of 12.58 min). The SC2D-C map representing the correlation between the HPLC chromatogram and the IR spectral region between 1800 and 700 cm^{-1} is presented in Figure 6.3. A contour on the map, termed a cross peak, represents a positive correlation between the intensities of the IR and HPLC peaks if the contour line is solid, indicating that the intensity changes are due to the same component. A broken contour line indicates a negative correlation between the IR and HPLC peaks, indicating that the intensity changes are from different components[33]. In the synchronous 2D correlation map in Figure 6.3, there are distinct cross peaks at the retention times of each sugar between 1500 and 750 cm^{-1}. For example, at a retention time of 13.25 min, at which glucose is eluted, there are positive cross peaks at 1033, 1080 and 1106 cm^{-1} on the wavenumber axis. A broad and negative cross peak is observed between 1700 and

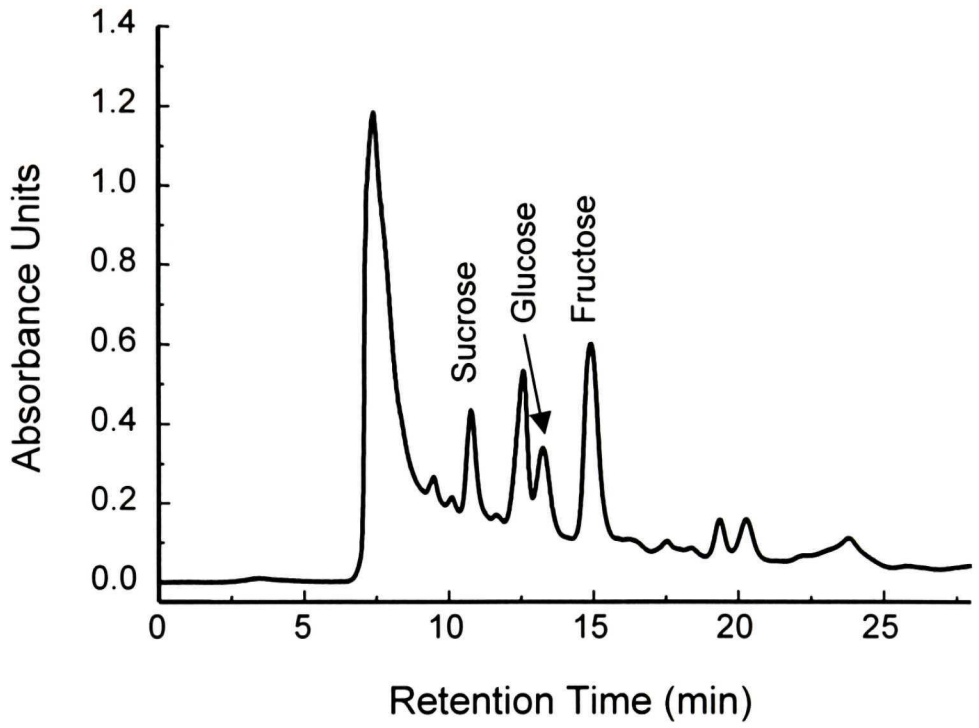

Figure 6.2. HPLC chromatogram of dry red wine sample spiked with 30 g/L of glucose, fructose and sucrose.

1500 cm^{-1} and is attributed to water absorption fluctuations. Thus, slice spectra were generated using only the region between 1500 and 750 cm^{-1} as most of the relevant information on the sugars, as revealed on the SC2D-C map, is in this region. Figure 6.4 illustrates the slice spectra of the three sugars obtained for their respective retention times on the 2D correlation map. The spectral features of each slice spectrum are quite different and a search of the spectral library after ATR correction of the slice spectra resulted in the correct identification of the sugars, with spectral matches of 78.93, 91.18 and 91.40% for glucose, fructose and sucrose, respectively. The lower spectral match for glucose could possibly be a result of lack of baseline separation of the glucose peak from that of tartaric acid in the HPLC chromatogram (Figure 6.2).

The above results demonstrate the feasibility of the SC2D-C approach, as it allowed for the correct identification of the three sugars despite the extensive overlap of their IR absorption bands. However, the spiked wine samples employed in this experiment represent an idealized situation in that the concentrations of the three sugars varied randomly against an invariant matrix. To assess the effect of a changing matrix on the identification of a single sugar, SC2D-C analysis was carried out on 14 samples of 7 different wines, half of which were spiked with varying amounts of sucrose. Figure 6.5 is the synchronous 2D correlation map generated from the FTIR spectral region between 1500 and 750 cm^{-1} and the HPLC data for retention times between 10 and 12 min. At the retention time of sucrose (10.77 min), cross peaks are found at 928, 999, 1057 and 1139 cm^{-1}. The corresponding slice spectrum was correctly identified as sucrose by a search of the spectral library, with a spectral match of 93.85%. Figure 6.6 compares this slice spectrum to the library spectrum of sucrose and the slice spectrum of sucrose obtained in the first experiment. Visually, the slice spectrum obtained in the second experiment is a better match to the library spectrum than that obtained in the first experiment, likely because in the latter case the samples had been spiked with other sugars as well. Nevertheless, the IR library spectral matches are almost identical (91% vs 94%), indicating that the spectral interferences from these sugars did not have a significant effect.

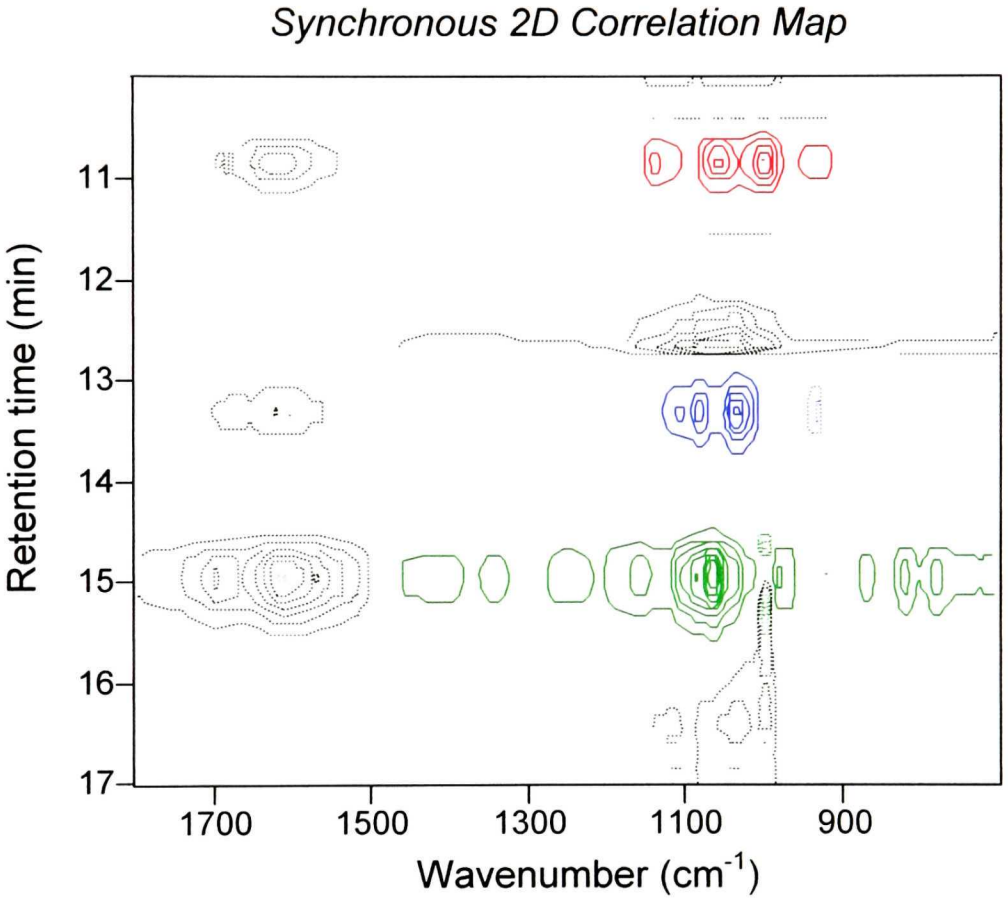

Figure 6.3. Synchronous 2D correlation map showing correlation between SB-ATR/FTIR spectra and HPLC chromatograms of 15 samples of a dry red wine spiked with varying amounts of glucose (blue), fructose (green) and sucrose (red).

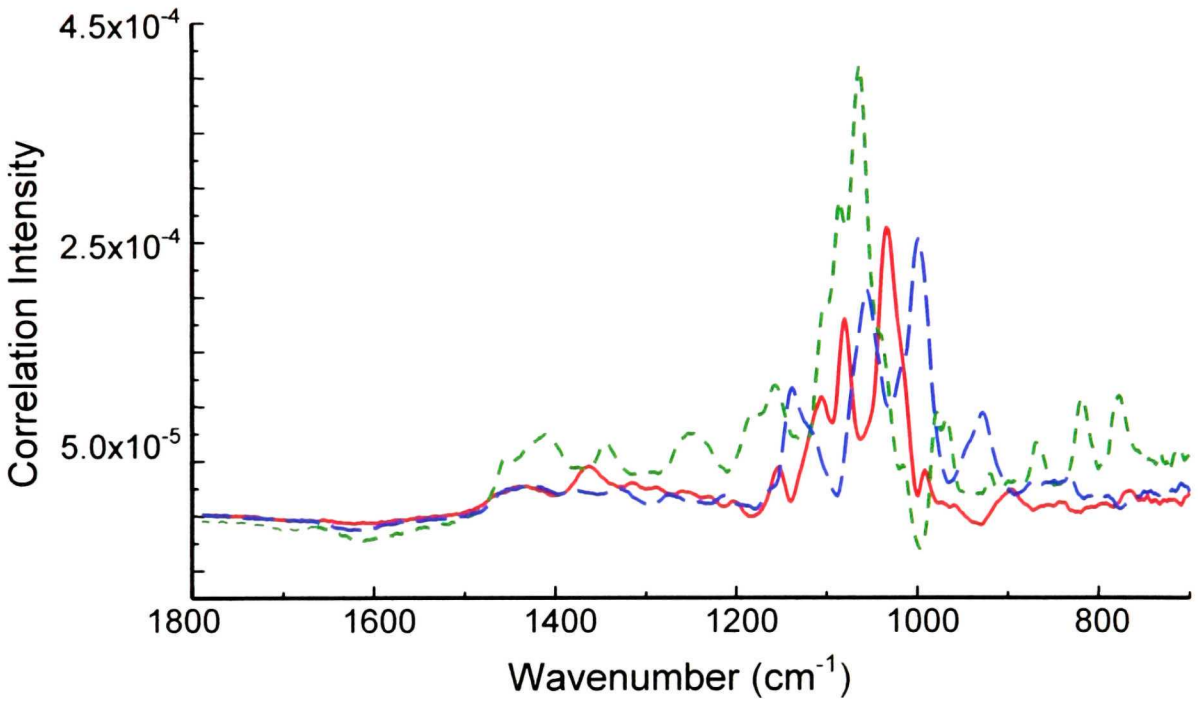

Figure 6.4. Slice spectra of glucose (———), fructose (- - - -) and sucrose (— —) obtained from the 2D correlation map in Figure 6.3.

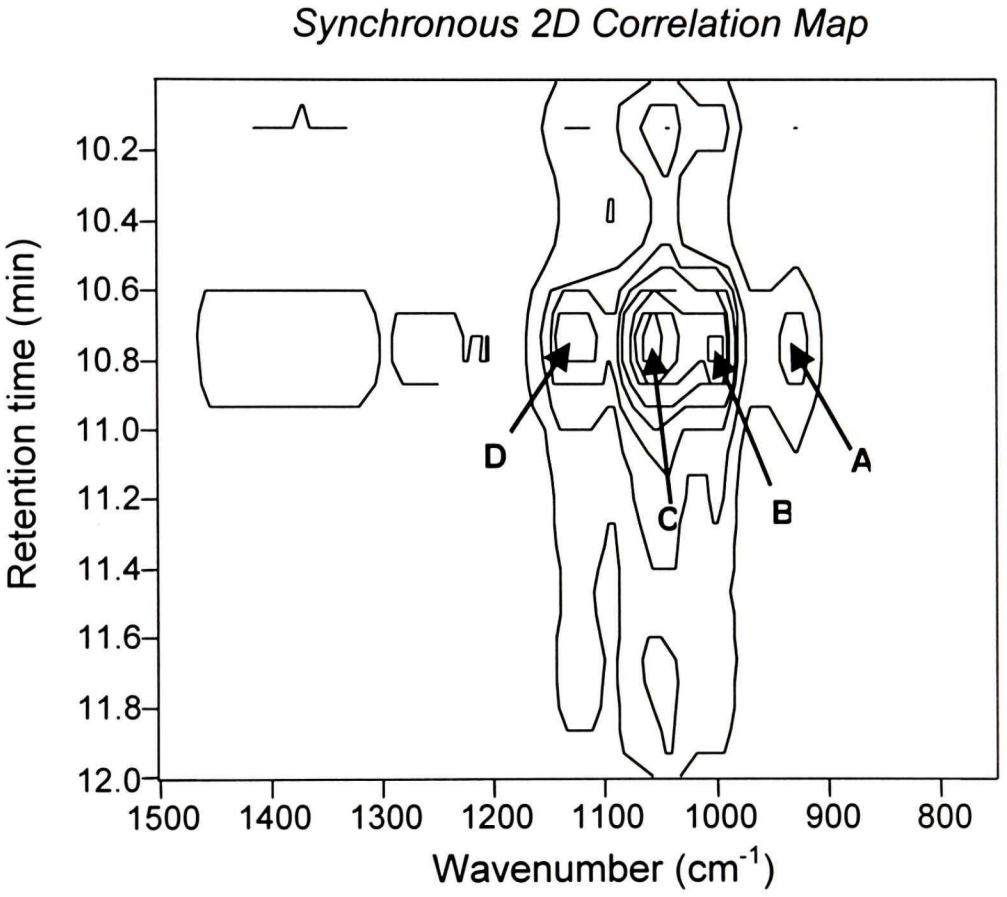

Figure 6.5. SC2D-C map showing correlation between SB-ATR/FTIR spectra and HPLC chromatograms of 7 unspiked and 7 sucrose-spiked wine samples with cross peaks at a retention time of 10.77 min with wavenumbers 928 (A) 999 (B), 1057 (C) and 1139 (D) cm^{-1}.

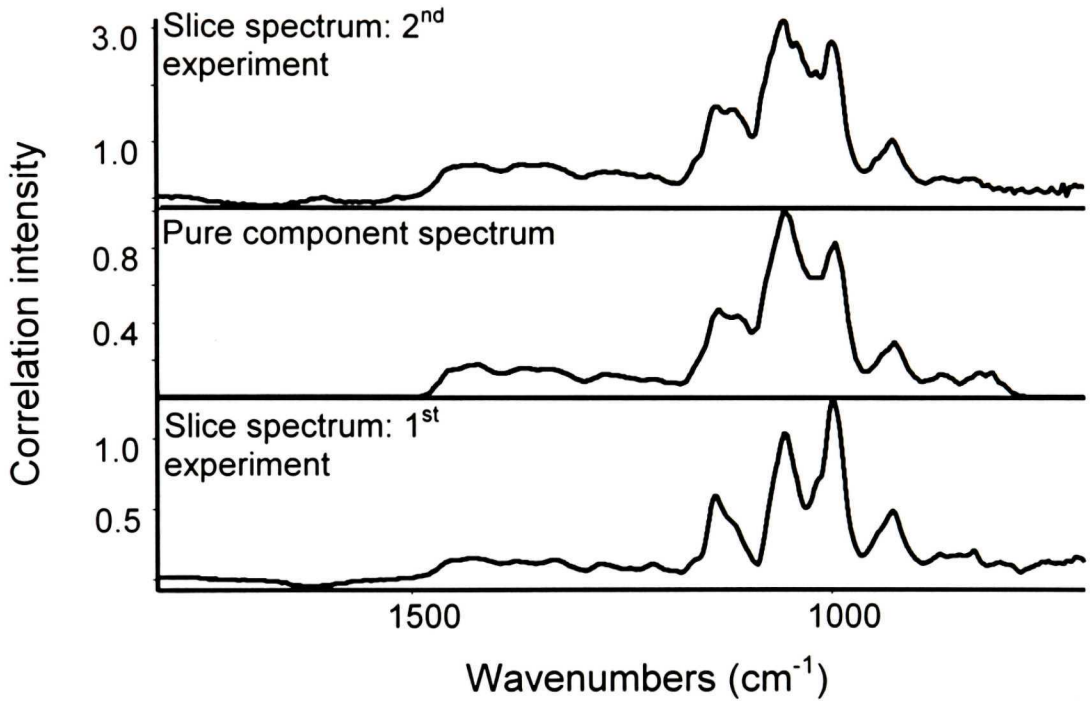

Figure 6.6. Slice spectra of sucrose obtained in the first and second experiments compared to the pure component spectrum.

6.4.2. Large Wine Data Set

To examine a more realistic analytical situation, IR spectra and HPLC chromatograms obtained for 149 wine samples previously used to calibrate an SB-ATR/FTIR spectrometer[29] for wine analysis were analyzed by SC2D-C. The data set included dry, semi-dry, semi-sweet, and sweet wine samples from several regions of the world in order to maximize variability. The most variable component, in terms of net concentration change, is ethanol, which varied from 7.3 to 17.6% (v/v), followed by glucose and fructose, which varied by 70 g/L in the data set, with all other components varying by less than 10 g/L. An HPLC chromatogram of a semi-dry wine from this data set is illustrated in Figure 6.7 and the retention times of several of the wine constituents are indicated. All IR spectra and HPLC chromatograms were subjected to mean centering prior to SC2D-C analysis and a slice spectrum for each chromatographic peak was generated from the synchronous 2D map. The slice spectrum for the HPLC peak of ethanol (25.56 min) exhibited three sharp bands at 1087, 1044 and 877 cm^{-1}, matching the bands in the spectrum of pure ethanol, and was correctly identified as ethanol by the IR spectral library search with a spectral match of 90.43%. The slice spectra for the HPLC peaks of glucose (11.38 min) and fructose (12.19 min), however, were incorrectly identified as ethanol and glucose, respectively. Comparative examination of the slice spectra of glucose and fructose in Figure 6.8 shows that they are virtually identical. It was considered that the slice spectra might match that of a mixture of glucose and fructose because in wines glucose and fructose tend to be found in a 1:1 ratio[34]. To verify this hypothesis, the pure component aqueous spectra of the two sugars were co-added and put into the IR spectral library. However, when the slice spectra were again matched against the library spectra, they were not classified as a glucose/fructose mixture. Since ethanol is a predominant component in wines, the co-added spectra of glucose/ethanol and fructose/ethanol were also added to the library. This time, the slice spectra for both glucose and fructose were identified as glucose/ethanol in the first ranking and fructose/ethanol in the second ranking, indicating the slice spectra had some spectral contributions from ethanol. This result indicates that there exists a collinear relationship not only between the two sugars, but also between the sugars and ethanol, which is also to be expected as very sweet wines normally have an alcohol content of

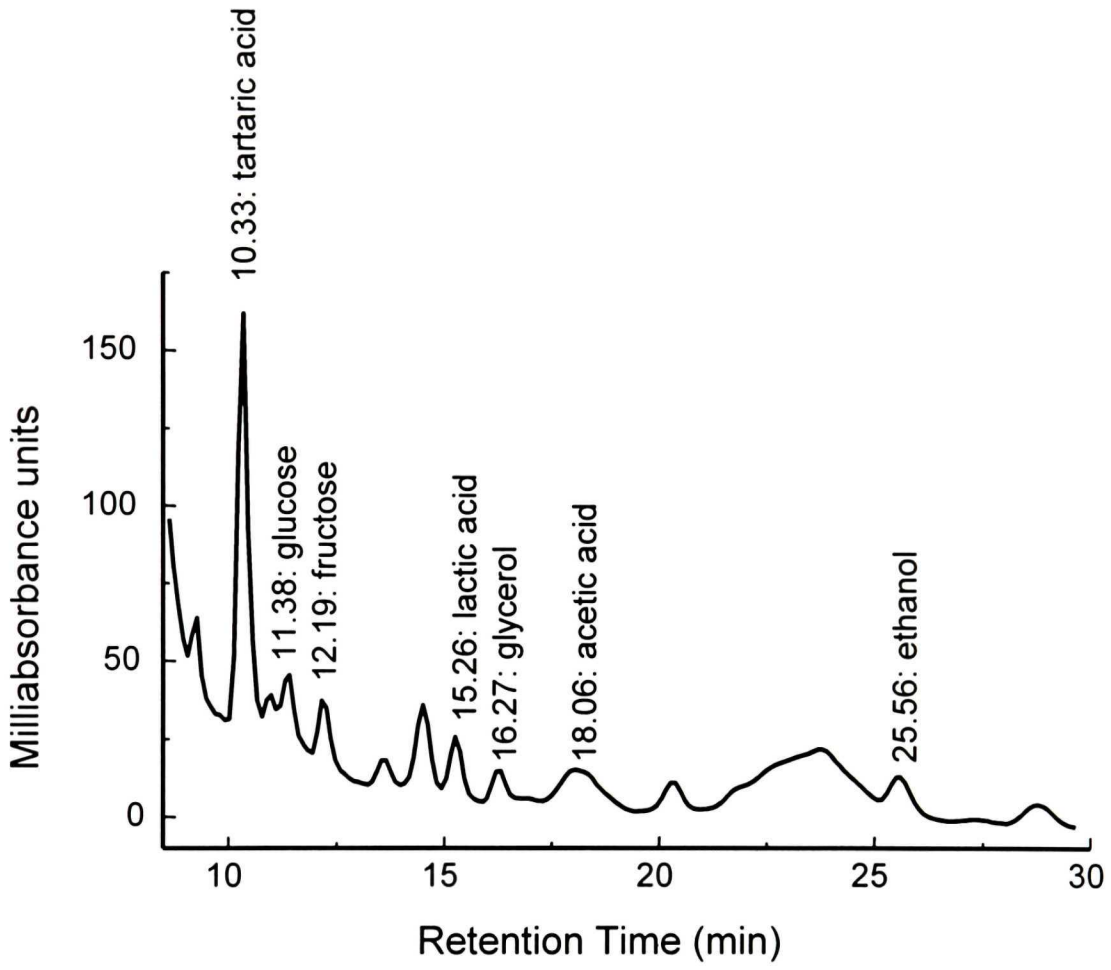

Figure 6.7. HPLC chromatogram of a semi-dry red wine.

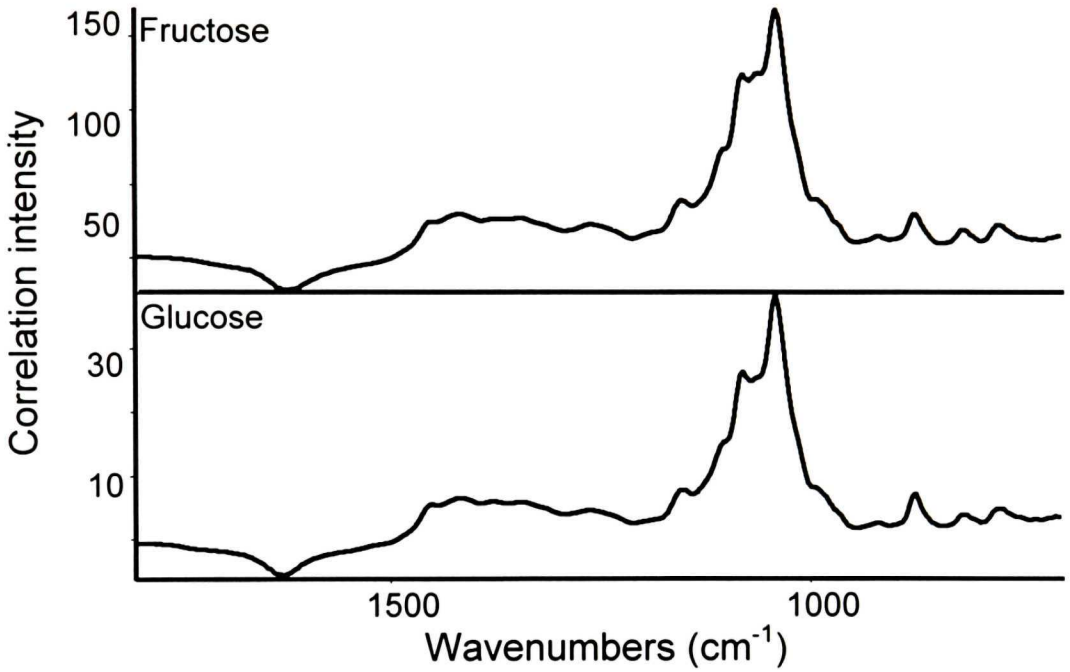

Figure 6.8. Slice spectra of glucose and fructose obtained using the large wine data set.

over 15% (v/v). Using the analysis data provided to us with these wine samples, this collinear relationship was confirmed by plotting alcohol content vs. total reducing sugar for wines that had >5 g/L of sugar. The plot yielded a correlation coefficient (R) of 0.72, explaining the presence of the spectral features of ethanol in the slice spectra for both glucose and fructose.

For the spectra of the wines in this data set, the changes in the absorption of ethanol are predominant owing to its high absorption coefficient and wide concentration range. In 2001, Sasic *et al.* have demonstrated that in such a situation, mean normalization, which gives equal statistical weight to all wavenumber points in the spectrum, is required to obtain optimal results from 2D correlation analysis[32]. After applying this pretreatment, the slice spectra for glucose and fructose, which were again virtually identical, were identified by the spectral library search as the addition spectrum of glucose/fructose. Figure 6.9 presents the slice spectrum of glucose before and after mean normalization pretreatment and the addition spectra of glucose and fructose and glucose and ethanol, illustrating the reduction of the ethanol absorption band by this pretreatment. Auto-scaling was also attempted as a pretreatment method; however, it was found that the spectra were seriously distorted, indicating that this pretreatment method is too drastic for this type of application.

SC2D-C analysis of the chromatographic peaks due to the various organic acids that are present as minor constituents in wines did not yield satisfactory results. The slice spectra exhibited a small carbonyl band, characteristic of organic acids. However, because of the low intensity of this band and the lack of the rest of the spectral signature, none of the slice spectra were identifiable by the spectral library search, with or without spectral pretreatment.

6.5 CONCLUSION

This study investigated a novel variant of generalized 2D correlation spectroscopy, SC2D-C, which correlates chromatographic and IR spectral data in an attempt to obtain the IR spectra of the compounds giving rise to the chromatographic peaks. This method is potentially useful for identification of chromatographic peaks

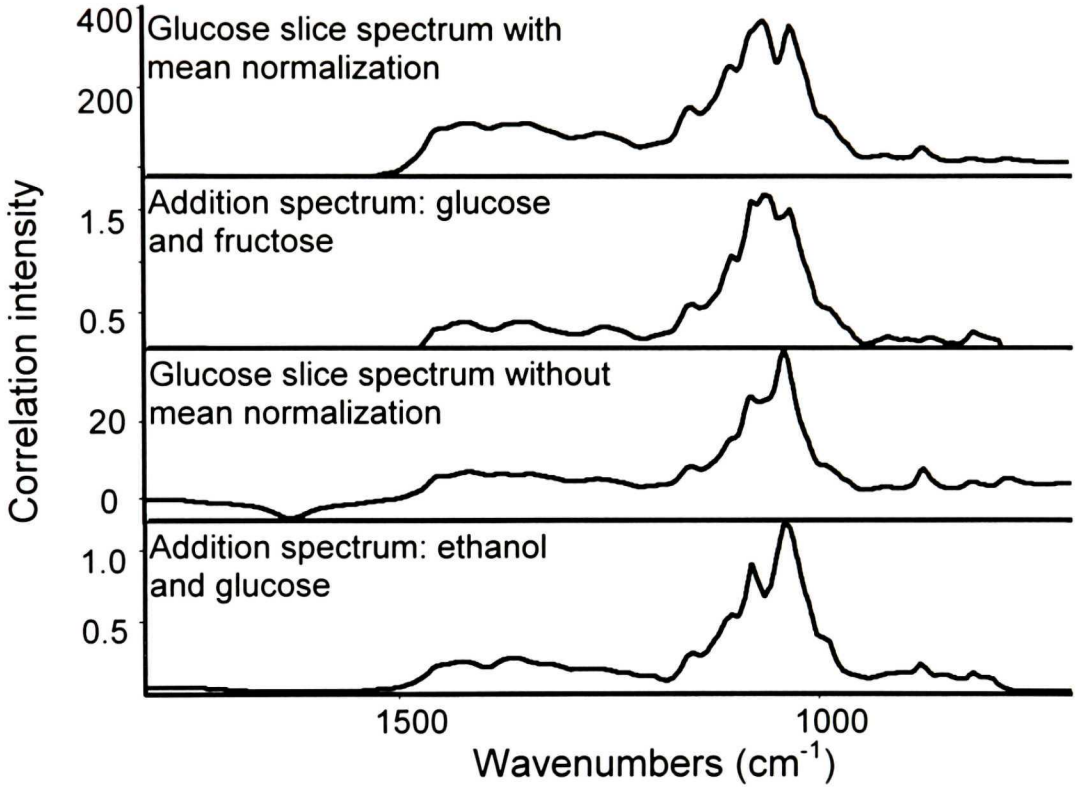

Figure 6.9. SC2D-C slice spectra of glucose before and after mean normalization as compared to addition spectra of glucose and fructose and ethanol and glucose.

without isolation of the eluted compounds and is much simpler than the alternative of interfacing an FTIR spectrometer to the chromatographic system. In this study, the proposed SC2D-C method for compound identification was applied to HPLC chromatograms and was shown to work well if the compound of interest has sufficient IR signal intensity and random variability within the set of samples subjected to SC2D-C analysis, which in principle may consist of only two samples. Although a component with a high absorption coefficient tends to obscure information related to other components, this limitation may be alleviated by employing certain data pretreatment methods, such as mean normalization. In addition to being simpler and much less costly to implement than HPLC-FTIR, the SC2D-C approach does not suffer from the limitations imposed by HPLC-FTIR on HPLC separation such as restrictions on the composition of the mobile phase and the necessity to use isocratic mobile phases, as the FTIR analysis is performed independently of the chromatographic separation. Conversely, for the FTIR analysis, samples may be dissolved in the most appropriate solvent for their FTIR spectral acquisition, irrespective of the solvent system employed for elution of the column. However, the SC2D-C approach has its own limitations as compound identification is not possible if there is strong collinearity between different components in the sample matrix or if the concentration of the compound is too low or insufficiently varying to give rise to significant IR spectral variability. Nevertheless, compound identification in complex samples subjected to chromatographic analysis could be facilitated by the availability of an FTIR software package incorporating a generalized 2D correlation algorithm, including mean centering and mean normalization pretreatment options, that can generate slice spectra at different retention time points, together with appropriate spectral libraries and library search algorithms.

REFERENCES

1. Ismail, A.A., van de Voort, F.R. and Sedman, J. (1997). Fourier transform infrared spectroscopy: Principles and applications. In: *Instrumental Methods in Food Analysis* (J.R.J. Paré and J.M.R. Bélanger eds., Elsevier, Amsterdam, The Netherlands), 93-139.

2. Hummel, D.O. (1997). Polymers, surfactants, and their mixtures. Computer-based search with special FTIR libraries, *Macromol. Symp.*, 119, 65-77.

3. Reeves, J.B. and Zapf, C.M. (1999). Spectral library searching: Mid-infrared versus near-infrared spectra for classification of powdered food ingredient, *Appl. Spectrosc.*, 53 (7), 836-844.

4. Koulis, C.V., Hymes, K.J. and Rawlins, J.L. (2000). A new infrared spectral library of controlled and noncontrolled drug standards using internal reflection spectroscopy, *J. Forensic Sci.*, 45 (4), 876-881.

5. Blanco, M. and Romero, M. (2001). Near-infrared libraries in the pharmaceutical industry: A solution for identity confirmation, *Analyst*, 126 (12), 2212-2217.

6. Kölhed, M., Lendl, B. and Karlberg, B. (2003). On-line infrared detection in aqueous micro-volume systems, *Analyst*, 128, 2-6.

7. Kölhed, M., Hinsmann, P., Svasek, P., Frank, J., Karlberg, B. and Lendl, B. (2002). On-line Fourier transform infrared detection in capillary electrophoresis, *Anal. Chem.*, 74, 3843-3848.

8. Somsen, G.W., Gooijer, C. and Brinkman, U.A.Th. (1999). Liquid chromatography-Fourier-transform infrared spectrometry, *J. Chromatogr. A*, 856, 213-242.

9. Vonach, R., Lendl, B. and Kellner, R. (1997). Hyphenation of ion exchange high-performance liquid chromatography with Fourier transform infrared detection for the determination of sugars in nonalcoholic beverages, *Anal. Chem.*, 69, 4286-4290.

10. Vonach, R., Lendl, B. and Kellner, R. (1998). High-performance liquid chromatography with real-time Fourier-transform detection for the determination of carbohydrates, alcohols and organic acids in wines, *J. Chromatogr. A*, 824, 159-167.

11. Edelmann, A., Diewok, J., Rodriguez Baena, J. and Lendl, B. (2003). High-performance liquid chromatography with diamond ATR-FTIR detection for the determination of carbohydrates, alcohols and organic acids in red wine, *Anal. Bioanal. Chem.*, 376, 92-97.

12. Noda, I. (1993). Generalized two-dimensional correlation method applicable to infrared, Raman, and other types of spectroscopy, *Appl. Spectrosc.*, 47 (9), 1329-1336.

13. Jung, Y.M., Shin, H.S., Czarnick-Matusewiscz, B., Noda, I. and Kim, S.B. (2002). Characterization of transition temperatures of a Langmuir-Blodgett film of poly(*tert*-butyl methacrylate) by two-dimensional correlation spectroscopy and principal component analysis, *Appl. Spectrosc.*, 56 (12), 1568-1574.

14. Shin, H.S., Jung, Y.M., Chang, T., Ozaki, Y. and Kim, S.B. (2002). Characterization of β-transition of poly(*tert*-butyl methacrylate) thin films by two-dimensional infrared correlation spectral analysis, *Vibr. Spectrosc.*, 29 (1-2), 73-77.

15. Noda, I., Liu, Y. and Ozaki, Y. (1996). Two-dimensional correlation spectroscopy study of temperature-dependent spectral variations of *N*-methylacetamide in the pure liquid state. 1. Two-dimensional infrared analysis, *J. Phys. Chem.*, 100, 8665-8673.

16. Ismoyo, F., Wang, Y. and Ismail, A.A. (2000). Examination of the effect of heating on the secondary structure of avidin and avidin-biotin complex by resolution-enhanced 2D infrared correlation spectroscopy, *Appl. Spectrosc.*, 54 (7), 939-947.

17. Schultz, C.P., Barzu, O. and Mantsch, H.H. (2000). Two-dimensional infrared correlation analysis of protein unfolding: Use of spectral simulations to validate structural changes during thermal denaturation of bacterial CMP kinases, *Appl. Spectrosc.*, 54 (7), 931-938.

18. Heinz, F., Mantsch, H.H. and Schultz, C.P. (2000). Sequential unfolding events in proteins monitored by 2D correlation analysis of FTIR spectra, *AIP Conference Proceedings*, 503, 95-102.

19. Ozaki, Y. and Noda, I. (1996). Potential of generalized two-dimensional correlation spectroscopy in the near infrared region, *J. Near Infrared Spectrosc.*, 4, 85-99.

20. Wang, Y., Tsenkova, R., Amari, M., Terada, F., Hayashi, T., Abe, A. and Ozaki, Y. (1998). Potential of two-dimensional correlation spectroscopy in analyses of NIR spectra of biological fluids. I. Two-dimensional correlation analysis of protein and fat concentration-dependent spectral variations of milk, *Analusis*, 26, (4), M64-M69.

21. Ozaki, Y., Sasic, S., Tanaka, T. and Noda, I. (2001). Two-dimensional correlation spectroscopy: Principle and recent theoretical development, *Bull. Chem. Soc. Jpn.*, 74, 1-17.

22. Noda, I. (1990). Two-dimensional correlation approach to the dynamic rheooptical characterization of polymers, *Chemtracts-Macromol. Chem.*, 1 (2), 89-105.

23. Barton II, F.E., Himmelsbach, D.S., Duckworth, J.H. and Smith, M.J. (1992). Two-dimensional vibration spectroscopy: Correlation of mid- and near-infrared regions, *Appl. Spectrosc.*, 46 (3), 420-429.

24. Czarnecki, M.A., Wu, P. and Siesler, H.W. (1998). 2D FT-NIR and FT-IR correlation analysis of temperature-induced changes of nylon 12, *Chem. Phys. Lett.*, 283 (5,6), 326-332.

25. Awichi, A., Tee, E.M., Srikanthan, G. and Zhao, W. (2002). Identification of overlapped near-infrared bands of glucose anomers using two-dimensional near-infrared and middle-infrared correlation spectroscopy, *Appl. Spectrosc.*, 56 (7), 897-901.

26. Noda, I., Liu, Y. and Ozaki, Y. (1996). Two-dimensional correlation spectroscopy study of temperature-dependent spectral variations of *N*-methylacetamide in the pure liquid state. 2. Two-dimensional Raman and infrared-Raman heterospectral analysis, *J. Phys. Chem.*, 100, 8674-8680.

27. McClure, W.F., Maeda, H., Dong, J., Liu, Y. and Ozaki, Y. (1996). Two-dimensional correlation of Fourier transform near-infrared and Fourier transform Raman spectra I: mixtures of sugar and protein, *Appl. Spectrosc.*, 50 (4), 467-475.

28. Kubelka, J., Pancoska, P., and Keiderling, T.A. (1999). Novel use of a static modification of two-dimensional correlation analysis. Part II: Hetero-spectral correlations of protein Raman, FT-IR, and circular dichroism spectra, *Appl. Spectrosc.*, 53 (6), 666-671.

29. Cocciardi, R.A., Ismail, A.A. and Sedman, J. Investigation of the potential utility of single-bounce attenuated total reflectance Fourier transform infrared spectroscopy in the analysis of distilled liquors and wines. To be submitted.

30. Sasic, S. and Ozaki, Y. (2001). Comparison of principal component analysis and generalized two-dimensional correlation spectroscopy: Spectral analysis of synthetic model system and near-infrared spectra of milk, *Appl. Spectrosc.*, 55 (1), 29-38.

31. Ozaki, Y., Sasic, S. and Jiang, H.J. (2001). How can we unravel complicated near infrared spectra? Recent progress in spectral analysis methods for resolution enhancement and band assignments in the near infrared region, *J. Near Infrared Spectrosc.*, 9, 63-95.

32. Sasic, S., Muszynski, A. and Ozaki, Y. (2001). New insight into the mathematical background of generalized two-dimensional correlation spectroscopy and the influence of mean normalization pretreatment on two-dimensional correlation spectra, *Appl. Spectrosc.*, 55 (3), 343-349.

33. Cocciardi, R.A., Ismail, A.A., Wang, Y. and Sedman, J. (2003). Heterospectral two-dimensional correlation spectroscopy of Fourier self-deconvolved Fourier transform near-infrared and Fourier transform mid-infrared spectra of sugar solutions. To be submitted.

34. Gallander, J.F. (1974). Chemistry of grapes and other fruits as the raw materials involved in winemaking. In: *Chemistry of Winemaking* (A.D. Webb and R.F. Gould eds., American Chemical Society, Washington D.C.), 11-49.

CHAPTER 7

SUMMARY OF CONTRIBUTIONS TO KNOWLEDGE AND CONCLUSIONS

Quantitative analysis of food products by mid-IR spectroscopy has been investigated for decades and has found several practical applications in the food industry. The significant advantages of Fourier transform infrared (FTIR) spectrometers over traditional dispersive and filter-based infrared (IR) instruments, particularly the speed of analysis (generally on the order of 1 min/sample) and amenability to automation, can translate into time and cost savings for the food industry[1]. However, wet-chemical, chromatographic and other spectroscopic techniques, particularly near-infrared (NIR) spectroscopy, continue to be much more widely used, in certain cases due to the higher sensitivity provided by these methods, but often due to sample-handling considerations, particularly difficulties encountered in IR analysis of aqueous systems, semi-solids and solids[2,3]. In addition to applications involving the direct analysis of foods, FTIR spectroscopy has also been coupled with high-pressure liquid chromatography (HPLC), gas chromatography (GC) and other separation techniques as means of detection providing high specificity. However, the complexities of interfacing an FTIR spectrometer to these systems result in both high cost and various limitations on the applicability of these so-called hyphenated techniques[4].

In this context, two approaches designed to enhance the utility of FTIR spectroscopy in food analysis were investigated in this thesis. The first involves the use of recently developed single-bounce attenuated total reflectance (SB-ATR) sample-handling accessories as a means of alleviating some of the sample-handling limitations associated with mid-IR spectroscopy. Attenuated total reflectance (ATR) is a well-established alternative to measurements in the transmission mode and is particularly useful in the analysis of aqueous samples, because it provides a short effective pathlength that allows the highly absorbing water bands to be on scale. By comparison with traditional multiple-bounce ATR (MB-ATR) accessories, SB-ATR accessories have a much shorter effective pathlength but nevertheless yield spectra of comparable quality because the optical design of the accessory, shown in Figure 2.4, allows for high optical throughput[5]. In addition, the small surface area of the ATR crystal eliminates many of the

temperature control and contamination problems associated with the various types of MB-ATR devices. It also allows for the use of much smaller sample volumes and superior optical contact with semi-solid and solid samples, particularly with the use of a diamond ATR crystal[6].

The second investigated approach is based on the application of generalized two-dimensional (2D) correlation spectroscopy, a technique that has undergone rapid development during the past decade, to establish correlations between SB-ATR/FTIR and Fourier transform near-infrared (FT-NIR) or HPLC data. In the first case, the objective of this approach is to make use of the high information content of mid-IR spectra to facilitate the development of NIR quantitative analysis methods, thereby exploiting some of the advantages of FTIR spectroscopy even when sample-handling limitations preclude its direct application as a quantitative analytical tool. The extension of this approach to the correlation of FTIR and HPLC data was undertaken to investigate the possibility of identifying peaks in HPLC chromatograms by FTIR spectroscopy without the need to either isolate the eluted compound or interface an FTIR spectrometer to the HPLC system.

The contributions to knowledge stemming from the research into these two approaches are summarized in the following paragraphs.

The feasibility of employing SB-ATR/FTIR spectroscopy to monitor enzymatic hydrolysis of lactose in the production of lactose-free and lactose-reduced milk was demonstrated in Chapter 3. A partial-least-squares (PLS) calibration model was developed to track the changes in the concentrations of lactose and its hydrolysis products, glucose and galactose, with sufficient accuracy to ascertain >95% completion of the hydrolysis reaction. The SB-ATR accessory was shown to be convenient for analysis of milk samples, and its small surface area allowed for simple and effective cleaning, thereby minimizing the possibility of cross contamination, and good temperature control, as required for accurate analyses. The method developed provides the dairy industry with a rapid and simple means of process monitoring in the production of lactose-free and lactose-reduced milk.

The potential utility of SB-ATR/FTIR spectroscopy for the analysis of distilled liquors and wines was explored in Chapter 4. The analytical performance of this

technique was evaluated relative to that of NIR spectroscopy, which is widely utilized by regulatory agencies to determine the alcohol content of distilled liquors and wines, as well as transmission FTIR spectroscopy, which is the mode of measurement employed in commercial FTIR wine analyzers. In addition, an SB-ATR/FTIR method for the simultaneous determination of 11 parameters important in the quality control of wines was developed and yielded satisfactory results for all but three components, which are present at too low concentrations in wine to be accurately quantified. This study demonstrated that SB-ATR/FTIR spectroscopy is a practical and versatile technique for the routine analysis of a wide variety of alcoholic beverages and provides a simple and cost-effective means of implementing FTIR wine analysis.

Among the findings of the research presented in Chapters 3 and 4 was the capability of SB-ATR/FTIR spectroscopy for the quantitative multicomponent analysis of sugars. This capability is due to the excellent quality of SB-ATR spectra in the 1200-950 cm^{-1} region, in which sugars exhibit intense and characteristic spectral profiles that allow them to be differentiated from each other. Accordingly, Chapter 5 addressed the possibility of utilizing this spectral information to assist in the selection of wavelengths for NIR multicomponent analysis of sugars through the use of heterospectral 2D correlation spectroscopy (H2D-CS). Although the possible use of H2D-CS in this manner has been suggested in the literature[7], this work represents the first study of its type. Potentially suitable NIR wavelengths for the determination of glucose, fructose and galactose in ternary aqueous solutions were identified by H2D-CS analysis of the SB-ATR/FTIR and FT-NIR spectra of binary aqueous solutions of these sugars. A multiple linear regression (MLR) calibration developed using the wavelengths selected by the H2D-CS approach gave better results than PLS calibrations and comparable results to those obtained by MLR using wavelengths selected by examination of 1^{st} and 2^{nd} derivative spectra of pure sugar solutions. This study demonstrated the validity of the principle of employing H2D-CS for the selection of wavelengths in the NIR region of the spectrum for use in the development of MLR calibrations. It was also noted that this approach has the added advantage of providing information on spectral variations induced by matrix effects, thereby potentially improving calibration performance.

In Chapter 6, the principles of H2D-CS were extended to the correlation of SB-ATR/FTIR spectral data with HPLC data. This novel application of 2D correlation, termed spectroscopic/chromatographic 2D correlation (SC2D-C), was devised because it offers the possibility of obtaining the IR spectrum of a constituent separated from a complex sample matrix by HPLC provided that this constituent is present at different concentrations in at least two samples. This approach bypasses the need to isolate the constituent and avoids the complexity and limitations of HPLC-FTIR. To study the feasibility of this approach, the HPLC chromatograms of wines were correlated to their respective SB-ATR/FTIR spectra using SC2D-C in order to generate IR slice spectra corresponding to the retention times of the chromatographic peaks. These slice spectra were then matched against an IR spectral library to identify the corresponding wine constituents. This approach worked well for random mixtures of sugars spiked into the same wine sample and for sucrose spiked into different wines as the slice spectrum of each component was correctly identified by the library search. However, when SC2D-C was carried out on 149 spectra and chromatograms of unspiked wine samples, the sugars and organic acids were not correctly classified due to collinearity effects and insufficient IR random spectral variability, respectively. Thus, this feasibility study based on wine as a model system showed the validity of the concept but also revealed several limitations that restrict its practical utility.

The research summarized above has laid the foundation for further applications of SB-ATR/FTIR spectroscopy and generalized 2D correlation spectroscopy in the area of food analysis. By facilitating sample-handling for FTIR analysis and calibration development for FT-NIR analysis, these recently developed techniques can broaden the scope and analytical performance of FTIR and FT-NIR spectroscopy. This may allow the food industry to make increased use of these rapid, automated instrumental methods and hence benefit from reductions in the time, labor costs and solvent and reagent use associated with wet-chemical and chromatographic methods of analysis.

REFERENCES

1. Ismail, A.A., van de Voort, F.R. and Sedman, J. (1997). Fourier transform infrared spectroscopy: Principles and applications. In: *Instrumental Methods in Food Analysis*

(J.R.J. Paré and J.M.R. Bélanger eds., Elsevier, Amsterdam, The Netherlands), 93-139.

2. Li-Chan, E.C.Y., Ismail, A.A., Sedman, J. and van de Voort, F.R. (2002). Vibrational spectroscopy of food and food products. In : *Handbook of Vibrational Spectroscopy*, (J.M. Chalmers and P.R. Griffiths eds., John Wiley & Sons Ltd., Chichester, England), 3629-3662.

3. Sedman, J., van de Voort, F.R. and Ismail, A.A. (1999). Attenuated total reflectance spectroscopy: Principles and applications in infrared analysis of food. In: *Spectral Methods in Food Analysis* (M.M. Mossoba ed., Marcel Decker Inc., New York, NY), 397-426.

4. McClure, G.L. (1993). General methods of sample preparation for the infrared hyphenated techniques. *In: Practical Sampling Techniques for Infrared Analysis* (P.B. Coleman ed., CRC Press, Boca Raton, FL), 165-216.

5. Brierley, P.R. (1999). Imaging stage for Fourier transform infrared spectrometer, *U.S. Patent* 5,965,889.

6. Brierley, P.R. (2000). Diamond anvil spectroscope, *U.S. Patent* 6,128,075.

7. Barton II, F.E., Himmelsbach, D.S., Duckworth, J.H. and Smith, M.J. (1992). Two-dimensional vibration spectroscopy: Correlation of mid- and near-infrared regions, *Appl. Spectrosc.*, 46 (3), 420-429.

APPENDIX A

2D IR CORRELATION SPECTROSCOPY ALGORITHM

In general, time-dependent variations in spectral intensity at a wavenumber, υ, under a small dynamic stimulus can be described as

$$A(\nu,t) = \bar{A}(\nu) + \tilde{A}(\nu,t) \quad [A.1]$$

where $\bar{A}(\nu)$ is the normal absorbance of the system without perturbation and $\tilde{A}(\nu,t)$ is the perturbation-induced fluctuation of absorbance, i.e. dynamic absorbance spectrum of the system. If the perturbation is sinusoidal with an angular frequency, ω, the dynamic absorbance signal will take the form

$$\tilde{A}(\nu,t) = \tilde{A}(\upsilon)\sin[\omega t + \beta(\upsilon)] \quad [A.2]$$

In general, not only the amplitude ($\tilde{A}(\upsilon)$), but also the phase angle ($\beta(\upsilon)$) is dependent on the wavenumber. The dynamic absorbance can also be expressed in terms of the sum of two orthogonal components

$$\begin{aligned}\tilde{A}(\upsilon,t) &= \tilde{A}'(\upsilon)\cos\beta(\upsilon)\sin\omega t + \tilde{A}(\upsilon)\sin\beta(\upsilon)\cos\omega t \\ &= A'(\upsilon)\sin\omega t + A''(\upsilon)\cos\omega t \quad [A.3]\end{aligned}$$

The terms $A'(\upsilon)$ and $A''(\upsilon)$ are the in-phase spectrum and quadrature spectrum of the dynamic absorbance, respectively.

A cross correlation function, $X(\tau)$, of dynamic IR absorbance spectra at two wavenumbers, $\tilde{A}(\upsilon_1, t)$ and $\tilde{A}(\upsilon_2, t)$, is defined as

$$X(\tau) = \lim_{T\to\infty} 1/T \int_{-T/2}^{T/2} \tilde{A}(\nu_1,t)\bullet \tilde{A}'(\nu_2,t+\tau)dt \quad [A.4]$$

The correlation time, τ, is regarded as the time interval between two measurements at υ_1 and υ_2. The correlation period, T, must span the full time of the process, i.e. $T\to\infty$. The cross correlation function is treated as a type of spectral intensity, also known as correlation intensity. By substituting equation A.3 into the above equation, the cross-correlation function reduces to a very simple form

$$X(\tau) = \Phi(\nu_1,\nu_2)\cos\omega\tau + \Psi(\nu_1,\nu_2)\sin\omega\tau \quad [A.5]$$

The synchronous (in-phase) and asynchronous (quadrature) 2D IR correlation intensities are $\Phi(\nu_1,\nu_2)$ and $\Psi(\nu_1,\nu_2)$, respectively, and are related to the dynamic IR spectral intensity variations as follows:

$$\Phi(\nu_1,\nu_2) = \tfrac{1}{2}[A'(\upsilon_1)A'(\upsilon_2) + A''(\upsilon_1)A''(\upsilon_2)] \quad [A.6]$$

$$\Psi(\upsilon_1,\upsilon_2) = \tfrac{1}{2}[A''(\upsilon_1)A'(\upsilon_2) - A'(\upsilon_1)A''(\upsilon_2)] \quad [A.7]$$

As can be seen from the above equations, the synchronous correlation intensity is maximal if the time-dependent variations of dynamic IR signals are in phase with each other and minimal when they are antiphase (π out of phase). The correlation intensity is near zero when the signals are orthogonal ($\pi/2$ out of phase) to one another. The asynchronous correlation intensity, on the other hand, is maximal when the signals are orthogonal to one another and near zero when the signals are exactly in phase or antiphase.

APPENDIX B

GENERALIZED 2D CORRELATION SPECTROSCOPY ALGORITHM

Generally, a dynamic IR spectrum $\tilde{y}(\upsilon,t)$ is defined as

$$\tilde{y}(\upsilon,t) = y(\upsilon,t) - \hat{y}(\upsilon) \text{ [B.1]}$$

where $\hat{y}(\upsilon)$ is the reference spectrum and usually set to be the static spectrum, which is the first spectrum in the set of dynamic spectra, or the time-averaged spectrum defined as

$$\hat{y}(\upsilon) = 1/T \int_{-T/2}^{T/2} y(\upsilon,t)dt \text{ [B.2]}$$

The above equation represents the procedure known as mean centering. It is necessary to Fourier transform each dynamic IR spectrum in the time domain into the frequency domain. The forward Fourier transform $\tilde{Y}_1(\omega)$ of the dynamic spectral intensity fluctuations $\tilde{y}(\upsilon_1,t)$ observed at some spectral variable υ_1 is given by

$$\tilde{Y}_1(\omega) = \int_{-\infty}^{\infty} \tilde{y}(\upsilon_1,t)e^{-i\omega t}dt$$

$$= \tilde{Y}_1^{Re}(\omega) + i\,\tilde{Y}_1^{Im}(\omega) \text{ [B.3]}$$

where $\tilde{Y}_1^{Re}(\omega)$ and $\tilde{Y}_1^{Im}(\omega)$ are the real and imaginary components of the Fourier transform and ω is an individual frequency component of the time-dependent variation of $\tilde{y}(\upsilon_1,t)$. The conjugate of the Fourier transform $\tilde{Y}_2^*(\omega)$ of dynamic spectral intensity fluctuations $\tilde{y}(\upsilon_2,t)$ observed at the spectral variable υ_2 is defined as

$$\tilde{Y}_2^*(\omega) = \int_{-\infty}^{\infty} \tilde{y}(\upsilon_2,t)e^{+i\omega t}dt$$

$$= \tilde{Y}_2^{Re}(\omega) - i\,\tilde{Y}_2^{Im}(\omega) \text{ [B.4]}$$

Given the two Fourier transforms, $\tilde{Y}_1(\omega)$ and $\tilde{Y}_2^*(\omega)$ above, the 2D correlation intensity between the two dynamic spectra $\tilde{y}(\upsilon_1,t)$ and $\tilde{y}(\upsilon_2,t)$ is defined as

$$\{\tilde{y}(\upsilon_1,t), \tilde{y}(\upsilon_2,t)\} = 1/\pi T \int_0^{\infty} \tilde{Y}_1(\omega) \bullet \tilde{Y}_2^*(\omega)\, d\omega$$

$$= \Phi(\upsilon_1,\upsilon_2) + i\Psi(\upsilon_1,\upsilon_2) \text{ [B.5]}$$

After calculating the correlation intensity of the dynamic spectra, the resulting components of the equation are the generalized 2D synchronous and asynchronous correlation spectra, $\Phi(\upsilon_1,\upsilon_2)$ and $\Psi(\upsilon_1,\upsilon_2)$, respectively. In generalized 2D correlation, the synchronous spectrum represents the overall similarities of the spectral intensity variations while the asynchronous spectrum represents the overall differences.

A simpler route to calculate generalized synchronous spectra without the need to Fourier transform the dynamic spectra is achieved by applying the Wiener-Khintchine theorem. The 2D cross-correlation function, as with 2D IR correlation spectroscopy, is given by

$$C(\tau) = 1/T \int_{T/2}^{T/2} \tilde{y}(\nu_1,t) \cdot \tilde{y}(\nu_2,t+\tau) dt \quad [B.6]$$

where τ is the correlation time and T is the correlation period. The cross correlation function can be related to the Fourier transforms of the dynamic IR spectra by the Wiener-Khintchine theorem as follows:

$$C(\tau) = 1/2\pi T \int_{-\infty}^{\infty} \tilde{Y}_1^*(\omega) \cdot \tilde{Y}_2(\omega) e^{i\omega\tau} d\omega \quad [B.7]$$

By setting $\tau = 0$, the above equation reduces to

$$C(0) = 1/2\pi T \int_{-\infty}^{\infty} \tilde{Y}_1^*(\omega) \cdot \tilde{Y}_2(\omega) d\omega$$

$$= 1/\pi T \int_{0}^{\infty} \tilde{Y}_1(\omega) \cdot \tilde{Y}_2^*(\omega) d\omega$$

$$= \Phi(\upsilon_1,\upsilon_2)$$

Therefore, the synchronous 2D correlation can be expressed as

$$\Phi(\upsilon_1,\upsilon_2) = 1/T \int_{T/2}^{T/2} \tilde{y}(\nu_1,t) \cdot \tilde{y}(\nu_2,t) dt \quad [B.8]$$

The synchronous 2D correlation spectrum is the time-averaged product of the dynamic spectral intensities.

The calculation of the asynchronous spectrum can be simplified by using a Hilbert transform. The Hilbert transform of a function is given by

$$h(t) = (1/\pi)\, pv \int_{-\infty}^{\infty} g(t')/t' - t\, dt' \quad [B.9]$$

The integration sign $pv \int_{-\infty}^{\infty}$ denotes that the Cauchy principal value is taken, i.e., the singularity of the point where $t' = t$ is excluded from the integration. The Hilbert transform $h(t)$ may be regarded as the convolution integral between the two functions, $g(t)$ and $1/t$. From the convolution theorem, the Fourier transform of $h(t)$ is proportional to the products of $g(t)$ and $1/t$.

$$H(\omega) = \int_{-\infty}^{\infty} h(t) e^{-i\omega t} dt = 1/\pi \int_{-\infty}^{\infty} 1/t\, e^{-i\omega t} dt \cdot \int_{-\infty}^{\infty} g(t) e^{-i\omega t} dt \quad [B.10]$$

and therefore, the Fourier transforms of functions $g(t)$ and $h(t)$ are related by

$$H(\omega) = i\text{sgn}(\omega) \bullet G(\omega) \text{ [B.11]}$$

The value of the signum function sgn(ω) is –1, 0, and 1 when ω is smaller than, equal to and greater than zero, respectively, and therefore:

$$H(\omega) = -G^{\text{Im}}(\omega) + iG^{\text{Re}}(\omega) \text{ when } \omega>0$$

$$H(\omega) = G^{\text{Im}}(\omega) - iG^{\text{Re}}(\omega) \text{ when } \omega<0$$

$$H(\omega) = 0 \text{ when } \omega=0$$

where $G^{\text{Im}}(\omega)$ and $G^{\text{Re}}(\omega)$ are the imaginary and real components of the Fourier transform of the function $g(t)$, respectively.

If we let the orthogonal spectrum $z(\upsilon_2,t)$ be the time-domain Hilbert transform of the dynamic spectrum $y(\upsilon_2,t)$, then

$$z(\upsilon_2,t) = (1/\pi)\, pv \int_{-\infty}^{\infty} y(\upsilon_2,t)/t' - t\, dt' \text{ [B.12]}$$

In the orthogonal spectrum, each Fourier component of the intensity variations of the dynamic spectrum is out of phase by $\pi/2$. The orthogonal correlation function $D(\tau)$ for a correlation time τ and correlation period T can consequently be expressed as

$$D(\tau) = 1/T \int_{-T/2}^{T/2} y(\nu_1,t) \bullet z(\nu_2,t+\tau)\text{d}t \text{ [B.13]}$$

Then by subsequently applying the Wiener-Khintchine theorem, the orthogonal correlation function can be related to the Fourier transforms of the dynamic and orthogonal spectra as follows:

$$D(\tau) = 1/2\pi\text{T} \int_{-\infty}^{\infty} \text{Y}_1^*(\omega) \bullet \text{Z}_2(\omega) e^{i\omega\tau}\, d\omega \text{ [B.14]}$$

where $Z_2(\omega)$ is the Fourier transform of $z(\upsilon_2,t)$. If τ is set to zero and if $Z_2(\omega) = i\text{sgn}(\omega) \bullet Y_2(\omega)$, the above equation reduces to

$$D(0) = \text{i}/2\pi\text{T} \int_{-\infty}^{\infty} \text{sgn}(\omega)\tilde{\text{Y}}_1^*(\omega) \bullet \tilde{\text{Y}}_2(\omega) d\omega \text{ [B.15]}$$

Since the signum function is an odd function, integration over the range of ω between -∞ and +∞ leaves only the imaginary component of the cross spectrum, which corresponds to the asynchronous 2D correlation spectrum. Thus

$$D(0) = \Psi(\nu_1,\nu_2) \text{ [B.16]}$$

Therefore, the asynchronous 2D correlation spectrum can be calculated from the time-averaged product of the dynamic spectral intensities and orthogonal spectral intensities measured at two different variables, ν_1 and ν_2:

$$\Psi(\upsilon_1,\upsilon_2) = 1/T \int_{-T/2}^{T/2} y(\nu_1,t) \bullet z(\nu_2,t) dt \quad [B.17]$$

Therefore, as with the calculation of the synchronous 2D correlation spectrum, the asynchronous 2D correlation spectrum can be calculated without needing to Fourier transform the dynamic spectral data.